



# Spin Waves 2011 International Symposium

## Program Abstracts

Ioffe Physical-Technical Institute  
Saint Petersburg, Russia  
June 5-11, 2011

# Contents

<b>Introduction.....</b>	<b>2</b>
<b>Conference Organization and Support.....</b>	<b>3</b>
<b>Invited Speakers.....</b>	<b>4</b>
<b>Symposium Program.....</b>	<b>5</b>
<b>Abstracts of Oral Sessions.....</b>	<b>14</b>
<b>Abstracts of Poster Session.....</b>	<b>79</b>
<b>Author Index.....</b>	<b>133</b>
<b>Symposium location map.....</b>	<b>138</b>

# Introduction

## **International Symposium on Spin Waves Saint Petersburg, Russia, June 5-11, 2011**

Since the sixties biennial Symposium on Spin Waves in St. Petersburg was aimed at providing an opportunity for discussion of the latest advances in fundamental studies of dynamic properties of various magnetically ordered materials. This year the Symposium will highlight the modern problems of magnetic dynamics and novel trends in magnetism. The Symposium will include discussions on the recently emerged research topics such as ultrafast phenomena of spin dynamics, current-induced and external-field-induced spin dynamics, spin dynamics of nanostructures, quantum magnets and multiferroics, X-ray and neutron probe of magnetism, and others. Recent advances in spintronics, spin-wave devices, magnetic and magneto-optical recording technology, as well as the prospects of exploiting the spin dynamical phenomena for ultrafast recording and processing of information will be discussed.



# Conference Organization and Support

## Organizing committee

- L. A. Prozorova, Chairwoman (Institute of Physical Problems, Moscow, Russia)
- S. O. Demokritov (Münster University, Münster, Germany)
- S. A. Nikitov (Institute of Radioengineering and Electronics, Moscow, Russia)
- R. V. Pisarev (Ioffe Physical-Technical Institute, St. Petersburg, Russia)

## Program committee

- A. I. Smirnov, Chairman (Institute of Physical Problems, Moscow, Russia)
- S. O. Demokritov (University of Münster, Münster, Germany)
- Yu. A. Filimonov (Saratov State University, Saratov, Russia)
- A. V. Kimel (Radboud University Nijmegen, Nijmegen, The Netherlands)
- S. V. Maleyev (Petersburg Nuclear Physics Institute, Gatchina, Russia)
- A. A. Mukhin (Prokhorov General Physics Institute, Moscow, Russia)
- V. V. Pavlov (Ioffe Physical-Technical Institute, St. Petersburg, Russia)
- V. A. Sanina (Ioffe Physical-Technical Institute, St. Petersburg, Russia)

## Local committee (Ioffe Physical-Technical Institute, St. Petersburg, Russia)

- R. V. Pisarev, Chairman
  - A. M. Kalashnikova
  - L. V. Lutsev
  - V. V. Pavlov
  - V. A. Sanina
  - P. A. Usachev
- In association with Agency for Science and Technology "Intellect"

## Sponsors

- Russian Academy of Sciences 
- Russian Foundation for Basic Research 
- Dynasty Foundation   
Dynasty
- St. Petersburg Scientific Center 
- Ioffe Physical-Technical Institute 



# Invited Speakers

- Dmitri Aristov (Petersburg Nuclear Physics Institute, Gatchina, Russia)
- Yuriy Bunkov (Institut Néel, Grenoble, France)
- Vladislav Demidov (University of Münster, Münster, Germany)
- Boris Kalinikos (Electrotechnical University, St. Petersburg, Russia)
- Stanislav Kamba (Institute of Physics, Prague, Czech Republic)
- Volodymyr Kruglyak (University of Exeter, Exeter, UK)
- Josep Nogués (Catalan Institute of Nanotechnology, Barcelona, Spain)
- Oleg Petrenko (University of Warwick, Coventry, UK)
- Andrei Pimenov (Vienna University of Technology, Vienna, Austria)
- Theo Rasing (Radboud University Nijmegen, Nijmegen, The Netherlands)
- Oleksandr Serha (Technical University, Kaiserslautern, Germany)
- Alexey Sherbakov (Ioffe Physical-Technical Institute, St. Petersburg, Russia)
- Sergey Sosin (Kapitza Institute of Physical Problems, Moscow, Russia)
- Oleg Starykh (University of Utah, Salt Lake City, USA)
- Leonid Svistov (Kapitza Institute of Physical Problems, Moscow, Russia)
- Georg Woltersdorf (University of Regensburg, Regensburg, Germany)

# **Symposium Program**

## International Symposium Spin Waves 2011 Oral Session Program

Monday, June 6

<b>10.00-10.10</b>	<b>Opening address</b>	
--------------------	------------------------	--

<b>10.10-11.10</b>	<b>Session 1</b>	<b>Spintronics</b>
10.10-10.40	J. Nogués (invited)	Controlling magnetic vortices using exchange bias p. 15
10.40-11.10	V.V. Kruglyak (invited)	Magnonics: exploiting spin waves in magnonic meta- materials and devices p. 16
<b>11.10-11.50</b>	<b>Coffee break and art exhibition</b>	

<b>11.50-12.35</b>	<b>Session 2</b>	<b>Ultrafast magnetization dynamics</b>
11.50-12.20	A. V. Scherbakov (invited)	Magnetization Precession Induced by Picosecond Acoustic Pulses in Ferromagnetic Materials p. 17
12.20-12.35	I. Razdolski	Time-Resolved imaging of spin reorientation in rare-earth orthoferrites p. 18
<b>13.00-14.30</b>	<b>Lunch</b>	

<b>14.30-15.45</b>	<b>Session 3</b>	<b>Quantum spin phenomena</b>
14.30-15.00	Yu. M. Bunkov (invited)	Magnon Bose-Einstein condensation p. 19
15.00-15.15	O. Dzyapko	Direct observation of first order quantum coherence and phase locking in magnon Bose-Einstein condensate p. 20
15.15-15.30	A. V. Klochkov	The first observation of magnon BEC in solid antiferromagnet CsMnF <sub>3</sub> p. 21
15.30-15.45	V. I. Kozub	Voltage-dependent electron distribution in a small spin valve: emission of nonequilibrium magnons and magnetization evolution p. 22
<b>15.45-16.15</b>	<b>Coffee break and art exhibition</b>	

<b>16.15-18.00</b>	<b>Session 4</b>	<b>Spintronics and magnetic films</b>
16.15-16.30	D. I. Kholin	Magneto-optical studies of interlayer coupling in Fe/Si/Fe tri-layers p. 23
16.30-16.45	Y. Matiks	Electronic phase transitions in nickel-oxide superlattices p. 24
16.45-17.00	E. Th. Papaioannou	Magneto-photonic behavior in 2D hexagonal patterns composed of 3d magnetic metals p. 25
17.00-17.15	V. A. Kosobukin	Plasmon-enhanced near-field magneto-optical Kerr effects and related scanning microscopy via a linear nanoprobe p. 26
17.15-17.30	D. Brunne	Spin-induced optical harmonic generation in the centrosymmetric semiconductors EuTe and EuSe p. 27
17.30-17.45	A. Stashkevich	Detection of buried layers in ferromagnetic metal films p. 28
17.45-18.00	R. M. Farzetdinova	Magnetic fluctuations as the reason of the metal-insulator transition in magnetic semiconductors p. 29
<b>18.00-19.30</b>	<b>Get-together party</b>	

**International Symposium Spin Waves 2011**  
**Oral Session Program**

**Tuesday, June 7**

<b>09.00-10.30</b>	<b>Session 5</b>	<b>Quantum and frustrated magnets</b>
09.00-09.30	L. E. Svistov (invited)	Magnetic phases of the frustrated $S=1/2$ chain compound $\text{LiCuVO}_4$ p. 30
09.30-09.45	A. V. Boris	Spin-fluctuation-mediated superconductivity in iron arsenides: complementary thermodynamics and optical studies p. 31
09.45-10.00	S. V. Maleyev	Spin waves in cubic helimagnets p. 32
10.00-10.15	A. N. Ignatenko	$Z_2$ -vortex unbinding transition for two-dimensional frustrated antiferromagnets p. 33
10.15-10.30	T. P. Gavrilova	Electron spin resonance in $\text{Ba}_3\text{Cr}_2\text{O}_8$ p. 34
<b>10.30-11.00</b>		<b>Coffee break</b>

<b>11.00-12.30</b>	<b>Session 6</b>	<b>Quantum and frustrated magnets</b>
11.00-11.30	O. A. Starykh (invited)	Breaking the spin waves: spinons in $\text{Cs}_2\text{CuCl}_4$ p. 35
11.30-11.45	K. Yu. Povarov	ESR modes in the spin-liquid phase of a two-dimensional frustrated quantum antiferromagnet $\text{Cs}_2\text{CuCl}_4$ p. 36
11.45-12.00	V. Ya. Krivnov	Low-temperature thermodynamics of frustrated classical spin chain near the critical point p. 37
12.00-12.15	V. R. Shaginyan	Properties of kagome lattice in $\text{ZnCu}_3(\text{OH})_6\text{Cl}_2$ p. 38
12.15-12.30	S. V. Demishev	Magnetic resonance in $\text{CeB}_6$ and ferromagnetic correlations p. 39
<b>13.00-14.30</b>		<b>Lunch</b>

<b>14.30-17.30</b>	<b>Session 7</b>	<b>Quantum and frustrated magnets</b>
14.30-15.00	O. A. Petrenko (invited)	Spin dynamics in the hyperkagome compound $\text{Gd}_3\text{Ga}_5\text{O}_{12}$ p. 40
15.00-15.30	D. N. Aristov (invited)	Asymmetric spin ladders: analytical and numerical studies p. 41
15.30-15.45	A. V. Syromyatnikov	Anomalously large damping of long-wavelength magnons caused by long-range interaction p. 42
15.45-16.00	V. N. Glazkov	Effects of weak interchain coupling on a spin-gap magnet p. 43
<b>16.00-16.30</b>		<b>Coffee break</b>
16.30-16.45	D. S. Inosov	Spin excitations in 122-ferropnictide superconductors studied by inelastic neutron scattering p. 44
16.45-17.00	A. M. Vasiliev	Magnetic anisotropy of 2D antiferromagnet with triangular lattice $\text{CuCrO}_2$ p. 45
17.00-17.15	A. V. Semeno	Probing of $\text{MnSi}$ by electron spin resonance p. 46
17.15-17.30	S. Sofronova	Magnetic anisotropy and exchange interactions of $\text{Ni}_3\text{B}_2\text{O}_6$ and $\text{Co}_3\text{B}_2\text{O}_6$ p. 47

<b>17.30-20.00</b>		<b>Poster session and refreshments</b>
--------------------	--	--

**International Symposium Spin Waves 2011**  
**Oral Session Program**

Wednesday, June 8

<b>09.00-11.15</b>	<b>Session 8</b>	<b>Multiferroics</b>
09.00-09.30	S. Kamba (invited)	Review of spin-phonon coupling in cubic SrMnO <sub>3</sub> , EuTiO <sub>3</sub> and hexagonal YMnO <sub>3</sub> antiferromagnets: radiofrequency, THz and far-infrared studies p. 48
09.30-10.00	A. Pimenov (invited)	Magnetic and magnetoelectric excitations in multiferroic manganites p. 49
10.00-10.15	A. A. Mukhin	Coupled R and Fe magnetic excitations in RFe <sub>3</sub> (BO <sub>3</sub> ) <sub>4</sub> multiferroics p. 50
10.15-10.30	A. P. Pyatakov	Spin flexoelectricity: magnetic domain walls and vortices as sources electric polarization p. 51
10.30-10.45	A. V. Malakhovskii	Hysteresis in magnetization of Nd <sub>0.5</sub> Gd <sub>0.5</sub> Fe <sub>3</sub> (BO <sub>3</sub> ) <sub>4</sub> single crystal p. 52
10.45-11.00	M. Ivanov	Evidence of <i>p-d</i> and <i>d-d</i> charge transfer and insulator-to-metal phase transitions in nonlinear optical response of (La <sub>0.6</sub> Pr <sub>0.4</sub> ) <sub>0.7</sub> Ca <sub>0.3</sub> MnO <sub>3</sub> p. 54
<b>11.00-12.00</b>		<b>Lunch</b>
<b>12.30-19.00</b>	<b>!!!!!!!!!!!!!!!!!!!!!!!!!!!! Excursion to Peterhof park and palace</b>	



**International Symposium Spin Waves 2011**  
**Oral Session Program**

Thursday, June 9

<b>09.00-11.15</b>	<b>Session 9</b>	<b>Nonlinear dynamics and nanostructures</b>
09.00-09.30	B. A. Kalinikos (invited)	Random formation of coherent spin-wave envelope solitons from incoherent microwave signal
09.30-10.00	G. Woltersdorf (invited)	Magnon magnetometry by XMCD and spin wave propagation in wires
10.00-10.15	M. A. Cherkasskii	Observation of black spin wave soliton pairs in yttrium iron garnet thin films
10.15-10.30	A. V. Kondrashov	Dual tunability of microwave chaos auto-generator based on ferrite-ferroelectric film structure
10:30-10:45	F. Mushenok	Non-linear spin-wave phenomena in chiral molecular magnets
10:45-11:00	S. V. Grishin	Self-generation of chaotic dissipative soliton trains in active feedback rings based on the ferromagnetic film
<b>11.00-12.00</b>		<b>Lunch</b>

<b>13.00-14.45</b>	<b>Session 10</b>	<b>Magnetization dynamics and nanostructures</b>
13.00-13.30	V. E. Demidov (invited)	Control of spin-wave emission characteristics of spin-torque nano-oscillators
13.30-13.45	J. Hellsvik	Atomistic spin dynamics simulations of ferrimagnetic resonance
13.45-14.00	N. B. Orlova	The model of ultrafast magnetization reversal without femtosecond spin dynamics
14.00-14.15	A. Taroni	Suppression of standing spin waves in low-dimensional magnets
14.15-14.30	T. V. Murzina	Optical and nonlinear-optical studies of Ni nanorods
14.30-14.45	N. S. Sokolov	Cobalt nanoparticle arrays on fluoride surfaces: growth and MOKE studies
<b>14.45-15.15</b>		<b>Coffee-break</b>

<b>15.15-17.00</b>	<b>Session 11</b>	<b>Magnetostatic waves</b>
15.15-15.30	S. Platonov	Magnetostatic spin waves propagation in wedge superlattices
15.30-15.45	A. Yarygin	Magnetostatic waves propagation in periodic magnetic structures with anisotropy
15.45-16.00	L. V. Lutsev	Spin waves in nanosized magnetic films
16.00-16.15	N. Volkov	Spin pumping and conversion of spin current into charge current in Co/Y <sub>3</sub> Fe <sub>5</sub> O <sub>12</sub> bilayer structure
16.15-16.30	M. Fayzullin	Possible mechanisms of magnon sidebands in KCuF <sub>3</sub>
<b>18.00-20.30</b>		<b>Conference dinner</b>

**International Symposium Spin Waves 2011**  
**Oral Session Program**

**Friday, June 10**

<b>09.00-11.00</b>	<b>Session 13</b>	<b>Trends in magnetism</b>
09.00-9.35	Th. Rasing (invited)	Ultrafast optical spin manipulation: challenges and opportunities p. 75
9.35-10.10	S. S. Sosin (invited)	Spin dynamics of Heisenberg and XY pyrochlore magnets studied by ESR p. 76
10.10-10.25	A. A. Sirenko	Far-IR excitations in multiferroics studied with Müller matrix ellipsometry and transmission spectroscopy using synchrotron radiation p. 77
10.25-11.00	A. A. Serga (invited)	Collapsing bullet and subwavelength spin-wave beams p. 78
<b>11.00-12.00</b>		<b>Closing remarks and coffee</b>

**International Symposium Spin Waves 2011**  
**Poster Session Program**

**Tuesday, June 7**  
**17:30-20:00**

- 01 G. Abramova, M. Boehm, **O. Bolsunovskaya**, B. Ouladdiaf  
Elementary excitation spectra of  $\text{Fe}_x\text{Mn}_{1-x}\text{S}$  single crystals p. 80
- 02 **A. A. Astretsov**, V. V. Pavlov, R. V. Pisarev, V. A. Rusakov, P. A. Usachev, A. I. Stognij,  
N. N. Novitski  
Optical and magneto-optical study of nanosized ferromagnetic metal-dielectric structures  
[Co/TiO<sub>2</sub>]<sub>n</sub>/Si p. 81
- 03 **A. G. Bazhanov**, A. M. Zyuzin  
Calculation of the resonant fields of SWR spectra with a smooth change of the symmetry boundary  
conditions in three-layer magnetic film p. 82
- 04 **E. N. Beginin**  
Propagation of microwave pulses through the nonlinear transmission line based on ferromagnetic  
structure p. 83
- 05 **E. N. Beginin**, S. A. Nikitov, Yu. P. Sharaevskii, S. E. Sheshukova  
Gap solitons in magnonic crystals at 3-wave interactions p. 84
- 06 V. D. Bessonov, **R. Gieniusz**, A. Maziewski, H. Ulrichs, V. E. Demidov,  
S. O. Demokritov, S. Urazhdin  
Resonant nonlinear frequency multiplication in microscopic magnetic elements p. 85
- 07 **P. Bondarenko**, B. A. Ivanov  
Dynamic properties of discrete solitons in 1D magnetic dots array p. 86
- 08 **A. Drozdovskii**, A. Ustinov, B. Kalinikos  
Pulsed excitation of surface spin-wave envelope solitons in magnonic crystal p. 87
- 09 **V. A. Dubovoj**, L. V. Lutsev, A. I. Firsenskov, A. E. Kozin, D. N. Fedin  
Traditional and perspective spin-wave devices for the microwave frequency band p. 88
- 10 **E. G. Ekomasov**, R. R. Murtazin, Sh. A. Azamatov, A. M. Gumerov, A. E. Ekomasov  
Nonlinear dynamics of the domain walls of the magnetic with 1D and 2D case nonhomogeneities  
modulation of the parameters of the magnetic anisotropy p. 89
- 11 **Yu. A. Fridman**, O. A. Kosmachev, Ph. N. Klevets  
Phase diagram in spin-1 easy-plane antiferromagnet p. 90
- 12 **A. A. Gippius**, N. E. Gervits, M. Baenitz, M. Schmitt, K. Koch, W. Schnelle, W. Liu,  
Y. Huang, H. Rosner  
NMR study of low dimensional spin system  $\text{Cu}_2[\text{PO}_3(\text{CH}_2)\text{PO}_3]$ : magnetic versus structural  
dimers p. 91
- 13 **A. Go**, L. Dobrzyński  
An influence of local environment on spin densities distribution in  $\text{Fe}_3\text{Al}$  and  $\text{Fe}_3\text{Si}$  doped with  
transition metals p. 92
- 14 **N. Grigoryeva**, B. Kalinikos  
Dipole-exchange spectrum of highly anisotropic ferromagnetic thin-film waveguides on terahertz  
frequencies p. 93
- 15 N. Grigoryeva, **R. Sultanov**, B. Kalinikos  
Dependence of the normal wave spectrum in multiferroic layered structure on surface spin-pinning  
conditions p. 94
- 16 S. V. Grishin, **D. V. Romanenko**, Yu. P. Sharaevskii  
Nonlinear model of a ferromagnetic film feedback ring at three-wave interactions p. 95



- 17 A. N. Ignatenko, **V. Yu. Irkhin**, A. A. Katanin  
Self-consistent spin wave theory, elementary excitations and Néel temperature in triangular-lattice antiferromagnets p. 96
- 18 P. A. Igoshev, A. V. Zarubin, A. A. Katanin, **V. Yu. Irkhin**  
Spin wave and one particle instabilities of ferromagnetic state in the Hubbard model p. 97
- 19 **D. Ilyushenkov**, D. Yavsin, V. Kozhevnikov, I. Yassievich, V. Kozub, S. Gurevich  
Magnetic properties of the Ni amorphous nanogranule films p. 98
- 20 V. P. Ivanov, **S. A. Manuilov**, A. M. Grishin, G. A. Nikolychuk  
Step forward to the new materials for MSSW devices p. 99
- 21 **A. S. Kamzin**, Fulin Wei, V. Ganeev, L. D. Zaripova  
Preparation and study of Fe/M ( $M=Co$  or Pt) thin films for ultrahigh-density magnetic recording p. 100
- 22 **A. N. Kalinkin**, V. M. Skorikov  
Skyrmion lattices in multiferroics p. 101
- 23 **E. Karashtin**, O. Udalov  
Properties of high frequency conductivity in noncollinear ferromagnets p. 102
- 24 **A. D. Karenowska**, A. V. Chumak, V. S. Tiberkevich, A. A. Serga, J. F. Gregg, A. N. Slavin, B. Hillebrands  
Oscillatory energy exchange between spin wave modes coupled by a dynamic magnonic crystal p. 103
- 25 **N. Khasanov**  
Some aspects of the influence of defects on the formation of thermoremanent magnetization in two-domain grains ensemble p. 104
- 26 **R. Khymyn**, V. E. Kireev, B. A. Ivanov  
Ground states of the triangular arrays of magnetic dots in the presence of the external magnetic field p. 105
- 27 M. I. Kobets, K. G. Dergachev, **E. N. Khatsko**, S. L. Gnatchenko  
Features of high-frequency properties of the crystal  $NdFe_3(BO_3)_4$  in the incommensurate magnetic phase p. 106
- 28 M. I. Kurkin, **N. B. Orlova**  
Equations to describe the femtosecond magneto-optics under the electric-dipole excitation of electrons p. 107
- 29 **A. P. Kuz'menko**, P. V. Abakumov  
Raman image of the magnetic structure in  $YFeO_3$  p. 108
- 30 N. Leo, D. Meier, **R. V. Pisarev**, S.-W. Cheong, M. Fiebig  
Role of the rare-earth magnetism in the magnetic-field induced polarization reversal in multiferroic  $TbMn_2O_5$  p. 109
- 31 **E. H. Lock**, A. V. Vashkovsky  
On the relationship between power and dispersion characteristics of a dipole spin waves p. 110
- 32 **L. V. Lutsev**, A. I. Stognij, N. N. Novitskii, A. S. Shulenkov  
Spin-wave and spintronic devices on the base of magnetic nanostructures p. 111
- 33 M. A. Morozova, **Yu. P. Sharaevskii**, S. E. Sheshukova, M. K. Zhamanova  
Self-action effects of magnetostatic waves in layered ferromagnetic structure p. 112
- 34 **N. V. Ostrovskaya**, V. V. Polyakova, A. F. Popkov  
Analysis of bifurcations in the model of a three-layered magnetic structure p. 113
- 35 **K. G. Patrin**, V. Yu. Yakovchuk, D. A. Velikanov, G. S. Patrin, S. A. Yarikov  
Magnetic, resonance and magnetoresistivity properties of trilayer NiFe/Bi/NiFe films p. 114

- 36 **V. V. Pavlov**, A. B. Henriques, A. Schwan, I. Akimov, R. V. Pisarev, D. Yakovlev, M. Bayer  
Picosecond spectroscopy of electronic-spin excitations in magnetic semiconductor EuTe p. 115
- 37 **Anna Pimenov**, Ch. Kant, A. Shuvaev, V. Tsurkan, A. Pimenov  
Synthesis, characterization and dynamic magnetic properties of multiferroic chromates p. 116
- 38 **V. K. Sakharov**, Y. V. Khivintsev, S. A. Nikitov, Y. A. Filimonov  
Magnetic structures based on periodically alternating cobalt and permalloy stripes p. 117
- 39 **V. K. Sakharov**, Y. V. Khivintsev, S. A. Nikitov, Y. A. Filimonov  
Magnetoresistance and domain structure in patterned magnetic microstructures based on cobalt and permalloy films p. 118
- 40 **A. V. Sizanov**, A. V. Syromyatnikov  
Magnetics with large single-ion easy-plane anisotropy p. 119
- 41 **P. M. Shmakov**, A. P. Dmitriev, V. Yu. Kachorovskii  
Spin waves in diluted magnetic quantum wells p. 120
- 42 **A. I. Smirnov**, K. Yu. Povarov, S. V. Petrov, A. Ya. Shapiro  
Magnetic resonance in ordered phase of spin-1/2 antiferromagnet Cs<sub>2</sub>CuCl<sub>4</sub> p. 121
- 43 **A. O. Sorokin**, A. V. Syromyatnikov  
Transitions in three-dimensional magnets with extra order parameters p. 122
- 44 **R. R. Subkhangulov**, B. R. Namozov, K. V. Kavokin, Yu. G. Kusraev, A. V. Koudinov  
Temperature dependence of multiple spin-flip Raman scattering in magnetic quantum wells p. 123
- 45 **S. M. Suturein**, L. Pasquali, A. G. Banshchikov, D. A. Baranov, V. V. Fedorov, K. V. Koshmak, Yu. A. Kibalin, P. Torelli, J. Fujii, G. Panaccione, N. S. Sokolov  
XMCD studies of magnetic properties and proximity effects in Co/MnF<sub>2</sub>(111) heterostructures p. 124
- 46 D. O. Tolmachev, A. S. Gurin, **N. G. Romanov**, P. G. Baranov, B. R. Namozov, Yu. G. Kusraev  
ODMR of Mn-related excitations in (Cd,Mn)Te quantum wells p. 125
- 47 **V. Tugarinov**, A. Pankrats, G. Petrakovskii, S. Kondyan, D. Velikanov, V. Temerov  
Antiferromagnetic resonance and magnetic investigations of rare-earth ferrobates p. 126
- 48 **O. G. Udalov**  
NMR spectrum in the non-collinear antiferromagnet Mn<sub>3</sub>Al<sub>2</sub>Ge<sub>3</sub>O<sub>12</sub> p. 127
- 49 **P. A. Usachev**, A. A. Astretsov, V. A. Rusakov, V. V. Pavlov, N. A. Tarima, S. A. Kitan', V. M. Iliyaschenko, N. I. Plusnin  
Magneto-optical properties of Fe and Fe/Cu layered nanostructures on Si(001) p. 128
- 50 **N. Useinov** and L. Tagirov  
Spin-polarized conductivity of double magnetic tunnel junction p. 129
- 51 A. G. Volkov, **A. A. Povzner**  
The nonlinear effect of external electric field on the spin excitations and the electronic structure of ferromagnetic semiconductors p. 130
- 52 **S. L. Vysotsky**, Yu. A. Filimonov, E. S. Pavlov, S. A. Nikitov  
Influence of metal on formation of forbidden gaps in SMSW spectrum of 1D ferrite magnonic crystal p. 131
- 53 **S. L. Vysotsky**, Yu. A. Filimonov, E. S. Pavlov, S. A. Nikitov  
Influence of three magnon parametric instability on MSSW Bragg resonances in 1D magnonic crystal p. 132

**Abstracts**

**Oral Sessions**

## Controlling magnetic vortices using exchange bias

J. Nogués<sup>1,2,3</sup>, G. Salazar-Álvarez<sup>4</sup>, J. J. Kavich<sup>2</sup>, M. Tanase<sup>5</sup>, A. Mugarza<sup>2</sup>, S. Stepanow<sup>6</sup>, V. Baltz<sup>7</sup>, A. Weber<sup>8</sup>, L. J. Heyderman<sup>8</sup>, A. K. Petford-Long<sup>5</sup>, O. Heinonen<sup>5</sup>, M. D. Baró<sup>3</sup>, B. Dieny<sup>7</sup>, K. S. Buchanan<sup>9</sup>, A. Hoffmann<sup>5</sup>, P. Gambardella<sup>1,2,3</sup>, J. Sort<sup>1,3</sup>

<sup>1</sup>*Institució Catalana de Recerca i Estudis Avançats (ICREA), Barcelona, Spain*

<sup>2</sup>*CIN2(ICN-CSIC), Catalan Institute of Nanotechnology, Campus UAB, Bellaterra, Spain*

<sup>3</sup>*Dept. de Física, Univ. Autònoma de Barcelona, Bellaterra, Spain*

<sup>4</sup>*Dept. of Materials and Environmental Chemistry, Stockholm University, Stockholm, Sweden*

<sup>5</sup>*Argonne National Laboratory, Argonne, Illinois, USA*

<sup>6</sup>*Max-Planck-Institut für Festkörperforschung, Stuttgart, Germany*

<sup>7</sup>*SPINTEC, CEA/Grenoble, Grenoble, France*

<sup>8</sup>*Lab. for Micro- and Nanotechnology, Paul Scherrer Institut, Villigen PSI, Switzerland*

<sup>9</sup>*Dept. of Phys., Colorado State Univ., Ft Collins, Colorado USA*

Nanostructured exchange biased systems, comprising exchange coupled antiferromagnetic (AFM) - ferromagnetic (FM) bilayers are at the heart of spintronic devices (e.g., read heads or MRAMs). In this talk the magnetic behavior of lithographically-patterned exchange coupled FM (permalloy) – AFM (IrMn) disks will be discussed. We have demonstrated that, for certain geometries, vortex formation remains the reversal mode in these FM-AFM dots although the loops are shifted along the field axis [1]. In fact, the actual magnetization reversal mechanism (coherent rotation vs. vortex formation) can be controlled by adjusting various parameters. For example, in circular dots measured away from the field cooling direction, a change in reversal mode occurs beyond a certain angle of measurement, which depends on the nucleation and bias fields (adjustable by intrinsic or extrinsic parameters). Moreover, if the system is field cooled, not in saturation but in a vortex state (i.e., using zero or small fields), either stabilized vortex states or a new type of asymmetric hysteresis loop are found. This asymmetry is characterized by the appearance of curved, reversible, central sections in the hysteresis loops, with non-zero remanent magnetization [2]. The origin of the new reversal is ascribed to the imprinting of magnetic vortices in the AFM during the cooling process, which results in a pinning of the vortex core. These imprinted states have been imaged using x-ray photoemission electron microscopy and magnetic circular dichroism [3]. Other asymmetries, e.g., in the vortex annihilation field, have been found and tentatively ascribed to tilted vortex states [4]. Moreover, exchange coupling significantly reduces the number of stochastic events, which are inherent in single layer ferromagnetic disks due to thermal activation, and results in magnetic behavior that is reproducible over time [5].

[1] J. Sort et al., Phys. Rev. Lett. **95**, 067201 (2005).

[2] J. Sort et al., Phys. Rev. Lett. **97**, 067201 (2006).

[3] G. Salazar-Alvarez et al., Appl. Phys. Lett. **95**, 012510 (2009).

[4] J. Sort et al., unpublished.

[5] M. Tanase et al., Phys. Rev. B **79**, 014436 (2009).

## **Magnonics: exploiting spin waves in magnonic meta-materials and devices**

V. V. Kruglyak<sup>1</sup>, Y. Au<sup>1</sup>, M. Dvornik<sup>1</sup>, R. V. Mikhaylovskiy<sup>1</sup>, T. Davison<sup>1</sup>, E. Hendry<sup>1</sup>,  
and E. Ahmad<sup>1</sup>

<sup>1</sup>*University of Exeter, EX4 4QL, Exeter, United Kingdom*

The recent renaissance of magnonics was a result of the remarkable technological, experimental, and theoretical progress that made it possible not only to study but also to explore ways to exploit spin waves in magnetic nanostructures [1]. In particular, a lot of interest has been generated by the prospectus for creation of magnonic meta-materials [2,3] and logic devices [1,4,5]. In this talk, we will review our most recent results along these research directions. We will demonstrate an architecture facilitating excitation of spin waves in multiple places on a magnonic logic chip. We will present opportunities arising from exploiting 3D magnetic geometries for design of spin wave resonances in magnonic metamaterials. Finally, we discuss opportunities and limitations for studies and exploitation of spin waves in THz frequency domain.

The research leading to these results has received funding from the European Community's Seventh Framework Programme (FP7/2007-2013) under Grant Agreements n°233552 (DYNAMAG) and n°228673 (MAGNONICS) and from the Engineering and Physical Research Council (EPSRC) of the UK.

- [1] V. V. Kruglyak, S. O. Demokritov, and D. Grundler, *J. Phys. D – Appl. Phys.* **43**, 264001 (2010).
- [2] V. V. Kruglyak, P. S. Keatley, A. Neudert, R. J. Hicken, J. R. Childress, and J. A. Katine, *Phys. Rev. Lett.* **104**, 027201 (2010).
- [3] R. V. Mikhaylovskiy, E. Hendry, and V. V. Kruglyak, *Phys. Rev. B* **82**, 195446 (2010).
- [4] S. V. Vasiliev, V. V. Kruglyak, M. L. Sokolovskii, and A. N. Kuchko, *J. Appl. Phys.* **101**, 113919 (2007).
- [5] Y. Au, T. Davison, E. Ahmad, P. S. Keatley, R. J. Hicken, and V. V. Kruglyak, *Appl. Phys. Lett.* **98**, 122506 (2011).

# Magnetization precession induced by picosecond acoustic pulses in ferromagnetic materials

A. V. Scherbakov

*Ioffe Physical-Technical Institute, 194021, St. Petersburg, Russia*

The methods of picosecond acoustics allow generating of ultrashort acoustic pulses and may be the powerful alternative to the optical methods of ultrafast control of magnetization. The control of magnetization by acoustic waves utilizes the strong sensitivity of magneto-crystalline anisotropy (MCA) of narrow ferromagnetic layers to the strain. The modulation of MCA by acoustic waves tilts the magnetization and induces coherent magnetization precession. Picosecond acoustic wave packet with the broad spectrum excites a number of magnon modes; however, the resonance effects are expected in the case of effective coupling between a certain magnon mode and an acoustic wave with a certain wave vector.

At experiment we inject high-amplitude acoustic pulse into a ferromagnetic semiconductor and monitor the induced modulation of magnetization by time-resolved Kerr rotation (KR) [1]. The structure studied is 200-nm-thick epitaxial  $\text{Ga}_{0.95}\text{Mn}_{0.05}\text{As}$  layer grown on a (001) GaAs substrate. The femtosecond optical pump excitation ( $\lambda=800$  nm, duration of 200 fs, excitation density up to  $5 \text{ mJ/cm}^2$ ) of a 100-nm-width Al film deposited on the polished back side of the substrate leads to the injection of the picosecond acoustic pulse into the sample. Broad acoustic wave packet containing only  $\epsilon_{zz}$  strain component propagates in the crystal, reaches ferromagnetic layer, and modulates MCA. The tilt and the resulting coherent precession of magnetization are monitored by means of the splitted from the same laser source linearly polarized probe beam focused at the magnetic layer exactly opposite to the pump beam. The variable optical delay between the pump pulse and the probe pulse provides femtosecond time resolution.

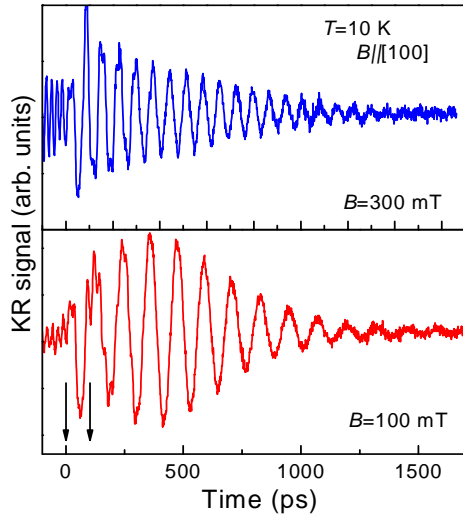


Fig. 1 KR signals at different magnetic fields. Acoustic pulse propagates in the magnetic layer at the time interval shown by the vertical arrows.

The experimental signals (Fig. 1) demonstrate strong dependencies of precession frequency and amplitude on the direction and strength of external magnetic field. We propose the model, which suggests linear dependence of MCA coefficients on  $\epsilon_{zz}$  and well quantitatively describes experimental results. We also show that both optical detection and acoustic excitation of magnetization precession possess different efficiency for different magnon modes. The frequency splitting between optically and acoustically active modes at certain direction and value of external magnetic field may lead to the pronounced beating in the KR signal (Fig. 1b).

The obtained experimental results demonstrate the great potential of picosecond acoustic methods for the ultrafast control of magnetization. The proposed technique are not limited by ferromagnetic semiconductors and low temperatures, but may be used in the wide range of ferromagnetic materials at room temperature.

[1] A.V. Scherbakov et al., Phys. Rev. Lett. **105**, 117204 (2010).

# Time-resolved imaging of spin reorientation in rare-earth orthoferrites

J. A. de Jong<sup>1</sup>, I. Razdolski<sup>1</sup>, A. M. Kalashnikova<sup>2</sup>, A. V. Kimel<sup>1</sup>, R. V. Pisarev<sup>2</sup>,  
A. M. Balbashov<sup>3</sup>, A. Kirilyuk<sup>1</sup> and Th. Rasing<sup>1</sup>

<sup>1</sup>Radboud University Nijmegen, IMM, 6525, AJ Nijmegen, The Netherlands

<sup>2</sup>Ioffe Physical-Technical Institute, RAS, 194021, St. Petersburg, Russia

<sup>3</sup>Moscow Power Engineering Institute, 105835, Moscow, Russia

Manipulation of magnetic states of a medium by means of femtosecond laser pulses is a promising approach to achieve the fastest ever processing of magnetic information [1,2]. It has been recently demonstrated that a circularly polarized laser pulse, acting as an effective magnetic field, can trigger a transition between two magnetic phases in HoFeO<sub>3</sub> [3]. Here we report a femtosecond time-resolved imaging of a novel laser-induced phase transition, where light has a twofold effect, both changing the magnetic anisotropy of a medium through heating and determining the magnetization direction in the new phase.

Single-shot time-resolved imaging and stroboscopic pump-probe experiments were performed on a weak ferromagnetic (Sm<sub>0.5</sub>Pr<sub>0.5</sub>)FeO<sub>3</sub> sample, kept at a temperature below the  $\Gamma_2 \rightarrow \Gamma_{24} \rightarrow \Gamma_4$  spin reorientation transition (SRT) range (95-130 K). A 40-fs circularly polarized pump pulse generates an effective magnetic field through the ultrafast inverse Faraday effect and simultaneously heating the sample over the SRT range. As the magnetic anisotropy of the sample changes rapidly with heating, this leads to a net magnetization reorientation. The out-of-plane net magnetization component was detected with a delayed probe femtosecond pulse.

Fig.1(a) shows the Faraday rotation dynamics for the initial temperature of 15 K. A circularly-polarized laser pulse induces the magnetization reorientation, its direction being clearly governed by the helicity of the pump polarization. The reorientation time depends on the initial temperature, being of the order of tens of ps for 15 K and decreasing down to a few ps for 90 K. The dynamics of the non-thermal contribution  $(\sigma_+ - \sigma_-)/2$  for different pump pulse energies is shown in Fig.1, (b). Its non-monotonous behaviour with respect to the pump energy explains the opposite reorientation directions in an unusual “ring-and-core” magnetization pattern, as shown in the images (Fig.1(b)).

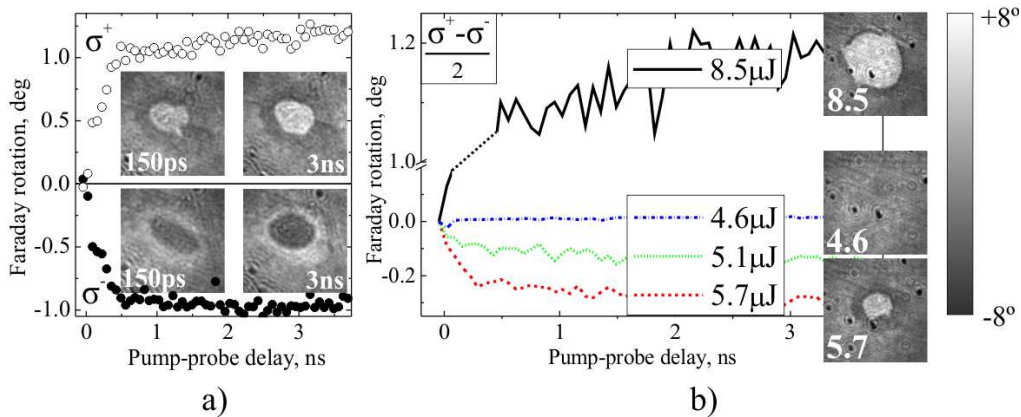


Fig.1. (a) Dynamics of the out-of-plane magnetization component during the spin reorientation in (Sm<sub>0.5</sub>Pr<sub>0.5</sub>)FeO<sub>3</sub> at 15 K for two opposite pump polarization helicities, as observed via the pump-probe Faraday rotation technique. Images represent magnetization patterns at the corresponding delays. (b) Pump pulse energy dependence of a non-thermal contribution  $(\sigma_+ - \sigma_-)/2$  to the spin reorientation dynamics. Images show the “ring-and-core” magnetization pattern at 3 ns delay.

[1] A. V. Kimel *et al.*, Nature **435**, 655 (2005).

[2] C. D. Stanciu *et al.*, Phys. Rev. Lett. **99**, 047601 (2007).

[3] A. V. Kimel *et al.*, Nat. Phys. **5**, 727 (2009).

# Magnon Bose-Einstein condensation

Yu. M. Bunkov

*Institut Neel 38042, Grenoble, France*

Superfluid  $^3\text{He}$  can be considered a quantum vacuum carrying various types of quasiparticles and topological defects. The structure of this system shows many similarities to that of our Universe. It can act as a model system for the study of many types of general physics experiments, which are difficult or even impossible in Cosmology, Atomic or Nuclear physics. There is a complete analogy between the Bose-Einstein condensation of atomic gases and the Bose-Einstein condensation of magnons in superfluid  $^3\text{He}$ . Four different states of magnon condensation have been found; the homogeneously precessing domain (HPD) in  $^3\text{He-B}$ ; the persistent signal, which is formed by a Q-ball in  $^3\text{He-B}$  at very low temperatures; coherent precession with fractional magnetization in  $^3\text{He-B}$  and coherent precession of magnetization in  $^3\text{He-A}$  and  $^3\text{He-B}$  in a squeezed aerogel [1]. All these cases are examples of the Bose-Einstein condensation of magnons with the interaction potential provided by specific spin-orbit coupling. The BEC phenomenon in the gas of magnons is readily accessible owing to the possibility of modifying the spin-orbit coupling. In some cases the BEC of magnons corresponds to almost 100% condensation.

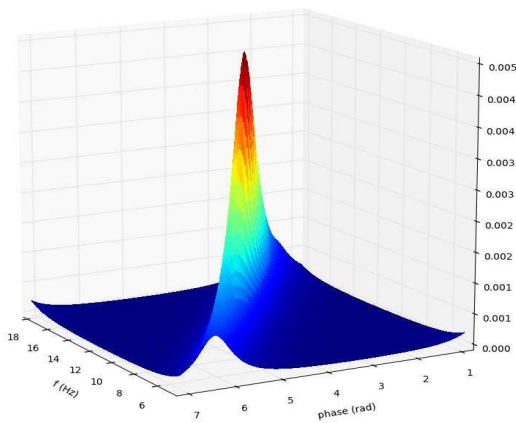


Fig. 1 Spin Waves condensation

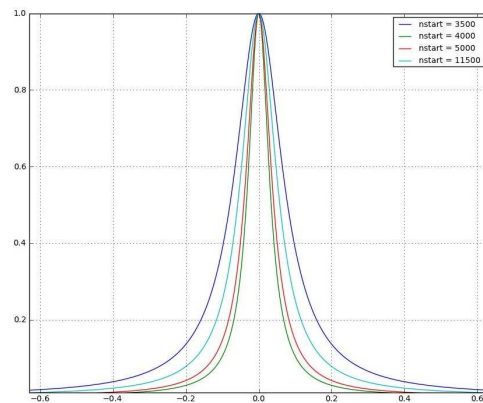


Fig. 2 The spectrum of BEC radiation after 70, 80, 100 and 230 msec after a RF pulse.

Fig.1 shows the frequency and phase distribution of BEC radiation. The accuracy of phase and frequency measurements is mixed due to the analogy with the uncertainty. Fig 2 shows the BEC radiation broadening. The broadening of magnetic field on the sample corresponds to 800 Hz!

[1] Yuriy M. Bunkov and Grigoriy Volovik, *J. Phys.: Condens. Matter* **22**, 164210 (2010).

[2] Yu. M. Bunkov “Spin superfluidity and magnons Bose–Einstein condensation”, *Physics-Uspokhi* **53**, 848 (2010).



# Direct observation of first order quantum coherence and phase locking in magnon Bose-Einstein condensate

P. Nowik-Boltyk, O. Dzyapko, V. E. Demidov and S. O. Demokritov  
*Institute for Applied Physics, University of Muenster, 48149 Muenster, Germany*

Bose-Einstein condensation (BEC) is one of the most fascinating quantum phenomena, as it brings quantum mechanical behavior of bosonic particles on to the macroscopic scale. The latter becomes possible due to emergence of spontaneous coherence between individual bosons comprising condensate, which makes all individual particles to act in a collective manner. Spontaneous coherence is a crucial point for BEC, determining BEC-based effects such as superconductivity superfluidity and Josephson effect.

Here we report on direct experimental observation of coherence in Bose-Einstein condensate of magnons in yttrium-iron garnet (YIG). Discovered by Demokritov [1], condensation of magnons was the first room temperature condensation. Besides, magnon BEC in tangentially magnetized films differs from all other known BEC systems by the fact that condensation occurs at non-zero value of wave vector  $|k_{\text{BEC}}| \neq 0$ , which results in degeneracy of the quantum state of the condensate (due to symmetry reasons magnons condensate at two points of phase space corresponding to  $\pm|k_{\text{BEC}}|$ ).

In our experiments we create magnon condensate by means of continuous parametric pumping. Continuous pumping allows for constant initial phase of the condensate during the whole measurements. Condensate properties are investigated by space and time resolved micro-focus Brillouin light scattering technique [2]. In the experiment we directly observe interference pattern, which results from the interference between two components of magnon condensate from different points of phase space. Stationary interference pattern appears as a result of phase locking between two condensates, which keeps difference between phases of individual condensates constant during the whole measurements. The phase locking arises as a result of nonlinear interaction between magnons from different condensates. This conclusion is corroborated by observation of increase of phase locking rate with pumping power.

- [1] S. O. Demokritov, V. E. Demidov, O. Dzyapko, G. A. Melkov, A. A. Serga, B. Hillebrands, and A. N. Slavin, *Nature* **443**, 430 (2006).
- [2] V. E. Demidov, S. O. Demokritov, B. Hillebrands, M. Laufenberg, and P. P. Freitas, *Appl. Phys. Lett.* **85**, 2866 (2004).

# The first observation of magnon BEC in solid antiferromagnet CsMnF<sub>3</sub>

A. V. Klochkov<sup>1</sup>, E. M. Alakshin<sup>1</sup>, Yu. M. Bunkov<sup>2</sup>, R. R. Gazizulin<sup>1</sup>, V. V. Kuzmin<sup>1</sup>,  
T. R. Safin<sup>1</sup>, M. S. Tagirov<sup>1</sup>

<sup>1</sup>Kazan (Volga region) Federal University, Kazan, Russia

<sup>2</sup>Institut Neel, Grenoble, France

The Spin Supercurrent and Bose-Einstein condensation of magnons similar to an atomic BEC was observed in 1984 in superfluid <sup>3</sup>He-B. The same phenomena should exist in solid magnetic systems. In this presentation we will report the first observation of magnon BEC in solid easy plain antiferromagnet CsMnF<sub>3</sub>. We have observed magnon BEC on a mode of coupled Nuclear-Electron precession. The dynamical properties of this mode have many similarities to NMR of superfluid <sup>3</sup>He-A. The coupled nuclear electron precession in CsMnF<sub>3</sub> shows a very peculiar dynamics. The electron precession frequency drops down to a near zero at zero fields. The <sup>55</sup>Mn NMR frequency in hyperfine field is very high, about 600 MHz. Due to crossover the two mixed modes of precession appear. We will speak about low frequency electron-nuclear precession mode. Its frequency depends on orientation of nuclear magnetization as it shown in Fig. 1. That is similar to the frequency dependence in <sup>3</sup>He-A where BEC of magnons have been proved [1]. Furthermore, the involvement of electron ordered subsystem gives the magnon-magnon interaction, spin waves and spin supercurrent, while the nuclear subsystem gives the relatively long time of relaxation. That is why the magnon BEC was predicted for CsMnF<sub>3</sub> [2].

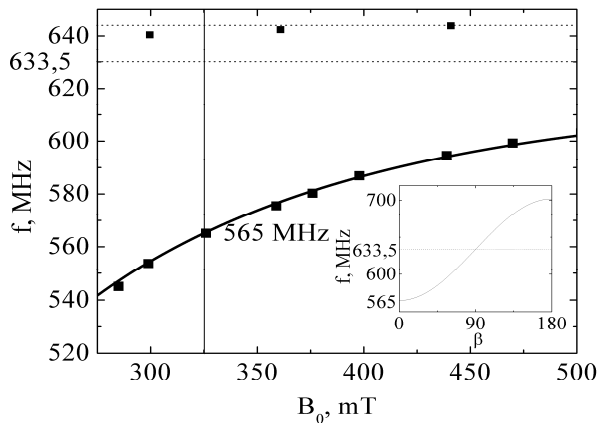


Fig. 1 The frequency of NMR mode on magnetic field and its dependence on angle of magnetization deflection at given field.

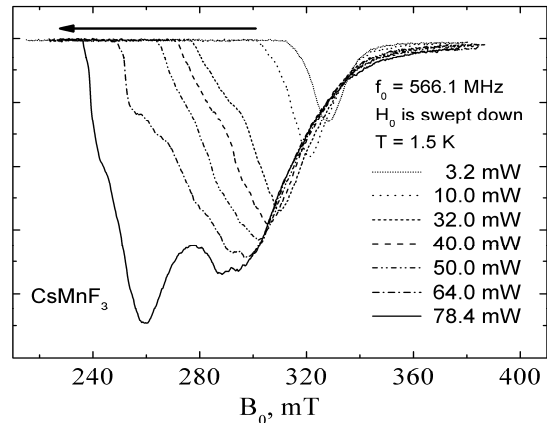


Fig. 2 The signal of CW NMR at different excitation levels. The system radiates on a non-resonance frequency that is correspond to formation of BEC

The experiment was done at the temperature of 1.5 K at a frequency of 566 MHz. The line of CW NMR at small RF excitation corresponds to 325 mT field. If we will increase the excitation and sweep down the field, the nuclear magnetizations deflects and keep the same frequency of radiation, as shown in Fig. 2. The amplitude of the radiation grows up. That means that we have created the magnon BEC with a deflected and homogeneously precessing magnetization. The stability of this state is due to the profile of magnon-magnon interaction and intrinsic spin supercurrent.

This work is supported by the Ministry of Education and Science of the Russian Federation (FTP "Scientific and scientific-pedagogical personnel of the innovative Russia" contract N02.740.11.5217)

[1] P. Hunger, Yu. M. Bunkov, E. Collin, H. Godfrin, J. Low Temp. Phys. **158**, 129–134 (2010).

[2] Ю. М. Буньков, УФН, 180, 884; Physics–Uspekhi, **53**:8, 848–853(2010).

# Voltage-dependent electron distribution in a small spin valve: emission of nonequilibrium magnons and magnetization evolution

V. I. Kozub<sup>1</sup>, J. Caro<sup>2</sup>

<sup>1</sup>*Ioffe Physical-Technical Institute, St. Petersburg 194021, Russian Federation*

<sup>2</sup>*Kavli Institute of NanoScience Delft, Delft University of Technology,  
Lorentzweg 1, 2628 CJ Delft, The Netherlands*

We describe spin transfer in a ferromagnet/normal metal/ferromagnet spin-valve point contact. Spin is transferred from the spin-polarized device current to the magnetization of the free layer by the mechanism of incoherent magnon emission by electrons. Our approach is based on the rate equation for the magnon occupation, using Fermi's golden rule for magnon emission and absorption and the non-equilibrium electron distribution for a biased spin valve. The magnon emission reduces the magnetization of the free layer. For anti-parallel alignment of the magnetizations of the layers and at a critical bias a magnon avalanche occurs, characterized by a diverging effective magnon temperature. This critical behavior can result in magnetization reversal and consequently to suppression of magnon emission. However the magnon-magnon scattering can lead to saturation of magnon concentration at large but finite value. The further behavior depends on the parameters of the system. In particular, gradual evolution of magnon concentration followed by the magnetization reversal is possible. Another scenario corresponds

to step-like increase of magnon concentration followed by slow decrease. In the latter case the spike in differential resistance is expected due to contribution of electron-magnon scattering. In the latter regime a telegraph noise of magnetoresistance can exist even at zero temperature. A comparison of the obtained results to existing experimental data and theoretical approaches is given. We demonstrate that our approach corresponds to the "bias-controlled regime" implying a given non-equilibrium electron distribution function controlled by the bias. We also give a critical review of the existing models of magnetization switching based mostly on the "spin-torque" approach started by J.C. Slonczewski, (*J. Magn. Magn. Mater.* v.159, L1 (1996)) and then extensively exploited by the group of G.E.W. Bauer, Y.Tserkovnyak, A.Brataas, (see e.g. *Phys. Rev. Lett.*, v. 88, 117601 (2002)). We show that the spin-torque approach corresponds to a "current-controlled regime" when the distribution function is adapted to the finite value of the incident spin current. It is shown that in any case our approach holds for the mutual orientation of the layers magnetizations close to the parallel or antiparallel. At the same time the scenario of the further evolution can depend on the system parameters. Then, the critical values of the switching current in our case appear to be much less than for spin-torque approach. We also give a criticism of the approach by Berger (*L. Berger, Phys. Rev. B* **54**, 9355 (1996) who - although using a concept of non-equilibrium magnons - has given an oversimplified picture basing on the artificially induced relaxation rates.

# Magneto-optical studies of interlayer coupling in Fe/Si/Fe tri-layers

D. I. Kholin, A. B. Drovosekov, S. V. Zasukhin, N. M. Kreines

*P.L. Kapitza Institute for Physical Problems RAS, ul. Kosygina 2, 119334 Moscow, Russia*

The problem of interlayer coupling in Fe/Si/Fe multilayer systems has attracted much attention for more than a decade [1-4] due to a possible use of these systems in high-tech applications. But experimental results in this field are rather contradictory mainly because of an uncontrollable diffusion of iron atoms into the silicon spacer. In this work, we study a series of Fe/Si/Fe tri-layers grown by means of the MBE technique. We varied the substrate temperature during the Si spacer formation for different samples from 300 to 77 K in order to change the concentration of Fe atoms in the spacer. The spacer thickness in each sample changed linearly from 0 to approximately 20 Å on a length of 10 mm, so that we could use the MOKE magnetometry to measure the dependence of the interlayer coupling on the spacer thickness. We had also made two samples with constant thicknesses of Si spacer, which suited for FMR and SQUID measurements [5], so we could compare the interlayer coupling parameters given by different experimental methods.

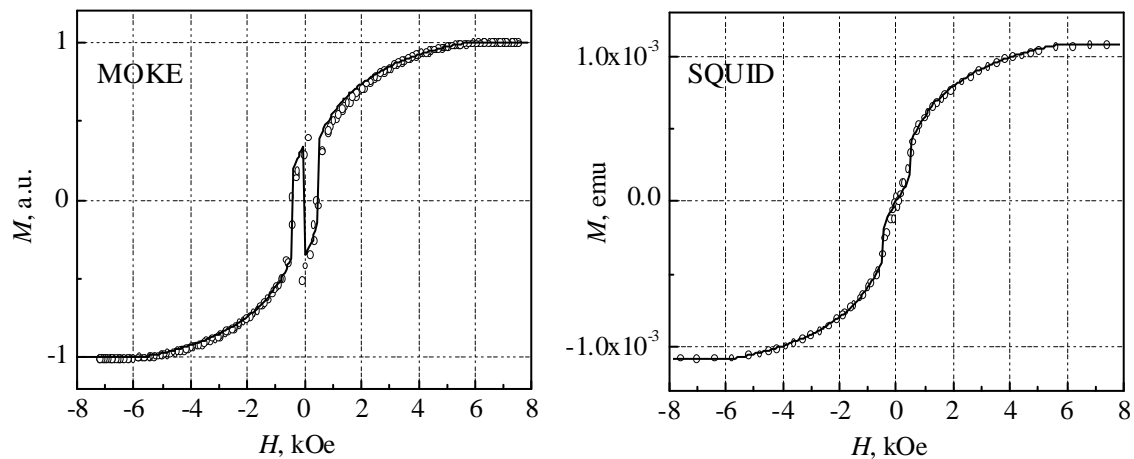


Fig. 1. Magnetization curves of a Fe(70 Å)/Si(12 Å)/Fe(70 Å) sample measured by MOKE and SQUID techniques. Dots – experimental data, solid lines – computer simulation based on the biquadratic coupling model. Magnetic field was applied in the film plane along the hard magnetisation axis of iron.

Unexpectedly, the shape of magnetisation curves measured by the MOKE and SQUID techniques differed significantly for the same samples (see Fig.1). In our talk we will show, that the results of MOKE, SQUID and FMR measurements can be all brought into conformity if we take into account a finite penetration depth of laser light and a twist of the magnetisation vector across the iron layers. This approach allowed us to obtain the dependence of the bilinear and biquadratic coupling constants on the spacer thickness for our samples.

The authors are grateful to D.E. Bürgler and R. Schreiber for the possibility to prepare the samples in Forschungszentrum Jülich. The work was partially supported by the Russian Foundation for Basic Research (grant No. 10-02-01110-a).

- [1] S. Toscano, B. Briner, H. Hopster and M. Landot, *J. Magn. Magn. Matter* **114**, L6 (1992).
- [2] D. Bürgler, M. Buchmeier, S. Cramm et al., *J. Phys.: Condens. Matter* **15**, S443 (2003).
- [3] S. N. Varnakov, S. V. Komogortsev, J. Bartolomé, et al., *Phys. Met. Metallogr.* **106**, 51 (2008).
- [4] A. Gupta, D. Kumar, and V. Phatak, *Phys. Rev. B* **81**, 155402 (2010).
- [5] A.B. Drovosekov, D.I. Kholin, N.M. Kreines, et al. EASTMAG2010, Abstracts book, 289 (2010).

## Electronic phase transitions in nickel-oxide superlattices

A. V. Boris<sup>1</sup>, Y. Matiks<sup>1</sup>, E. Benckiser<sup>1</sup>, T. Prokscha<sup>2</sup>, E. Morenzoni<sup>2</sup>,  
G. Cristiani<sup>1</sup>, H.-U. Habermeier<sup>1</sup>, and B. Keimer<sup>1</sup>

<sup>1</sup>Max Planck Institute for Solid State Research, Heisenbergstrasse 1, D-70569 Stuttgart, Germany

<sup>2</sup>Laboratory for Muon Spin Spectroscopy, PSI, CH-5232 Villigen PSI, Switzerland

The competition between collective quantum phases in materials with strongly correlated electrons depends sensitively on the dimensionality of the electron system, which is difficult to control by standard solid-state chemistry. We have fabricated superlattices of the paramagnetic metal LaNiO<sub>3</sub> and the wide-gap insulator LaAlO<sub>3</sub> with atomically precise layer sequences. Using optical ellipsometry and low-energy muon spin rotation, superlattices with LaNiO<sub>3</sub> as thin as two unit cells are shown to undergo a sequence of collective metal-insulator and antiferromagnetic transitions as a function of decreasing temperature, whereas samples with thicker LaNiO<sub>3</sub> layers remain metallic and paramagnetic at all temperatures. Metal-oxide superlattices thus allow control of the dimensionality and collective phase behavior of correlated-electron systems [1].

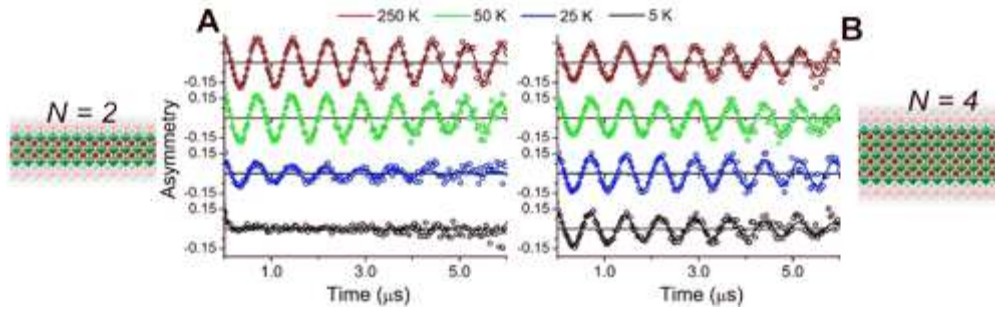


Fig. 1. Muon spin relaxation spectra in a weak transverse magnetic field of 100 G in the LaNiO<sub>3</sub> ( $N$  u.c.) | LaAlO<sub>3</sub> ( $N$  u.c.) superlattices with (A)  $N = 2$  and (B)  $N = 4$  on LaSrAlO<sub>4</sub> substrate.

We carried out low-energy muon spin rotation measurements using the  $\mu$ E4 beamline at the Paul Scherrer Institute, Switzerland, where positive muons with extremely reduced velocity can be implanted into specimens and brought to rest between the substrate and the LaAlO<sub>3</sub> capping layer. We used 100 G transverse field measurements to determine the fraction of muons,  $f_m$ , experiencing static local magnetic fields  $B_{loc} > B_{TF}$ . Fig. 1A indicates that the  $N = 2$  SL shows a transition from an entirely paramagnetic muon environment ( $f_m = 0$ ) to a nearly full volume of static internal fields, with a sharp onset at  $T_N = 50$  K. The continuous temperature dependence of  $f_m$  and the absence of thermal hysteresis indicate that the magnetic transition for the  $N = 2$  SLs is second-order. At the same time SLs with thicker LaNiO<sub>3</sub> layers remain paramagnetic down to the lowest temperatures, see Fig. 1B, as in bulk LaNiO<sub>3</sub>.

[1] A. V. Boris, Y. Matiks, E. Benckiser *et al.*, Science (in press).

# Magneto-photonic behaviour in 2D hexagonal patterns composed of 3d magnetic metals

E. Th. Papaioannou<sup>1</sup>, E. Melander<sup>1</sup>, E. Östman<sup>1</sup>, V. Kapaklis<sup>1</sup>, G. Ctistis<sup>2</sup>, P. Patoka<sup>3</sup>,  
M. Giersig<sup>3</sup> and B. Hjörvarsson<sup>1</sup>

<sup>1</sup>Department of Physics and Astronomy, Uppsala University, Box 516, 751 20 Uppsala, Sweden

<sup>2</sup>Complex Photonic Systems (COPS), MESA + Institute for Nanotechnology, University of Twente, 7500 AE, Enschede, The Netherlands

<sup>3</sup>Institut für Experimentalphysik, Freie Universität Berlin, 14195 Berlin, Germany

Magnetophotonics has become a flourishing field nowadays due to surprising effects in combining photonics structures with magnetic materials and magnetic field. Surface plasmons are usually studied for a metallic-dielectric system where the metal is highly conductive (Ag, Au, Al). For the case of highly absorbing magnetic metals (Fe, Co, Ni) the surface plasmons undergo a strong internal damping. However, recently, experimental and theoretical works have shown reveal the generation of surface plasmons in magnetic nanostructures and their influence to the enhancement of various magneto-optical surface effects.[1-2]

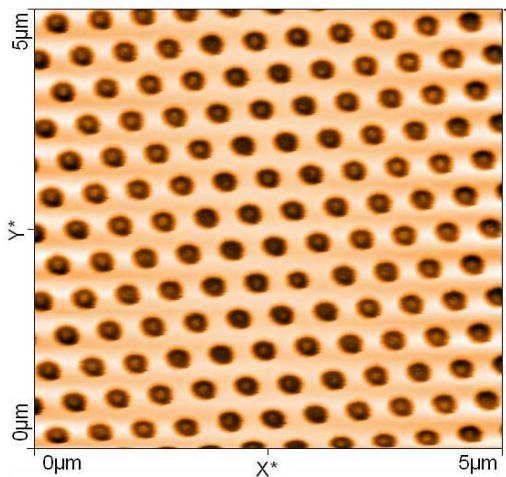


Fig. 1 Atomic force micrograph of a 100 nm-thick Ni film with hexagonal arrays of holes. The pitch size of the array is  $a = 470$  nm and the hole size is  $d = 275$  nm.

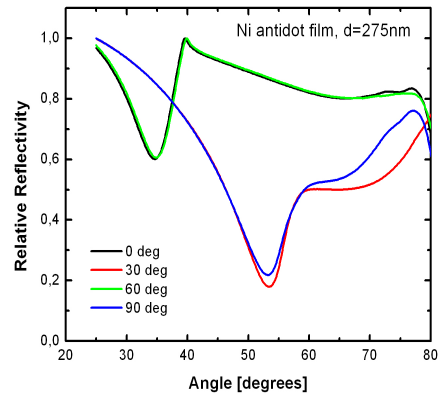


Fig. 2 Minima in Reflectivity spectra due to surface plasmons excitations as a function of angle of incidence and of symmetry direction of the hexagonal pattern of a Ni antidot film with  $a = 470$  nm and  $d = 275$  nm.

In this work we present optical and magneto-optical measurements of hexagonal arrays of circular holes of different diameters in thin films of the 3d magnetic metals. Drops in reflectivity and enhanced magneto-optical activity are reported in the cases of Co, Fe and Ni films which are closely connected with the existence of surface plasmons. How the propagation of surface plasmons is influenced by the 2D hexagonal symmetry of the patterns and by external magnetic field is revealed through magneto-diffraction measurements.

[1] E. Th. Papaioannou, V. Kapaklis, P. Patoka, M. Giersig, P. Fumagalli, A. Garcia-Martin, E. Ferreiro-Vila, G. Ctistis, Phys. Rev. B **81**, 054424 (2010).

[2] V.I. Belotelov, D.A. Bykov, L.L. Doskolovich, A. N. Kalish and A.K. Zvezdin, J. Opt. Soc. Am. B **26** (2009).

# Plasmon-enhanced near-field magneto-optical Kerr effects and related scanning microscopy via a linear nanoprobe

V. A. Kosobukin

*Ioffe Physical-Technical Institute, 194021, St. Petersburg, Russia*

Developed earlier was a theory of near-field magneto-optics [1] and scanning microscopy [2] with quasi-point probes. In conformity with the scheme of operated microscope [3], a single silver nanoparticle was a source of near field resulting in magneto-optical Kerr effects in scattering mode. Presently, a variety of linear plasmonic nano-objects is available, and treating the near-field magneto-optics with probes of this kind is topical [4].

This work reports on a theory of resonant near-field magneto-optical Kerr effects in elastic scattering of light and the related scanning nanoscopy using a linear nanoprobe. As a model, a cylinder and laterally non-uniform ultrathin magnetic layer embedded in a sample host are considered, the two entities being nearby the sample surface and parallel to it. The probe is thought of as a noble-metal nanowire or needle possessing long-lived local (surface) plasmons to enhance the magneto-optical effects. The problem of near-field Kerr-type magneto-optics is solved within the Green function technique [1, 2]. The plasmon-resonant dielectric polarization of the complex «probe+image» is treated self-consistently. The magneto-optical scatterings are studied for polar and longitudinal magnetizations. Since the planes of incidence and scattering of light coincide, classification of the scattering events in terms of TM ( $p$ -polarized) and TE ( $s$ -polarized) waves looks like that for conventional Kerr reflection. Scanning near-field microscopy is treated in varying the in-surface distance  $|X|$  between the probe (nanowire) and a laterally nano-sized magnetic domain. Polarization, angle and spectroscopy characteristics of the magneto-optical scatterings are found to be principally different for linear and point probes. In microscopy, the size of the domain «image» is estimated as  $w + h$  in terms of the lateral domain width  $w$  and the vertical probe-domain distance  $h$ . Figure 1 illustrates the efficiency of magneto-optical scatterings versus the scanning coordinate  $X$ , i.e. lateral distance between Ag cylinder and domain of width  $w = 10$  nm in ultrathin Co layer embedded in Au. The scattering is seen to be essentially enhanced at the plasmon resonance  $\hbar\omega = 3.55$  eV as compared with non-resonant excitation ( $\hbar\omega = 3.8$  eV). To conclude, the above ideas could be of general interest for nanophotonics of magnet/noble-metal composites and metamaterials.

The work was partly supported by the RFBR, grant No. 11-02-00304.

- [1] V. A. Kosobukin, Proc. SPIE **2535**, 9 (1995); Surf. Sci. **406**, 32 (1998).
- [2] V. A. Kosobukin, Proc. SPIE **3791**, 93 (1999).
- [3] T. J. Silva, S. Schultz and D. Weller, Appl. Phys. Lett. **65**, 658 (1994).
- [4] V. A. Kosobukin, Proc. SPIE **7996**, 79960F (2011).

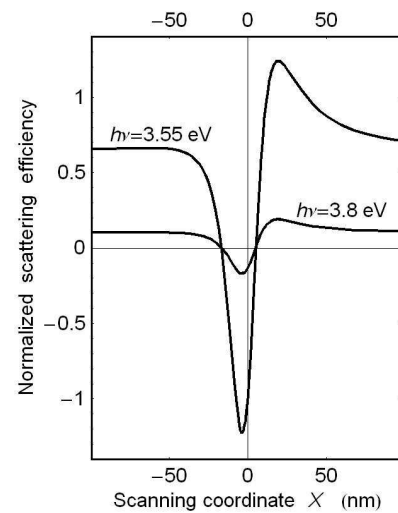


Fig. 1 Efficiency of magneto-optical scattering (near-field contrast) vs. lateral scanning coordinate  $X$  of Ag nanowire relative to a domain with width  $w = 10$  nm in Co layer embedded in Au host.

# Spin induced optical harmonic generation in the centrosymmetric semiconductors EuTe and EuSe

D. Brunne<sup>1</sup>, B. Kaminski<sup>1</sup>, M. Lafrentz<sup>1</sup>, R. V. Pisarev<sup>2</sup>, D. R. Yakovlev<sup>1</sup>, V. V. Pavlov<sup>2</sup>,  
A. B. Henriques<sup>3</sup>, G. Springholz<sup>4</sup>, G. Bauer<sup>4</sup>, E. Abramof<sup>5</sup>, P. H. O. Rapp<sup>5</sup>,  
and M. Bayer<sup>1</sup>

<sup>1</sup>Experimentelle Physik 2, Technische Universität Dortmund, D-44221 Dortmund, Germany

<sup>2</sup>Ioffe Physical-Technical Institute, Russian Academy of Sciences, 194021 St. Petersburg, Russia

<sup>3</sup>Instituto de Física, Universidade de São Paulo, 05315-970 São Paulo, SP, Brazil

<sup>4</sup>Institut für Halbleiter- und Festkörperphysik, Johannes Kepler Universität Linz, 4040 Linz, Austria

<sup>5</sup>LAS-INPE, 12227-010 São José dos Campos, SP, Brazil

The magnetic europium chalcogenide semiconductors EuTe and EuSe were investigated by the spectroscopy of second and third harmonic generation (SHG/THG) in the vicinity of the optical band gap [1-3]. In such materials with centrosymmetric crystal lattice the electric-dipole SHG process is symmetry forbidden so that no signal is observed in zero magnetic field. Signal appears, however, in applied magnetic field with the SHG intensity being proportional to the square of magnetization. The magnetic field and temperature dependencies of the induced SHG and THG allow us to introduce a type of nonlinear optical susceptibility determined by the magnetic-dipole contribution in combination with a spontaneous or induced magnetization. The experimental results can be described qualitatively by a phenomenological model.

In the metamagnetic semiconductor EuSe the SHG is strongly dependent on the different magnetic phases as shown in Fig. 1. This effect can clearly be attributed to the spinstructure in the magnetic phases.

Furthermore the results could be verified with THG spectroscopy. Since THG is allowed even in centrosymmetric structures it is a powerful tool to investigate the interference between the crystallographic and the spin contributions to the harmonic generation as shown in Fig. 2.

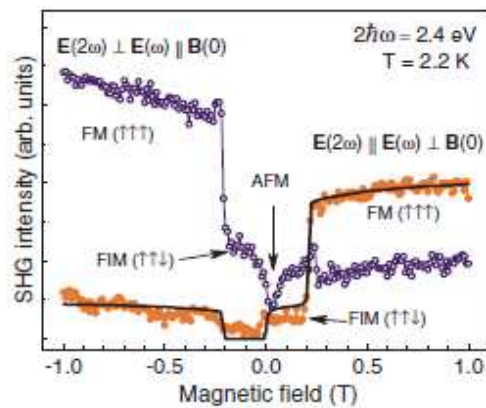


Fig. 1. SHG intensity as function of magnetic field strength at an energy of 2.4 eV in EuSe.

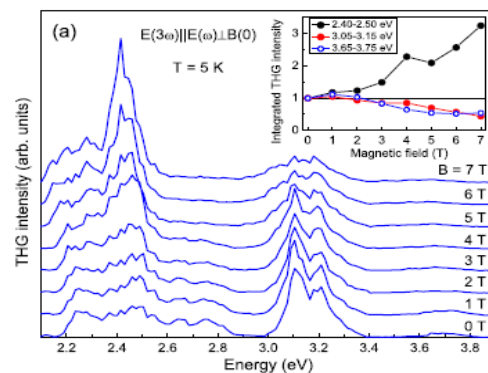


Fig. 2. THG intensity as function of magnetic field strength in EuTe.

- [1] B. Kaminski, et al., Phys. Rev. Lett. **103**, 057203 (2009).
- [2] M. Lafrentz, et al., Phys. Rev. B **82**, 235206 (2010).
- [3] B. Kaminski, et al., Phys. Rev. B **81**, 155201 (2010).



## Detection of buried layers in ferromagnetic metal films

M. Kostylev<sup>1</sup>, A. Stashkevich<sup>2</sup>, A. O. Adeyeye<sup>3</sup>

<sup>1</sup>*School of Physics, the University of Western Australia,  
35 Stirling Highway, Crawley 6009 WA, Australia*

<sup>2</sup>*LSPM CNRS (UPR 3407), Université Paris13, 93430 Villetaneuse, France*

<sup>3</sup>*Department of Electrical and Computer Engineering, National University of Singapore, Singapore*

It is generally accepted that microwave conductivity effects (CE) on spin wave dynamics in magnetic conducting samples *with thicknesses bellow the microwave magnetic skin depth* (sub skin depth samples (SSD)) are negligible. Indeed, the models established for insulating samples work extremely well for these samples [1]. However, it was recently shown that CE can have a profound effect on the excitation of microwave magnetic dynamics in SSD samples [2-4].

In this work we discuss the effect of sample conductivity on the microwave magnetic dynamics. More specifically, we have made use of the influence of the eddy current induced inhomogeneity of the exciting microwave field, produced by a micro-strip antenna, on the excitation efficiency for higher spin-wave modes. Typically it is supposed that the spin wave *dispersion* is practically unaffected by CE, in agreement with previous treatments [4]. This is the main reason, why usually results of investigation of thermal magnons using Brillouin light scattering technique (BLS) are in excellent agreement with the theories for insulators [1]. However, as it has been shown in Ref.5, any symmetry breaking in the distribution of the structure's magnetic properties in the direction normal to its plane will invariably lead to a characteristic asymmetry in the spin wave spectra, with respect to the inversion of the direction of the spin wave propagation. In terms of the BLS spectroscopy this means an asymmetry in the frequencies of the Stokes and Anti-Stokes spectral lines. That is why, to make our conclusions more reliable, we have used the BLS spectroscopy as a complementary means of characterization.

In this talk, we have demonstrated the efficiency of the broadband microstrip FMR technique for detection and characterization of a hidden magnetic inhomogeneity in a film sample. Based on the nonreciprocity of the microstrip FMR response with respect to the direction of penetration of the exciting microwave field in the sample, it is especially effective in the case when the hidden layer breaks the symmetry of the ferromagnetic structure. In the particular case of a 100 nm thick Permalloy film, an additional magnetically depleted top sublayer has been detected and characterized. These results have been confirmed by BLS spectroscopy revealing, surprisingly, the fact that the optical properties of the additional sublayer do not differ much from those of the bulk of the film. In a broader context, the proposed technique can be regarded as a nondestructive express method to detect the presence of magnetic inhomogeneity in conducting ferromagnetic films.

[1] K. Yu. Guslienko et al. *Phys.Rev.B* **66**, 132402 (2002).

[2] M. Kostylev, *J. Appl. Phys.*, **106**, 04390 (2009); M.Kostylev et al., *J. Appl. Phys.* **108**, 103914 (2010); Y.V. Khivintsev et al., *J. Appl. Phys.* **108**, 023907 (2010);

[3] K.J. Kennewell et al., *J. Appl. Phys.* **108**, 073917 (2010).

[4] N.S.Almeida and D.L.Mills, *Phys. Rev.B* **53**, 12232 (1996).

[5] M. Vohl, P. Barnas, and J. Grünberg, *Phys. Rev.B* **39**, 12003 (1989).

## Magnetic fluctuations as the reason of the metal-insulator transition in magnetic semiconductors

E. Z. Meilikhov, R. M. Farzetdinova  
*Kurchatov Institute, 123182, Moscow, Russia*

The role of large-scale fluctuations of the electric potential in traditional (*non-magnetic*) doped semiconductors is well known. Such a fluctuating potential appears usually in highly-compensated semiconductors where concentrations of charged impurities (donors and acceptors) are high and the concentration of screening mobile charge carriers is low, that results in a large screening length, defining the spatial scale of electric potential fluctuations. In that case, the average amplitude of the fluctuation potential is also high that leads to the localization of charge carriers and results in the activation character of the system conductivity: it is controlled by the thermal activation of charge carriers from the Fermi level to the percolation level and falls down exponentially with lowering temperature. In the absence of the impurity compensation, the charge carrier concentration is so high that any perturbations of the electro-static nature are effectively screened, and the spatial scale of the potential coincides with the extent of impurity density fluctuations. The depth of such a short-scale potential relief is relatively shallow and does not lead to the charge carrier localization – the conductivity keeps being a metal one.

In diluted (but nevertheless, highly-doped) *magnetic* semiconductors (of  $\text{Ga}_{1-x}\text{Mn}_x\text{As}$  type), in addition to above mentioned fluctuations of the electric potential, the new perturbation source appears - specifically, fluctuations of the “magnetic potential” concerned with fluctuations of the local magnetization in such a semiconductor. That potential is, in fact, the potential of the exchange interaction of mobile charge carriers with magnetic impurities (for instance, via the RRKKY mechanism) which fluctuates in accordance with fluctuations of the concentration and the local magnetization of those impurities. Within the “wells” of the magnetic potential, mobile charge carriers with a certain spin direction are accumulated while the carriers of the opposite spin direction are pushed out. The spatial scale  $l$  of magnetic fluctuations is now determined not by the electrostatic screening but by the characteristic length of the magnetic interaction of impurities and the correlation length of their arrangement in the semiconductor bulk. However, in diluted magnetic semiconductors, there is usually  $l \sim l_s$  and, thus, spatial scales of the magnetic (exchange) and Coulomb potentials agree closely. That means the constructive superposition of both reliefs, and so the average total amplitude of the potential relief becomes to be higher. The medium arises where the concentration and the spin polarization of charge carriers are strongly non-uniform, and the degree of that non-uniformity is substantially defined by the local magnetization of the system. Increasing magnetization with lowering temperature promotes strengthening the spatial localization of charge carriers and in a number of cases could stimulate the metal-insulator transition. Percolative metal conductivity, characteristic for non-uniform systems, changes into the conductivity of the activation type. That occurs when under some external factors (such as temperature, magnetic field, etc.) the Fermi level falls below the percolation level. One of possible mechanisms is as follows. The fluctuating potential leads to appearing the density of states tail into which both the percolation and Fermi levels are pulled. Rates of those levels' movement are different, and if they change the relative position the metal-insulator transition occurs. It is just the model that is investigated in the present work.

# Magnetic phases of the frustrated $S=1/2$ chain compound $\text{LiCuVO}_4$

L. A. Prozorova, A. I Smirnov, L. E. Svistov

*P. L. Kapitza Institute for Physical Problems RAS, Moscow, Russia*

N. Büettgen, H.-A. Krug von Nidda, W. Kraetschmer  
*Center for Electronic Correlations and Magnetism EKM,  
Experimentalphysik V, Universität Augsburg, Germany*

T. Fujita, M. Hagiwara, Z. Honda, S. Kimura, K. Omura, H. Yamaguchi  
*KYOKUGEN, Osaka University, Japan*

A. Prokofiev

*Institut für Festkörperphysik Technische Universität Wien, Austria*

Unconventional magnetic orders and phases in frustrated quantum spin chains are attractive issues, because they appear under a fine balance of the exchange interactions and are sometimes caused by much weaker interactions or fluctuations. A kind of frustration in quasi-one-dimensional chain magnet  $\text{LiCuVO}_4$  is provided by competing interactions when the intra-chain nearest neighbor exchange is ferromagnetic and the next nearest neighbor exchange is antiferromagnetic. Theoretical investigations of frustrated one dimensional model with the exchange parameters of  $\text{LiCuVO}_4$  have predicted a set of exotic phases in a magnetic field such as vector chiral, spin density wave and nematic phases<sup>1,2,3</sup>. The order parameters of these phases are the quadratic forms of components of neighbor spins.

We discuss the experimental investigation of low temperature magnetic phases of  $\text{LiCuVO}_4$  and compare these phases with those obtained theoretically in frame of different models. For the field range less than 10 T the magnetic properties of  $\text{LiCuVO}_4$  were studied with ESR and NMR spectroscopy<sup>4,5</sup>. For the fields below 7 T the planar spiral spin structure is realized. At  $H \sim 7$  T the transition to spin-modulated phase was observed. In this phase the ordered component of spins is parallel to static field and its value changes along the chain. The low field magnetic phases are long range ordered and are characterized by magnetic correlations, similar to that of 1D theory.

To study high field magnetic phases were studied the magnetization of  $\text{LiCuVO}_4$  compound up to saturation field ( $\sim 50$ T) with pulse technique<sup>6</sup>. Besides the transition from the planar spiral to spin modulated structure an additional transition was observed just below the saturated field. This high field magnetic phase is considered as a spin nematic phase, which was predicted theoretically not only for 1D model, but also in frame of more realistic quasi 2-dimensional model in Ref. 7. For the nematic phase the ordered spin components should be zero, and a correlator of transversal components of neighboring spins is an order parameter. The critical fields and the slope of magnetization in this phase are in a good agreement with calculated one.

[1] T. Hikihara, L. Kecke, T. Momoi, A. Furusaki, Phys. Rev. B **78**, 144404(2008).

[2] J. Sudan, A. Lüscher, A. M. Läuchli, Phys. Rev. B **80**, 140402(R) (2009).

[3] F. Heidrich-Meisner, I. P. McCulloch, A. K. Kolezhuk, Phys. Rev. B **80**, 144417 (2009).

[4] N. Büettgen, H.-A. Krug von Nidda, L.E. Svistov, L.A. Prozorova, A. Prokofiev, W. Assmus, Phys. Rev. B **76**, 014440 (2007).

[5] N. Büttgen, W. Kraetschmer, L. E. Svistov, L. A. Prozorova, and A. Prokofiev, Phys. Rev. B **81**, 052403 (2010).

[6] L.E. Svistov, T. Fujita, H. Yamaguchi, S. Kimura, K. Omura, A. Prokofiev, A.I. Smirnov, Z. Honda, M. Hagiwara, JETP Lett. **93**, 21 (2011).

[7] M. E. Zhitomirsky and H. Tsunetsugu, Europhys. Lett. **92**, 37001 (2011).

# Spin-fluctuation-mediated superconductivity in iron arsenides: complementary thermodynamics and optical studies

A. Charnukha, O. V. Dolgov, A. N. Yaresko, C. T. Lin, B. Keimer, and A. V. Boris  
*Max Planck Institute for Solid State Research, Heisenbergstrasse 1, D-70569 Stuttgart, Germany*

Interplay between spin fluctuations and superconducting pairing is a challenge to our current understanding of the origin of the remarkably high critical temperature in superconductors near magnetic phases. We report specific heat and full complex dielectric function measurements on high-purity  $\text{Ba}_{0.68}\text{K}_{0.32}\text{Fe}_2\text{As}_2$  single crystals with  $T_c = 38.5$  K [1,2]. We discuss the microscopic origin of superconductivity-induced electronic specific heat,  $C_p$ , and infrared optical anomalies in the framework of a multiband Eliashberg theory with two distinct superconducting gap energies  $2\Delta_A \approx 6 k_B T_c$  and  $2\Delta_B \approx 2.2 k_B T_c$ . The observed unusual suppression of the optical conductivity in the superconducting state at energies up to  $14 k_B T_c$  can be ascribed to spin-fluctuation-assisted processes in the clean limit of the strong-coupling regime.

We critically examine that the superconducting state of the iron pnictides appears to fit reasonably well into a BCS framework in which phonons are replaced by spin fluctuations. We observe, however, a superconductivity-induced suppression of an absorption band at an energy of 2.5 eV, two orders of magnitude above the superconducting gap energy [3]. Based on density-functional calculations, this band is assigned to transitions from As-p to Fe-d orbitals crossing the Fermi surface. The optical anomaly we observed can be explained as a consequence of non-conservation of the total number of unoccupied states involved in the corresponding optical transitions due to the opening of the superconducting gaps and redistribution of the occupation of the different bands below  $T_c$ . It requires a lowering of the material's chemical potential in the superconducting state, which can potentially enhance superconductivity in iron-pnictides. However, even a generalization of the standard BCS theory to the multiband case does not take into account this effect. Therefore, self-consistent treatment of a variable chemical potential at the superconducting transition is needed.

We identify a related effect at the spin-density-wave transition in parent compounds of the 122 family. Interactions of electrons in different energy bands at the Fermi level may provide a common framework for an explanation of the optical anomalies in the SDW and superconducting compounds. It is important to note that these anomalies affect only a small fraction of the interband transitions, which involve initial states of As p-orbital character deep below the Fermi level. This indicates that these orbitals significantly influence electronic instabilities in the iron arsenides, possibly due to the high polarizability of the As-Fe bonds.

[1] P. Popovich *et al.*, Phys. Rev. Lett. **105**, 027003 (2010).

[2] A. Charnukha *et al.*, Preprint: arXiv:1103.0938 (2011).

[3] A. Charnukha *et al.*, Nature Communications **2**, 219 (2011).

## Spin waves in cubic helimagnets

S. V. Maleyev

*Petersburg Nuclear Physics Institute, 188300, Gatchina, Russia*

In this report we discuss the B20 helimagnets (MnSi, FeGe, etc). In them the Dzyaloshinskii-Moriya interaction (DMI) leads to the spin-wave mixture with momenta  $\vec{q}$  and  $\vec{q} \pm n\vec{k}$  where  $\vec{k}$  is the helix wave-vector and  $n = 1, 2, \dots$ . As a result the spin-wave spectrum displays strong anisotropy at  $q \ll k$ .  $\varepsilon_{\vec{q}} = (Aq_{\parallel}^2 + 3Aq_{\perp}^4/8 + \Delta^2 - 3H_{\perp}^2/8)^{1/2}$ , where  $\parallel, \perp$  denote vector components along and perpendicular to  $\vec{k}$  respectively and  $\Delta$  is the spin-wave gap which appears due to the spin-wave interaction. At  $q > k$  we have  $\varepsilon_{\vec{q}} = Aq(q^2 + k^2)^{1/2}$ . It is shown also, that  $H_{\perp}$  dependence of the spin-wave energy appears due to similar  $(q, k)$  mixing in perpendicular field.

The so-called A-phase is the most striking phenomenon observed in B20 magnets. In this state just below  $T_c$  the helix vector rotates perpendicular to the field and then with increasing of  $T$  returns to initial direction along the field. From above expression for  $\varepsilon_{\vec{q}}$  we see that the perpendicular state becomes instable at  $H > H_{A2} = \Delta\sqrt{8/3}$ . It is the upper bound of the A-phase state. The lower boundary is a result of the infra-red divergences (IRD) at  $H_{\perp} \rightarrow H_{A2}$  which appear in the  $1/S$  expansion for the magnetic energy due to very soft spin-wave spectrum at  $q < k$ . In fact the A-phase has to be at all  $T > Ak^2$  but it is very narrow and can be observed just below  $T_c$  due to critical slowing down. Rather rough estimations are in agreement with existing experimental results.

From the above results we conclude that the field behaviour of the multiferroics with the DMI could be understood if one takes into account the field induced spin-wave mixing which has to appear in the field directed in the plain of the spin rotation.

## **$Z_2$ -vortex unbinding transition for two-dimensional frustrated antiferromagnets**

A. N. Ignatenko

*Institute of Metal Physics, 620990, Ekaterinburg, Russia*

Two-dimensional frustrated Heisenberg antiferromagnet with non-collinearly ordered ground state at finite temperature is known to have transition related to the decay of vortex pairs [1]. In contrast to the famous Berezinsky-Kosterlitz-Thouless (BKT) phase transition, which appears in systems with abelian XY-like symmetry, in the present case even without vortices magnetic fluctuations are so strong that they not only destroy magnetic order, which is in accordance with Mermin-Wagner theorem, but also produce finite correlation length at any finite temperature and the phenomenon of quasi-long range order does not occur.

In this contribution the influence of magnetic classical and quantum fluctuations on the vortex subsystem is studied. If one simply neglects fluctuations by considering vortices inserted at some points into ideally ordered background, one obtains an ensemble of point particles equivalent to classical Coulomb plasma in two dimensions. In this picture long-range logarithmic potential at low temperatures is able to bind *all* vortices into pairs (dipoles); the latter begin to dissolve only at Kosterlitz-Thouless temperature. Therefore neglect of fluctuations leads to usual BKT phase transition.

It is shown that magnetic fluctuations exponentially screen the interaction between vortices at distances  $r \gg \xi$  ( $\xi$  is correlation length). Correspondingly the energy of one vortex which is equal to half the energy of infinitely large pair is finite. Hence even at arbitrary small temperatures not all vortices are bound into pairs, and there exist finite, but exponentially small, density of free  $Z_2$  – vortices. Therefore there is no principal difference between low and high temperature regimes: at high temperatures density of vortices is simply much larger than at low temperatures. *Thereby the process of dissociation of  $Z_2$  – vortex dipoles is a crossover and not a phase transition.*

In the renormalized classical region ( $T$  is low in comparison with ground state spin stiffness) this crossover is sufficiently narrow due to exponentially large correlation length  $\xi \sim \exp(1/T)$ . At distances  $1/T \ll r \ll \xi$  the repulsive double logarithmic interaction  $-T \log(r)^2$ , which is induced by fluctuations in addition to bare attractive logarithmic potential  $\log(r)$ , leads to substantial reduction of the crossover temperature. Under the enhancement of frustration, when the system is approached to quantum phase transition into spin liquid ground state, the crossover is smeared by quantum fluctuations.

Backward influence of  $Z_2$  – vortices on the spin fluctuations (spin correlation functions), in particular the possibility of vortex mechanism of spinon's confinement, is also discussed.

[1] H. Kawamura and S. Miyashita, J. Phys. Soc. Japan **53**, 9 (1984); **53**, 4138 (1984).

## Electron spin resonance in $\text{Ba}_3\text{Cr}_2\text{O}_8$

T. P. Gavrilova<sup>1</sup>, R. M. Eremina<sup>1</sup>, J. Deisenhofer<sup>2</sup>, A. Loidl<sup>2</sup>

<sup>1</sup> *Zavoisky Physical -Technical Institute, 420029, Sibirsky tract, 10/7, Kazan Russia*

<sup>2</sup> *Institute for Physics, Augsburg University, D-86135 Augsburg, Germany*

Very recently, a new family of dimerized antiferromagnet, namely  $\text{A}_3\text{M}_2\text{O}_8$  ( $\text{A}=\text{Ba}, \text{Sr}$   $\text{M}=\text{Mn}, \text{Cr}$ ), has shown Bose-Einstein condensation of magnons ( $H_c = 12.5$  T for  $\text{Ba}_3\text{Cr}_2\text{O}_8$  [1]). The systems also uniquely show the presence of dimerized  $\text{MO}_4^{3-}$  tetrahedra with an M ion in the unusual 5+ oxidation state and the presence of competing exchange interactions, since the dimers are arranged in a triangular lattice presenting a high degree of geometrical frustration. The fitting of the temperature dependence of the magnetic susceptibility in  $\text{Ba}_3\text{Cr}_2\text{O}_8$  by modified Bleaney-Bowers equation with interdimer interactions confirmed the formation of a spin-singlet ground state at low temperature and allowed to determine the intradimer isotropic exchange interaction  $J^{\text{is}}=27.3$  K [2]. All these interesting facts stimulated

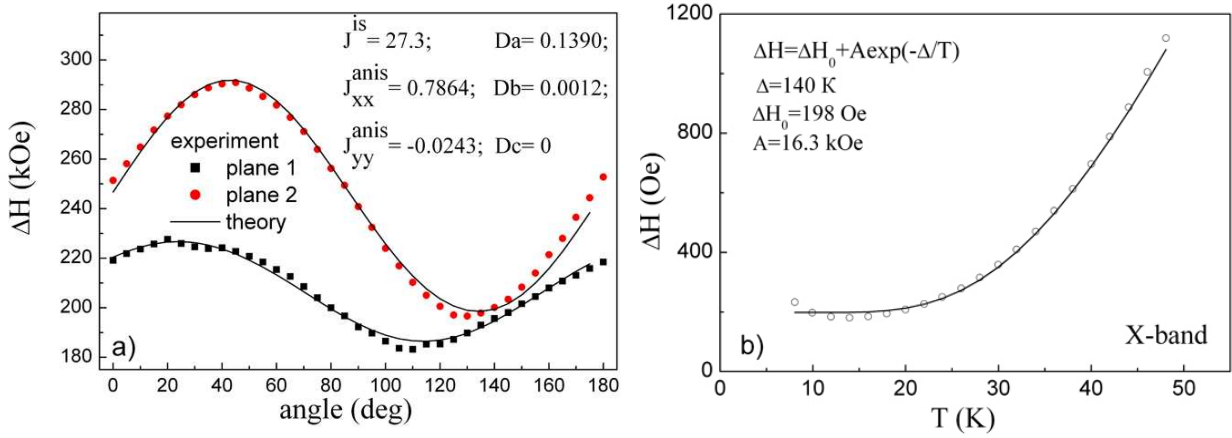


Fig.1. a) Angular dependencies of ESR linewidth in  $\text{Ba}_3\text{Cr}_2\text{O}_8$  in X-band at  $T=12$  K; b) Temperature dependence of the ESR linewidth in X-band frequency.

our study of  $\text{Ba}_3\text{Cr}_2\text{O}_8$  single crystals by the ESR method. ESR measurements were performed at X-band (9.47 GHz) frequency in the temperature range  $4.2 < T < 300$  K. The ESR spectrum consists of one Lorentzian-shaped line with  $g \sim 2$ . The experimental angular dependencies of  $g$ -factors and ESR linewidths in two different planes are presented in Fig.1. Black curves correspond to the theoretical calculations. It was necessary to take into consideration the intradimer symmetric and antisymmetric anisotropic exchange interaction to fit the experimental data. The presence of DM interaction was confirmed also by high-frequency ESR measurement [3].

The temperature dependence of the ESR linewidth is presented in Fig.1 c. As shown in Fig.1 c, the linewidth increases with increasing temperature from 200 Oe at 10K up to about 1100 Oe at 50K. The intensity of the ESR signals becomes very low at the temperature above 70 K, so the lines are not detected at the highest temperatures. The exponential increase of the ESR linewidth indicates that the relaxation of the excited spin occurs via an Orbach process.

We acknowledge partial support by the program UMNiK 8765r/11225.

[1] A. Aczel, H. Dabkowska, G. Luke, *et al.*, Comm. APS, March-Meet. Abst.: **32**, 00013 (2008).

[2] T. Nakajima, H. Mitamura, and Yu. Ueda, *JPSJ* **75**, 054706 (2006).

[3] M. Kofu, H. Ueda, H. Nojiri, *et al.*, *PRL* **102**, 177204 (2009).

## **Breaking the spin waves: spinons in $\text{Cs}_2\text{CuCl}_4$**

Oleg A. Starykh

*University of Utah, UT 84112, Salt Lake City, USA*

Modern investigations in quantum magnetism are driven by a relentless search for exotic disordered spin-liquid ground states. I describe several recent advances in this field focusing on materials with spatially anisotropic triangular structure. I show that the excitation spectrum in these magnets is composed of incoherent continuum, arising from the one-dimensional spinons of individual spin chains, and a sharp dispersing peak, due to coherently propagating ‘triplon’, an  $S = 1$  bound states of two spinons. I present a direct and parameter-free comparison of the calculated dynamical spin correlations with inelastic neutron measurements on  $\text{Cs}_2\text{CuCl}_4$ . I also describe crucial role of small residual interactions, primarily inter-layer exchange and several symmetry-allowed Dzyaloshinskii-Moriya interactions (DMI), in selecting the low-temperature ordered states.

I conclude by presenting an analogy between the system of critical spinons subject to uniform DMI and that of electrons in quantum wires subject to spin-orbit interaction of Rashba type. I show that this analogy provides a straightforward explanation of the recent ESR experiments in the paramagnetic phase of  $\text{Cs}_2\text{CuCl}_4$ .



# ESR modes in the spin-liquid phase of a two-dimensional frustrated quantum antiferromagnet $\text{Cs}_2\text{CuCl}_4$

K. Yu. Povarov<sup>1</sup>, A. I. Smirnov<sup>1,2</sup>, O. A. Starykh<sup>3</sup>, S. V. Petrov<sup>1</sup>, A. Ya. Shapiro<sup>4</sup>

<sup>1</sup>*P. L. Kapitza Institute for Physical Problems, RAS, 119334 Moscow, Russia*

<sup>2</sup>*Moscow Institute for Physics and Technology, 141700, Dolgoprudny, Russia*

<sup>3</sup>*Department of Physics and Astronomy, University of Utah, Salt Lake City, Utah 84112, USA*

<sup>4</sup>*A.V.Shubnikov Institute of Crystallography, RAS, 119333 Moscow, Russia*

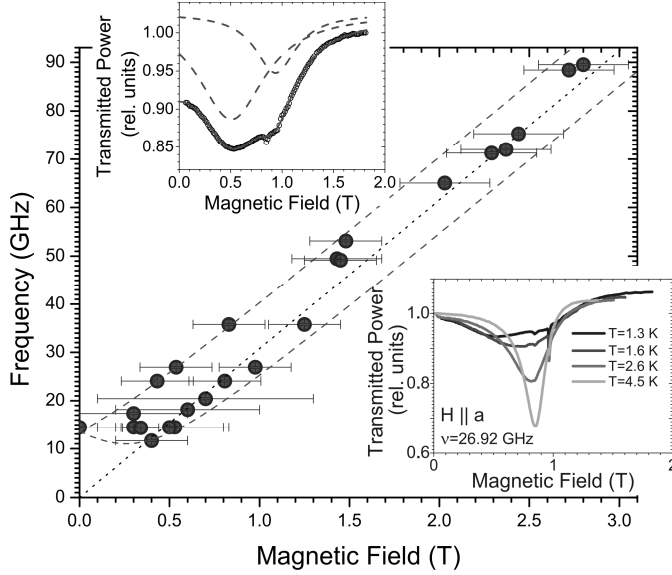


Fig. 1. Frequency-field dependence at  $T=1.3$  K and  $\mathbf{H}\parallel\mathbf{a}$ . Dotted line is a para-magnetic resonance at  $T=10$  K, dashed line presents

presence of the *uniform* Dzyaloshinskii-Moriya interaction (DMI) [3]. This kind of DMI, which represents a distinct feature of  $\text{Cs}_2\text{CuCl}_4$ , the DM vector is oriented in a unique direction for all pairs of spins within a chain. In the molecular field approximation the uniform DMI results in a spiral spin structure with the wavevector of order  $q_{\text{DM}}\sim D/J$ . In case of a spin  $S=1/2$  chain, which has critical ground state, such a DMI results in a shift of the spinon continuum by the value of  $q_{\text{DM}}$ , giving rise to two ESR frequencies, which represent upper and lower boundaries of the continuum transposed to zero wavevector by the DMI [3]. Such a transformation of the spin excitations spectrum implies a specific polarization dependence of the ESR absorption at  $H=0$ , with a maximum at the microwave field perpendicular to DMI vector, i.e. at  $\mathbf{h}\parallel\mathbf{b}$ . Precisely such polarization dependence was indeed observed at a frequency of 14 GHz. Using theoretical predictions of [3], we estimate the components of the DMI vector to be  $D_a/(4\hbar)=8\pm 2$  and  $D_c/(4\hbar)=11\pm 2$  GHz, correspondingly.

[1] O. A. Starykh, H. Katsura, L. Balents, Phys. Rev. B **82**, 014421 (2010).

[2] D. C. Dender et al., Phys. Rev. Lett. **79**, 1750 (1997).□

[3] S. Gangadharaiah, J. Sun, O. A. Starykh, Phys. Rev. B **78**, 054436 (2008).

We report new effects in the low frequency spin dynamics of  $S=1/2$  antiferromagnet  $\text{Cs}_2\text{CuCl}_4$ . This spin system realizes distorted triangular lattice, with spin chains effectively decoupled because of frustration [1]. In a correlated state, below the Curie-Weiss temperature  $\Theta_{\text{CW}}=4$  K and above the ordering temperature  $T_N=0.62$  K, we observe a shift of ESR frequency, developing with cooling. Besides, in a magnetic field  $\mathbf{H}\parallel\mathbf{a}$ ,  $\mathbf{H}\parallel\mathbf{c}$ , we observe a splitting of ESR in two lines, also emerging with cooling. At  $T=1.3$  K the effective gap in the magnetic resonance spectrum is 14 GHz, and the splitting reaches 10 GHz. These findings are quite unusual for  $S=1/2$  magnet in a paramagnetic phase, nevertheless, they are naturally described by a consideration of the spectrum of spinons in  $S=1/2$  spin chain [2] in

# Low-temperature thermodynamics of frustrated classical spin chain near the critical point

V. Ya. Krivnov and D. V. Dmitriev

*Institute of Biochemical Physics of RAS, Kosygin str.4, Moscow, Russia*

Last year much attention has been paid to the 1D  $J_1$ - $J_2$  Heisenberg model that exhibit frustration. Its Hamiltonian has a form

$$H = J_1 \sum S_n S_{n+1} + J_2 \sum S_n S_{n+2} \quad (1)$$

where  $J_1 < 0$  is the ferromagnetic (NN) coupling while  $J_2 > 0$  is the antiferromagnetic (NNN) interaction. This model is basic one for the description of magnetic properties of recently synthesized edge-shared cuprate chain compounds. The model is characterized by the frustration parameter  $\alpha = J_1/|J_1|/J_2$ . The ground state of the model is ferromagnetic for  $\alpha < 1/4$ . At the critical point  $\alpha = \alpha_c = 1/4$  the ground state phase transition to the incommensurate singlet phase with helical spin correlations takes place. Remarkably, this transition point does not depend on a spin value, including the classical limit  $s = \infty$ . The important question related to this model is the influence of the frustration on the low-temperature thermodynamics near the transition point because there are several edge-shared cuprates with  $\alpha \approx 1/4$  which are of particular interest. At present the low temperature thermodynamics of quantum  $s=1/2$  model (1) can be studied only either by using of numerical calculations of finite chains or by approximate methods. In this work this problem is studied for the classical version of (1) for which exact thermodynamics at  $T \rightarrow 0$  can be obtained. It is expected that main qualitative features of the quantum low-temperature thermodynamics can be reproduced correctly in the framework of the classical model.

The calculation of the partition and spin correlation functions is reduced to quantum mechanics problem of a particle in a potential well. It is shown that exactly in a the transition point the correlation length  $l$  behaves at  $T \rightarrow 0$  as  $T^{-1/3}$  and zero field susceptibility  $\chi$  diverges as  $T^{-4/3}$  in contrast with the Heisenberg ferromagnet ( $\alpha=0$ ) where  $l \sim T^{-1}$  and  $\chi \sim T^{-2}$ . Corresponding numerical factors for  $l$  and  $\chi$  are found. We compare these results with those obtained by modified spin wave method.

The behavior of the low-temperature susceptibility in the helical phase at  $\alpha \gg \alpha_c$  is studied. The main feature of this behavior in the limit  $T \rightarrow 0$  and  $\delta = (\alpha - \alpha_c) \rightarrow 0$  with  $t = T/\delta^{3/2}$  fixed is the universal dependence of the scaling variable  $t$ . In particular,  $\chi(T)$  has a maximum at  $T_m \sim \delta^{3/2}$  and  $\chi_m \sim \delta^2$ . The obtained dependence  $\chi(T)$  is in qualitative agreement with that observed in edge-shared cuprates with  $\alpha$  close to  $\alpha_c$ . The dependencies of  $T_m$  and  $\chi_m$  on  $\alpha$  are also in accord with the experimental observations. The static structure factor  $S(k)$  has the maximum at  $k = k_m(T)$ .  $k_m$  vanishes at  $t = t_c$  and the value  $t_c$  determines the Lifshitz boundary on  $(T, \delta)$  plane, separating the ferromagnetic and the helical phases. The vanishing of  $k_m$  on the Lifshitz boundary is characterized by the critical index  $1/2$ .

# Properties of kagome lattice in $\text{ZnCu}_3(\text{OH})_6\text{Cl}_2$

V. R. Shaginyan

*Petersburg Nuclear Physics Institute, Gatchina, 188300, Russia*

Strongly correlated Fermi systems are among the most intriguing and fundamental systems in physics, whose realization in some compounds is still to be discovered. We show that the kagome lattice of  $\text{ZnCu}_3(\text{OH})_6\text{Cl}_2$  can be viewed as a strongly correlated Fermi system whose thermodynamic is defined by quantum critical spin liquid located at the fermion condensation quantum phase transition (FCQPT) [1]. For the first time we calculate the susceptibility, magnetization and specific heat  $C$  as functions of temperature  $T$  versus magnetic field  $B$ . Our calculations are in good agreement with the experimental facts and their scaling behavior coincides with that observed in heavy-fermion (HF) metals and  $2\text{D } ^3\text{He}$ . We have also demonstrated that  $\text{ZnCu}_3(\text{OH})_6\text{Cl}_2$  exhibits the Landau-Fermi liquid, non-Fermi liquid and transition behavior as HF metals and  $^3\text{He}$  do.

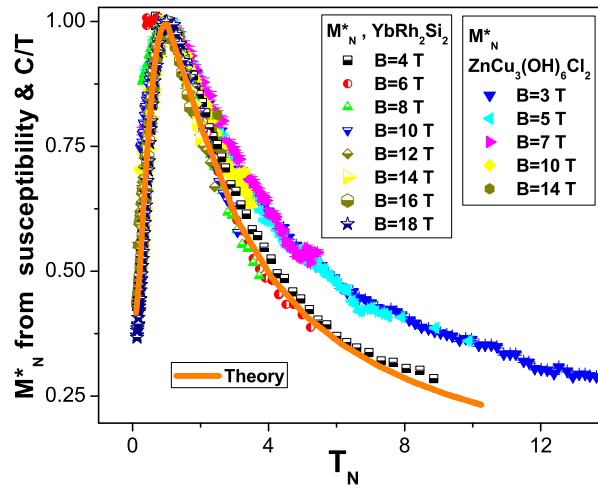


Fig. 1

Strongly correlated behavior of  $\text{ZnCu}_3(\text{OH})_6\text{Cl}_2$  can be illuminated by comparing with that of  $\text{YbRh}_2\text{Si}_2$  as it is shown in Fig. 1. It is convenient to introduce the normalized effective mass  $M^*_N$  and the normalized temperature  $T_N$  dividing the effective mass  $M^*$  by its maximal values,  $M^*_M$ , and temperature  $T$  by  $T_M$  at which the maximum occurs [1]. Then, we can compare the behavior of the susceptibility proportional to  $M^*$  measured on  $\text{ZnCu}_3(\text{OH})_6\text{Cl}_2$  in magnetic fields  $B$  [2] with  $C/T$  proportional to  $M^*$  obtained on  $\text{YbRh}_2\text{Si}_2$  in magnetic fields  $B$  [3] representing  $M^*$  as the normalized effective mass  $M^*_N = M^*/M^*_M$  versus the normalized temperature  $T_N = T/T_M$ . In Fig. 1, the corresponding fields  $B$  are listed in the legends. Our calculations shown by the solid curve that traces the scaling behavior of  $M^*_N$  located at FCQPT [1,4] are in good agreement with the experimental facts.

- [1] V.R. Shaginyan, M.Ya. Amusia, A.Z. Msezane, and K.G. Popov, *Phys. Rep.* **492**, 31 (2010).
- [2] J.S. Helton *et al.*, *Phys. Rev. Lett.* **104**, 147201 (2010).
- [3] P. Gegenwart *et al.*, *New J. Phys.* **8**, 171 (2006).
- [4] V. R. Shaginyan *et al.*, *Europhys. Lett.* **93**, 17008 (2011).

## Magnetic resonance in CeB<sub>6</sub> and ferromagnetic correlations

S. V. Demishev<sup>1</sup>, A. V. Semeno<sup>1</sup>, A. V. Bogach<sup>1</sup>, T. V. Ishchenko<sup>1</sup>, V. B. Filipov<sup>2</sup>,  
N. Yu. Shitsevalova<sup>2</sup> and N. E. Sluchanko<sup>1</sup>

<sup>1</sup>A.M.Prokhorov General Physics Institute of RAS, 119991, Moscow, Russia,

<sup>2</sup>Institute for Problems of Materials Science of NASU, 03680, Kiev, Ukraine

Studying of the magnetic resonance in strongly correlated metals, dense Kondo systems and heavy fermion materials has recently attracted much attention [1-3]. Although strong spin fluctuations in these systems seem to destroy magnetic resonance, it was shown theoretically that this difficulty may be overcome by ferromagnetic correlations [1-2]. However the magnetic resonance in the co-called antiferro-quadrupole phase (phase II) of CeB<sub>6</sub> has been observed [4], whereas this material is supposed to be an archetypical dense Kondo system with orbital ordering, which is governed by the *antiferromagnetic* interactions. In the present

work we have applied new technique of absolute measurements of the high frequency (60-100 GHz) ESR in strongly correlated metals [5,6], which allows finding full set of the spectroscopic parameters including g-factor, line width and oscillating magnetisation. It is found that approaching to the phase II-paramagnetic phase transition temperature  $T_{I-II}$  results in strong broadening of the resonance (the line width increases 3 times in the range  $1.8 \leq T \leq 3.8$  K) whereas g-factor  $g = 1.59$  remains temperature independent. Magnetic resonance data suggests that the magnetization of CeB<sub>6</sub> in the phase II consists of several contributions, one of which is responsible for the observed magnetic resonance (fig. 1). This term in magnetization is missing in the paramagnetic phase and corresponds to ferromagnetically interacting

localized magnetic moments. The magnitude of the oscillating part of magnetization is less than total magnetization in the range  $T^* < T < T_{I-II}$  and coincide with the total magnetization for  $T < T^*$ , where  $T^* \sim 2$  K. We argue that (i) ferromagnetic correlations plays a key role in the observed phenomenon in analogy with the theoretical results on magnetic resonance in the dense Kondo systems [1-2] and (ii) the antiferro-quadrupole model of orbital ordering contradicts to the experimental data on the magnetic resonance in CeB<sub>6</sub>. It is found that effective quantum number for the oscillating magnetic moment is  $J = 1/2$ , which suggests that the ground state of the Ce<sup>3+</sup> ion is  $\Gamma_7$  rather than  $\Gamma_8$ . This result demands further development of the theory of static and dynamic magnetic properties of this heavy fermion metal.

The work was supported by the Programme of the Russian Academy of Sciences ‘‘Strongly correlated electrons’’ and by the Federal Programme ‘‘Scientific and Educational Human Resources of Innovative Russia’’.

- [1] E. Abrahams and P. Wölfle, Phys. Rev. B, **78**, 104423 (2008).
- [2] P. Schlottmann, Phys. Rev. B, **79**, 045104 (2009).
- [3] J. Sichelschmidt, et al. Phys. Rev. Lett. **91**, 156401 (2003).
- [4] S.V. Demishev, et al., phys. stat. sol. (b) **242**(3), R27 (2005).
- [5] A.V. Semeno, et al., Phys. Rev. B, **79**, 014423(2009).
- [6] S.V. Demishev, et al., Phys. Rev. B, **80**, 245106 (2009).

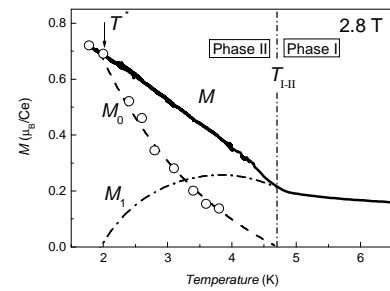


Fig. 1 Magnetisation structure of the phase II of CeB<sub>6</sub>: total magnetisation ( $M$ ), oscillating magnetisation ( $M_0$ ), non-oscillating background ( $M_1$ ).

# Spin dynamics in the hyperkagome compound $\text{Gd}_3\text{Ga}_5\text{O}_{12}$

O. A. Petrenko<sup>1</sup>, P. P. Deen<sup>2</sup>, G. Balakrishnan<sup>1</sup>, B. D. Rainford<sup>3</sup>,  
C. Ritter<sup>4</sup>, L. Capogna<sup>5</sup>, H. Mutka<sup>4</sup> and T. Fennell<sup>4</sup>

<sup>1</sup>Department of Physics, University of Warwick, Coventry CV4 7AL, UK

<sup>2</sup>European Spallation Source ESS AB P.O Box 176, SE-221 00 Lund, Sweden

<sup>3</sup>Department of Physics and Astronomy, Southampton University Southampton SO17 0BJ, UK

<sup>4</sup>Institut Laue Langevin, 6 rue Jules Horowitz, 38042 Grenoble, France

<sup>5</sup>Istituto Officina dei Materiali (IOM)-CNR, OGG 6 rue J. Horowitz, 38042 Grenoble, France

We present the first neutron inelastic scattering results on the magnetic state of the frustrated hyperkagome compound  $\text{Gd}_3\text{Ga}_5\text{O}_{12}$  (GGG) at low temperatures [1] and in applied magnetic field [2]. Our neutron scattering studies reveal a remarkable range of timescales. Short-range spatial correlations observed previously in the neutron diffraction experiments [3] appear static within the instrumental resolution ( $50 \mu\text{eV}$ ). Three distinct inelastic modes are found at  $0.04(1)$ ,  $0.12(2)$  and  $0.58(3)$  meV at  $0.06$  K (see Fig. 1). The application of a magnetic field up to  $2.5$  tesla reveals disparate behavior of the magnetic excitations. In zero applied field, the lowest and highest energy excitations show spatial dependencies indicative of dimerised short-range antiferromagnetic correlations that survive to high temperatures, comparable to the nearest neighbor exchange interactions. Our results suggest that the ground state of a three-dimensional hyperkagome compound differs distinctly from its frustrated counterparts on a pyrochlore lattice and reveal a juxtaposition of cooperative paramagnetism and strong dimerised coupling. These results are surprising since GGG is often classified as a strongly frustrated system with a manifold of connected states for which one would expect a continuum of gapless excitations.

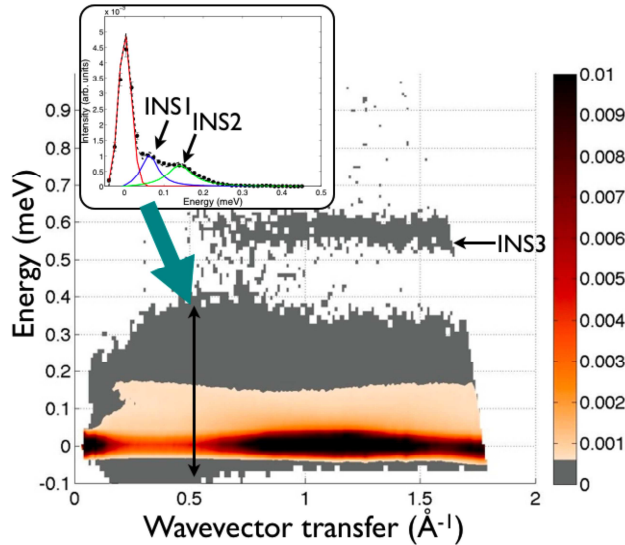


Fig. 1 Powder-averaged scattering function  $S(Q, \omega)$  of GGG at  $0.06$  K with incident energy  $1.94$  meV. Insert is a cut at wave-vector transfer of  $Q=0.5 \text{ \AA}^{-1}$  showing the elastic lineshape and two low-lying excitations with the corresponding fits.

[1] P. P. Deen, O. A. Petrenko, G. Balakrishnan, B.D. Rainford, C. Ritter, L. Capogna, H. Mutka, and T. Fennell, *Phys. Rev. B* **82**, 174408 (2010).

[2] P. P. Deen *et al.*, unpublished (2011).

[3] O. A. Petrenko, *et al.*, *Phys. Rev. Lett.* **80**, 4570 (1998).

# Asymmetric spin ladders: analytical and numerical studies

D. N. Aristov<sup>1,2</sup>

<sup>1</sup>*Petersburg Nuclear Physics Institute, 188300, Gatchina, Russia,*

<sup>2</sup>*St. Petersburg State University, 198504, St. Petersburg, Russia*

Conventional spin ladders [1] contain several equal spin chains coupled by interchain interaction. We consider asymmetric spin-1/2 two-leg ladders [2] with non-equal antiferromagnetic (AF) couplings  $J_{\parallel}^{1(2)}$  along legs, 1(2), and ferromagnetic rung coupling,  $J_{\perp}$ . Similar to conventional case, [3] this model possesses a gap  $\Delta$  in the spectrum of spin excitations and exponential decay of correlations. [4,5] In the limit of large  $J_{\perp}$  this gap is equivalent to Haldane gap for AF spin-1 chain, irrespective of asymmetry of the ladder. The behavior of the gap at small rung coupling depends on the asymmetry of the ladder. For weak asymmetry, and particularly for conventional symmetric ladder,  $J_{\parallel}^1 = J_{\parallel}^2$ , one has linear scaling,  $\Delta \sim J_{\perp}$ . Strong asymmetry of the

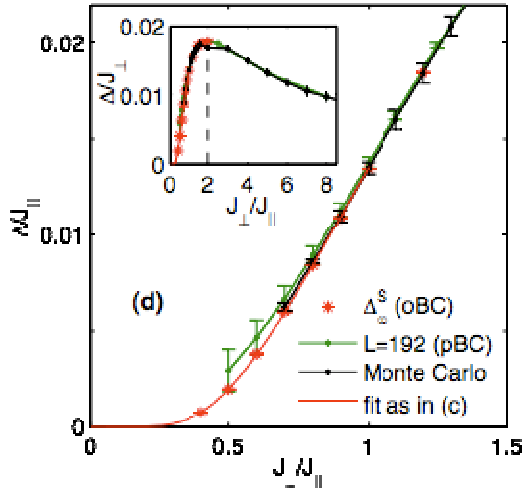


Fig. 1. DMRG and QMC data for the spin gap for the extreme ladder asymmetry.

coupling along legs,  $J_{\parallel}^2 \ll J_{\perp} \ll J_{\parallel}^1$ , is characterized by two energy scales: exponentially small gap in spin excitations spectrum,  $\Delta \sim J_{\perp} \exp(-J_{\parallel}^1/J_{\perp})$ , and the width of the dense band of low-lying excitations, induced by Suhl-Nakamura indirect exchange,  $\sim J_{\perp}^2/J_{\parallel}^1$ . We report the numerical results obtained by exact diagonalization technique, DMRG and large-scale quantum Monte Carlo (QMC) simulations for various spin correlation functions. [6] Particularly the string order parameter, characterizing the hidden AF order in Haldane phase, behaves differently at weak and strong asymmetry. On the basis of our numerical data for strongly asymmetric case, we propose the low-energy theory of effective spin-1 variable, pertaining to large blocks on the

decimated lattice. This theory combines the spin-wave analysis, in spirit of original Haldane's paper, with Kadanoff's decimation procedure.

- [1] T. Giamarchi, Quantum Physics in One Dimension (Clarendon Press, 2003).
- [2] M. N. Kiselev, D. N. Aristov, and K. Kikoin, Phys. Rev. B **71**, 092404 (2005).
- [3] D. G. Shelton, A. A. Nersisyan, and A. M. Tsvelik, Phys. Rev. B **53**, 8521 (1996).
- [4] F. H. L. Essler, T. Kuzmenko, and I. A. Zaliznyak, Phys. Rev. B **76**, 115108 (2007).
- [5] C. Brünger, F.F. Assaad, S. Capponi, F. Alet, D.N. Aristov, and M.N. Kiselev, Phys. Rev. Letters **100**, 017202 (2008).
- [6] D.N. Aristov, C. Brünger, F.F. Assaad, M.N. Kiselev, A. Weichselbaum, S. Capponi, and F. Alet, Phys. Rev. B **82**, 174410 (2010).

# Anomalously large damping of long-wavelength magnons caused by long-range interaction

A. V. Syromyatnikov

*Petersburg Nuclear Physics Institute, Gatchina, Orlova Rosha 188300, Russia*

We discuss the spin-wave interaction in 3D and 2D Heisenberg ferromagnets (FMs) with dipolar forces at  $T_c \gg T \geq 0$  using  $1/S$  expansion. A comprehensive analysis is carried out of the first  $1/S$  corrections to the spin-wave spectrum. We observe a number of quite unusual phenomena: the spin-wave gap caused by spin-wave interaction and anomalously large damping of long-wavelength magnons in 3D FM.

We demonstrate that the spin-wave interaction leads to the *gap*  $\Delta$  in the spectrum  $\varepsilon_{\mathbf{k}}$  in both 3D [1] and 2D [2] FMs renormalizing greatly the bare gapless spectra at small momenta  $k$ . This spin-wave gap, which has been steadily ignored in the literature, resolves the problem of infrared divergent corrections to the longitudinal spin susceptibility [3] and to the spin-wave stiffness [4] in 3D FM. This gap resolves also the problem of long-wavelength magnons instability in 2D FM [5].

Expressions for the spin-wave damping  $\Gamma_{\mathbf{k}}$  are derived. We observe thermal enhancement of both  $\Gamma_{\mathbf{k}}$  and  $\Gamma_{\mathbf{k}}/\varepsilon_{\mathbf{k}}$  at small momenta in both 2D and 3D FMs. In particular, a peak appears in  $\Gamma_{\mathbf{k}}/\varepsilon_{\mathbf{k}}$  at  $k = k_c \sim \Delta/\sqrt{TD}$ , where  $D$  is the spin-wave stiffness. The height of this peak is of the order of  $T/T_c \ll 1$  in 2D FMs for  $S \sim 1$ . Thus, we conclude that *magnons are well-defined quasi-particles in 2D FM at  $T \ll T_c$* . Amazingly, the spin-wave damping appears to be much larger in 3D FM: the peak height in  $\Gamma_{\mathbf{k}}/\varepsilon_{\mathbf{k}}$  is of the order of unity at  $T \ll T_c$ . Thus, we find that *long-wavelength magnons in 3D FM are heavily damped at small  $T$* . [6]

Particular estimations show that  $k_c < 10^{-3} \text{ \AA}^{-1}$  in the majority of materials. Such a small value can explain the surprising fact that such an unusual phenomenon has not been observed so far. Moreover, the magnetocrystalline anisotropy normally screens this effect completely. We point out a number of real compounds with  $k_c \sim 10^{-2} \div 10^{-3} \text{ \AA}^{-1}$  and negligible anisotropy, which are suitable for experimental verification of our predictions.

[1] A. V. Syromyatnikov, Phys. Rev. B **74**, 014435 (2006).

[2] A. V. Syromyatnikov, Phys. Rev. B **77**, 144433 (2008).

[3] B. P. Toperverg, A. G. Yashenkin, Phys. Rev. B **48**, 16505 (1993).

[4] T. S. Rahman, D.L. Mills, Phys. Rev. B **20**, 1173 (1979).

[5] A. Kashuba, Ar. Abanov, V. L. Pokrovsky, Phys. Rev. Lett. **77**, 2554 (1996); Phys. Rev. B **56**, 3181 (1997).

[6] A. V. Syromyatnikov, Phys. Rev. B **82**, 024432 (2010).

# Effects of weak interchain coupling on a spin-gap magnet

V. N. Glazkov<sup>1</sup>, A. I. Smirnov<sup>1</sup>, A. Zheludev<sup>2</sup>, B. C. Sales<sup>3</sup>

<sup>1</sup>*Kapitza Institute, Moscow, Russia*

<sup>2</sup>*Laboratory for Neutron Scattering and Magnetism, ETH-Zurich, Zurich, Switzerland*

<sup>3</sup>*Oak Ridge National Laboratory, Oak Ridge, USA*

Spin-gap magnet NTENP ( $\text{Ni}(\text{C}_9\text{H}_{24}\text{N}_4)\text{NO}_2(\text{ClO}_4)$ ) is an example of a  $S=1$  spin chain with alternating exchange interaction. Spin sublevels of the triplet excitations are strongly split by an effective crystal field, originating from single-ion anisotropy on  $\text{Ni}^{2+}$ . This system is a good test probe for different phenomena, related to the physics of spin-gap systems. Closing of the gap by an applied magnetic field, induced order above critical field, effects of magnon decay were studied by neutron scattering and electron spin resonance (ESR) techniques (see [1] and references therein).

Different sorts of ESR transitions are available for observation in NTENP: thermoactivated inter-triplet transitions, transitions between singlet ground state and triplet sublevels, antiferromagnetic resonance above critical field. They can be identified by characteristic temperature dependences and characteristic  $f(H)$  dependences for different modes. We observed that certain ESR modes are split, which can not be accounted for in the simple model of one-dimensional spin-gap system (Figure 1).

We propose that the observed splittings are due to the weak dispersion of excitations in the direction, transverse to the chain. Since effective crystal field parameters are  $\mathbf{k}$ -dependent, splitting of the triplet sublevels is slightly different in the true minimum of  $E(\mathbf{k})$  and in the saddle point at the edge of Brillouin zone. Difference of singlet-triplet transition frequencies allows to measure directly amplitude of the dispersion in the transverse direction and to estimate strength of the interchain interaction as  $J_{\perp} \sim 0.05\text{K}$ .

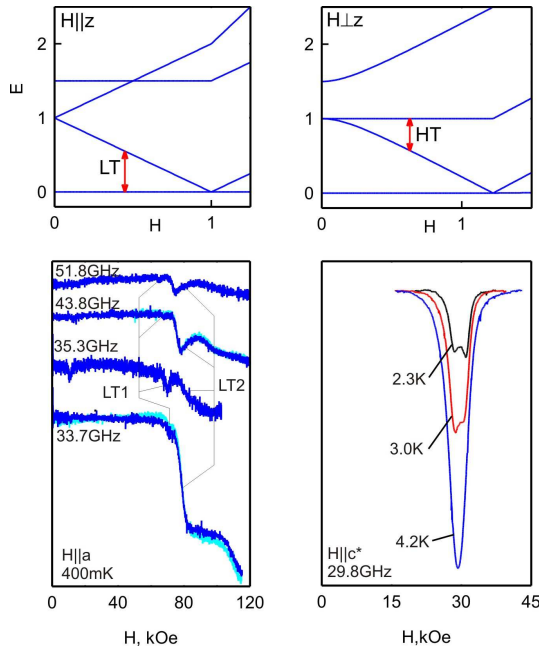


Fig. 1. (Upper panels) Schematic representation of the energy levels and expected resonance transitions for low-temperature (LT) and thermoactivated (HT) modes. (Lower panels) Experimentally observed splitting of the LT and HT modes.

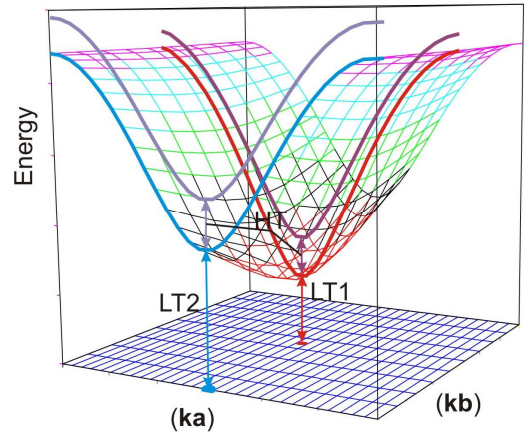


Fig. 2. Dispersion of the lower excitations branch in the transverse (b) direction causes difference in the resonance frequencies (transverse dispersion is shown out of scale for clarity).

[1] V.N. Glazkov, A.I. Smirnov, A. Zheludev, B.C. Sales, Phys.Rev. B **82**, 184406 (2010).



# Spin excitations in 122-ferropnictide superconductors studied by inelastic neutron scattering

D. S. Inosov, J. T. Park, Yuan Li, D. Haug, A. Yaresko, V. Hinkov, B. Keimer  
*Max-Planck-Institute for Solid State Research, Heisenbergstr. 1, 70569 Stuttgart, Germany*

Inelastic neutron scattering studies on  $\text{BaFe}_{1.85}\text{Co}_{0.15}\text{As}_2$  and  $\text{BaFe}_{1.91}\text{Ni}_{0.09}\text{As}_2$  electron-doped ferropnictide superconductors will be presented. In the iron arsenides, the proximity of superconductivity and antiferromagnetism in the phase diagram, the apparently weak electron–phonon coupling and the ‘resonance peak’ in the superconducting spin-excitation spectrum have fostered the hypothesis of magnetically mediated Cooper pairing. To assess the spectral weight and the symmetry of the pairing boson, we have extensively studied spin excitations in these systems over a wide range of temperatures and energies, and for different doping levels [1, 2]. In contrast to high- $T_c$  cuprate superconductors, the spin-excitation spectrum agrees well with predictions of the theory of nearly antiferromagnetic metals. The temperature evolution of the resonance energy monotonically follows the closing of the superconducting energy gap, as expected from conventional Fermi-liquid models. Our observations point to a surprisingly simple theoretical description of the spin dynamics in the iron-based superconductors and provide a solid foundation for models of magnetically mediated superconductivity [1].

We have also studied the anisotropy of spin excitations in the transverse and longitudinal directions of the reciprocal space [2]. Optimally doped samples that exhibit neither static magnetic phases nor structural phase transitions have revealed that the spin excitation spectrum does not follow the  $4_2/m$  screw symmetry around the  $(\frac{1}{2} \frac{1}{2} L)$  axis, which belongs to the  $I4/mmm$  space group of the crystal. This is seen both in the in-plane anisotropy of the normal- and superconducting-state spin dynamics and in the out-of-plane dispersion of the spin resonance mode. The in-plane anisotropy can be qualitatively reproduced in the normal-state DFT calculations, and therefore does not necessarily imply a symmetry-broken ground state. Below  $T_c$ , the resonance energy, its intensity, and the SC spin gap inherit the normal-state modulation along the out-of-plane direction  $L$  with a period twice larger than expected from crystal symmetry. The amplitude of this modulation decreases with doping. The amplitude of this modulation decreases with doping and is therefore associated with the 3D character of magnetic coupling between itinerant electrons, providing an analogy to the even-odd resonance splitting in copper oxides.

Combining our and previous data, we have shown [2, 3] that at odd  $L$  a universal linear relationship  $\omega_{\text{es}} = 4.3 k_B T_c$  holds for all Fe-based superconductors, independent of their carrier type. Yet, an extensive comparison of the  $2\Delta/k_B T_c$  ratios has revealed that contrary to the recently suggested universality of this ratio in Fe-based superconductors, the coupling in pnictides ranges from weak, near the BCS limit, to strong, as in cuprates, bridging the gap between these two extremes. An important consequence of this result for ferropnictides is that the separation in energy between the excitonic spin-resonance mode and the particle-hole continuum, which determines the resonance damping, no longer appears independent of  $T_c$ .

- [1] D. S. Inosov *et al.*, *Nature Physics* **6**, 178 (2010).
- [2] J. T. Park *et al.*, *Phys. Rev. B* **82**, 134503 (2010).
- [3] D. S. Inosov *et al.*, arXiv:1012.4041 (unpublished).

# Magnetic anisotropy of 2D antiferromagnet with triangular lattice $\text{CuCrO}_2$

L. A. Prozorova<sup>1</sup>, L. E. Svistov<sup>1</sup>, V. Tsurkan<sup>2</sup>, A. M. Vasiliev<sup>1</sup>

<sup>1</sup>*P. L. Kapitza Institute for Physical Problems RAS, Moscow, Russia*

<sup>2</sup>*Center for Electronic Correlations and Magnetism EKM,  
Experimentalphysik V, Universität Augsburg, Germany*

For more than a decade, the study of frustrated antiferromagnets has been a fascinating subject of condensed-matter physics. Unconventional types of magnetic ordering and phases in frustrated quantum spin chains are attractive issues, because they appear under a fine balance of the exchange interactions and are sometimes caused by much weaker interactions or fluctuations.

$\text{CuCrO}_2$  compound is an example of the quasi-two dimensional antiferromagnet ( $S=3/2$ ) on a triangular lattice with easy axis anisotropy. At temperatures lower than transition temperatures ( $T_{N1}=23.6$  K and  $T_{N2}=24.2$  K) the magnetic system of  $\text{CuCrO}_2$  is long range ordered in the triangular planes and has short range correlations between planes. The planar spiral spin structure with the incommensurate vector  $(0,328; 0,328; 0)$  was recently detected in  $\text{CuCrO}_2$  compound [1]. The small deviation from 120-degree magnetic structure is probably caused by small distortion of triangular lattice, so that the exchange parameter along one side of the triangle differs from two others (Fig. 1).

In our work we study the magnetic structure of  $\text{CuCrO}_2$  single crystals using the ESR technique. The frequency and angle dependencies of ESR spectra can be well described in the model of a planar spiral spin structure with biaxial anisotropy [2]. One anisotropy axis is directed along  $C_3$   $(0,0,1)$  and the second is arranged along  $(1,-1,0)$ . The weak in-plane anisotropy is connected with the distortion of triangular planes mentioned above. The in-plane anisotropy does not change at the spin-reorientation transition, which means that this distortion is not connected with magnetostriction.

The value of anisotropy of the exchange susceptibility of the spin structure, the constants of anisotropy and the fields of spin reorientation transitions were obtained.

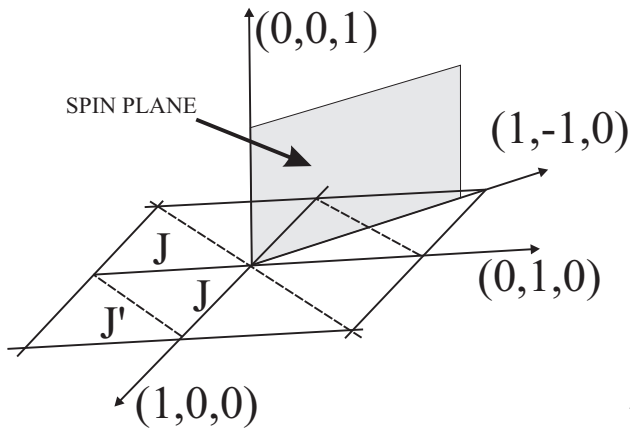


Fig. 1

[1] M. Poienar, F. Dumay, C. Martin, V. Hardy, A. Maignan, and G. Andre, *Phys. Rev. B* **79**, 0144412 (2009).

[2] K. Kimura, H. Nakamura, S. Kimura, M. Hagiwara, and T. Kimura, *Phys. Rev. Lett.* **103**, 107201 (2009).

## Probing of MnSi by electron spin resonance

A. V. Semeno, A. V. Bogach, V. V. Glushkov, N. E. Sluchanko, N. A. Samarin,  
and S.V. Demishev

*Prokhorov General Physics Institute, Russian Academy of Sciences, ul. Vavilova 38,  
Moscow, 119991 Russia*

High frequency (60 GHz) electron spin resonance (ESR) in manganese monosilicide (MnSi) single crystals is studied [1]. The measurements have been performed within the temperature range 1.8–60 K at the applied magnetic field up to 70 kOe. A single resonance line is observed at all temperatures. Values of the line intensity obtained in the units of magnetic permeability evidence that the density of magnetic moments contributing to ESR coincides well with static magnetization of MnSi. Analysis of the lineshape within Dyson model for itinerant electrons exhibits that the ESR lineshape corresponds to the limit of localized magnetic moments. The low limit value of diffusion time through the skin layer is defined from the simulation. Strong growth of the linewidth of ESR is found below Neel transition temperature  $T_N < 29\text{K}$ . At the same time the  $g$ -factor only slightly depends on temperature:  $g \sim 1.9\text{--}2.0$ . Such behavior of ESR parameters has been analyzed in the framework of Moriya theory using the  $SL(T)$  function. The revealed deviations from the model of weak itinerant-electron magnetism, which is commonly used for the description of the magnetic properties of MnSi, indicate a possible spin-polaron nature of the unusual magnetic properties of this strongly correlated metal.

[1] S. V. Demishev *et. al.*, JEPT Letters, **93**, 213 (2011).

# The magnetic anisotropy and exchange interactions of $\text{Ni}_3\text{B}_2\text{O}_6$ and $\text{Co}_3\text{B}_2\text{O}_6$

S. Sofronova<sup>1,2</sup>, N. Volkov<sup>1</sup>, L. Bezmaternykh<sup>1</sup> and E. Eremin<sup>1,2</sup>

<sup>1</sup>*Kirensky Institute of Physics SB RAS, 660036, Krasnoyarsk, Russia*

<sup>2</sup>*Siberian State Aerospace University, Krasnoyarsk, Russia*

The orthorhombic antiferromagnetic single crystals of  $\text{Ni}_3\text{B}_2\text{O}_6$  ( $T_N = 46,3$  K) and  $\text{Co}_3\text{B}_2\text{O}_6$  ( $T_N = 34,1$  K) were grown using a  $\text{Bi}_2\text{Mo}_3\text{O}_{12}$  and  $\text{Na}_2\text{O}$  flux. The seeds were obtained by spontaneous nucleation from the same flux. The magnetic properties of the crystals were investigated using ac and dc magnetization measurements performed with a physical property measurement system (PPMS, Quantum Design) for magnetic fields applied along the a, b, c orthorhombic axis in the temperature range from 2 K to 350 K at magnetic fields up to 90 kOe. The magnetic susceptibility of highly anisotropic  $\text{Co}_3\text{B}_2\text{O}_6$ , measured along a and b orthorhombic axis, clearly reveal the anomalies at 10 K (Fig.1). Suggesting that there is the spin-reorientation transition at 10 K. Calculations of Ni-O-Ni and Co-O-Co interactions made in the framework of an indirect coupling model [1]. Some of calculated Co-O-Co exchange interactions are highly anisotropic in contrast isotropic Ni-O-Ni exchange interactions. The probable magnetic structures of  $\text{Ni}_3\text{B}_2\text{O}_6$  and  $\text{Co}_3\text{B}_2\text{O}_6$  are considered based on the experimental data and results of calculations.

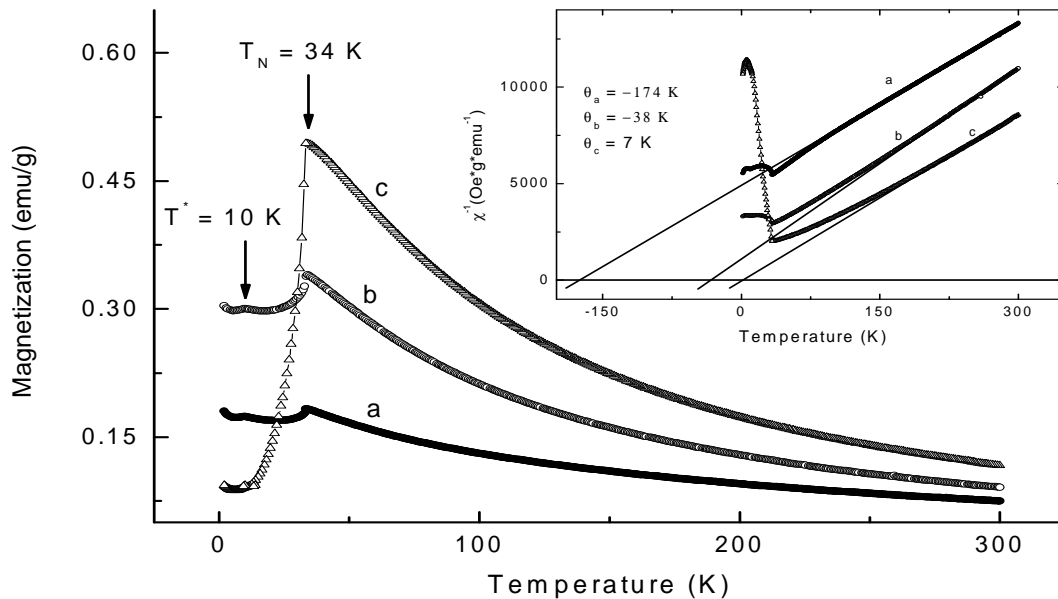


Fig. 1 The temperature dependencies of magnetization of  $\text{Co}_3\text{B}_2\text{O}_6$  for magnetic field 1 kOe along the a, b, c orthorhombic axis. The inset shows the temperature dependencies of inverse magnetic susceptibility.

## Acknowledgements

This study was supported by Federal Special-Purpose Program 'Scientific, Academic and Teaching Staff of Innovative Russia, 2009–2013.

[1] O.A. Bayukov, A.F. Savitskii, Phys. stat. sol.(b) **155**, 249 (1989).

# Review of spin-phonon coupling in cubic SrMnO<sub>3</sub>, EuTiO<sub>3</sub> and hexagonal YMnO<sub>3</sub> antiferromagnets: radiofrequency, THz and far-infrared studies

S. Kamba<sup>1</sup>, V. Goian<sup>1</sup>, V. Skoromets<sup>1</sup>, C. Kadlec<sup>1</sup>, P. Kužel<sup>1</sup>, A. Belik<sup>2</sup>,  
J. H. Lee<sup>3</sup>, K. M. Rabe<sup>3</sup>, K. Kohn<sup>4</sup>, and R. V. Pisarev<sup>5</sup>

<sup>1</sup>*Institute of Physics ASCR, Na Slovance 2, 182 21 Prague 8, Czech Republic*

<sup>2</sup>*International Center for Materials Nanoarchitectonics (MANA), National Institute for Materials Science (NIMS), 1-1 Namiki, Tsukuba, Ibaraki 305-0044, Japan*

<sup>3</sup>*Department of Physics and Astronomy, Rutgers University, Piscataway, New Jersey 08854-8019, USA*

<sup>4</sup>*Waseda University, Department of Physics, Tokyo 169-8555, Japan*

<sup>5</sup>*Ioffe Physical Technical Institute, Russian Academy of Sciences, 194021, St. Petersburg, Russia*

e-mail: [kamba@fzu.cz](mailto:kamba@fzu.cz)

In this contribution we review results of our investigations of a spin-phonon coupling in various non-conducting antiferromagnets. The strength of the spin-phonon coupling is manifested by a drop-down of dielectric permittivity  $\epsilon'$  below the Néel temperature  $T_N$ . A decrease of  $\epsilon'$  by 3 %, 6 % and 32 % was observed below  $T_N$  in EuTiO<sub>3</sub>, YMnO<sub>3</sub> and SrMnO<sub>3</sub>, respectively. We demonstrate that the observed dielectric anomalies are caused blue shifts of low-frequency phonons near  $T_N$ . Simultaneously, we show that the magnetocapacitance effect in EuTiO<sub>3</sub>, i.e. change of  $\epsilon'$  with magnetic field  $B$ , is caused by tuning of a phonon frequency with  $B$ .

The strongest spin-lattice coupling we have observed is in the cubic SrMnO<sub>3</sub> ceramics. The lowest-frequency polar phonon revealed in IR reflectivity spectra exhibits strong (17 %) hardening on cooling below  $T_N=230$  K resulting in a 32 % decrease of the static  $\epsilon'$  below  $T_N$ . This decrease of  $\epsilon'$  is one order of magnitude larger than that observed in EuTiO<sub>3</sub>. Such a huge change of the permittivity due to antiferromagnetic ordering has never been observed and it gives evidence of extremely strong spin-phonon coupling in SrMnO<sub>3</sub> bulk ceramics. The experimental results correspond to theoretical values obtained from our first-principles calculations of bulk SrMnO<sub>3</sub>. The confirmation of huge spin-phonon coupling in cubic SrMnO<sub>3</sub> opens the possibility to prepare thin films with a simultaneous ferroelectric and ferromagnetic order, which could be induced due to the spin-phonon coupling in strained thin films as recently suggested from first principles [1]. By achieving to elaborate films strained by more than 3%, both ferroelectric and ferromagnetic critical temperatures should appear near 150 K, i.e. much more than we recently experimentally confirmed in the strained EuTiO<sub>3</sub> films [2].

In the last part of our contribution we will report about time-domain THz study of AFM resonance in hexagonal YMnO<sub>3</sub>. The AFM resonance lies near 42 cm<sup>-1</sup> at 10 K and its frequency decreases on heating towards  $T_N = 70$  K [3]. This excitation seen in magnetic THz permeability disappears above  $T_N$  but above  $T_N$  another excitation with similar frequency appears in *dielectric* spectra. It reminds paraelectromagnon, but we will explain it by multiphonon or phonon-magnon absorption.

[1] J. H. Lee and K. M. Rabe, *Phys. Rev. Lett.* **104**, 207204 (2010)

[2] J. H. Lee, L. Fang, E. Vlahos, X. Ke, Y-W. Jung, S. Kamba et al. *Nature*, **466**, 954 (2010).

[3] V. Goian, S. Kamba et al. *Phase Transitions* **83**, 931 (2010).

# Magnetic and magnetoelectric excitations in multiferroic manganites

Andrei Pimenov

*Institute of Solid State Physics, Vienna University of Technology, A-1040 Vienna, Austria*

Multiferroics are materials simultaneously showing ferromagnetic and ferroelectric order. Two order parameters are coupled in these materials, which leads to such unusual effects like magnetic switching of electric polarization and dielectric constant. As can be expected already from the first principles, changes in the static properties of multiferroics must be accompanied by dynamic effects like characteristic magnetoelectric excitations. Indeed, such excitations could be recently observed in the spectra and were called electromagnons. Contrary to the conventional magnons, the electromagnons are excited by the electric component of the electromagnetic wave and contribute substantially to the static dielectric permittivity. In addition to the strong electric activity of the electromagnons a series of other excitations of magnetic and magnetoelectric nature are observed in the same frequency range as electromagnons. The systematics of the existing modes and the current state of the art in the understanding of the underlying mechanisms is summarized [1].

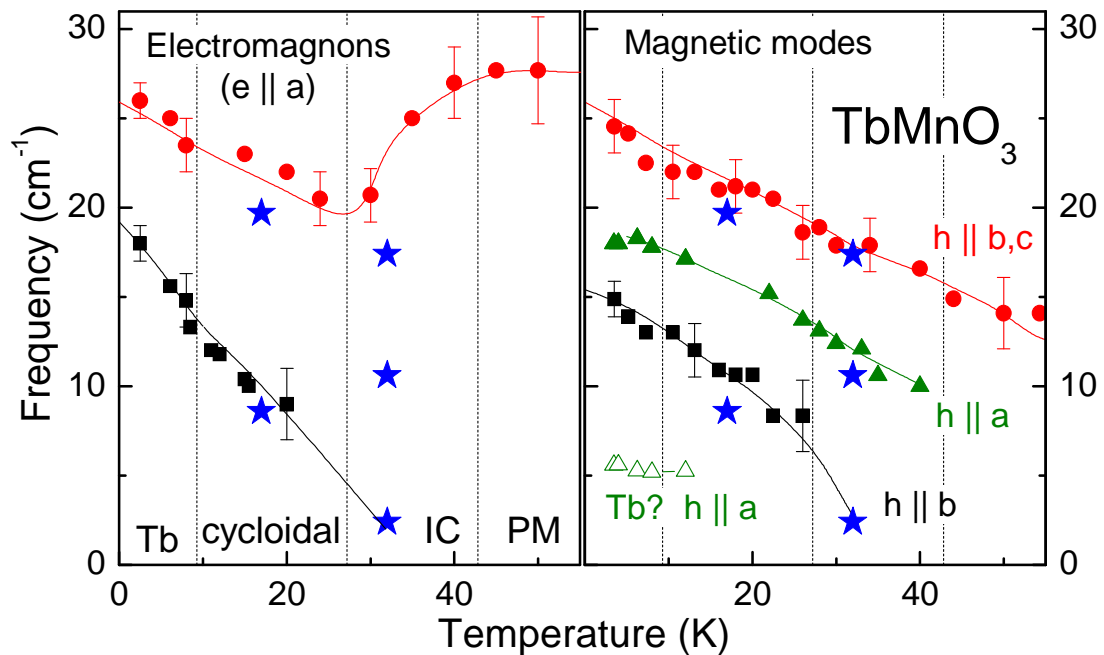


Fig. 1. Frequencies of the magneto-active and electro-active excitations in  $\text{TbMnO}_3$  compared with the results by inelastic neutron scattering (INS) [2]. The INS data are shown as stars. Left panel: electric modes (electromagnons). Right panel: magnetic modes. Symbols represent the experimental data, solid lines are drawn to guide the eye. The excitation conditions of the magnetic excitations are indicated at the curves. The electromagnons are excited in the geometry  $e \parallel a$  only. Dashed lines represent the boundaries between different magnetic phases. PM - paramagnetic, IC - incommensurate (sinusoidal) antiferromagnetic, cycloidal – cycloidal antiferromagnetic, Tb - phase with ordered Tb sublattice.

[1] A. M. Shuvaev, A. A. Mukhin, and A. Pimenov, Topical Review in: *J. Phys.: Condens. Matter* **23**, 113201 (2011).

[2] D. Senff et al., *J. Phys.: Condens. Matter*, **20**, 434212 (2008).

## Coupled R and Fe magnetic excitations in $R\text{Fe}_3(\text{BO}_3)_4$ multiferroics

A. M. Kuzmenko, A. A. Mukhin, V. Yu. Ivanov  
*Prokhorov General Physics Institute of the RAS, 119991 Moscow, Russia*

Rare-earth iron borates  $R\text{Fe}_3(\text{BO}_3)_4$  are a new family of multiferroics ( $T_N = 30\text{-}40$  K) possessing non-centrosymmetrical trigonal crystal structure and exhibiting interesting magnetic, magnetoelectric and other properties which strongly depend on an exchange interaction of antiferromagnetic Fe and paramagnetic rare-earth (R) ions. We have studied the submillimeter magnetic resonance properties of easy plane Nd, Sm, Gd-based iron borates to get additional data on R-Fe interaction and its effect on magnetic excitations in Fe- and R-subsystems. Polarization measurements of transmission spectra of single crystalline *a*-cut plates were carried out by a submillimeter quasioptical backward-wave-oscillator technique at the frequency range  $3\text{-}20\text{ cm}^{-1}$  at the temperatures  $3\text{-}300$  K. One or two resonance modes were observed for both ac electro-magnetic field polarizations ( $\mathbf{h}\parallel b, \mathbf{e}\parallel c$  and  $\mathbf{h}\parallel c, \mathbf{e}\parallel b$ ). They were identified as magnetic excitations in the exchange coupled Fe- and R-subsystems originated from antiferromagnetic resonance (AFMR) of Fe ions and electron transitions inside a ground state (doublet) of R ions split by R-Fe exchange field. A qualitatively different resonance mode behavior was found for various R-ions. It was established both experimentally and theoretically an existence of a strong dynamical coupling of the magnetic Fe and R ions oscillations accompanied by their anti-crossing and intensity redistribution between the modes of the same symmetry.

An increase of the Nd-mode frequencies (up to  $13\text{ cm}^{-1}$ ) as compare with the static exchange  $\text{Nd}^{3+}$  doublet splitting ( $8.8\text{ cm}^{-1}$ ) was observed in  $\text{NdFe}_3(\text{BO}_3)_4$  as a result of R-mode anti-crossing with underlying Fe AFMR mode ( $h\parallel b$ ) which was soften. The mode anti-crossing was reduced with dilution of Nd ions in  $\text{Nd}_{0.4}\text{Y}_{0.6}\text{Fe}_3(\text{BO}_3)_4$ . Similar increasing of Sm-mode frequencies as compare with the  $\text{Sm}^{3+}$  doublet splitting was also observed in  $\text{SmFe}_3(\text{BO}_3)_4$ , which, however, was accompanied by the increasing of AFMR mode frequency ( $h\parallel b$ ) in contrast to  $\text{NdFe}_3(\text{BO}_3)_4$ . This is explained by a significant anisotropy of exchange Sm-doublet splitting in the easy plane and easy axis states as compare with Nd one.

An unusual hiding of expected Gd-modes was revealed in pure  $\text{GdFe}_3(\text{BO}_3)_4$ . It was attributed to a peculiar compensation of contributions of Fe and Gd ions to permeability for the high frequency (exchange) mode due to almost equality of their gyromagnetic ratios. However, in mixed  $\text{Gd}_{0.5}\text{Nd}_{0.5}\text{Fe}_3(\text{BO}_3)_4$  system the Gd-modes were well observed along with Nd ones. Their frequencies ( $\sim 17\text{ cm}^{-1}$ ) turned out more then two times higher of Gd levels exchange splitting.

An explanation and quantitative description of the observed effects have been performed and corresponding parameters of magnetic interactions have been extracted. A role and contribution of magnetoelectric (electro dipolar active) excitations, i.e. electromagnons in the phenomena studied have been also analyzed.

This work was supported by RFBR (10-02-00846 and 09-02-01355).

# Spin flexoelectricity: magnetic domain walls and vortices as sources of electric polarization

A. K. Zvezdin <sup>1</sup>, A. P. Pyatakov<sup>1,2</sup>

<sup>1</sup> A. M. Prokhorov General Physics Institute, 38, Vavilova st., 119991, Moscow, Russia

<sup>2</sup> Physics Department, M.V. Lomonosov MSU, Leninskie gori, 119992, Moscow, Russia

The magnetoelectric coupling in multiferroic materials with coexisting ferroelectric and magnetic ordering is now an issue of keen interest from the fundamental point of view and because it offers a low-energy-consuming way in spin electronics and magnetic storage. A common scenario of magnetoelectric coupling is the *spin flexoelectricity*, i.e. the electric polarization induced by spatially modulated spin structures [1-3]. This mechanism is responsible for improper ferroelectricity in the so-called spiral multiferroics [4].

However it is not generally known that this principle has far-reaching implications beyond the field of multiferroic materials. Micromagnetic structures like domain walls and magnetic vortices can also be considered as a source of ferroelectricity due to the local symmetry violation in the material. Recently the motion of domain walls in the gradient of the electric field provided by a tip electrode has been observed in rare-earth iron garnet films [5].

In this report several aspects of coupling between the spatial spin modulation and the electric polarization in the field of micromagnetism are considered:

- 1) electric field control of magnetic domain walls [6]
- 2) domain wall electric polarity switching by magnetic field [7]
- 3) chiral domain structure in magnetic films with broken central symmetry [7]
- 4) the possibility of magnetic vortex/antivortex nucleation by electric field [8]

It should be noted that ferroelectricity developed from micromagnetic structure is universal phenomenon and can appear in every magnetic insulator even in centrocymmetric one. Besides its fundamental importance the electric charge density associated with magnetic inhomogeneities provides new means for the electrical control of the magnetic state. This fits the novel trend in low-power-consumption spintronics and magnetic memory that is based on domain wall engineering. Low spin damping in iron garnet films compared to multiferroic materials makes them also interesting in the context of electrically tuned spin wave propagation.

[1] V.G. Bar'yakhtar, V.A. L'vov, and D.A. Yablonskii, JETP Lett. **37**, 673 (1983).

[2] A. Sparavigna, A. Strigazzi, and A. Zvezdin, Phys. Rev. B **50**, 2953 (1994).

[3] A.P. Pyatakov, A.K. Zvezdin, The Eur. Phys. J. B **71**, 419 (2009).

[4] S.-W. Cheong, M. Mostovoy, Nature Materials **6**, 13 (2007).

[5] A.S. Logginov et al, JETP Letters **86**, 115 (2007).

[6] A.S. Logginov et al, APL **93**, 182510 (2008).

[7] A.P. Pyatakov et al, EPL **93**, 17001 (2011).

[8] A.P. Pyatakov, G.A. Meshkov, A.S. Logginov, Moscow University Phys. Bulletin, **65**, 329 (2010).



# Hysteresis in magnetization of $\text{Nd}_{0.5}\text{Gd}_{0.5}\text{Fe}_3(\text{BO}_3)_4$ single crystal

A. V. Malakhovskii<sup>1</sup>, E. V. Eremin<sup>1</sup>, D. A. Velikanov<sup>1,2</sup>, A. V. Kartashev<sup>1</sup>,  
A. D. Vasil'ev<sup>1</sup>, I. A. Gudim<sup>1</sup>

<sup>1</sup>*L.V. Kirensky Institut of Physics, SB RAS, 660036 Krasnoyarsk, Russia,*

<sup>2</sup>*Siberian Federal University, 660041 Krasnoyarsk, Russia*

Some ferrobates with the general formula  $\text{RFe}_3(\text{BO}_3)_4$  (R – rare earth ion) are multiferroics and crystals  $\text{GdFe}_3(\text{BO}_3)_4$  and  $\text{NdFe}_3(\text{BO}_3)_4$ , in particular. These two crystals demonstrate substantially different magnetic properties (see, e.g., [1, 2]). Therefore it was of interest to study crystal with the mixed Gd and Nd ions.

Magnetic properties of  $\text{Nd}_{0.5}\text{Gd}_{0.5}\text{Fe}_3(\text{BO}_3)_4$  single crystal have been studied in the main crystallographic directions in the field up to 90 kGs and in the temperature range 2 – 300 K. Heat capacity has been also measured in the temperature range 2 – 300 K. At temperature 32 K a transition into easy plane antiferromagnetic state has been revealed. This state remains down to 2 K. A hysteresis has been discovered in the field interval 1 – 3.5 kGs during magnetization in the easy plane perpendicular to the trigonal axis of the crystal (Fig. 1). In the same field interval a spin-flop transitions take place in domains in the easy plane. At temperature 11 K in the field  $B < 1$  kGs a singularity on the temperature dependence of magnetic susceptibility in the easy plane is observed (Fig. 2). At the same temperature the hysteresis appears, i. e., at the higher temperatures the thermal energy is enough for overcoming a potential barrier between domains with three energetically equivalent directions of magnetic moments, and the crystal in any point tunnels between these states. In the field  $B > 3.5$  kGs the crystal goes over to one domain state, and the singularity on the temperature dependence of the susceptibility disappears (Fig. 2). Thus, this singularity is connected with appearance of fixed domains and, consequently, of fixed domain walls. Just the presence of the fixed domain walls distinguishes the crystal state at  $T < 11$  K from the state at  $T > 11$  K. Analysis of the experimental results has shown, that behavior of magnetization in the fields 1 – 3.5 kGs is conditioned by moving of the domain walls and also by spin-flop transitions and by rotation of magnetic moments to the magnetic field direction not only in the domains but in the domain walls as well.

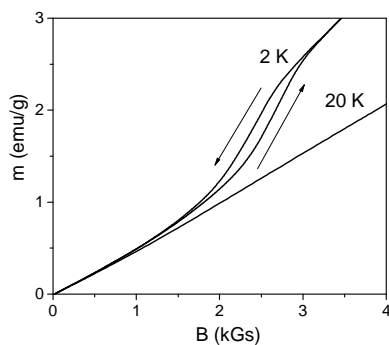


Fig. 1. Magnetization in the easy plane.

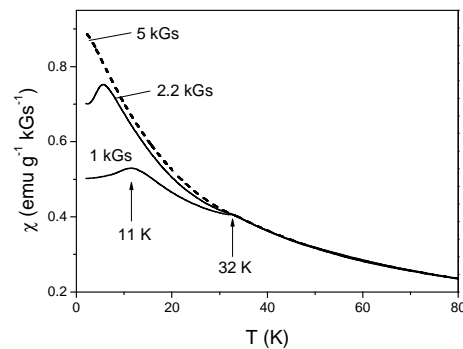


Fig. 2. Susceptibility in the easy plane.

- [1] A. D. Balaev, L. N. Bezmaternykh, I. A. Gudim, V. L. Temerov, S. G. Ovchinnikov and S. A. Kharlamova, *J. Magn. Magn. Mater.* **258-259**, 532 (2003).
- [2] Е. А. Попова, Н. Тристан, Х. Хесс, Р. Клингелер, Б. Бюхнер, Л. Н. Безматерных, В. Л. Темеров и А.Н. Васильев, *ЖЭТФ* **132**, 121 (2007).

# Nonreciprocity of electromagnon polaritons of TbMnO<sub>3</sub> at its boundary with a metal in a magnetic field

I. E. Chupis

*B. Verkin Institute for Low Temperature Physics and Engineering,  
National Academy of Sciences of Ukraine, pr. Lenina 47, Kharkov 61103, Ukraine*

Recently gigantic magnetoelectric (ME) effects were found in orthorhombic manganite TbMnO<sub>3</sub> with incommensurate antiferromagnetic (AF) structure below  $T_N = 42\text{K}$  [1]. Inhomogeneous ME interaction induces a small electric polarization in noncollinear AF state below  $T_c = 27\text{K}$ . Hybrid spin- electric excitations in TbMnO<sub>3</sub> were firstly observed in an alternating electric fields [2]. These results have been qualitatively explained [3].

In this work the spreading of electromagnetic wave in a semi-infinite TbMnO<sub>3</sub> ( $z > 0$ ) at its boundary with an ideal metal ( $z < 0$ ) in a magnetic field  $\mathbf{H}$  directed along x-axis in a contact surface was analyzed. Surface electromagnetic wave is running along the modulation vector  $\mathbf{k}$  of AF structure,  $\mathbf{q} \parallel \mathbf{k} \parallel y$ . The alternating fields in a wave  $\mathbf{e}, \mathbf{h} \sim \exp[i(qy - \omega t) - k_0 z]$  where  $k_0$  is the inverse value of the depth penetration of the field into the TbMnO<sub>3</sub>. Electromagnon spectrum would be calculated using the equations for Lagrange's function. The coupling of AF magnons and optical phonons are described by the ME terms  $P_i(A_i \partial_y A_y - A_y \partial_y A_i)$  where  $\mathbf{P}$  – electric polarization,  $\mathbf{A}$ - AF vector,  $i=x,y,z$ . The interaction of electric polarization with magnetic field is described by the dynamic ME energy  $[\vec{P}\vec{H}]\dot{\vec{P}}$  where  $\dot{\vec{P}} = \partial_t \vec{P}$  [4]. Dispersion equations were received in a linear approximation for small deviations  $\mathbf{a}$  and  $\mathbf{p}$  from their equilibrium values restricting in the first harmonic. The components  $(a_z, p_z, p_y)$  are coupled in a sinusoidal AF and paraelectric state ( $T_c < T < T_N$ ). In the ferroelectromagnetic state ( $T < T_c$ ) electromagnon is the excitation of  $(a_z, a_y, p_z, p_y)$ . Taking into account the Maxwell equations and boundary conditions the surface polariton spectrum in the terahertz region was obtained.

Strong nonreciprocity of the spectrum ( $\omega(-\vec{q}) \neq \omega(\vec{q})$ ) was revealed. The modes of electromagnon polaritons appreciably differ in opposite directions of the magnetic field or the propagation of the wave. Electromagnon polariton with the given frequency propagates only in one direction with respect to the magnetic field, which is the effect of rectification of surface electromagnetic waves. The inversion of the magnetic field results in 'switching on' or 'switching off' surface wave. The existence of radiant surface electromagnon modes was predicted. The depth of penetration of electromagnetic wave in TbMnO<sub>3</sub>  $k_0^{-1} \sim H^{-1}$  appreciably depends on the frequency. Incommensurate AF structure and magnetic field induce the gaps in the spectrum.

[1] T. Kimura, T. Goto, H. Shintani, K. Ishizaka, T. Arima, and Y. Tokura, *Nature (London)*, **426**, 55 (2003).

[2] A. Pimenov, A. A. Mukhin, V. Yu. Ivanov, V. D. Travkin, A. M. Balbashov, and A. Loidl, *Nature Phys.* **2**, 97 (2006).

[3] I. E. Chupis, *FNT*, **35**, 1101 (2009).

[4] I. E. Chupis, *Ferroelectrics*, **204**, 173 (1997).

# Evidence of $p-d$ and $d-d$ charge transfer and insulator-to-metal phase transitions in nonlinear optical response of $(\text{La}_{0.6}\text{Pr}_{0.4})_{0.7}\text{Ca}_{0.3}\text{MnO}_3$

M. Ivanov<sup>1</sup>, E. Mishina<sup>1</sup>, V. Moshnyaga<sup>2</sup>, M. Fiebig<sup>3</sup>

<sup>1</sup> *Moscow State Institute of Radioengineering, Electronics and Automation, prosp. Vernadskogo 78, 119454 Moscow, Russia*

<sup>2</sup> *Universitaet Goettingen, Friedrich-Hund- Platz 1, 37077, Goettingen, Germany*

<sup>3</sup> *Universitaet Bonn, Nussallee 14-16, 53115, Bonn, Germany*

We report the evidence of  $p-d$  and  $d-d$  charge transfer transition and insulator-to-metal phase transitions in optical second harmonic generation (SHG) in  $(\text{La}_{0.6}\text{Pr}_{0.4})_{0.7}\text{Ca}_{0.3}\text{MnO}_3$  (LPCMO) thin film. LPCMO perovskite is an  $O'$  - orthorhombic manganate with  $P6_3/mmm$  space group with four- and three-electron energy levels of the  $\text{Mn}^{3+}(d^4)$  and  $\text{Mn}^{4+}(d^3)$  states, respectively, in octahedral crystal field.

SHG spectra for specific light polarization combinations show two bands at 3.4 and 2.8 eV. Considering the influence of applied magnetic field and Jahn-Teller effect on the SHG spectra, as well as taking into account the data on electronic structure of the orthorhombic manganites we conclude that the observed energy bands correspond the doubled energy of the well known charge transfer transitions  $\text{Mn} (^5\Gamma_1 \rightarrow ^5\Gamma_6)$  and  $\text{Mn} (^5\Gamma_1 \rightarrow ^5\Gamma_5)$  at 1.725 eV and 1.4 eV, respectively [1].

Colossal magnetoresistance manganites, particularly LPCMO, are characterized by electronic phase separation with coexisting paramagnetic insulating and ferromagnetic metallic phases [2]. In LPCMO an insulator-to-metal transition temperature,  $T_{\text{IM}}$ , is very close to Curie temperature,  $T_{\text{C}}$ , i.e.  $T_{\text{IM}}=T_{\text{C}}=190$  K. To distinguish insulator-to-metal transition the temperature measurements of SHG intensity at resonant laser pump energy of 1.725 eV were carried out. The SHG intensity decreases significantly near  $T_{\text{IM}}$  as the temperature increases. A minimum of the SHG signal at  $T_{\text{IM}}=190$  K is shifted by about 15 K when magnetic field of 6 kOe is applied; this is consistent with the field-induced shift of insulator-to-metal transition, observed by other techniques [3].

The work is partly supported by DAAD.

[1] A. S. Moskvina et al., Phys. Rev. B **82**, 035106 (2010).

[2] G. Singh-Bhalla, A. Biswas, A. F. Hebard. Phys. Rev. B **80**, 144410 (2009).

[3] T. Z. Ward et al., Nature Phys. **5**, 885 (2009).

## Random formation of coherent spin-wave envelope solitons from incoherent microwave signal

L. D. Carr<sup>1</sup>, B. A. Kalinikos<sup>2</sup>, P. Krivosik<sup>3</sup>, W. Tong<sup>3</sup>, C. E. Patton<sup>3</sup>, and M. Wu<sup>3</sup>

<sup>1</sup>*Department of Physics, Colorado School of Mines, Golden, Colorado 80401, USA*

<sup>2</sup>*St. Petersburg Electrotechnical University, 197376, St. Petersburg, Russia*

<sup>3</sup>*Department of Physics, Colorado State University, Fort Collins, Colorado 80523, USA*

For many years envelope solitons generally have been taken as coherent entities (see e.g. [1]). In recent years, however, there has been increased interest in the formation of incoherent solitons from incoherent waves. The concept of incoherent solitons was suggested as early as in 1977 [2]. The experimental observation of such solitons, however, has taken nearly 20 years to be realized. Specifically, it has been discovered that incoherent optical spatial solitons could be formed from spatially and temporally incoherent light beams [3,4]. For the formation of such incoherent optical solitons, the medium must have a non-instantaneous nonlinearity.

This work reports on the formation of temporal spin-wave envelope solitons from incoherent waves in a medium with an instantaneous nonlinearity. The obtained results demonstrate the first realization of coherent solitons from incoherent waves. It is found that if one excites a temporal packet of incoherent waves in a one-dimensional nonlinear dispersive medium, one can observe a fundamentally new type of soliton, a so-called random soliton. Such solitons randomly appear from the propagating wave packet, with random peak amplitude, random timing, and a short lifetime. In spite of the incoherent nature of the propagating wave packet and the random nature of the soliton generation process, the solitons, when realized, show coherent properties of the sort found for usual bright, gray, and black envelope solitons.

The experiments were performed for the so-called backward volume spin waves and surface spin waves in a magnetic yttrium iron garnet (YIG) film strip. Pulses of microwave noise were used to excite incoherent spin-wave packets at one end of the YIG strip. The propagation of such packets along the YIG strip was probed by microstrip line transducers.

The nonlinear response time of the YIG film is inversely proportional to the power of the carrier SW. The correlation time of the incoherent packet is determined by the bandwidth of the incoherent spin-wave signals. When the spin-wave amplitude is sufficiently large to push the nonlinear response time below the correlation time, the carrier spin waves experience an instantaneous nonlinearity and random coherent solitons appear [5].

In conclusion, the investigated type of random spin-wave soliton phenomena should be common to a wide range of nonlinear dispersive soliton supporting systems.

[1] M. Remoissenet, *Waves Called Solitons: Concepts and Experiments* (Springer-Verlag, Berlin, 1996).

[2] A. Hasegawa, *Phys. Fluids* **20**, 2155 (1977).

[3] M. Mitchell, et al., *Phys.Rev. Lett.*, **77**, 490 (1996).

[4] Z. G. Chen, et al., *Science* **280**, 889 (1998).

[5] W. Tong, M. Wu, L. D. Carr, and B. A. Kalinikos, *Phys. Rev. Lett.*, **104**, 037207 (2010).

## Magnon magnetometry by XMCD and spin wave propagation in wires

G. Woltersdorf, H. G. Bauer , P. Majchrak, A. Ranzinger and C. H. Back  
*University of Regensburg, 93040, Regensburg, Germany*

Using X-ray magnetic circular dichroism (XMCD) we directly measure the transverse components of the precessing magnetization in a thin Permalloy films under cw microwave excitation. Since the dynamic signal can be calibrated by XMCD hysteresis loops the excursion angle of the magnetization can be evaluated. At large microwave fields the susceptibility becomes non-linear due to the excitation of parametric spin waves (Suhl instability) [1]. In addition the XMCD experiment also allows us to measure the decrease of the time averaged longitudinal component of the magnetization at ferromagnetic resonance [2]. By combining both measurements it is possible to separate coherent and incoherent components of the magnetic excitation in the non-linear regime. In doing so we are able to determine the density and lifetime of the magnons involved in the non-linear processes

The wave length of propagating spin waves has been determined in thin ferromagnetic films and more recently in structured Permalloy [3-4]. Thin stripes are of particular interest for micron-sized spin wave devices as they may serve as spin wave guides for spin wave logic. For the realization of such devices the knowledge of the damping length of propagating spin waves within the structure is essential. We used a TR-MOKE setup to study propagating magnetostatic spin waves in micron and submicron wide Permalloy stripes. In these experiments the wave length and the damping length can both be directly measured. These results are compared to analytical calculations taking the excitation profile into account. In addition the analytical calculations are used for the interpretation of spin wave Doppler experiments performed using Permalloy wires [5].

- [1] H. Suhl, J. Phys. Chem. Solids **1**, 209 (1957)
- [2] G. Boero *et al.* Appl. Phys. Lett., **87**, 152503 (2005)
- [3] V. E. Demidov *et al.*, Phys. Rev. B **77**, 064406 (2008)
- [4] S. Neusser *et al.*, Phys. Rev. Lett. **105**, 067208 (2010)
- [5] V. Valminck and M. Bailleul, Science **322**, 410 (2009)

## Observation of black spin wave soliton pairs in yttrium iron garnet thin films

M. A. Cherkasskii<sup>1</sup>, Z. Wang<sup>2</sup>, M. Wu<sup>2</sup>, and B. A. Kalinikos<sup>1</sup>

<sup>1</sup>*St. Petersburg Electrotechnical University, 197376, St. Petersburg, Russia*

<sup>2</sup>*Colorado State University, 80523, Fort Collins, Colorado, USA*

A dip in the envelope of a linear carrier wave broadens due to dispersion as the wave propagates. If the wave is nonlinear and its nonlinearity is repulsive, however, this broadening can be cancelled by the nonlinear effect and the dip can become a stable localized excitation – an envelope black soliton. A black soliton has several unique features, and one of them is a phase jump of  $180^\circ$  at the soliton centre. From a physical point of view, a straightforward way to excite a black soliton is to use a black pulse, in other words, a continuous wave with a narrow dip. This approach has indeed been used to excite black solitons for surface spin waves in a single-crystal yttrium iron garnet (YIG) thin film [1]. Theoretically, however, an initial black pulse should not evolve into a single black soliton. Rather, it should develop into a pair of black solitons so that the net phase change is  $0^\circ$  or  $360^\circ$ . This phase condition is needed because the initial excitation signal has no phase difference across the black pulse region and this phase property should be conserved [2]. This presentation reports for the first time the formation of a pair of black solitons from a single black spin-wave pulse. As in [1], experiments were done with a YIG film strip in a surface spin-wave configuration. A pair of black solitons with opposite  $180^\circ$  phase jump was observed in certain power and pulse width ranges. Beyond those ranges, one also observed a single black soliton and multiple black or grey solitons. No matter what the number of solitons was, however, the net phase change across the soliton region was always zero. The experimental results were confirmed by numerical simulations which were based on the complex Ginzburg-Landau equation and the experimental parameters.

This work was supported in part by and the Russian Foundation for Basic Research and the U. S. National Science Foundation.

[1] M. Chen, M. A. Tsankov, J. M. Nash, and C. E. Patton, *Phys. Rev. Lett.* **70**, 1707 (1993).

[2] A. N. Slavin, *IEEE Trans. Magn.* **31**, 3479 (1995).

# Dual tunability of microwave chaos auto-generator based on ferrite-ferroelectric film structure

A. V. Kondrashov<sup>1</sup>, A. B. Ustinov<sup>1</sup>, B. A. Kalinikos<sup>1</sup>, and H. Benner<sup>2</sup>

<sup>1</sup>*St. Petersburg Electrotechnical University, 197376, St. Petersburg, Russia,*

<sup>2</sup>*Darmstadt University of Technology, D-64289, Darmstadt, Germany*

This work reports for the first time generation of chaotic signal in a feedback active ring structure based on ferrite-ferroelectric (“multiferroic”) delay line (DL) with dual magnetic and electric tuning. Experimentally it was observed that the active ring can generate different types of signals, namely, c.w. signal, soliton train and chaotic signals. It was demonstrated that the properties of these auto-generated signals can be controlled by varying of the magnetic field, electric bias field (voltage), and ring gain coefficient.

Our experiments were performed using the YIG-film-based as well as the multiferroic-based feedback ring. The active resonance ring comprising serially connected DL fabricated on ferrite-ferroelectric (multiferroic) structure, a semiconductor microwave amplifier, a tunable attenuator, and a directional coupler. The DL played the role of a nonlinear frequency-controlling element of the active ring. The amplifier compensated for microwave losses in the DL and attenuator. Using the attenuator, it was possible to control the gain for microwave signal circulating in the ring. The signal circulated in the ring was sampled through a directional coupler for spectrum analysis in the frequency domain and waveform analysis in the time domain.

The multiferroic waveguide used in the delay line was manufactured from a YIG film grown on a gadolinium gallium garnet substrate and a barium strontium titanate (BST) ceramic layer, which was pressed from below to the surface of the YIG film. The metallic electrodes covered the BST layer from below and top were used to apply voltage creating a bias electric field. All the experiments were done for the three common directions of the bias magnetic field. To excite and receive waves in the multiferroic waveguide two microstrip antennae were used.

The experiments demonstrated that with increasing the gain coefficient for all the investigated directions of magnetic field and the magnitudes of electric field the auto-generation regime was changing from monochromatic generation to generation of periodic sequence of pulses, and then to wide-band chaotic signal generation. It was observed that a change of the magnetic field direction led to a slope change in the fractal dimension vs. gain dependence. It means that it is possible to tune the parameters of the chaotic generator through choosing a combination of magnetic field and gain coefficient. Also, tuning of the generator can be realized by changing electric bias voltage applied to the ferroelectric layer. In particular, it was shown that increasing of the bias voltage led to increase of the fractal dimension of the generated microwave dynamical chaos, as shown on Fig.1.

This work was supported in part by the Russian Foundation for Basic Research, the Ministry of Education and Science of the Russian Federation, and by the Deutsche Forschungsgemeinschaft.

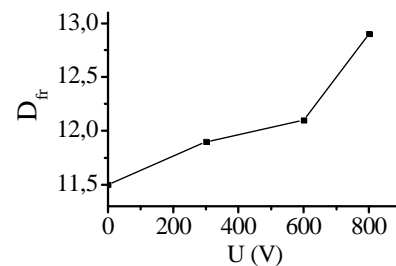


Fig.1 Dependence of fractal dimension on bias voltage

# Non-linear spin-wave phenomena in chiral molecular magnets

R. Morgunov<sup>1</sup>, F. Mushenok<sup>1</sup>, O. Koplak<sup>2</sup>

<sup>1</sup>*Institute of Problems of Chemical Physics, 142432, Chernogolovka, Russia*

<sup>2</sup>*Taras Shevchenko University of Kyiv and NAS of Ukraine, 01033, Kyiv, Ukraine*

Molecular metal-organic magnets provide an inimitable possibility of relatively straightforward tailoring of their electronic and magnetic structure by chemical methods and, thus, open vast prospects for research and management of spin-wave processes in crystals. One of the most important examples of such a chemical design is chiral molecular magnets. The structural chirality of these compounds induces the chirality of the spin density. The goal of this work is determination of feature of spin excitation in chiral molecular ferrimagnet  $[\text{Mn}\{(\text{R/S})\text{-pn}\}_2][\text{Mn}\{(\text{R/S})\text{-pn}\}_2\text{H}_2\text{O}][\text{Cr}(\text{CN})_6]$  (YN) at different spin precession amplitudes.

At low amplitude of spin precession (microwave power  $P < 0.2$  mW) FMR spectra of YN crystal contain two line sequences [1]. “Left-hand” sequence **1a**, **2a**, **3a**... are peaks whose amplitudes decrease as the magnetic field decreases. Resonant fields of left-hand sequence obey to conditions of spin-wave resonance in thin films. “Right-hand” sequence **1b**, **2b**, **3b**... are peaks whose amplitudes decrease as the magnetic field increases (fig. 1). Dependence of resonant fields of right-hand sequence on the peak number is in agreement with theoretical prediction for spin-soliton excitation in chiral magnets [2].

At microwave power higher threshold value  $P_{\text{th}} \sim 0.2 - 1$  mW sharp transformation of the line shape and change of the ferromagnetic resonance field were observed in the YN crystal. FMR spectra obtained at increasing and decreasing magnetic field are different (fig. 2). The obtained results are explained by development of spin-wave instability due to high amplitude of spin precession (foldover) [2].

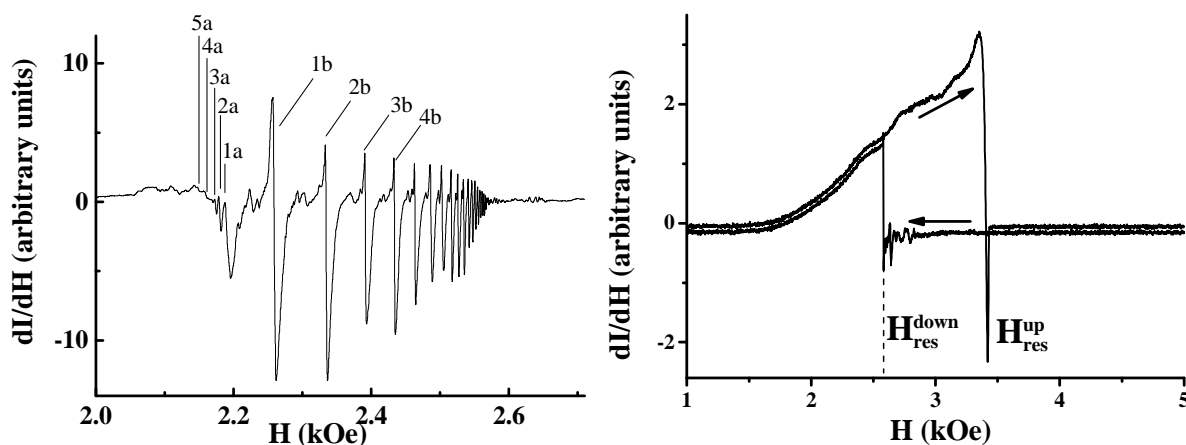


Fig. 1. FMR spectra of YN crystal,  $T=4$  K,  $P = 0.02$  mW.

Fig. 2. FMR spectra of YN crystal obtained at different directions of the magnetic field sweep,  $T=4$  K,  $P = 2$  mW.

Thus, in chiral molecular ferrimagnet  $[\text{Mn}\{(\text{R/S})\text{-pn}\}_2][\text{Mn}\{(\text{R/S})\text{-pn}\}_2\text{H}_2\text{O}][\text{Cr}(\text{CN})_6]$  non-linear spin excitations were detected. At low angle of spin precession spin-soliton and spin-wave resonances is observed. At angle of spin precession exceeding threshold value spin foldover is appearing.

[1] R.B. Morgunov, M.V. Kirman, K. Inoue et al., *Phys. Rev. B* **77**, 184419 (2008).

[2] J. Kishine, K. Inoue, Y. Yoshida, *Prog. Theor. Phys.* **159**, 82 (2005).

[3] R.B. Morgunov, F.B. Mushenok, O. Kazakova *Phys. Rev. B* **82**, 134439 (2010).



# Self-generation of chaotic dissipative soliton trains in active feedback rings based on the ferromagnetic film

S. V. Grishin, Yu. P. Sharaevskii and E. N. Beginin  
*Saratov State University, 410012, Saratov, Russia*

It is well known, that self-generation of a chaotic microwave (MW) signal in active feedback rings based on the ferromagnetic film is observed when parametric three-wave interactions of spin waves are presented [1, 2]. The last experimental investigations have shown that quasiperiodical chaotic MW pulse trains can be generated in ferromagnetic film feedback rings [3-5]. These structures are formed, when the following three conditions are met: i) existence of parametric three-wave interaction; ii) presence of a frequency filtration; and iii) synchronization of spin-wave self-modulation frequencies. In this case, a power spectrum is continuous, an envelope quasiperiodical changes in time, and a phase change of envelope is chaotic. Structures localized in space or time, formed in the systems with amplification and loss, are known as dissipative solitons [6]. The quasiperiodical dissipative soliton trains which have a chaotic phase change we will call the chaotic dissipative solitons.

In this paper, we demonstrate two methods of the self-generation of chaotic dissipative soliton trains. First method is based on self-synchronization of the spin-wave self-modulation frequencies. Self-synchronization is observed in the case of one mode or multimode excitation in the active feedback rings. In the case of one mode excitation, the self-generation of the chaotic dissipative soliton trains appears either of the self-synchronization of the spin-wave self-modulation frequencies on a small nonlinearity of the power amplifier [4] or of the self-synchronization of the spin-wave self-modulation frequencies with the parametric satellites of the second type. In the case of multimode excitation, a self-generation of the chaotic dissipative soliton trains appears because of the self-synchronization of the spin-wave self-modulation frequencies of two modes [3].

Second method is based on a passive synchronization of the spin-wave self-modulation frequencies. It is well known, that parametric three-wave interactions lead to the presence of the magnetostatic spin wave (MSW) nonlinear loss. The last causes, in particular, the occurrence of saturable absorption of an MW signal, passing through a microstrip transmission line loaded on the ferromagnetic film. In the MW range, a nonlinear element that has the saturable absorption of an MW signal is known as an MSW signal-to-noise enhancer. Passive synchronization is carried out by the various types of MSW signal-to-noise enhancers used in the active feedback rings [5]. In this case, the dissipative solitons have a pulse ratio greater than a pulse ratio of the dissipative solitons obtained by the self-synchronization.

This work was supported by the Grants from Russian Foundation for Basic Research (project No. 11-02-00057), the President of Russian Federation for Support of Leading Scientific Schools (project No. 3407.2010.2) and the Government of Russian Federation for Support of Scientific Research in the Russian Universities Under the Guidance of Leading Scientists (project No. 11.G34.31.0030).

- [1] V. E. Demidov and N. G. Kovshikov, *Tech. Phys. Lett.* **24**, 274 (1998).
- [2] A. M. Hagerstrom, W. Tong, M. Wu, B. A. Kalinikos, R. Eykholt, *Phys. Rev. Lett.*, **102**, 207202 (2009).
- [3] E. N. Beginin, S. V. Grishin, and Yu. P. Sharaevsky, *JETP* **88**, 647 (2008).
- [4] S. V. Grishin, B. S. Dmitriev, Yu. D. Zharkov and et al., *Tech. Phys. Lett.* **36**, 76 (2010).
- [5] E. N. Beginin, S. V. Grishin, and Yu. P. Sharaevskii, *Tech. Phys. Lett.* **36**, 1042 (2010).
- [6] N. N. Akhmediev and A. Ankiewicz (Eds.), *Dissipative solitons* (Springer-Verlag, Berlin, 2005).

# Envelope solitons formation in magnonic crystals near the band gap

M. A. Morozova, Yu. P. Sharaevskii and S. E. Sheshukova  
*Saratov State University, 410012, Saratov, Russia*

In recent years, because of rapid advances in the technology of thin-film magnetic materials and development of new approaches to obtain periodic structures, the production of crystals based on magnetic materials - magnonic crystals (MC), has produced great interest. The MC, by analogy with the photonic crystals, demonstrate more interesting nonlinear phenomena in comparison with the effects observed in homogeneous ferromagnetic films. However, we can conclude that the nonlinear processes in such periodic structures, including those associated with the peculiarities of formation of solitons, are insufficiently investigated. There are very few specific studies in this field [1, 2] that show the experimental and numerical simulation results based on one-dimensional nonlinear Schrodinger equation (NSE).

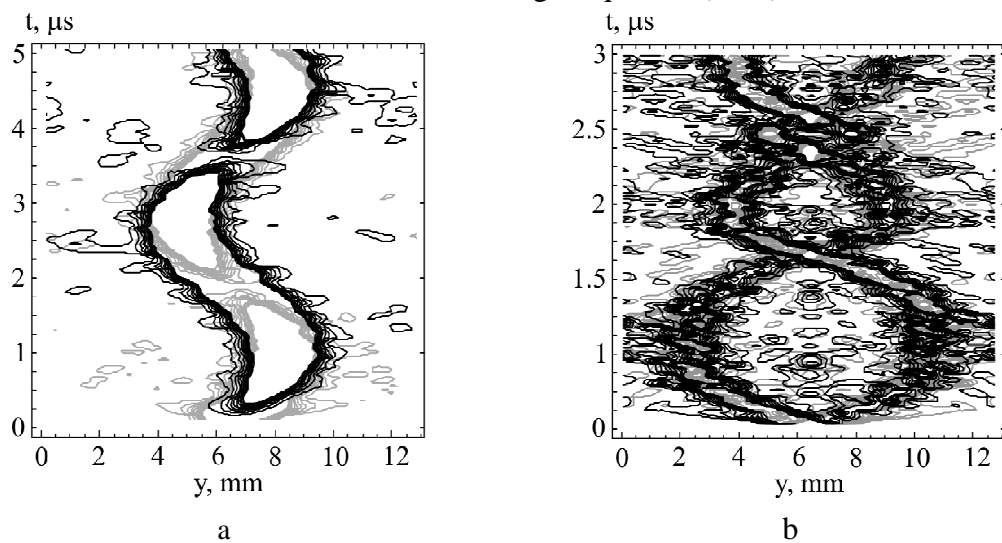


Fig. 1 Lines of equal level of envelope amplitudes for forward wave  $\varphi_f$  (shown by gray color) and backward wave  $\varphi_b$  (shown by black color); when  $\varphi_f \neq 0, \varphi_b = 0$  (a),  $\varphi_f = \varphi_b \neq 0$  (b).

In this work, the model based on coupled NSE for the envelope amplitude forward and backward waves was used to calculate the parameter spaces corresponding to solitons, similar Bragg solitons (BS) with different properties. In particular, the basic mechanism of formation of solitons, similar to BS, and solitons, localized on the limited length of structure (Fig.1), is mutual capture of pulses on the forward and backward waves, which move with the cumulative velocity. Features of wave evolution depending on coupling parameter and group velocity and the areas of parameters corresponding to formation of pulses, similar to BS and solitons localized on the limited length of structure, are investigated.

This work was supported by Federal Targeted Programme of the Ministry of Education and Science (project № 2010-1.2.2-123-019-002) and the Government of Russian Federation (project № 11.G34.31.0030).

[1] A. B. Ustinov, N. Yu. Grigoreva and B. A. Kalinikos, JETP Lett. **88**, 31 (2008).

[2] A. V. Drozdovskii, M. A. Cherkasskii, A. B. Ustinov, N. G. Kovshikov and B. A. Kalinikos, JETP Lett. **91**, 16 (2010).

## Control of spin-wave emission characteristics of spin-torque nano-oscillators

Vladislav E. Demidov<sup>1</sup>, Sergei Urazhdin<sup>2</sup>, and Sergej O. Demokritov<sup>1</sup>

<sup>1</sup>*Institute for Applied Physics, University of Muenster, 48149, Muenster, Germany*

<sup>2</sup>*Department of Physics, West Virginia University, WV 26506, Morgantown, USA*

In this talk I review our recent achievements in experimental investigations of spin-wave emission by spin-torque nano-oscillators (STNOs) and studies on the control of the emission characteristics. The experiments were performed by using micro-focus Brillouin light scattering (BLS) spectroscopy [1], which allowed recording of two-dimensional spin-wave intensity patterns with the spatial resolution of about 250 nm. The studied STNOs were lithographically-prepared point contacts with dimensions below 100 nm made on an extended permalloy film.

We show that STNOs emit spin waves in a form of highly-directed beams perpendicular to the direction of the static magnetic field [2]. The efficiency of emission is strongly affected by the nonlinear frequency shift. We demonstrate that the propagation length of the emitted spin waves can be controlled by nonlinear frequency conversion [3], as well as by modification of the internal magnetic fields under the point contact using micro-magnets built into STNO devices.

[1] S. O. Demokritov and V. E. Demidov, *IEEE Trans. Mag.* **44**, 6 (2008).

[2] V. E. Demidov, S. Urazhdin and S. O. Demokritov, *Nature Materials* **9**, 984 (2010).

[3] V. E. Demidov et al., *Phys. Rev. B* **83**, 060406(R) (2011).

## Atomistic spin dynamics simulations of ferrimagnetic resonance

J. Hellsvik<sup>1,3</sup>, J. H. Mentink<sup>2</sup>, L. Bergqvist<sup>1</sup>, D. Iușan<sup>1,3</sup>, A. Bergman<sup>1</sup>, Th. Rasing<sup>2</sup>,  
M. Katsnelson<sup>2</sup>, and O. Eriksson<sup>1</sup>

<sup>1</sup>*Department of Physics and Astronomy, Uppsala University, Sweden,*

<sup>2</sup>*Radboud University Nijmegen, Institute for Molecules and Materials, The Netherlands,*

<sup>3</sup>*Consiglio Nazionale delle Ricerche, CNR-SPIN, L'Aquila, Italy*

Atomistic spin dynamics simulations [1,2] have been used to investigate the dynamic properties of a two-component ferrimagnet (FiM) as function of temperature. We demonstrate that there is a distinct difference between a two-macrospin description and an atomistic description. At temperatures where the magnetic system is close to the magnetic and angular momentum compensations points, the relaxation in a uniaxial easy axis anisotropy resembles results in recent experiments on FiM resonance [3].

The simulations were performed for a model FiM with two different species of magnetic atoms, with magnetic moments  $M_1=2.0\mu_B$  and  $M_2=1.0\mu_B$ . The exchange interactions were chosen so that magnetic compensation occurs at  $T_M=180$  K and the Curie temperature is  $T_C\approx 700$  K. With unequal Landé g-factors for the  $M_1$  atoms and the  $M_2$  atoms, the angular momentum compensation temperature  $T_A$  is shifted above  $T_M$  to  $T_A=200$  K.

To distinguish the effects between dynamics in external magnetic field and in magneto-crystalline anisotropy field, separate simulations were performed with only one kind of driving field present at the time. The primary case is relaxation in an external field. Starting at an angle to the external field, the magnetization evolves in damped precession towards the energy minimum. As expected for a FiM, both the precession frequency and the relaxation time depends on the temperature. Due to the strong exchange coupling the magnetic sublattices remain close to antiparallel, also in the immediate vicinity of the compensation points. The frequencies related to the magnetization components transversal to the applied field are associated with the ferromagnetic (FM) mode [4] and the exchange mode [5] respectively. Far away from the compensation points the FM mode has similar frequencies for the case of the commonly used expression from linearised FiM theory, macrospin simulations and atomistic simulations. Approaching the compensation points, the frequency branches separate, with the linearised theory giving a divergence-like peak, the macrospin simulations a strong peak and the atomistic simulations only a modest peak. We analyse the differences between the three models and argue that the atomistic model is the only one that show both proper precession frequencies and relaxation times when compared to damped precession of actual FiMs.

The simulations of precession in a uniaxial anisotropy were performed with the initial magnetic configuration tilted from the symmetry axis. Remarkable is here that the frequency of the FM mode does not drop to zero around  $T_M$ . This is precisely what was observed in experiments on FiM resonance of GdFeCo [3].

[1] B. Skubic *et al.*, J. Phys.: Condens. Matter **20**, 315203 (2008).

[2] J. H. Mentink, *et al.*, J. Phys.: Condens. Matter **22**, 176001 (2010).

[3] C. D. Stanciu *et al.*, Phys. Rev. B. **73**, 220402(R) (2006).

[4] R. K. Wangsness, Phys. Rev. **93**, 68 (1954).

[5] C. Kittel, Phys. Rev. B **82**, 565 (1951).

# The model of ultrafast magnetization reversal without femtosecond spin dynamics

M. I. Kurkin<sup>1</sup> and N. B. Orlova<sup>2</sup>

<sup>1</sup>*Institute of Metal Physics UrB RAS, 620041, Ekaterinburg, Russia*

<sup>2</sup>*Department of Applied and Theoretical Physics, Novosibirsk State Technical University, 630092  
Novosibirsk, Russia*

The formation of the reverse magnetization domain under the effect of circularly polarized pumping with the duration  $\tau_p = 40\text{fs} = 4 \cdot 10^{-14}\text{s}$  [1] is considered as the challenge for the existing theory of spin magnetism, according to which the corresponding times of the spin dynamics  $\tau_s$  must belong to the nanosecond range ( $\tau_s > 10^{-10}\text{s}$ ). To overcome such a strong discrepancy between theoretical predictions and experimental results the model is suggested [2] based on the existence of the intermediary state between the optical pumping ( $h\nu$ ) and ordered spins (S). The intermediary state should have time to respond to the femtosecond optical pumping with the duration  $\tau_p$  and should keep the consequences of this reaction in the nanosecond time intervals. For the role of such the intermediary state, the orbital angular momentum of the electrons L (Fig. 1) is proposed [2].

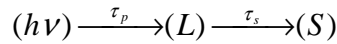


*Fig 1.*

Three properties of the electron spectrum in the crystals may conflict with the role of the orbital angular momentum as an intermediary state:

1. The quenching of the electrons orbital momenta in crystals that prohibits the magnetic quantum number  $m$  to determine the equilibrium states of the electrons.
2. Strong Coulomb interactions determining the dynamics and kinetics of the electrons orbital momenta prevent the existence of slow processes with nanosecond durations.
3. Fast relaxation of excited electrons with femtosecond time scales  $\tau_R$  casts doubt on the ability to save the information on the parameters of the optical pumping during the nanosecond time intervals.

In the report we discuss the possibility of overcoming the obstacles (1) - (3) with the use of conservation laws and the "energy – time" uncertainty relations.

This work was partly supported by Russian Foundation for Basic Research (project 11-02-00093).

[1] C. D. Stanciu et al., Phys. Rev. Lett. **99**, 047601 (2007).

[2] M. I. Kurkin, N. B. Bakulina and R. V. Pisarev, Phys. Rev. B **78**, 134430 (2008).

# Suppression of standing spin waves in low-dimensional magnets

A. Taroni<sup>1</sup>, A. Bergman<sup>1</sup>, L. Bergqvist<sup>2</sup>, J. Hellsvik<sup>1</sup> and O. Eriksson<sup>1</sup>

<sup>1</sup>Department of Physics and Astronomy, Uppsala University, PO Box 516, 751 20 Uppsala, Sweden,

<sup>2</sup>Department of Materials Science and Engineering, KTH Royal Institute of Technology, 100 44 Stockholm, Sweden

Spin-polarized electron energy loss spectroscopy (SPEELS) has recently developed to the point of becoming a powerful method with which to probe spin waves at surfaces and in thin film structures [1]. Landmark experiments have included the measurement of the magnon spectrum of ultrathin Co films on Cu(001) [2], and of a single monolayer (ML) of Fe on W(110) [3]. The experimental accessibility of these properties challenge theoreticians to address a host of issues in nanoscale magnetic structures, from accurately describing the exotic ground states that arise from relativistic spin-orbit coupling effects, to a correct treatment of the dynamics of their spin motions.

We investigate the magnetic properties of a range of thin magnetic films, using a combination of first-principles calculations and atomistic spin dynamics simulations. In particular, we focus on the experimental absence of standing spin wave modes in such systems. Using Co on Cu(001) as a model system, we demonstrate that by increasing the number of layers, the “optical” branches predicted from adiabatic first-principles calculations appear strongly suppressed, in agreement with SPEELS measurements reported in the literature [2]. Our results suggest that, while a direct interpretation of experimental data in terms of linear spin wave theory is insufficient [4], a dynamical analysis is sufficient in order to capture the strong damping of the standing modes.

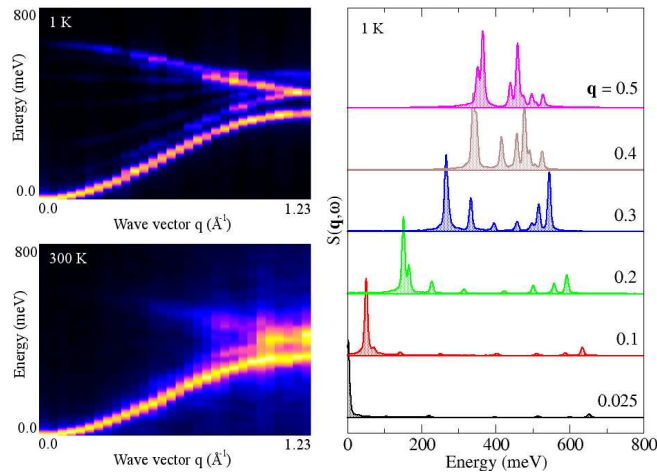


Figure 1: Dynamical structure factor  $S(\mathbf{q}, \omega)$  obtained from ASD simulations for 8 ML Co/Cu(100).

[1] M. Plihal, D. L. Mills and J. Kirschner, *Phys. Rev. Lett.* **82**, 2579 (1999).

[2] R. Vollmer *et al.*, *Phys. Rev. Lett.* **91**, 147201 (2003).

[3] J. Prokop *et al.*, *Phys. Rev. Lett.* **102**, 177206 (2009).

[4] A. T. Costa, R. B. Muniz and D. L. Mills, *Phys. Rev. B* **69**, 064413 (2004).

## Optical and nonlinear-optical studies of Ni nanorods

I. A. Kolmychek<sup>1</sup>, V. L. Krutianskiy<sup>1</sup>, S. I. Mitryukovskiy<sup>1</sup>, E. A. Gan'shina<sup>1</sup>, R. Pollard<sup>2</sup>, R. Atkinson<sup>2</sup>, W. Hendren<sup>2</sup>, A. Murphy<sup>2</sup>, A. V. Zayats<sup>3</sup> and T.V. Murzina<sup>1</sup>

<sup>1</sup>Department of Physics, Moscow State University, 119992 Moscow, Russia

<sup>2</sup>Centre for Nanostructured Media, Queen's University of Belfast, Belfast BT7 1NN, UK

<sup>3</sup>Department of Physics, King's College London, Strand, London WC2R 2LS, UK

Artificial magnetic nanostructures that possess strong structural asymmetry are of high interest as they can reveal new optical and magneto-optical properties. It has been shown in a number of papers that magnetic nanorods can demonstrate plasmonic properties [1] as well as a strong shape-induced anisotropy of their magnetic behavior [2]. Second harmonic generation (SHG) is known as a powerful method sensitive to the main parameters of metallic nanostructures. It allows one to characterize the spectral properties of a medium in two spectral ranges, i.e. corresponding to the fundamental and SHG wavelengths and providing an information on electronic, magnetic and symmetry properties of the structures. In this work, the resonant optical and nonlinear-optical properties of 2D arrays of Ni nanorods are studied.

Nickel nanorods with the diameter of 20 nm and the height of 180 nm were fabricated by electrodeposition of Ni in porous aluminum. Fig. 1 shows the reflectivity spectra measured for different polarizations of the pump beam and reveal a pronounced anisotropy of the optical properties of the samples. Magneto-optical (MO) transversal Kerr effect studied for the magnetic field of 2.5 kOe demonstrates strong discrepancies with the MO response of bulky nickel samples.

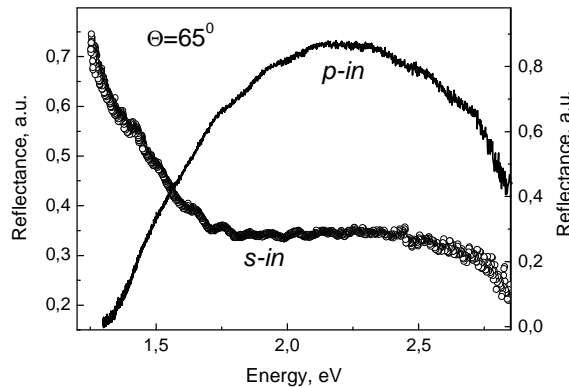


Fig. 1 Reflectance spectra measured at the angle of incidence  $\Theta=65^\circ$  for p- and s-polarizations of the fundamental radiation.

The SHG experiments were performed using a tunable femtosecond Ti-sapphire laser as a fundamental radiation. Pronounced spectral dependencies of the SHG and magnetization-induced SHG are observed. The optical and nonlinear-optical effects are described in terms of resonant plasmon excitation in elongated Ni nanostructures.

[1] G. A. Wurtz, W. Dickson, D. O'Connor, R. Atkinson, W. Hendren, P. Evans, R. Pollard, and A. V. Zayats, *Opt. Express* **16**, 7460 (2008).

[2] A. A. Stashkevich, Y. Roussigné, P. Djemia, S. M. Chérif, P. R. Evans, A. P. Murphy, W. R. Hendren, R. Atkinson, R. J. Pollard, A. V. Zayats, G. Chaboussant, and F. Ott, *Phys. Rev. B* **80**, 144406 (2009).

## Cobalt nanoparticle arrays on fluoride surfaces: growth and MOKE studies

N. S. Sokolov, S. M. Sutorin, S. V. Gastev, A. G. Bانشchikov, D. A. Baranov,  
K. V. Koshmak, V. V. Fedorov, A. V. Nashchekin, A. A. Sitnikova and B. B. Krichevtsov  
*Ioffe Physical-Technical Institute, 194021, St. Petersburg, Russia*

Studies of self-organized magnetic nanoparticle array formation and their magnetic properties attract considerable attention due to increasing needs for high density advanced magnetic storage. In this work, growth by molecular beam epitaxy and magnetic properties of Co nanoparticle arrays on vicinal  $\text{CaF}_2(111)$  and  $\text{MnF}_2(111)$  as well as on grooved and ridged  $\text{CaF}_2(110)$  surfaces were studied. For characterization of the array morphology and shape of the nanoparticles atomic force microscopy (AFM) and electron microscopy (SEM, TEM) have been applied. Structure of the nanoparticles was studied using reflection high-energy electron diffraction during growth and grazing incidence X-ray diffraction at the Photon Factory in Tsukuba (Japan). Magnetic properties of the nanoparticles were characterized by measurements of longitudinal and polar magneto-optical Kerr effects (MOKE).

It was shown that changing growth conditions one can control density and size of the nanoparticles in a wide range. It was found that for small Co exposures the nanoparticles form chains aligned along  $\text{CaF}_2(111)$  surface steps. Structural studies showed dominance of fcc phase and co-orientation of Co and  $\text{CaF}_2$  crystal lattices. Well-pronounced magnetic anisotropy was observed with easy axis along the direction of the chains. Dependence of magnetic anisotropy on Co exposure was studied; the anisotropy was explained by magneto-dipole interaction between the nanoparticles. At higher exposures (up to 50 nm) formation of large (150-200 nm) well-faceted Co epitaxial islands was observed. Hysteresis loops for this case had the shape characteristic of magnetic vortexes formation.

Very strong dependence of surface morphology, crystal structure and magnetic properties on growth conditions was revealed for Co growth on grooved and ridged  $\text{CaF}_2(110)$  surface. Well-pronounced *in-plane* magnetic anisotropy was observed for Co arrays grown at the temperatures below 300°C. In this case cubic (fcc) crystal structure of the nanoparticles was identified. However for growth at 500°C hexagonal crystal structure of the nanoparticles was observed. Measurements of polar MOKE clearly showed presence of *out-of-plane* remanent magnetization.

Interestingly it was found that the coercivity measured by MOKE at room temperature was 3-5 times less for Co nanoparticles grown on  $\text{CaF}_2(111)$  than for those grown on  $\text{MnF}_2(111)$  given the same effective cobalt film thickness of 3-5 nm. Though atomic force microscopy measurements did not show any considerable difference in the surface morphology of the structures, to exclude its possible contribution into the decrease in coercivity of Co on  $\text{MnF}_2(111)$ , additional experiments have been carried out. Half of the sample with Co nanoparticle array grown on  $\text{CaF}_2(111)$  was capped by thin  $\text{MnF}_2$  layer, afterwards whole structure was overgrown by protective thin  $\text{CaF}_2$  layer. Considerable (up to two times) decrease of the coercivity was found in the part of the sample, where Co nanoparticles contacted with  $\text{MnF}_2$  layer. This makes it quite probable that the decrease of the coercivity in Co/ $\text{MnF}_2$  structures is due to the increased magnetic interaction between Co nanoparticles contacting with  $\text{MnF}_2$  layer. This phenomenon has some similarity with the proximity effect observed in Ref. [1], where blocking temperature of Co superparamagnetic nanoparticles was considerably increased when they were covered by Pt layer.

[1] J. Bartolomé et al., Journal of Magnetism and Magnetic Materials **316**, e9 (2007).



# Magnetostatic spin waves propagation in wedge superlattices

Platonov Sergey<sup>1,2</sup>, Nikitov Sergey<sup>1,2</sup>

<sup>1</sup> Russian Academy of Sciences, Institute of Radioengineering and Electronics,  
125009, Moscow, Russia,

<sup>2</sup> Moscow Institute of Physics and Technologies, 141700, Moscow, Russia

Magnonic crystals (MC) are materials with periodically modulated magnetic parameters and represent spin-wave counterpart of photonic crystals [1]. The study of MC has been intensively growing recently; nonetheless there is no general theory of magnetostatic wave propagation in 2D periodic structures [2]. In our work we have studied surface magnetostatic wave propagation in both one-dimensional and 2D magnetic wedge multi-layered structure. Structure thickness linearly depends on MC length. Thickness dependence upon element of the structure prevents us from applying Bloch's theorem in determining the spectrum of magnetostatic waves [3].

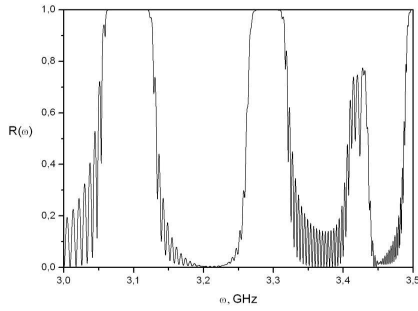


Fig. 1 The frequency dependence of the reflection coefficient

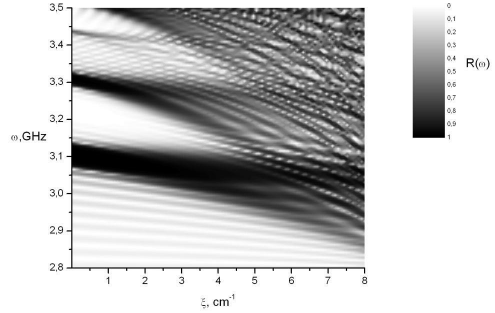


Fig. 2 The frequency dependence of the reflection coefficient for various values of the angular parameter

We use transfer matrix method (TMM) for calculating transmission and reflection spectrum of magnonic crystal [4]. The spectrum of magnetostatic waves in MC forms band structure with forbidden gaps. We have found forbidden band gap width and position dependence on the angle of the wave vector with periodicity direction of the wedge 2D magnonic crystal. It has also been found dependence of band gaps width and position on angular parameter. Forbidden band gaps in spectrum of magnonic crystal are blurred out due to violations of the Bragg's resonance condition for large values of the angular parameter.

The work is supported by Ministry of Education and Science of Russia (agreement #II556).

- [1] Yu.V. Gulyaev and S. A. Nikitov, "Magnonic Crystals and Spin Waves in Periodic Structures," Dokl. Akad. Nauk 380 (4), 469–471 (2001) [Dokl.-Phys. 46 (10), 687–689 (2001)].
- [2] V. V. Kruglyak, S. O. Demokritov, and D. Grundler, J. Phys. D: Appl. Phys. 43, 264001 (2010).
- [3] A.G. Gurevich and G.A. Melkov, *Magnetization Oscillations and Waves*. New York: CRC, (1996).
- [4] M. Born and E. Wolf, *Principles of optics: electromagnetic theory of propagation, interference and diffraction of light*. Oxford, Pergamon Press, (1964).

# Magnetostatic waves propagation in periodic magnetic structures with anisotropy

Yarygin Andrey<sup>1,2</sup>, Platonov Sergey<sup>1,2</sup>, Nikitov Sergey<sup>1,2</sup>

<sup>1</sup> Russian Academy of Sciences, Institute of Radioengineering and Electronics,  
125009, Moscow, Russia,

<sup>2</sup> Moscow Institute of Physics and Technologies, 141700, Moscow, Russia

Magnetic periodic structures have attracted much attention during several past decades. Spectra of magnetostatic wave excitations in such structures are significantly different from those of uniform media and exhibit features such as band gaps, where magnetostatic wave propagation is entirely prohibited.

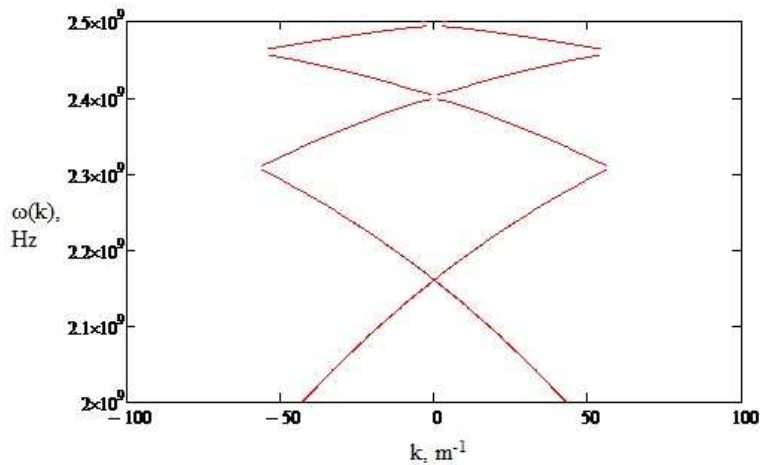


Fig. 1 The frequency dependence of the wave number

In this paper it is shown that the magnetostatic wave dispersion relation takes a simple analytic form when the static magnetization lies in the plane defined by the normal to the plate and the applied magnetic field. Also we have considered dispersion relation with a glance of anisotropy in magnonic crystal [1, 2]. This crystal consists of two ferromagnetic layers of YIG with different magnetization and constants of anisotropy. As a result we obtain the frequency dependence of wave propagation of their wave number. It is plotted qualitative model of the frequency bands allowed for magnetostatic wave propagation.

- [1] A. G. Gurevich and G. A. Melkov, *Magnetization Oscillations and Waves*. New York: CRC, (1996).
- [2] Yu. V. Gulyaev, S. A. Nikitov, L. V. Zhivotovskii, A. A. Klimov, Ph. Tailhades, et al., "Ferromagnetic films with magnon band gap periodic structures: Magnon crystals" [*JETP Letters*, Vol. 77, No. 10, 2003, pp. 567–570.]

# Universal formula for angular width of a diffractive spin wave beam

E. H. Lock

*Kotel'nikov Institute of Radio Engineering and Electronics of Russian Academy of Sciences  
(Fryazino branch)*

*141190, Vvedensky sq.1, Fryazino, Moscow region, Russia*

An examples of well-known physical laws for isotropic media are the laws of geometrical optics and the formula, describing angular width of diffractive beam as a ratio of incident wavelength  $\lambda_0$  and slit length  $D$ . Evidently the question is appear: is it possible to deduce similar universal formula for anisotropic media 2-D geometries? So an attempt is taken to obtain such formula through the study of spin wave diffraction in ferrite slab (for more details see [1]).

To describe dipole spin waves, named usually magnetostatic waves (MSWs), let's use magnetostatics equations  $\text{rot } \mathbf{h} = 0$  and  $\text{div } \mathbf{b} = 0$  and introduce magnetostatic potential  $\Psi$  in agree with formula  $\mathbf{h} = \text{grad}\Psi$  (see [2]). Due to potential  $\Psi$  is scalar function, the study of MSW diffraction become simpler – and we can follow in general by the widely known analytical way, applied for isotropic media, with taking into account noncollinear character of MSW. In particular, for diffraction of the plane surface MSW (MSSW) on the wide slit (MSSW with noncollinear wavevector  $\mathbf{k}$  and group velocity vector  $\mathbf{V}$  is incident on the slit in opaque thin screen with arbitrary orientation) it was shown, that angular distribution of magnetic potential  $\Psi$  in the far-field region is described by the expression of type  $\sim \sin\Phi/\Phi$ , where the phase function  $\Phi$  is more complex, than for isotropic media. It is possible to obtain analytical formula, describing angular width  $\Delta\psi$  of main diffractive MSSW beam in the far-field region:

$$\Delta\psi = \frac{\lambda_0}{D} \left| \frac{d\psi}{d\varphi}(\varphi_0) \right| F \quad (1)$$

Here  $D$  is the length of slit,  $\lambda_0$  – the wavelength of incident MSSW,  $\varphi_0$  – the orientation of the wave vector  $\mathbf{k}_0$  of incident MSSW,  $d\psi/d\varphi$  and  $\psi(\varphi)$  – respectively, derivative and dependence of MSSW group velocity vector orientation angle  $\psi$  on MSSW wavevector orientation angle  $\varphi$ ,  $F$  – function, depending on  $\varphi_0$ , slit orientation  $\theta$  and angular derivative of isofrequency dependence (ID) at  $\varphi = \varphi_0$ . All angles are counted respect to collinear propagation axis, along which vectors  $\mathbf{k}$  and  $\mathbf{V}$  are collinear. Thus, the angular width  $\Delta\psi$  is defined substantially by mathematic properties of ID for the certain wave. If vector  $\mathbf{k}_0$  is normal to the slit line, then  $F \equiv 1$ . In this case for isotropic media (whose ID is circumference, dependence  $\psi(\varphi)$  has the form  $\psi = \varphi$  and  $d\psi/d\varphi \equiv 1$ ) we find from (1) well-known expression  $\Delta\psi = \lambda_0/D$ .

There is a hope, that formula (1), deduced for MSW, will be valid for any anisotropic media and structures for 2-D geometries, including metamaterial structures, that characterized by ID too. As it is seen from the formula (1) an unusual phenomenon may be appear in anisotropic 2-D geometries: if incident wave is characterized by such value  $\varphi_0$  that  $d\psi/d\varphi = 0$  at  $\varphi = \varphi_0$  then  $\Delta\psi = 0$ ! It means, the diffractive beam conserve its wide during propagation! Mention must be made, that ID for not any medium contains the point(s), where  $d\psi/d\varphi = 0$ , but such points present on ID for MSSWs with frequencies near the beginning of the spectrum.

This work is partially supported by the Program “Development of the Scientific Potential of High School” (project No. 2.1.1/1081).

[1]. Lock E. H. Electronic Journal «Investigated in Russia» **084**, 975-1005 (2010).

<http://zhurnal.ape.relarn.ru/articles/2010/084.pdf>.

[2]. Damon R. W., Eshbach J. R. J. Phys. Chem. Solids **19**, 308 (1961).

## Reorientation of 2D magnetic domain patterns in pulsed fields

M. Logunov, M. Gerasimov, N. Loginov and A. Spirin  
National Research Mordovia State University, 430005, Saransk, Russia

2D magnetic domain patterns with  $Cmm2$ ,  $Cmm6$ ,  $P2$ ,  $Pab2$ ,  $P6$  and other symmetry can be formed in garnet films in pulsed or harmonious magnetic fields at presence of constant magnetizing field [1-2]. The patterns consist from topologically modified bubble domains and patterns are statically steady after removal of magnetic fields. Interest to 2D magnetic domain patterns connects with an opportunity of creation on their base operated magneto-phonic devices [3]. Processes of formation of 2D domain structures are actively investigated by means of computer simulations [4-5], including as analogue of processes of ordering in various physical and chemical systems.

In the present work it is generated nine types of the 2D domain patterns described by five space symmetry groups, in the same garnet film with uniaxial anisotropy. Faraday effect was used for observation of domain structure. Labyrinthal domain structure was characteristic structure in demagnetized film. Conditions at which reorientation of patterns (fig.) is possible were found.

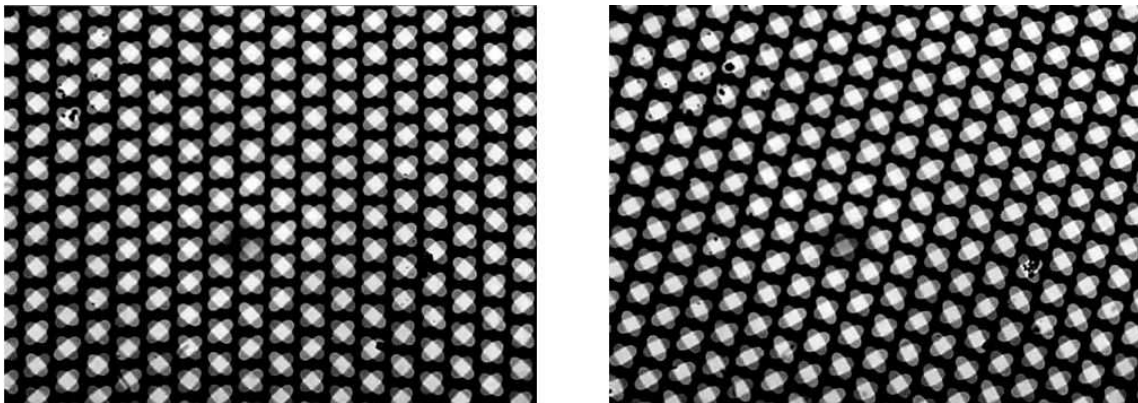


Fig. Initial (left) and reoriented (right) dynamic domain patterns  
(2D pattern with symmetry  $Pab2$  in statics)

Reorientation of domain patterns with  $Cmm6$ ,  $Pab2$ , and  $P6$  symmetry has been studied. It is necessary to put  $10^3 - 10^4$  pulses of magnetic field for turn of patterns on a corner of 90 degrees. Turn of patterns, possibly, is caused by action of gyrotropic forces on extending domains in pulsed field [6]. Parameters of pulses of magnetic field depend on symmetry of 2D pattern and constant magnetizing field.

- [1] F. V. Lisovskii and E. G. Mansvetova, JETP Lett. **55**, 32 (1992), **58**, 784 (1993).
- [2] M. V. Logunov and M. V. Gerasimov, JETP Lett. **74**, 491 (2001).
- [3] Yu. V. Gulyaev, S. A. Nikitov, L. V. Zhivotovskii et al., JETP Lett. **77**, 567 (2003).
- [4] E. Ascitutto, C. Roland, and C. Sagui, Phys. Rev. E **72**, 021504 (2005).
- [5] K. Kudo, K. Nakamura. Phys. Rev. B **76**, 036201; 054111 (2007).
- [6] A. P. Malozemoff, J. C. Slonczewski, *Magnetic Domain Walls in Bubble Materials* (Acad. Press, N.Y., 1979).

# Spin waves in nanosized magnetic films

L. V. Lutsev

*Ioffe Physical-Technical Institute of the Russian Academy of Sciences, 194021, St. Petersburg, Russia*

A microscopic theory is developed for spin-wave excitations in nanosized magnetic films. Generalized Landau-Lifshitz equations and spin wave damping are derived by the spin operator diagram technique for the Heisenberg model with magnetic dipole (MDI) and exchange interactions [1,2]. Spin excitations, which are determined by poles of effective Green functions, are given by solutions of the Landau-Lifshitz equations and the equation for the magnetostatic potential. Spin-wave dispersion relations in normal magnetized 2D spin monolayer and in  $N$ -layered structures are found. The spectrum of spin waves in  $N$ -layered structures has the mode-type character and consists of  $N$  modes. Due to the MDI, the dispersion curve of the first mode at the small wavevector  $q$  is the linear function of  $q$ .

$$\sum_{\substack{(1\mu)(1\nu) \\ (\mu,\nu = +,-)}} = \frac{1}{2B} \begin{array}{c} \text{---} \text{---} \text{---} \\ \text{---} \text{---} \text{---} \\ \text{---} \text{---} \text{---} \end{array} + \frac{1}{(2B)^2} \begin{array}{c} \text{---} \text{---} \text{---} \\ \text{---} \text{---} \text{---} \\ \text{---} \text{---} \text{---} \end{array}$$

$\mu, q, j, \omega_m$        $\nu, q, j', \omega_m$        $\mu, q, j, \omega_m$        $\nu, q, j', \omega_m$

Fig. 1 Self-energy diagrams in the one-loop approximation, which makes a major contribution to the spin-wave relaxation. The factor  $B$  is expressed by the Brillouin function.

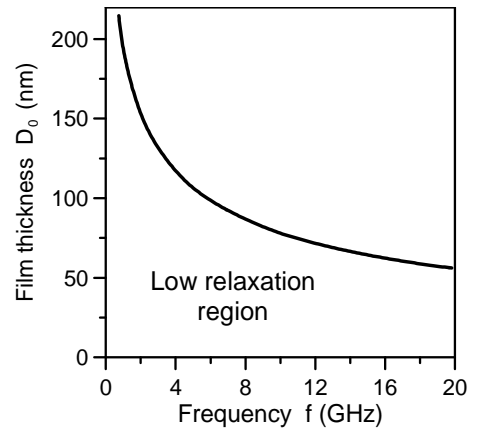


Fig. 2 Low relaxation spin-wave region for normal magnetized YIG films at different frequencies. For film thickness  $D < D_0$  first spin-wave mode with low damping is observed.

The spin-wave damping has been calculated in the one-loop approximation for a diagram expansion of the Green functions. It is found that for the first mode the MDI makes a major contribution to the long-wavelength spin-wave relaxation in comparison with the exchange interaction. The one-loop diagrams correspond with the three-magnon confluence processes induced by the MDI (Fig. 1). If at the given frequency  $f$  the thickness of magnetic film is less than a certain thickness  $D_0$ , then for the first mode the MDI cannot induce three-magnon processes and the one-loop diagrams are equal to zero (Fig. 2). In this case, spin-wave relaxation is determined by non-trivial diagrams only in the two-loop approximation and a low relaxation spin-wave region exists. This gives opportunity to construct low damping spin-wave devices (filters, delay lines) and high quality resonators. This study was supported by the Russian Foundation for Basic Research (project no. 10-02-00516).

[1] L.V. Lutsev, *J. Phys.: Condensed Matter*, **17**(38), 6057 (2005).  
 [2] L.V. Lutsev, *Diagram technique for quantum models with internal Lie-group dynamics*, in: *Mathematical Physics Research Developments*, Editor: Morris B. Levy, (Nova Science Publishers, Inc., 2009), 141.

# Spin pumping and conversion of spin current into charge current in Co/Y<sub>3</sub>Fe<sub>5</sub>O<sub>12</sub> bilayer structure

N. Volkov<sup>1,2</sup>, M. Rauckii<sup>1</sup>, D. Smolyakov<sup>1,2</sup>, E. Eremin<sup>1</sup>, G. Patrin<sup>2</sup>, I. A. Turpanov<sup>1</sup>,  
V. I. Jushkov<sup>1,2</sup>, L. A. Lee<sup>1</sup>

<sup>1</sup>L.V. Kirensky Institute of Physics SB RAS, 660036, Krasnoyarsk, Russia

<sup>2</sup>Siberian Federal University, 660041, Krasnoyarsk, Russia

A great expectation of the spintronics relates to possibilities to manipulate the spin degrees of freedom of the electrons using theirs for the processing, transmitting and storing of information. It is clear, that main efforts of the researches are concentrated on the searching the effective ways to control the spins. The one of the key question here is how easily convert between charge and spin currents? There are two types of carriers for non-equilibrium spin currents: one is a conduction electron, the other is collective motion of magnetic moment. Here we present the results of the study which demonstrate the generation of the spin current from magnetization motion, the spin pumping from a ferrimagnetic insulator to ferromagnetic metal, and, more principal, the converting the spin current into the charge current in the interior of the metal ferromagnetic film. Schematic illustration of the experimental set-up is

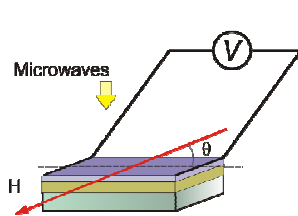


Fig. 1

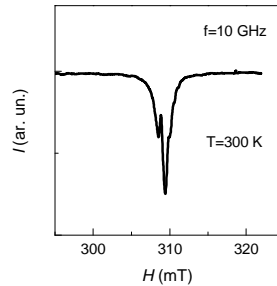


Fig. 2

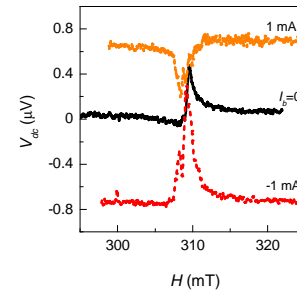


Fig. 3

shown in the Fig. 1. The sample is Co/Y<sub>3</sub>Fe<sub>5</sub>O<sub>12</sub> bilayer film, composed of 1- $\mu$ m-thick garnet layer and 20-nm-thick Co layer. Structure with electrodes attached to the cobalt film is placed at center of a 10 GHz microwave cavity. A static in-plane magnetic field  $H$  is applied during measurement. When  $H$  fulfils ferromagnetic resonance condition, precession of the magnetization in Y<sub>3</sub>Fe<sub>5</sub>O<sub>12</sub> layer is induced (Fig. 2). The main result is shown in Fig. 2. When the resonance precession is excited in Y<sub>3</sub>Fe<sub>5</sub>O<sub>12</sub> layer, the d. c. voltage  $V_{dc}$  is generated in the Co layer. The data in Fig. 3 are obtained at  $\theta=90^\circ$  ( $\theta$  is defined in Fig. 1.),  $V_{dc}$  decreases with decreasing  $\theta$ , and at  $\theta=0^\circ$  the effect vanishes completely. The bias current  $I_b$  through Co layer influences the value and sign of the effect. It depends also on microwave power. The mechanism of voltage generation in our experiments is not clear entirely. Now we can conclude only that observed effect is irrelevant to electromagnetic artefacts, and, in our opinion, it relates to following processes. At first, the spin angular momentum is transferred from magnetization-precession motion to conduction-electron spin trough the Y<sub>3</sub>Fe<sub>5</sub>O<sub>12</sub>/Co interface, as a result, spin current is pumped into Co layer. After that, the spin current in this layer is converted into the charge current. The origin of such conversion in the ferromagnetic metal is lacking for the present (in the case of the paramagnetic metal, the conversion takes place due to spin-orbit interaction [1]). We hope that planned studies allow us to clarify the details of the spin pumping and spin-charge current conversion mechanisms.

[1] Y. Kajiwara, K. Harii, S. Takahashi et al. Nature (London) **464**, 262 (2010).

## Possible mechanisms of magnon sidebands in $\text{KCuF}_3$

M. Eremin, M. Fayzullin

*Institute for Physics, Kazan (Volga Region) Federal University, 420008, Kazan, Russia*

Recently very narrow sidebands were observed in optical absorption spectra of  $\text{KCuF}_3$  for  $T < T_N$  [1], which cannot be described in the framework of conventional mechanisms [2]. For a possible explanation in paper [3] was suggested the following effective operator

$$H_{\text{eff}}^{\text{MD}}(a \rightarrow a') = \frac{\mu_B}{2\Delta} \sum_b \langle a | H_\alpha I_a^\alpha | a' \rangle J_{ab} (\mathbf{S}_a \mathbf{S}_b - 1/4), \quad (1)$$

where  $J_{ab}$  is the superexchange coupling parameter of copper ions in the ground states, and  $\Delta$  is the transfer energy of electron from site (b) to site (a),  $I_a^\alpha$  is  $\alpha$  component of the orbital momentum operator. The virtual process scheme is shown in Fig.1.

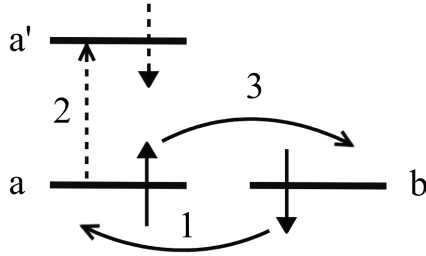


Fig. 1 Virtual scheme of the exchange-induced magnetic dipole transition. Numbers 1 and 3 correspond to electron hopping.

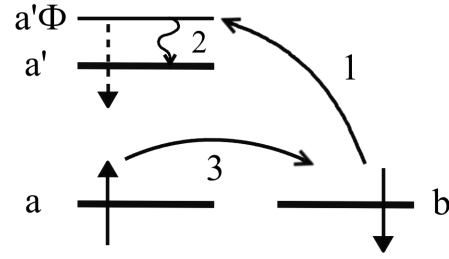


Fig. 2 Virtual scheme of the exchange-induced electric dipole transition. Label 2-corresponds to phonon vibration of bridging fluorine ion.

Now we analyze in addition another possible mechanism of exciton-magnon absorption involving phonon related electric dipole transition. Derived effective operator of magnon related optical absorption is written as

$$H_{\text{eff}}^{\text{ED}}(a \rightarrow a') = \frac{\varepsilon |e|}{\Delta} \sum_b \frac{t_{b,a'\Phi} \langle a'\Phi | E_\alpha u_\alpha | a' \rangle t_{ab}}{|\Delta_{b,a'\Phi}|} (\mathbf{S}_a \mathbf{S}_b - 1/4), \quad (2)$$

where  $\varepsilon$  and  $t$  are dielectric constant and effective hopping integral, correspondently,  $u_\alpha$  is vibration coordinate of fluorine bridge ion. In Fig.2 the spin down of electron from Cu site (b) excites to the state  $a'$  plus phonon  $|a'\Phi\rangle$ , then due to coupling with electric field component  $E_\alpha$  phonon disappear and electron transfer to state  $|a'\rangle$  and finally the spin up from state  $|a\rangle$  jumps to site (b). In both cases summation over surrounding neighbors (index b in Eq. 1, Eq.2) is assumed. Calculations of optical absorptions showed, that discrete sideband structure corresponds to low energy singularities in the magnon density of states. The energy dispersion of the magnons was taken according to neutron scattering data [4].

[1] J. Deisenhofer, I. Leonov, M.V. Eremin et al., Phys. Rev. Lett. **101**, 157406 (2008).

[2] Y. Tanabe, T. Moriya, S. Sugano, Phys. Rev. Lett. **15**, 1023 (1965).

[3] M. V. Eremin, J. Deisenhofer, M.A. Fayzullin et al., Solid State Phenomena **168-169**, 113 (2011).

[4] S.K. Satija, J.D. Axe, G. Shirane et al., Phys. Rev. B **21**, 2001 (1980).

# Ultrafast optical spin manipulation: challenges and opportunities

Theo Rasing

*Radboud University Nijmegen, Institute for Molecules and Materials,  
6525AJ, Nijmegen, The Netherlands*

The interaction of sub-picosecond laser pulses with magnetically ordered materials has developed into an extremely exciting research topic in modern magnetism and spintronics. From the discovery of sub-picosecond demagnetization over a decade ago to the recent demonstration of magnetization reversal by a single 40 femtosecond laser pulse, the manipulation of spins by ultra short laser pulses has become a fundamentally challenging topic with a potentially high impact for future spintronics, data storage and manipulation and quantum computation.

Single-shot pump-probe magneto-optical imaging results show that circularly polarized subpicosecond laser pulses steer the magnetization reversal in a Transition Metal-Rare Earth alloy along a novel and ultrafast route, which does not involve precession but occurs via a strongly nonequilibrium state. However, the nature of this phase and the dynamics of the individual TM and RE moments remained elusive so far. Recent experiments indicate a possible difference in the dynamics of the TM and RE moments at time scales that are currently limited by the pulse widths of the optical excitations employed (~100 fs). To investigate such highly nonequilibrium phases requires both excitation and probing at ultra short time scales and selectivity for the individual moments.

In addition, when the time-scale of the perturbation approaches the characteristic time of the exchange interaction (~10-100 fs), the magnetic dynamics may enter a novel coupling regime where the exchange interaction may even become time dependent. Using ultrashort excitations, we might be able to manipulate the exchange interaction itself. Such studies require the excitation and probing of the spin and angular momentum contributions to the magnetic order at timescales of 10 fs and below, a challenge that might be met by the future fs X-ray FEL's.

- [1] A.V. Kimel et al, *Nature* **435** (2005), 655-657.
- [2] C.D. Stanciu et al, *Phys. Rev. Lett.* **99**, 047601 (2007).
- [3] A.V. Kimel et al, *Nature Physics* **10**, 727-731 (2009).
- [4] K. Vahaplar et al, *Phys. Rev. Lett.* **103**, 117201 (2009).
- [5] A. Kirilyuk et al, *Rev. Mod. Phys.* **82**, 2731-2784 (2010).
- [6] I. Radu et al, *Nature* (2011).



# Spin dynamics of Heisenberg and XY pyrochlore magnets studied by ESR

S. S. Sosin<sup>1</sup>, L. A. Prozorova<sup>1</sup>, O. A. Petrenko<sup>2</sup> and M. E. Zhitomirsky<sup>3</sup>

<sup>1</sup>*P. Kapitza Institute for physical problems, 119334, Moscow, Russia,*

<sup>2</sup>*Department of Physics, University of Warwick, Coventry CV4 7AL, UK,* <sup>3</sup>*SPSMS/INAC/CEA, F-38054 Grenoble, France*

The strong frustration of a nearest-neighbour (NN) exchange interaction in spin systems on a pyrochlore crystal lattice enhances the role of other interactions and fluctuations in magnetic ordering. Various combinations of these forces produce large variety of magnetically ordered states observed in different pyrochlore materials. Using the electron spin resonance spectroscopy (ESR) we compare the low energy spin dynamics of two compounds:  $\text{Gd}_2\text{Sn}_2\text{O}_7$  and  $\text{Er}_2\text{Ti}_2\text{O}_7$ . The first system with weak anisotropy and large  $S=7/2$  of magnetic  $\text{Gd}^{3+}$  ion orders below  $T_N=1$  K in a “plane cross” structure [1]. Three gapped resonance modes were detected in the ordered phase (Fig. 1). The gap values at  $H=0$  are well described by the spin-wave theory (SWT) with natural parameters for the NN exchange, dipolar interaction and single ion anisotropy. The theory also predicts a lowest gap, which determines the exponential decrease in the specific heat at low temperature. The field evolution of two of these branches is peculiar to a planar magnetic structure with an isotropic susceptibility. In the saturated phase ( $H>H_s$ ), weakly dispersive soft modes with linear field dependence are detected [2].

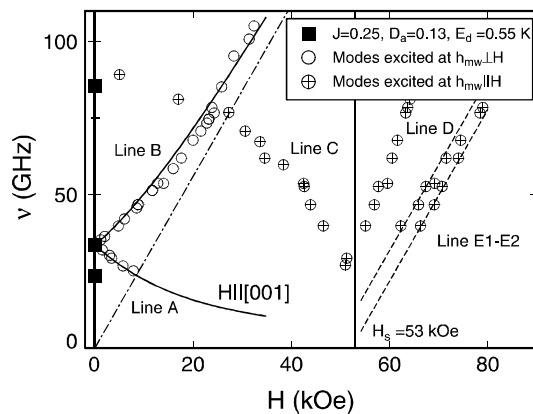


Fig. 1 Frequency-field diagram of  $\text{Gd}_2\text{Sn}_2\text{O}_7$  at  $T=0.45$  K, closed squares are gaps expected from SWT, solid lines is the theory for a “rigid” planar structure at  $H \ll H_s$ .

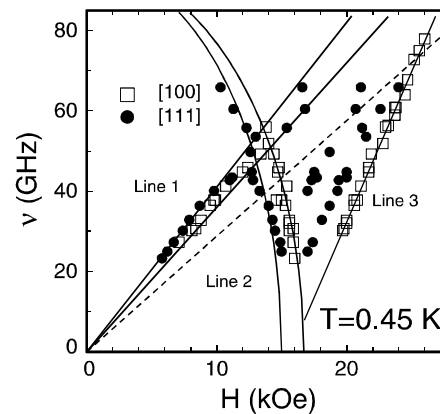


Fig. 2 Three branches of the resonance spectrum of  $\text{Er}_2\text{Ti}_2\text{O}_7$  measured in the ordered phase in two directions of applied magnetic field. Solid lines are guide-to-eyes.

The orbital splitting of  $\text{Er}^{3+}$  ions in the second compound leads to an effective  $S=1/2$  spin system with the strong local XY anisotropy of magnetic moments. The noncoplanar ordering observed at  $T_N=1.2$  K is supposed to result from the effect of fluctuations (order by disorder) [3]. Our ESR measurements reveal the existence of a Goldstone mode acquiring an isotropic “Zeeman” gap under field (see Fig. 2). The second mode has a gap softening near  $H_c \approx 15-16$  kOe at the II order transition into a state with spin canting from local easy planes. The approximately linear in field branch (Line 3) is observed above  $H_c$ . The spin-wave calculations of the excitation spectra in the simplest XY-model should verify that (i) zero-point oscillation can indeed stabilize the required  $H=0$  spin structure and (ii) the resonance spectra observed in various field directions are correctly reproduced by the theory.

[1] A.S. Wills *et al.*, *J. Phys.: Condens. Matter* **18**, L37 (2006).

[2] S.S. Sosin *et al.*, *Phys. Rev B* **79**, 014419 (2009).

[3] J.D.M. Champion *et al.*, *Phys. Rev. B* **68**, 020401(R) (2003).

# Far-IR excitations in multiferroics studied with Müller matrix ellipsometry and transmission spectroscopy using synchrotron radiation

P. D. Rogers<sup>1</sup>, E. Standard<sup>1</sup>, T. D. Kang<sup>1</sup>, M. Kotelyanskii<sup>1,2</sup>, and A. A. Sirenko<sup>1</sup>  
<sup>1</sup>Department of Physics, New Jersey Institute of Technology, Newark, NJ 07102, United States  
<sup>2</sup>Rudolph Technologies Inc., Flanders, NJ 07836, United States

The measurements of both the complex dielectric function  $\varepsilon(\omega)$  and the magnetic permeability  $\mu(\omega)$  spectra using a combination of ellipsometry and transmittance can reveal details of the coupling between magnetic and electric excitations in multiferroic materials. Recently we developed a full-Mueller matrix far-IR spectroscopic ellipsometer (Fig. 1) at the U4IR beamline of the National Synchrotron Light Source (NSLS) in Brookhaven National Laboratory (BNL) [1]. The main application of our ellipsometer is for multiferroic materials, magnetic samples with  $\mu \neq 1$ , and metamaterials [2]. An exceptional brightness of synchrotron radiation allows for measurements in a broad spectral range between 10 and 4,000  $\text{cm}^{-1}$ . For

the quantitative analysis of the optical spectra for materials with  $\mu(\omega) \neq 1$ , we developed an adequate modelling approach, which is based on Berreman's  $4 \times 4$  matrix formalism. Our approach allows to model experimental optical spectra, including spectra of electromagnons in anisotropic magnetic materials, and to separate  $\varepsilon(\omega)$  and the  $\mu(\omega)$  tensor components (Fig. 2). Experimental data for a number of multiferroic and magneto-electric crystals, such as  $RE\text{Mn}_5\text{O}_5$  and  $RE_3\text{Fe}_5\text{O}_{12}$  garnets ( $RE$ =rare earth) will be presented [3-5]. In addition to purely dielectric (phonons) and magnetic modes (magnons, crystal field excitations), we observed several hybrid modes with a mixed magnetic and electric dipole activity [3]. The hybrid modes originate from the ligand field transitions in the  $f$ -shell of the  $RE$  ions modified by exchange interaction with magnetic ions (Fe, Mn). The observed vanishing of certain hybrid modes in the reflectivity spectra has been explained in terms of the adjusted oscillator strength matching condition  $\mu(\omega_h) \cdot S_e = \varepsilon(\omega_h) \cdot S_m$  [3].

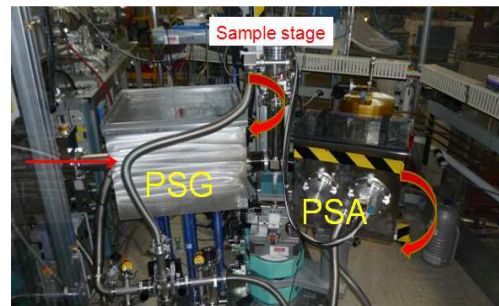


Fig. 1 Ellipsometer at U4IR, NSLS, BNL

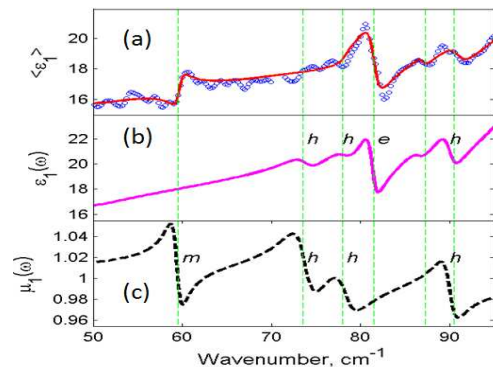


Fig. 2 (a) Ellipsometry data and modelling results for  $\varepsilon(\omega)$  (b), and  $\mu(\omega)$  (c) for  $\text{Dy}_3\text{Fe}_5\text{O}_{12}$  magneto-electric crystal.

- [1] T. D. Kang, E. Standard, G. L. Carr, T. Zhou, M. Kotelyanskii, and A. A. Sirenko, *Thin Solid Films*, **519**, 2698 (2011).
- [2] P. D. Rogers, T. D. Kang, T. Zhou, M. Kotelyanskii, and A. A. Sirenko, *Thin Solid Films* **519**, 2668 (2011).
- [3] P. D. Rogers, Y. J. Choi, E. Standard, T. D. Kang, K. H. Ahn, A. Dudroka, P. Marsik, C. Bernhard, S. Park, S-W. Cheong, M. Kotelyanskii, and A. A. Sirenko, *Phys. Rev. B* (2011) arXiv:1101.2675v1 [cond-mat.str-el].
- [4] T. D. Kang, E. Standard, K. H. Ahn, and A. A. Sirenko, G. L. Carr, S. Park, Y. J. Choi, M. Ramazanoglu, V. Kiryukhin, and S-W. Cheong, *Phys. Rev. B* **82**, 014414 (2010).
- [5] A. A. Sirenko, S. M. O'Malley, and K. H. Ahn, S. Park, G. L. Carr, and S-W. Cheong, *Phys. Rev. B* **78**, 174405 (2008).

# Collapsing bullet and subwavelength spin-wave beams

A. A. Serga<sup>1</sup>, M. P. Kostylev<sup>2</sup>, and B. Hillebrands<sup>1</sup>

<sup>1</sup>*Fachbereich Physik and Forschungszentrum OPTIMAS, Kaiserslautern University of Technology, Kaiserslautern 67663, Germany*

<sup>2</sup>*School of Physics, University of Western Australia, WA 6009, Crawley, Australia*

The formation of quasi-two-dimensional nonlinear spin-wave eigenmodes – so-called guided spin-wave bullets [1] – in longitudinally magnetized stripes of a ferrimagnetic (yttrium iron garnet) film has been experimentally observed using time and space-resolved Brillouin light scattering (BLS) spectroscopy and confirmed by numerical simulation.

Spin-wave bullets are stable spin-wave packets which propagate along a waveguide structure, for which both transverse instability and interaction with the edges of the waveguide are important. It has been found that if its amplitude is increased, a bullet can become destabilized. Under these circumstances a pronounced two-dimensional compression of the spin-wave packet followed by a wave collapse are observed [2]. We show both theoretically and experimentally that a collapsing two-dimensional wave packet in a medium with cubic nonlinearity and a two-dimensional dispersion of higher than parabolic order radiates untrapped dispersive waves (Fig. 1).

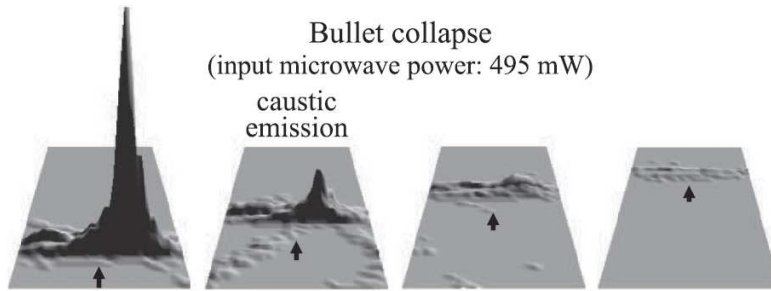


Fig. 1 Snapshots of collapsing spin-wave bullet measured at 50 ns time intervals by time- and space-resolved BLS spectroscopy. Arrows show the bullet propagation direction.

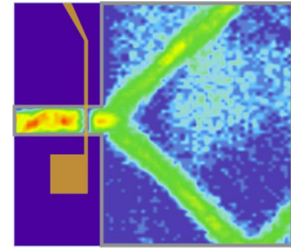


Fig. 2 Measured intensity of the spin-wave beams irradiated by an immobile point source.

Induced uniaxial anisotropy in an in-plane magnetized ferrimagnetic film sample leads to the formation by these waves of narrow beams symmetrically arranged relative to the bias magnetic field. We describe the radiation from a collapsing spin-wave bullet with reference to our observations of the excitation of non-diffractive spin-wave beams with a stable sub-wavelength transverse aperture – spin-wave caustics – by an immobile point source (see Fig. 2) [3]. We demonstrate that the caustic angles to the bullet's propagation direction are significantly modified by the motion of the source. The contribution of both the inverse Doppler frequency shift [4] and a Galilean transformation to the angles' values is analysed. The peculiarities of the phenomenon are well described by the theoretical model. Support by the DFG within the SFB/TRR 49, the Australian Research Council, and the University of Western Australia is gratefully acknowledged.

- [1] A. A. Serga, M. P. Kostylev, and B. Hillebrands, *Phys. Rev. Lett.* **101**, 137204 (2008).
- [2] M. P. Kostylev, A. A. Serga, and B. Hillebrands, *Phys. Rev. Lett.* **106**, 134101 (2011).
- [3] T. Schneider et al., *Phys. Rev. Lett.* **104**, 197203 (2010).
- [4] A. V. Chumak et al., *Phys. Rev. B* **81**, 140404(R) (2010).

**Abstracts**

**Poster Session**

## Elementary excitation spectra of $\text{Fe}_x\text{Mn}_{1-x}\text{S}$ single crystals

G. Abramova<sup>1</sup>, M. Boehm<sup>2</sup>, O. Bolsunovskaya<sup>1</sup>, B. Ouladdiaf<sup>2</sup>

<sup>1</sup>L. V. Kirensky Institute of Physics, Russian Academy of Sciences, Siberian Branch,  
Krasnoyarsk, 660036 Russia

<sup>2</sup>Institut Laue-Langevin, 38042 Grenoble, Cedex 9, France

$\text{Fe}_x\text{Mn}_{1-x}\text{S}$  ( $0 < x < 0.3$ ) are new Mott-type substances with rock salt structure of  $\alpha\text{-MnS}$  and belong to the MnO-type substances with strong electron correlations. Applying hydrostatic pressure to such a system leads to a number of possibilities, including an insulator-metal transition, moment reduction (that is, a high-spin to low-spin transition), a change in crystal symmetry [1, 2]. The pressure effects on their magnetic and crystal structures still are not fully understood [3]. We have used the chemical pressure (the cation substitution in the MnS matrix) in order to induced the change of the physical properties, which is similar of applying hydrostatic pressure. In present work the results of inelastic neutron scattering of  $\text{Fe}_x\text{Mn}_{1-x}\text{S}$ , single crystals synthesized on the base of  $\alpha\text{-MnS}$  are compared with the calculated spectra of elementary excitations. X-ray and neutron diffraction studies [4] have shown that the cubic NaCl parameter decreases from 5,224 Å ( $x=0$ ) to 5,165 Å ( $x=0,29$ ) with increasing of the cation substitution in  $\text{Fe}_x\text{Mn}_{1-x}\text{S}$  single crystals. The Neel temperature increases from 150K to 200K. The inelastic neutron scattering spectra measured on IN3 in the temperature range 2 - 270K and energy const-E scans between  $2 \leq E \leq 10$  meV along the main symmetry axis (qqq) and (00q). The magnetic Lauegram are shown on Fig.1. The measured spectra Fig. 2 are have been fitted with a function:  $E=D*\cos(\pi*q)$ , with  $D=41$  meV for the qqq direction and  $D=20$  meV for the 00q direction.

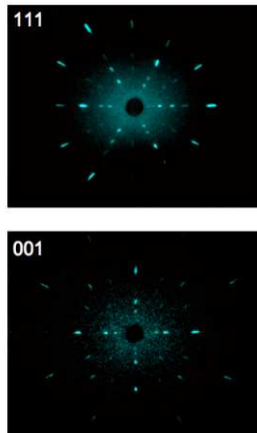


Fig. 1 Magnetic Lauegram measured on the OrientExpress (Laue diffractometer) at 10K.

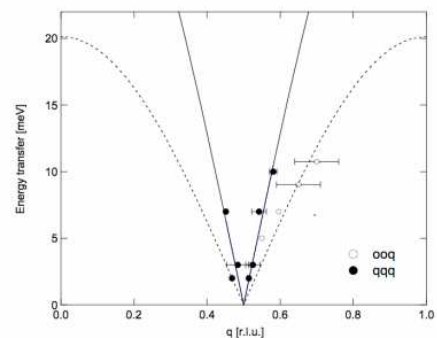


Fig. 2 Dispersion along the main symmetry axis qqq and 00q.

Theoretical analyses of spin-wave spectra for MnS and its solid solutions are made in the frame of Heisenberg model.

[1] D. Kasinathan, et al. PRB **74**, 195110 (2006).

[2] R. E. Cohen, I. I. Mazin, D. G. Isaak, Science **275**, 654 (1997).

[3] Yang Ding, et al, PRB **74**, 144101 (2006).

[4] Abramova G. et al, JMMM **320**, I23, 3261 (2008).

# Optical and magneto-optical study of nanosized ferromagnetic metal-dielectric structures $[\text{Co}/\text{TiO}_2]_n/\text{Si}$

A. A. Astretsov<sup>1,2</sup>, V. V. Pavlov<sup>1</sup>, R. V. Pisarev<sup>1</sup>, V. A. Rusakov<sup>1</sup>, P. A. Usachev<sup>1</sup>,

A. I. Stognij<sup>3</sup>, N. N. Novitski<sup>3</sup>

<sup>1</sup>*Ioffe Physical-Technical Institute of RAS, 194021, St. Petersburg, Russia*

<sup>2</sup>*Physics and Technology Centre, 194021, St. Petersburg, Russia*

<sup>3</sup>*Scientific and Production Materials Research Centre of NASB, 220072, Minsk, Belarus*

Artificial multilayer structures of alternating layers of magnetic and nonmagnetic materials are of large interest both for fundamental physics and for various technological applications. Such structures can find applications as media for ultrahigh density magnetic storage, high sensitive sensors of magnetic fields, magneto-resistive memory. We present results on optical and magneto-optical phenomena in ferromagnetic metal-dielectric structures  $[\text{Co}/\text{TiO}_2]_n/\text{Si}$ . Three different compositions of these structures were prepared by the ion beam deposition technique [1]. Optical dielectric constants were obtained using a standard ellipsometry technique in broad spectral range of 0.6-5.5 eV. Figure 1 shows magnetic hysteresis loops measured by means of the longitudinal magneto-optical Kerr effect. Comparison of polar and longitudinal Kerr effects establishes an easy-magnetization axis is in plane of structure with an effective anisotropy field of about 16 kOe. On the basis of anisotropic model in the effective medium approximation for optical dielectric function [2, 3], the optical and magneto-optical effect were calculated, see e.g. Fig. 2. Thus, using optical and magneto-optical methods it is possible to get important information about electronic and magnetic structures of nanosized ferromagnetic metal-dielectric multilayers: optical dielectric constants, optical and magnetic anisotropy or parameters of technical magnetization process.

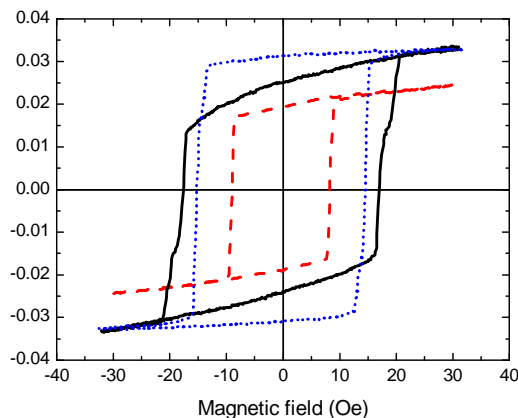


Fig. 1. Hysteresis loops of three different composition of structures  $[\text{Co}/\text{TiO}_2]_n/\text{Si}$

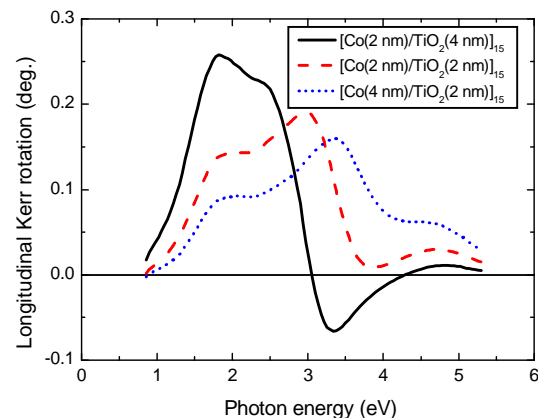


Fig. 2. Modelling of the longitudinal Kerr effect for three different compositions of structures  $[\text{Co}/\text{TiO}_2]_n/\text{Si}$

Using the anisotropic model on the basis of effective medium approximation one can easily justify necessary parameters of nanosized ferromagnetic metal-dielectric structures demanded for practical applications or fundamental physical studies.

[1] A. I. Stognij, M. V. Pashkevich, N. N. Novitski, *et al.*, *Tech. Phys. Lett.* **36**, 426 (2010).

[2] B. Wood, J. B. Pendry and D. P. Tsai, *Phys. Rev. B* **74**, 115116 (2006).

[3] Y. A. Dynnik, I. S. Edelman, T. P. Morozova, *et al.*, *JETP Lett.* **65**, 555 (1997).



# Calculation of the resonant fields of SWR spectra with a smooth change of the symmetry boundary conditions in three-layer magnetic film

A. G. Bazhanov, A. M. Zyuzin

Mordovia State University, 430005, Saransk, Russia

The aim of this work was experimental investigation and theoretical calculation of the values of resonance fields  $H_n$  of spin-wave resonance (SWR) with gradual change in the symmetry boundary conditions (spin pinning symmetry). Smooth change in the symmetry of spin pinning, a gradual decrease in the thickness  $h_{pin}$  of the upper layer with high damping (pinning layer) in a three-layer film by layer-etching. The study found that as the thickness  $h_{pin}$  where the boundary conditions are gradually moving from symmetric to asymmetric, the resonant field of zero spin-wave (SW) mode  $H_0$  remains almost unchanged. For the first and subsequent modes for  $h_{pin} \leq 0.4$  mkm a change in the value  $H_n$  close to periodic. At full etching thickness  $h_{pin}$  of the top of the pinning layer, where the boundary conditions are asymmetric, and the resonance field starts to decrease monotonically. A further decrease in the thickness of the excitation layer  $h_{ex}$  values  $H_n$  also decrease monotonically. To explain these results was calculated, which recorded the equations of motion of the magnetization for each of the layers, as well as the exchange boundary conditions at the interface between layers [1]. Conducted in this paper, the calculation showed that the observed change in the value  $H_n$  due to the fact that at thicknesses  $h_{pin}$  greater length damped spin waves in the pinning layer  $h_{pin} > l$  no effect on the value of the wave phase at the interlayer boundary is not happening. When  $h_{pin} \leq 0.4$  mkm length damped spin waves in the pinning layer  $l$  becomes comparable to the value  $h_{pin}$  and the value of the wave phase at the interlayer boundary begins to state the spin fluctuations on the free boundary. Phase value, in turn, greatly affects the wave numbers  $k_{1n}, k_{2n}^I, k_{2n}^{II}$ , which determine, in turn, the resonance fields  $H_n$  of SW modes.

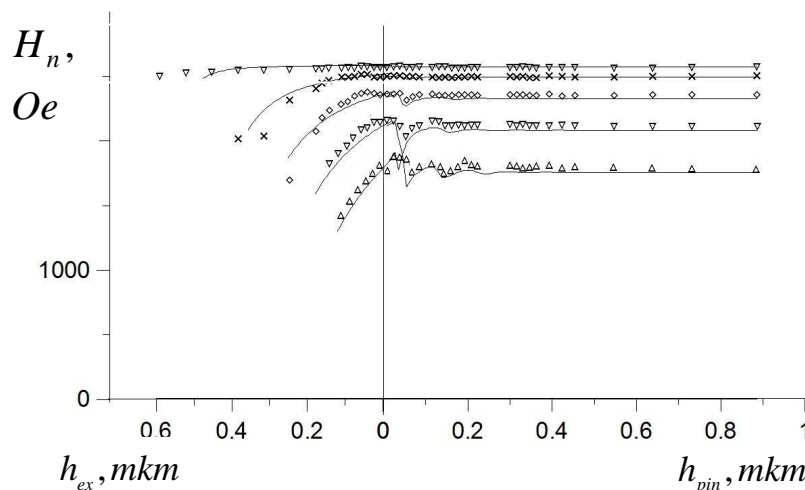


Fig.1. Dependence of the resonant mode fields of the spin-wave resonance on the thickness of the pinning layer  $h_{pin}$  for parallel orientation of the external field relative to the film. Badges - experiment, solid line - calculation.

[1] A.G. Bazhanov, Physics Metals and Metallography **101**(4), 354 (2006).

# Propagation of microwave pulses through the nonlinear transmission line based on ferromagnetic structure

E. N. Beginin

*Saratov State University, 410012, Saratov, Russia*

The active investigation of magnetostatic waves (MSW) in thin ferrite films is caused by the opportunity of creation linear and nonlinear devices (based on them) for microwave signals processing. An example of a nonlinear device is a microstrip transmission line (MTL) with thin ferrite film on it and placed in a uniform magnetic field. Passing through MTL a microwave signals with power  $P$  less than some threshold level  $P_0$  are attenuated more than signals with power  $P > P_0$  [1]. It is possible at frequencies when three-magnon decay processes are allowed. Theoretical analysis of this device has significant difficulties, since the nonlinearity is occurred due to parametric coupling between exited MSW and other types of spin waves [2]. The model of a two-level absorbing medium was used for theoretical investigation of nonlinear MTL. In this model, the power of electromagnetic wave passing through the MTL and its absorption coefficient  $\alpha(z,t)$  at the signal frequency  $f$  are described by a system of rate equations:

$$\frac{dP}{dz} = \alpha P$$
$$\frac{d\alpha}{dt} = -\frac{\alpha}{T} \left( \frac{P}{P_s} + 1 \right) + \frac{\alpha_0}{T},$$

The system of these equations contain such parameters:  $T$  – a system relaxation time,  $P_s$  – a saturation power,  $\alpha_0$  - low signal absorption factor at given frequency. Numerical value of these parameters were determined experimentally. The solution of the system of rate equations set accordance between an instantaneous values of signal at the output  $P_2$  (when  $z = L$ ) and the input  $P_1$  (when  $z = 0$ ) of the MTL. The numerical solution of these equations was performed using the Runge-Kutta method. The experimental investigation of propagation of continuous wave and pulsed microwave signals with different power levels at fixed frequency  $f=2,76$  GHz through MTL were performed to verify the theoretical model. The nonlinear MTL has the following parameters:  $P_s=9$  dBm,  $T=3$   $\mu$ s. These investigations demonstrate that the proposed model describes well the experimental results of the MTL in pulse regime if the pulse repetition period is greater than the system relaxation time  $T$ . For the lesser period the discrepancy with experimental results is observed. It can be explained by the absence of the opposite influence of MSW on the microwave signal in the model description. This work was supported by Government of Russian Federation (project №11-02-00057).

[1] J.D. Adam et al., Appl. Phys. Lett. **36**, 485 (1980).

[2] G. T. Kazakov et al., J. of Comm. Tech. and Elect. **51**, 440 (2006)



## Gap solitons in magnonic crystals at 3-wave interactions

E. N. Beginin<sup>1</sup>, S. A. Nikitov<sup>2</sup>, Yu. P. Sharaevskii<sup>1</sup> and S. E. Sheshukova<sup>1</sup>

<sup>1</sup>Saratov State University, 410012, Saratov, Russia,

<sup>2</sup>Kotel'nikov Institute of Radio Engineering and Electronics of Russian Academy of Sciences, 125009 Moscow, Russia

First observation of gap solitons (GP) in magnonic crystal (MC) was reported in [1]. The authors observed these solitons at frequencies higher than 4 GHz in conditions of 4-wave interactions. In current work we investigate possibility of GP formation in MC at frequencies less than 3 GHz when 4-wave interactions are forbidden by conservation laws. In this case the amplifier of monochromatic spin waves is restricted by 3-wave decay processes. MC was made as a periodic system of etched grooves at the surface of a YIG film with the thickness 4  $\mu\text{m}$ . The grooves have the depth – 0.7  $\mu\text{m}$ , the width – 70  $\mu\text{m}$  and the period – 100  $\mu\text{m}$ . Magnetostatic waves (MSW) delay line was used for measurement with microstrip antennas having the width 30  $\mu\text{m}$ . The distance between them was 4 mm. Thus, 40 periods of MC were located between the antennas. The delay line was subjected to the magnetic field with intensity  $H_0=276$  Oe parallel to the YIG film surface and the antennas. Surface MSW (MSSW) were excited in such geometric configuration. The band gaps were observed within the MSSW spectrum at the frequencies where the Bragg reflection conditions are satisfied (for the MSSW wave number). The central frequency of the first band gap is  $f_0=2.574$  GHz, the depth of rejection is 30 dB, the frequency width of the band gap is 15 MHz at power level -3 dB. The rectangular microwave pulses with power  $P_{\text{in}}$  were supplied to the input of the delay line; the pulse duration was 120 ns, the repetition period was 4  $\mu\text{s}$  and the carrier frequency was  $f_0$ . Time dependences of the amplitude envelope had two spikes corresponding to the fronts of the input pulse. When  $P_{\text{in}} < -5$  dBm, most of the input signal is reflected as from the linear Bragg grating. With increasing  $P_{\text{in}}$  (fig.1), pulse train appeared at the output. Number of pulses was changed from 1 to 3 and the pulse duration varied in the range 15-30 ns. It was determined by  $P_{\text{in}}$ . Some pulses passing through the grating were formed as GS with almost constant phase (fig. 2).

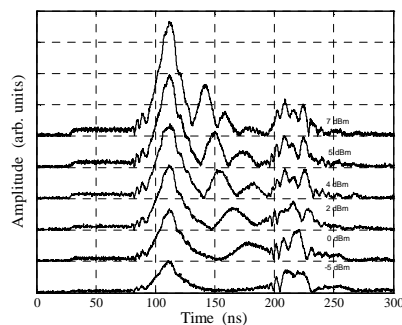


Fig. 1 The amplitude of the transmitted signal at several levels of input power

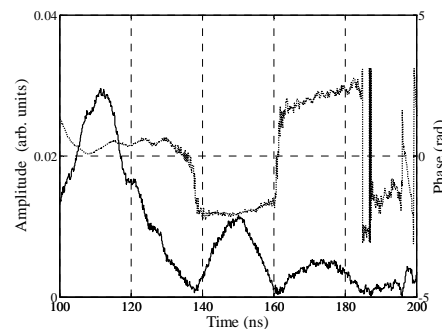


Fig. 2 The amplitude (solid line) and phase (dotted line) of the transmitted signal at input power  $P_{\text{in}}=5$  dBm

This work was supported by Federal Targeted Programme of the Ministry of Education and Science (project №2010-1.2.2-123-019-002) and the Government of Russian Federation (project No. 11.G34.31.0030).

[1] A. Ustinov, B. Kalinikos, *et al.*, Phys. Rev. B **81**, 180406 (2010).

## **Resonant nonlinear frequency multiplication in microscopic magnetic elements**

V. D. Bessonov<sup>1</sup>, R. Gieniusz<sup>1</sup>, A. Maziewski<sup>1</sup>, H. Ulrichs<sup>2</sup>, V. E. Demidov<sup>2</sup>,  
S. O. Demokritov<sup>2</sup>, S. Urazhdin<sup>3</sup>

<sup>1</sup>*Faculty of Physics, University of Białystok, Lipowa 41, 15-424 Białystok, Poland*

<sup>2</sup>*Institute for Applied Physics and Center for Nonlinear Science, University of Muenster,  
Corrensstrasse 2-4, 48149 Muenster, Germany*

<sup>3</sup>*Department of Physics, West Virginia University, Morgantown, WV 26506, USA*

Here we report on the experimental study of nonlinear frequency multiplication in Permalloy-film ellipses subjected to intense microwave magnetic field. The ellipses had lateral dimensions of 1 by 0.5  $\mu\text{m}$  and the thickness of 10 nm and were prepared by e-beam lithography on top of 1- $\mu\text{m}$ -wide microwave transmission line used for the excitation of magnetization dynamics. The experiments were performed by micro-focus Brillouin light scattering spectroscopy with the spatial resolution of about 250 nm and the frequency resolution of 100 MHz.

We show that the resonant modes of the magnetic elements can be excited by applying a microwave signal at a frequency which is by a factor of two or even three smaller compared to the resonant frequency. We study the spatial characteristics of the nonlinearly excited modes and show that the double-frequency excitation is efficient for modes with anti-symmetric spatial profiles, whereas the triple-frequency excitation is efficient for modes with symmetric profiles. The latter process shows an especially high efficiency, which makes it promising for technical applications.

Our results contribute to the deep understanding of large-amplitude magnetization dynamics in nanostructures and open new opportunities for implementation of nano-scale magnetic devices for microwave technology.

# Dynamic properties of discrete solitons in 1D magnetic dots array

P. Bondarenko<sup>1</sup>, B. A. Ivanov<sup>1,2</sup>

<sup>1</sup>Institute of Magnetism NASU and MESU, 03142, Kyiv, Ukraine,

<sup>2</sup>T. Shevchenko National University of Kyiv, 03022, Kyiv, Ukraine

The magnetic dots are organized in linear chain and defined by rather high spatial regularity. The dots have no direct contact between each other, therefore the sole source of their interaction is the magnetic dipolar interaction. The dynamic and static topological solitons in magnetic dot arrays are computed numerically and analytically. Next conclusions for the static domain walls are drawn:

1. Long-range dipole coupling leads to the power-like interaction between domain wall centre and moments on the periphery.
2. Kinks are attracted to the chain edges with Coulomb-like forces due to dipole-dipole interaction between dots.

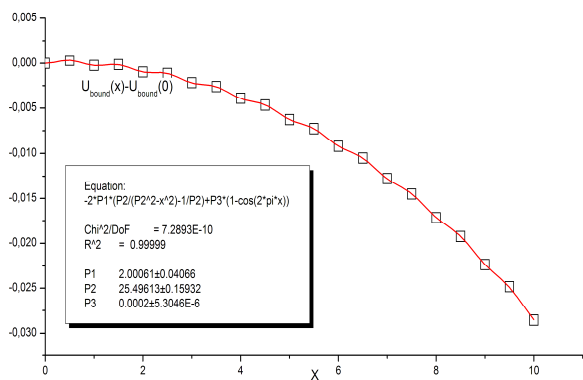


Fig.1 Dependence of attracting potential between domain wall and array edge on soliton centre coordinate relative to the chain centre.

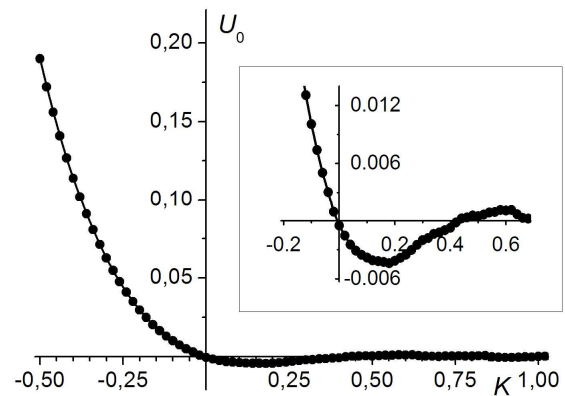


Fig.2 Dependence of Peierls-Nabarro barrier for static kink on easy-axis dot anisotropy.

Analytical results are derived from exact solution for discrete kinks in 1D spin chain with pure uniaxial exchange anisotropy (Gochev's solution [1]). The dynamic properties of kinks are examined within the framework of previously mentioned analytical approach. It is shown that Peierls-Nabarro barrier [2] is negligible in comparison with the kink energy in the absence of single dot anisotropy. The dependence of pinning potential on kink velocity is found. Velocity values are obtained for which soliton can move through the chain with nonzero anisotropy without being pinned.

[1] I. G. Gochev, JETP Lett. **85**, (1983).

[2] F. R. N. Nabarro, Theory of Crystal Dislocations (Oxford Univ. Press, Oxford, England, 1967).

# Pulsed excitation of surface spin-wave envelope solitons in magnonic crystal

A. Drozdovskii, A. Ustinov, and B. Kalinikos

*St. Petersburg Electrotechnical University, 197376, St. Petersburg, Russia*

One of the fundamental physical phenomena observed in different media are the envelope solitons of waves of various nature, the nonlinear localized wave packets that are formed during the propagation of a pulsed perturbation owing to the compensation of the spreading effect of dispersion by the grouping effect of nonlinearity [1]. The envelope solitons can be also formed due to the development of intrinsic or induced modulation instability under the continuous propagation of finite-amplitude waves in a nonlinear dispersive medium [1, 2]. The aim of this work is to study the possibility of the formation and propagation of bright envelope solitons under the pulsed microwave excitation of spin-wave packets in a magnonic crystal.

We note that the formation of bright solitons was observed in the spectral regions with a strong dispersion, which are situated near the stop-bands caused by the Bragg resonances. The excitation and detection of spin-wave packets was performed utilizing a delay-line structure with 2-mm long, 50- $\mu\text{m}$  wide, short-circuited input and output microstrip antennae. The distance between the antennae was 7.2 mm. Experimentally investigated magnonic crystal sample had a thickness of 11.6  $\mu\text{m}$ , a width of 2 mm, and a length of 55 mm. Grooves with a depth of 2  $\mu\text{m}$ , a width of 50  $\mu\text{m}$ , and a period of 400  $\mu\text{m}$  were etched over the entire width of the yttrium iron garnet film waveguide perpendicular to its longer axis. The experimental sample was placed in a homogeneous static magnetic field of 1206 Oe between the poles of an electromagnet. The field was directed along the spin-wave antennae in the plane of the magnonic crystal.

Thus, the input antenna excited the surface spin wave packets in a periodic structure. Owing to the nonreciprocity in the excitation of such waves, the major part of the energy propagated towards the output antenna. The carrier waves, which propagate in the opposite direction towards the beveled end of the magnonic crystal, were attenuated and did not affect the measurement results.

We studied the possibility of the formation of bright spin-wave solitons in the magnonic crystal by short RF pulses supplied to the input antenna. For this purpose, the carrier frequency, duration, and amplitude of the input pulses were systematically changed. The formation of solitons was detected in the first three stop bands. This formation always occurred at the frequencies corresponding to the right (high-frequency) slopes of the stop bands, where the group velocity of the spin waves increases rapidly with frequency. In other words, the formation of bright solitons was observed in the regions of strong positive dispersion. The formation of solitons in the spectral intervals between the stop bands was not observed in the power interval of 1–500 mW provided by the experimental set-up.

This work was supported in part by Russian Foundation for Basic Research, the Ministry of Education and Science of Russia, and by the grant of the President of Russia.

[1] M. Remoissenet, *Waves Called Solitons: Concepts and Experiments* (Springer, Berlin, 1996).

[2] Yu. S. Kivshar and G. P. Agrawal, *Optical Solitons: From Fibers to Photonic Crystals* (Academic, San Diego, CA, 2003; Fizmatgiz, Moscow, 2005).

## Traditional and perspective spin-wave devices for the microwave frequency band

V. A. Dubovoj<sup>1</sup>, L. V. Lutsev<sup>2</sup>, A. I. Firsenkov<sup>1</sup>, A. E. Kozin<sup>1</sup>, D. N. Fedin<sup>1</sup>

<sup>1</sup>*Magneton J.S. Co., 194223, St. Petersburg, Russia,*

<sup>2</sup>*Ioffe Physical-Technical Institute, Russian Academy of Sciences, 194021, St. Petersburg, Russia*

Traditional spin-wave devices (SWD) were developed formerly during several decades and are developed today by a number of foreign firms [1] and Russian enterprises [2]. At present the most perspective traditional devices on spin waves (SW) are tunable band pass and band reject filters, delay lines, resonators, generators, signal-to-noise enhancers, power restrictors. The main feature of SWD is the opportunity to govern their characteristics and the working frequency by the formation of profile of the applied magnetic field and by the variation of its value in monocystal ferrite films of 3 - 60  $\mu\text{m}$  thickness.

The most known and used traditional SWDs are filters. SW filters operate in frequencies from 1.2 GHz up to 18 GHz and have losses up to 2 .5 dB in this range. The main characteristics of these filters are: the pass band is in the range from 12 MHz up to 200 MHz, the level of parasitic resonances leads to 40 dB, the out-of-band attenuation reaches 70 dB, the tunable time can reach 20  $\mu\text{s}$ . The rectangular factor of the pass and reject bands can reach 1.8. This corresponds to the selectivity of the 6-chain filters on YIG spheres. At present there are produced SW filters on fixed frequencies of small sizes. Such SW devices have dimension sizes of 12 $\times$ 8 $\times$ 12 mm.

Additional opportunities for creation SWDs on ferrite films with enhanced characteristics can be based on the nonlinear relaxation of the magnetization in ferrite films. Power restrictors, signal-to-noise enhancers and magnetic soliton generators are created on the base of nonlinear properties of ferrite devices.

SW filters belong to the class of electrical-tuned devices and have a number of positive properties in comparison with analogous functional devices. In comparison with tunable filters based on varactors, SW filters have considerably better parameters of their amplitude-frequency characteristics. They have low signal losses, high quality, linear tunable characteristics, selectivity. However, SW filters lose to the varactor filters in dimensions, cost and in expenditure of energy. In this connection, it is need to continue further development of spin wave devices, which based on heterostructures containing sputtered ferrite films [3]. Devices of the new, second generation should be made by the integration technology on a single substrate, should have small dimensions, must be suitable for surface fit operations, and should have low cost.

We consider one of the variant of SW devices of the new generation. Device has been produced as the chip, which was made on a substrate. SW device contains the multilayered structure, which consists of epitaxial YIG film, SW guide and microstrip circuit located above the spin wave guide. In dependence of the distance between generating and receiving antennae in the applied magnetic field this SW device has amplitude-frequency characteristics of a filter or a delay line.

[1] G. M. Vapne. *Microwave devices on magnetostatic waves*. Reviews on electronic engineering.

Microwave Electronics. Moscow. CNII Electronica. **8** (1984) [in Russian].

[2] [www.magneton.ru](http://www.magneton.ru) *Pre-production models of filters on magnetostatic waves*.

[3] S. A. Manuilov, R. Fors, S. I. Khartsev, and A. M. Grishin, *J. Appl. Phys.*, **105**, 033917 (2009).

## **Nonlinear dynamics of the domain walls of magnetics with 1D and 2D case nonhomogeneities modulation of the parameters of the magnetic anisotropy**

E. G. Ekomasov, R. R. Murtazin, Sh. A. Azamatov, A. M. Gumerov, A. E. Ekomasov  
*Bashkir State University, 450074, Ufa, Russia*

It is known that in real magnetics the appearance of magnetic parameters local changes happens due to structural and chemical non-homogeneities and local influence (mechanical, thermal or solar) [1]. As it is usually difficult to make a precise (microscopic) calculation, one is to model the functions, which describe the parameters of a non-homogeneous material [2, 3]. The case is especially interesting, when the size of a magnetic non-homogeneity and the size, describing a non-homogeneity of parameters of a stuff, are of the same order. It results in considerable complication of Landau-Lifshitz equation for the magnetization. Although the task of excitation and distribution of the magnetization waves, under certain conditions, is reduced to the studies of the modified sine-Gordon equation with floating factor [4]. The investigation of the big perturbations influence on the solution of the modified sine-Gordon equation in general case can be investigated only with the help of numerical methods. In dynamic, when a temporally or spatial non-homogeneous perturbation acts in the area of such non-homogeneities (or defects), under certain conditions, a strongly non-linear waves of magnetic character can be aroused. Such waves are weakly investigated.

This research considers our studies of the domain walls (DW) dynamics in ferromagnetics with an optional size one and two dimensional modulation of the magnetic anisotropy constant in terms of stimulation and radiation of the nonlinear waves. For the nonhomogeneity of the constant of the magnetic anisotropy (NCMA) case the reflection of the DW from the NCMA region was observed. It was connected with the DW resonant interaction with the magnetic nonhomogeneity of the breather type, stimulated in the NCMA region. Also the possibility of the DW quasitunneling involving several NCMA regions (i.e. when the particle crosses the barrier with the speed below ultimate) and the origin of the magnetic nonhomogeneities of the multi-pulson type in the form of kink and breather bound state cophased and antiphased with the oscillating breathers was shown.

We have investigated for the case of 2D nonhomogeneity of the origin and evolution of the magnetic nonhomogeneities of pulson and 2D soliton types, localized in defect region. The dependences of the maximum amplitude solitary bending waves on the DW speed and on the non-homogeneities region characteristics in the case of DW inertial motion and DW motion in the external magnetic fields were found. The analytical form of the solitary bending waves amplitude, that gives qualitative description of our results, was found. The dependences of maximum deflection magnetization in magnetic nonhomogeneities of pulson and 2D soliton types on time, nonhomogeneities region characteristics and DW speed were received.

[1] S. V. Vonsovskii, *Magnetism*, Nauka, Moscow, (1971) [in Russian].

[2] D. I. Paul, *J.Phys.C: Solid State Phys.*, **12**, 585-593 (1979).

[3] M. A. Shamsutdinov et al., *Ferro- and antiferromagnitodynamic. Nonlinear oscillations, waves and solitons*, Ufa: Gilem, 2007, 368 c. [in Russian]

[4] E. G. Ekomasov, Sh. A. Azamatov, R. R. Murtazin, *FMM* **105**, 341-349 (2008) [in Russian].

[5] E. G. Ekomasov, Sh. A. Azamatov, R. R. Murtazin, *FMM*, **108**, № 6, 566-571 (2009) [in Russian].

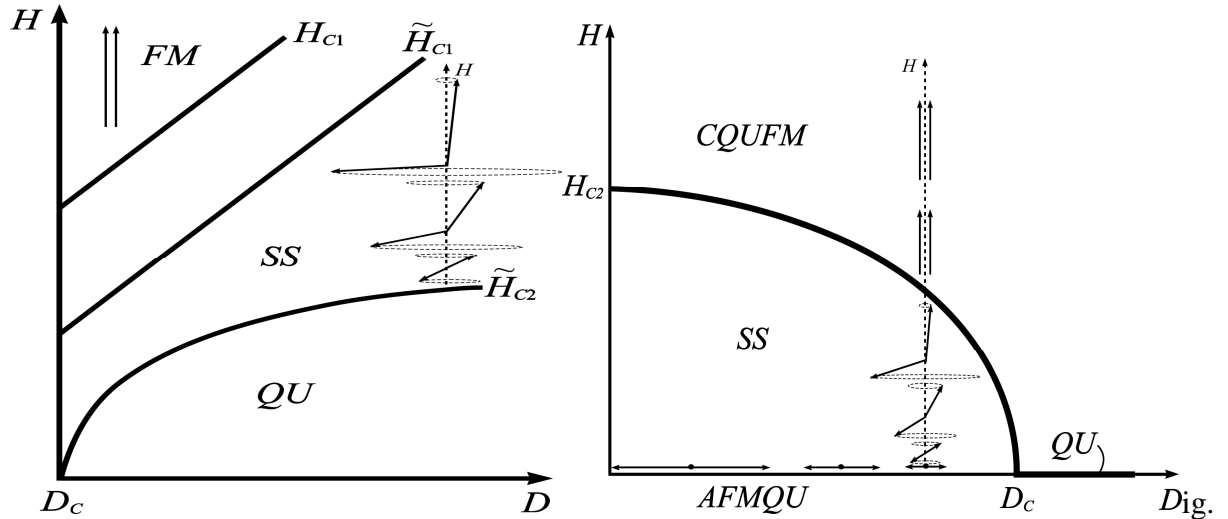
## Phase diagram in spin-1 easy-plane antiferromagnet

Yu. A. Fridman, O. A. Kosmachev, Ph. N. Klevets  
*V.I. Vernadskiy Taurida national university*  
*Academician Vernadskiy ave., 4, Simferopol, 95007, Ukraine*

We investigated the phase states of strongly anisotropic easy-plane antiferromagnetic with intersublattice exchange anisotropy in both the longitudinal and the transverse magnetic field. It was shown that the magnetic phase akin to the “super-solid” (SS) phase, found in the solid  $^4\text{He}$ , realizes for both orientations of the magnetic field. Our results obtained for the longitudinal orientation of the magnetic field are in good agreement with the results of other studies [1-3]. Besides, we showed that the SS phase realizes also for the case of transverse orientation of the magnetic field. It should be noted that this result was obtained earlier, for example, in [2]; however, it was not interpreted as the SS phase. Our results for the case of transverse orientation of the magnetic field are in good agreement with the previous results [2]. It must be noted that we did not make any simplifying assumptions like, for example, in [3], and take into account relativistic interactions exactly.

Besides, we showed that the behavior of strongly anisotropic easy-plane antiferromagnetic differs a lot in longitudinal and transverse magnetic fields. First of all, this difference is exhibited in the formation of the ferromagnetic (FM) state. In longitudinal field (when field is greater than the stability field), the antiferromagnetic passes from the SS phase into the FM phase through the phase transition of the first kind. If the field is along the basal plane, the system is in the collinear quadrupolar-ferromagnetic phase (CQUFM) and asymptotically (at  $H \rightarrow \infty$ ) tends to saturation.

We built the phase diagrams for both orientations of the magnetic field. The phase diagram for the longitudinal orientation of the magnetic field is in quality agreement with [3]. And the phase diagram for the case of the transverse orientation of the magnetic field was obtained at first.



1. Phase diagrams of strongly anisotropic easy-plane antiferromagnetic in the longitudinal (a) and transverse (b) magnetic field. QU denotes the quadrupolar phase, AFMQU – the quadrupolar antiferromagnetic state.

- [1] P. Sengupta and C. D. Batista, Phys. Rev. Lett. **98**, 227201 (2007).
- [2] V.M. Kalita, I. Ivanova, V.M. Loktev, Phys. Rev. B **78**, 104415 (2008).
- [3] C. J. Hamer, O. Rojas, and J. Oitmaa, Phys. Rev. B **81**, 214424 (2010).

# NMR study of low dimensional spin system $\text{Cu}_2[\text{PO}_3(\text{CH}_2)\text{PO}_3]$ : magnetic versus structural dimers

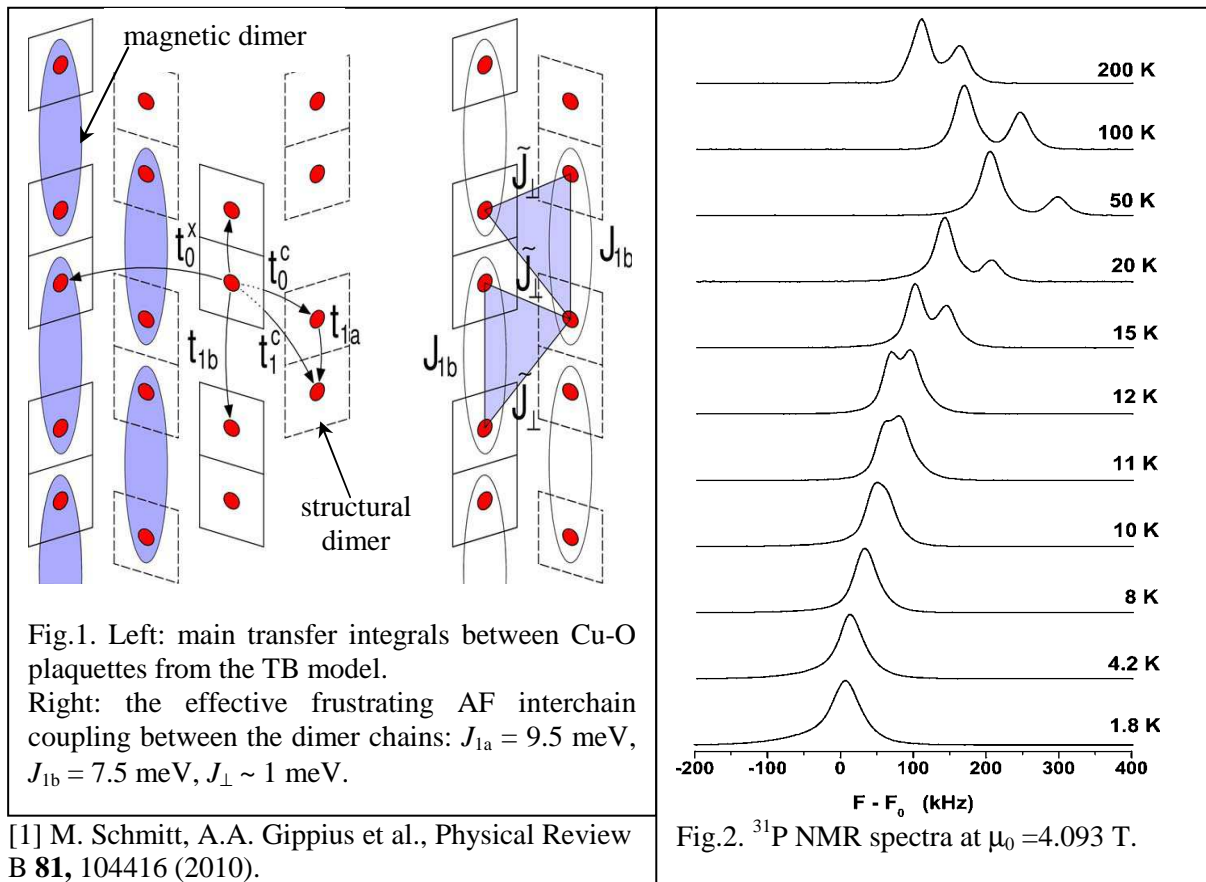
A. A. Gippius<sup>1,2</sup>, N. E. Gervits<sup>1</sup>, M. Baenitz<sup>2</sup>, M. Schmitt<sup>2</sup>, K. Koch<sup>2</sup>,  
W. Schnelle<sup>2</sup>, W. Liu<sup>2</sup>, Y. Huang<sup>2</sup>, H. Rosner<sup>2</sup>

<sup>1</sup>Faculty of Physics, M.V. Lomonosov Moscow State University, 119991, Moscow, Russia,

<sup>2</sup>Max Planck Institute for Chemical Physics of Solids, 01187, Dresden, Germany,

Due to their large variety of unprecedented exotic ground states, low-dimensional magnetic compounds have always attracted great interest in solid-state physics. For spin 1/2, the influence of quantum fluctuations becomes crucial for the ground state of the system. From crystallographic point of view,  $\text{Cu}_2(\text{PO}_3)_2\text{CH}_2$  could be considered either as an alternating spin chain or as a dimer system (Fig.1).

At high temperature  $^{31}\text{P}$  NMR spectra exhibit two peak structure coinciding with two crystallographic P sites (Fig.2). Below 10 K two peaks merge evidencing that the spin part of magnetic susceptibility is freezing out due to formation of a singlet ground state with a gap in magnetic excitation spectrum of about 25 K [1]. Surprisingly, the leading antiferromagnetic (AF) exchange of about 75 K can be assigned by density-functional band-structure calculations to a coupling between the structural  $\text{Cu}_2\text{O}_6$  dimers, whereas the intra-dimer coupling is strongly reduced due to sizable ferromagnetic contributions leading to unique situation when magnetic and structural dimers do not coincide. The present NMR, NQR, magnetic susceptibility and specific heat experimental data can be consistently described within a scenario of coupled alternating AF Heisenberg chains.



[1] M. Schmitt, A.A. Gippius et al., Physical Review B **81**, 104416 (2010).



# An influence of local environment on spin densities' distribution in Fe<sub>3</sub>Al and Fe<sub>3</sub>Si doped with transition metals

A. Go<sup>1</sup> and L. Dobrzyński<sup>1,2</sup>

<sup>1</sup>Faculty of Physics, University of Białystok, Lipowa 41, 15-424 Białystok, Poland,

<sup>2</sup>The Soltan Institute for Nuclear Studies, 05-400 Otwock-Świerk, Poland

Electronic structure and spin densities' distribution in Fe<sub>3</sub>Al and Fe<sub>3</sub>Si doped with transition metals strongly depend on the configuration of the nearest neighbourhood. Changes of atoms' arrangement in the first coordination sphere of Fe can lead to radical modifications of the symmetry of Fe spin densities. Detailed analysis of those effects is carried out by TB-LMTO-ASA method. This method, based on the supercell approach, allows investigation of different local environments of Fe and influence of the crystal field on the spin density distribution.

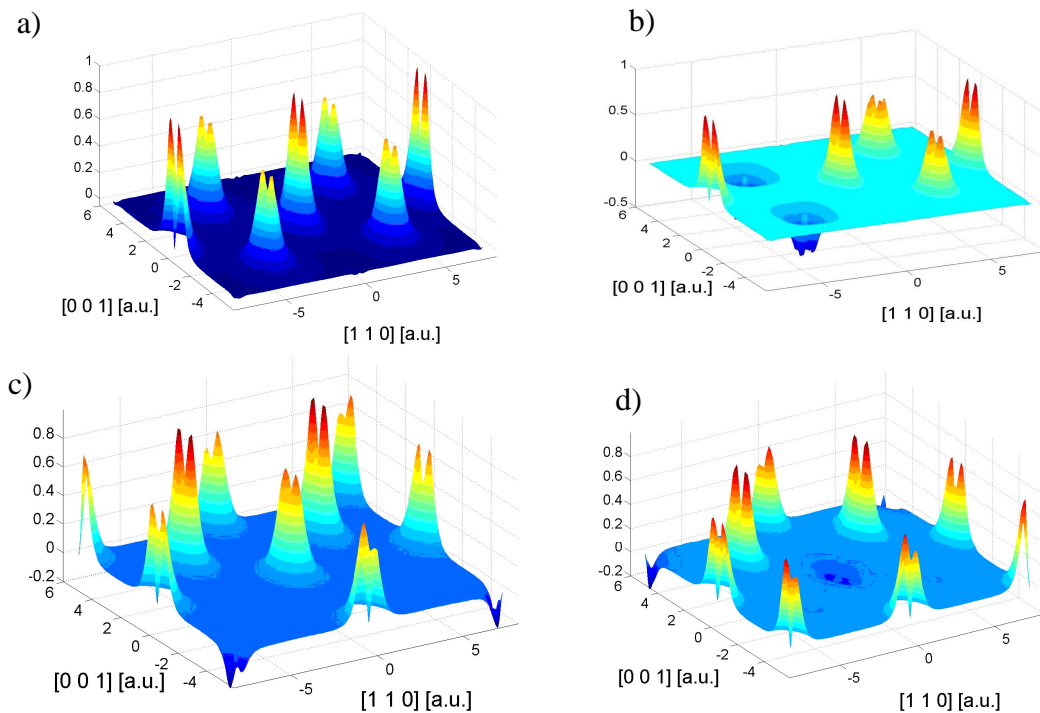


Fig. 1 Spin density in Fe<sub>2,5</sub>Mn<sub>0,5</sub>Al. Central atom Fe surrounded by a) 8 Fe , b) 4Fe4Mn, c) 4Fe4Al, d) 4Mn,4Al atoms.

Fig. 1 a) shows spin density in Fe<sub>2,5</sub>Mn<sub>0,5</sub>Al in the (110) plane, where central Fe atom is surrounded by 8 Fe atoms. When 4 neighbouring Fe atoms are substituted by Mn (Fig. 1 b) or Al (Fig. 1 c) atoms Fe spin density decreases. However, if the first coordination sphere consists of 4 Mn and 4 Al atoms (Fig. 1 d), a reversion of Fe spin density is observed.

# Dipole-exchange spectrum of highly anisotropic ferromagnetic thin-film waveguides on terahertz frequencies

N. Grigoryeva and B. Kalinikos

*Saint Petersburg Electrotechnical University, 197376, St. Petersburg, Russian Federation*

Rapidly growing interest to terahertz (THz) frequency technology stimulates the theoretical and experimental investigation of highly anisotropic ferromagnetic materials in general and hexaferrite thin films in particular [1]. Hexagonal ferrite materials have large effective uniaxial anisotropy field of about 15-25 kOe and can be easily tuned at frequencies of 60–100 GHz and higher with relatively small applied bias magnetic fields [2]. Recent advances in the growth technology of hexagonal barium ferrite films with low microwave losses make these materials particularly attractive for high-frequency applications [3].

On the other hand, a demand of miniaturisation in nanoelectronics leads to size reduction of the practically used elements. It is well known that the dispersion characteristics of any type of the confined waveguiding elements differ drastically from the infinite plane ones. From these perspectives, commonly used approximate theoretical methods, that relate spin-wave spectra for infinite-width and finite-width waveguiding structures, should be accurately considered.

Here we present an eigen-mode theory for the highly anisotropic ferromagnetic thin-film waveguides. The dipole-exchange spectrum of spin waves was obtained analytically using the method of tensorial Green's function together with the spin-wave mode approach elaborated in our previous work. A finite width of the waveguiding structure was taken into account simultaneously with the magnetic anisotropy of the hexagonal ferrite material.

The considered model includes the dipole-dipole and exchange interactions in the ferromagnetic waveguide, as well as it takes into account the surface and volume anisotropies. The surface anisotropy is taken into account through the surface spin-pinning conditions on all sides of the magnetic waveguide. The uniaxial volume anisotropy of the hexaferrite film is included through corresponding tensorial demagnetization factor. The derived dispersion relations are obtained in analytical form. They can be used in calculations of the spin-wave spectrum for an arbitrary direction of the external bias magnetic field and for an arbitrary direction of the uniaxial volume anisotropy of the waveguide.

To illustrate the theoretical conclusions, the numerical calculations were done for the most common case when the uniaxial anisotropy is perpendicular to the film plane when the waveguiding structure was magnetized in the same direction by the external magnetic field. It is demonstrated that the approximate methods, which were widely used previously to account the finite width of the waveguide, give a large discrepancy with the exact calculations. Moreover, the traditionally used approximate methods cannot take into account the intermode interaction, which can cause a very pronounced dipole gaps in the spin-wave spectrum.

This work was supported in part by the Russian Foundation for Basic Research, by the RF Ministry of Education and Science under contracts 02.740.11.0231 and 02.740.11.0465, and the grant of the President of RF NSh-3783.2010.2.

- [1] Ce-Wen Nan, M. I. Bichurin, Shuxiang Dong, D. Viehland and G. Srinivasan, *J. Appl. Phys.* **103**, 031101 (2008).
- [2] N. Yu. Grigoryeva, R. A. Sultanov and B. A. Kalinikos, *Electronics Letters* **47**(1), 35 (2011).
- [3] J. Das, B. A. Kalinikos, A. R. Barman and C. E. Patton, *Appl. Phys. Lett.* **91**, 172516 (2007).

# Dependence of the normal wave spectrum in multiferroic layered structure on surface spin-pinning conditions

N. Grigoryeva, R. Sultanov and B. Kalinikos

*Saint Petersburg Electrotechnical University, 197376, St. Petersburg, Russian Federation*

It is well-known that multiferroics (ferrite-ferroelectric layered structures) provide a possibility of simultaneous broadband magnetic field tuning and fast electric field tuning [1]. This gives a unique opportunity for the construction of cost effective, fast and broadband devices for a wide range of high frequency applications. Moreover, recent advances in the growth technology of thin ferroelectric films on the surface of the gold coated ferrite films with low microwave losses make these structures particularly attractive for a variety of tunable microwave components and devices for millimeter-wave and terahertz applications [2]. However, the fabrication of such complex structure in one technological cycle causes the uncontrollable spin pinning on the ferrite film interfaces. As it was mentioned earlier in a set of works [3], [4], spin pinning on the surface of a free ferromagnetic film causes the crucial modification of the normal spin-wave modes spectrum and produces attenuation “notches” in the spin-wave transmission response. The non-symmetrical spin pinning on two surfaces of the ferromagnetic film produces more complex modifications of the spin-wave spectrum.

Recently the previously elaborated analytical theory of the hybrid dipole-exchange electromagnetic-spin waves in ferrite-ferroelectric layered structures was extended to the case of the arbitrary spin pinning conditions on both surfaces of the ferrite film [5]. This general theory allows one to determine the changes in the spin-wave spectrum owing to the different spin pinning conditions on both sides of the ferrite film.

Here we present the investigation of the dependence of the normal wave spectrum in multiferroic layered structure on surface spin-pinning conditions. Hybrid dipole-exchange electromagnetic-spin wave spectrum is calculated for the case of an arbitrary spin-pinning parameters on both surfaces of the ferromagnetic film. Three main configurations of the bias magnetic field are considered: perpendicular to the film plane, tangential along and perpendicular to the spin-wave propagation direction. One of the most common structures, namely, ferroelectric-ferrite-dielectric substrate-air with one metallic screen placed near the ferroelectric layer is considered. Symmetric and antisymmetric surface spin pinning conditions are studied. The detailed analysis is performed for the case of tangentially magnetized structure in the direction of spin-wave propagation. The dependence of the size of the dipole gaps in the spin-wave spectrum vs. spin-pinning parameters is calculated.

This work was supported in part by the Russian Foundation for Basic Research, by the RF Ministry of Education and Science under contracts 02.740.11.0231 and 02.740.11.0465, and the grant of the President of RF NSh-3783.2010.2.

- [1] Ce-Wen Nan, M. I. Bichurin, Shuxiang Dong, D. Viehland and G. Srinivasan, *J. Appl. Phys.* **103**, 031101 (2008).
- [2] J. Das, B. A. Kalinikos, A. R. Barman and C. E. Patton, *Appl. Phys. Lett.* **91**, 172516 (2007).
- [3] D. Adam, T. W. O’Keeffe and R. W. Patterson, *J. Appl. Phys.* **50(3)**, 2446 (1979).
- [4] B. A. Kalinikos, A. N. Slavin, *J. Phys. C: Solid State Phys.* **19**, 7013 (1986).
- [5] N. Yu. Grigoryeva, R. A. Sultanov and B. A. Kalinikos, *Phys. Solid State* **53(5)**, 971 (2011).

# Nonlinear model of a ferromagnetic film feedback ring at three-wave interactions

S. V. Grishin, D. V. Romanenko, and Yu. P. Sharaevskii  
*Saratov State University, 410012, Saratov, Russia*

As shown experimentally [1], self-generation of a chaotic signal is observed in ferromagnetic film feedback rings at three-wave interactions. The first model, describing three-wave interactions in parametric media with linear amplification, was proposed in [2]. This model describes parametric interactions of waves of various natures, including spin waves in the system with amplification [3]. Transition to chaos in such a model is observed at the detuning  $\delta$  of spin-wave frequencies from the half-frequency of magnetostatic wave (MSW) of  $\sim 8$  MHz. Such value is too large and not observed in experiments [4].

In this paper, the model of three-wave interactions of spin waves in the ferromagnetic film feedback ring is presented. This model is based on the system of three complex equations with a time delay and a nonlinearity of the power amplifier. Presence of power amplifier nonlinearity and the time delay in the model allows to observe a single-frequency generation regime and transition to chaos at the  $\delta \sim 100$ -300 kHz. At small values of a ring gain (see Fig. 1a), regime of constant amplitude, which corresponds to the single-frequency generation regime of the investigated feedback ring, is observed. At the certain ring gain value, the periodical quasi-sinusoidal modulation is observed. At the increase of the ring gain value (see Fig. 1b), the period of modulation decreases, and an envelope has a form of relaxation oscillation train. At the further increase of the ring gain value, the modulation becomes more complicated, and a chaotic modulation is observed at some values of the ring gain (see Fig. 1c). The obtained results have a good agreement with the experimental data [4].

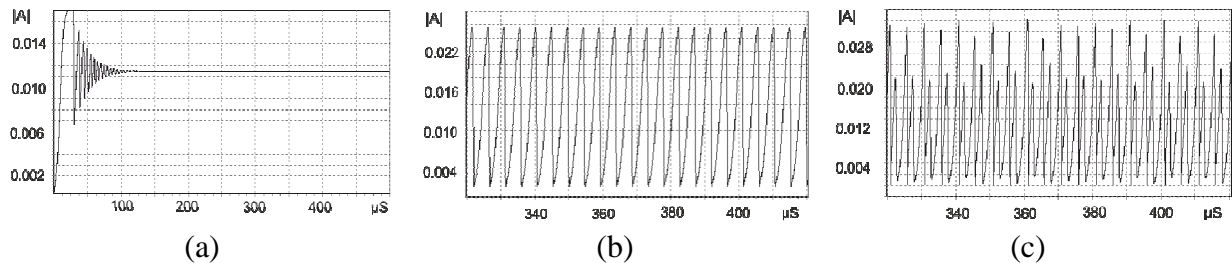


Fig. 1. Evolution of complex amplitude of MSW at various values of the ring gain  $\gamma$ : 0.30 (a), 0.95 (b) and 1.50 (c).

This work was supported by the Grants from Russian Foundation for Basic Research (project No. 11-02-00057), the President of Russian Federation for Support of Leading Scientific Schools (project No. 3407.2010.2) and the Government of Russian Federation for Support of Scientific Research in the Russian Universities Under the Guidance of Leading Scientists (project No. 11.G34.31.0030).

- [1] V. E. Demidov and N. G. Kovshikov, *Tech. Phys. Lett.* **24**, 274 (1998).
- [2] S. A. Vyskind and M. I. Rabinovich, *JETP* **44**, 292 (1976).
- [3] V. E. Demidov and N. G. Kovshikov, *Tech. Phys.* **44**, 960 (1999).
- [4] E. N. Beginin, S. V. Grishin, and Yu. P. Sharaevsky, *JETP* **88**, 647 (2008).

## Self-consistent spin wave theory, elementary excitations and Neel temperature in triangular-lattice antiferromagnets

A. N. Ignatenko, V. Yu. Irkhin and A. A. Katanin  
<sup>1</sup>*Institute of Metal Physics, 620990, Ekaterinburg, Russia*

A number of Heisenberg antiferromagnets (e.g., VCl<sub>2</sub>, VBr<sub>2</sub>, LiCrO<sub>2</sub>) possess a layered structure with triangular lattice in a layer. Due to geometrical frustration of this lattice the magnetic order becomes non-collinear. In contrast to conventional collinear antiferromagnets, we have two types of excitations: spin waves and  $\mathbb{Z}_2$ -vortices (visons). These vortices are to some extent similar to vortices in the XY model: they also have a finite activation temperature  $T_{KT}$  which is an analog of the Kosterlitz-Thouless temperature.

Spin-wave spectrum of isotropic non-collinear antiferromagnets contains three gapless Goldstone modes. Therefore the formulation of the self-consistent spin wave theory (SSWT) for these systems turns out to be non-trivial since two of the modes acquire gaps in a naive SSWT treatment. These unphysical gaps are formally similar to the gaps owing to magnetic anisotropy or dipole interactions. Opening of these gaps disturbs magnetic properties and should be eliminated. We construct a version of SSWT without this drawback.

For layered frustrated antiferromagnets SSWT is insufficient at not to low temperatures since it does not take into account vortices [4]. The vortices give the main contribution to sublattice magnetization for  $T > T_{KT}$  and determine the Neel temperature. However, SSWT can be used to determine exchange parameters from the experimental sublattice magnetization at low temperatures.

To estimate vortex contribution to the Neel temperature we use the Monte-Carlo results for the correlation length of the purely two-dimensional triangular antiferromagnet,  $\xi(T) = A \exp\left[b/\sqrt{T - T_{KT}}\right]$  for  $T > T_{KT}$ , where  $T_{KT} = 0.28 JS^2$  and  $b = 0.77$  [3]. We determine the Neel temperature for the quasi-2D model as a temperature where a crossover from 2D to 3D regime occurs, so that  $\xi(T_{Neel}) \approx a\sqrt{J'/J}$ , and

$$T_{Neel} \approx T_{KT} + 2.37 JS^2 \ln^{-2}\left(\frac{2J'}{J}\right).$$

The Table contains the experimental and calculated Neel temperature for layered triangular-lattice antiferromagnets ( $S = 3/2$ ,  $\Delta T = T_N^{calc} - T_{KT}$ ).

	$J$ , K	$J'/J$	$\Delta T/T_N$	$T_N^{exp}$ , K	$T_N^{calc}$ , K
VBr <sub>2</sub>	32	0.06	0.6	29	56.6
VCl <sub>2</sub>	44	0.006	0.3	36	39.8
LiCrO <sub>2</sub>	80	0.0013	0.2	62	62.5

- [1] H. Kadowaki, K. Ubukoshi, K. Hirakawa, J.L. Martinez, and G. Shirane, J. Phys. Soc. Japan **56**, 4027 (1987).  
[2] V. Yu. Irkhin and A.A. Katanin, Phys. Rev. B **55**, 12318 (1997); **57**, 379 (1998).  
[3] M. Wintel, H.U. Everts, and W. Apel, Phys. Rev. B **52**, 13480 (1995).  
[4] A.N. Ignatenko, V. Yu. Irkhin, and A.A. Katanin, Solid State Phenomena, **152-153**, 257 (2009).

# Spin wave and one particle instabilities of ferromagnetic state in the Hubbard model

P. A. Igoshev, A. V. Zarubin, A. A. Katanin, V. Yu. Irkhin  
Institute of Metal Physics, 620990, Ekaterinburg, Russia

We analyze the criterion of ferromagnetism for a two-dimensional (2D) itinerant electron system on the square lattice with the Fermi level near a van Hove singularity. The corresponding electronic spectrum has the form  $\varepsilon_k = -2t(\cos k_x + \cos k_y) + 4t'(\cos k_x \cos k_y + 1)$ ,  $t, t'$  being transfer integrals for nearest and next-nearest neighbours.

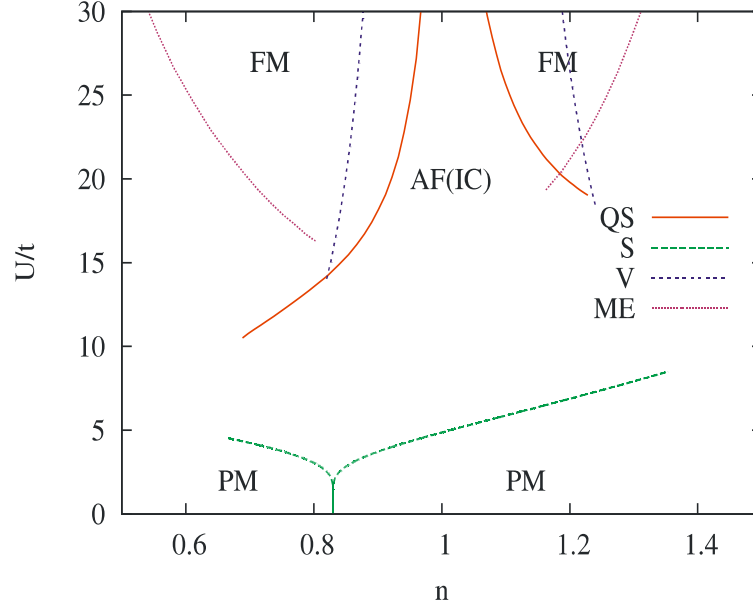


Fig. 1 Phase diagram of the 2D Hubbard model with  $t'=0.2t$ ,  $n$  being the electron concentration. *Line QS* separating FM and AF (including incommensurate, IC) phases is the result of the quasistatic approximation, *line S* is the boundary of the FM and PM phases in the simple Stoner theory, *line V* is the Visscher's boundary of phase separation of FM–AF (Neel) phase in the limit of large Hubbard repulsion  $U$ , *line ME* is the boundary of the FM and PM phases in the method of decoupling the equation of motion for the Green's functions for Hubbard's operators [3]

The results of the mean-field approach [1] are improved with the help of quasi-static (QS) approximation [2]. A comparison is performed with the method by Visscher (see [1]) and the result of decoupling the equation-of-motion sequence for the Green's functions in the Hubbard operator representation [3]. The phase diagram has the following phases: ferromagnetic (FM), antiferromagnetic (AF), incommensurate and paramagnetic (PM). It is shown that near half filling ( $n = 1$ ) the ferromagnetic state is characterized by instability of the spin-wave type, while away from half-filling the one-electron (spin-polaron) instability. Combined magnetic phase diagram for  $t' = 0.2t$  including all the instabilities is shown in Fig. 1.

- [1] P. A. Igoshev, M. A. Timirgazin, A. A. Katanin, A. K. Arzhnikov, V. Yu. Irkhin, Phys. Rev. B **81**, 094407 (2010).
- [2] P. A. Igoshev, A. A. Katanin, V. Yu. Irkhin, Sov. Phys. JETP **105**, 1043 (2007).
- [3] V. Yu. Irkhin, A. V. Zarubin, Solid State Phenomena, **168-169**, 469 (2011).

## Magnetic properties of the Ni amorphous nanogranule films

D. Ilyushenkov, D. Yavsin, V Kozhevin, I. Yassievich, V. Kozub and S. Gurevich  
*Ioffe Physico-Technical Institute, the Russian Academy of Sciences, 194021, St. Petersburg, Russia*

We report on structural and magnetic properties of granular films consisting of 2.5nm Ni nanoparticles. The films are fabricated by the original laser electrodispersion technique, which allows producing nearly monodisperse and amorphous particles.

Atomic force microscopy (AFM) study shows that in 10 nm thickness films the particles are self-assembled in clusters with the lateral size 100–150nm and the height of about 10 nm. Performed by SQUID, the films magnetization measurements reveal super- paramagnetic behaviour, characteristic for an ensemble of non-interacting single domain magnetic particulates. It is found that the magnetic moment of the particulate is equal to that of about 3000 individual Ni nanoparticles and the blocking temperature is close to room temperature. Defined from magnetic measurements, the size of single domain particulates correlates well with the size of the clusters determined from AFM images. We propose that exchange interaction plays an important role in the formation of the particulates by aligning the magnetic moments of the individual Ni nanoparticles inside the clusters. Presence of magnetic clusters with high blocking temperature makes the fabricated films potentially useful for high-density magnetic data storage applications.

We have studied theoretically (including computer simulations) magnetic properties of aggregates of ferromagnetic amorphous nanogranules in the presence of direct exchange between the neighboring granules and random anisotropy fields. We show that such a system can be considered as ferromagnetic glass. We demonstrate (basing on analytical considerations as well as on the results of numerical simulations) that the system is decomposed to clusters or domains with nearly collinear orientation of magnetization. The size of the domains depends on the ratio of the exchange interaction and random anisotropy. For quasi-2D structures we predict that the dipole–dipole interactions between the granules lead to a formation of magnetic vortices. Moreover, the computer simulations also reproduce the puzzling increase of the thermoremanent magnetization observed experimentally in 50 nm thickness films, which is expected to be a result of a temperature-dependent decrease in the anisotropy (or a temperature dependent increase in the exchange). We also consider the structures with weak intergranular exchange and show that they are characterized by the presence of two critical temperatures.

- [1] D.S. Ilyushenkov, V.I. Kozub, I.N. Yassievich, et al., *J. Magn. Magn. Mater.*, **323**, 1588 (2011).
- [2] D.S. Ilyushenkov, V.I. Kozub, D.A. Yavsin, et al., *J.Magn.Magn.Mater.*, **321(5)**, 343 (2009).

## Step forward to the new materials for MSSW devices

V. P. Ivanov<sup>1</sup>, S. A. Manuilov<sup>2</sup>, A. M. Grishin<sup>2</sup>, G. A. Nikolychuk<sup>1</sup>

<sup>1</sup>Research Institute Ferrit-Domen, 196084, Saint-Petersburg, Russia,

<sup>2</sup>Royal Institute of Technology, SE-16440, Stockholm, Sweden

Yttrium iron garnet (YIG) films are well known to be used in different kinds of magnetostatic wave (MSW) devices. The liquid phase epitaxy (LPE) is well established technique for high quality low loss YIG films synthesis. Therefore thick LPE grown YIG films are still have no rivals. Here one more time we try to promote the new sub-micron YIG films synthesised by the means of pulse laser deposition (PLD) technique. Previously authors described the films growth process and they magnetic properties [1-3]. Shortly, PLD grown Fe-deficient films in combination with low coercivity  $H_c = 40$  mOe and moderate magnetic losses  $\Delta H = 0.9$  Oe posses recordly hight value of uniaxial anisotropy  $H_u = -0.88$  kOe with saturation magnetization  $4\pi M_s$  around 1.8 kGs. All these make PLD synthesised films attractive for miniaturised and highly tunable devices with lowered power consumption.

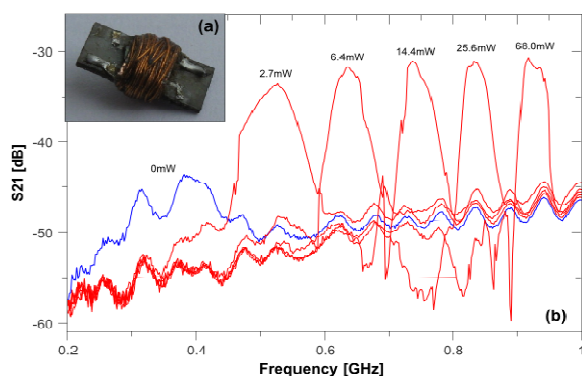


Fig. 1 MSSW filter with integrated coil: (a) photo of  $10 \times 6.4 \times 4.3$  mm<sup>3</sup> device and (b) transmission characteristics of the device taken at different powers supplied to the integrated coil. External magnet wasn't used here.

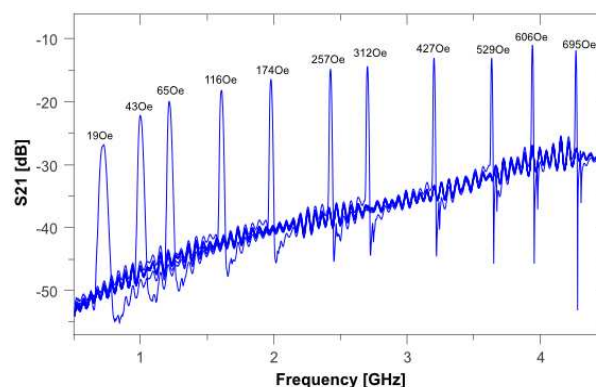


Fig. 2 Performance of MSSW filter in the wide frequency range. External magnet was used to sweep magnetic field  $H$  from 19 Oe up to 695 Oe, while integrated coil was kept deenergized.

The constructed device is MSSW filter based on PLD grown 0.45  $\mu\text{m}$  thick YIG film with tuning coil directly wound onto alumina plate with MSSW excitation transducers and laid on them YIG film. The photo of the device is shown in Fig.1a. Figure Fig.1b represents device tuning in the range of 0.5 GHz with the power feed to the tuning coil ranged from 0 to 68 mW. The rejection level around 47 dB and minimum insertion loss of 30 dB gives 17dB to the MSSW assisted filter transmission. The wide range inspection of the filter performance is presented in Fig.2 where external magnet has been used with turned off power of the integrated turning coil. Filter transmission characteristics measured in the range of 0.5 – 4.5 GHz reveal insertion loss minimum of 11 dB at 3.9 GHz with rejection level of 30 dB.

The value of the losses achieved in the constructed MSSW filter combined with low power consumption and possible miniaturization promises for PLD grown YIG films applicability in the new and well known MSW devices.

[1] S. A. Manuilov, R. Fors, S. I. Khartsev, and A. M. Grishin, J. Appl. Phys. **105**, 033917 (2009).

[2] S. A. Manuilov, S. I. Khartsev, and A. M. Grishin, J. Appl. Phys. **106**, 123917 (2009).

[3] S. A. Manuilov and A. M. Grishin, J. Appl. Phys. **108**, 013902 (2010).



## Preparation and study of Fe/M (M=Co or Pt) thin films for ultrahigh-density magnetic recording

A. S. Kamzin<sup>1</sup>, Fulin Wei<sup>2</sup>, V. Ganeev<sup>3</sup> and L. D. Zaripova<sup>3</sup>

<sup>1</sup>*Ioffe Physical-Technical Institute of RAS, 194021, St. Petersburg, Russia,*

<sup>2</sup>*Research Institute of Magnetic Materials, Lanzhou University, 730000, Lanzhou, China*

<sup>3</sup>*Kazan (Privolzhsky) Federal University, 420008, Kazan, Russia*

The further increase in the density of recording on magnetic media, one has, on the one hand, to create magnetic films as recording media with a high coercivity. On the other hand, in order to write information on the high coercivity media, recording head materials with high saturation magnetization, high permeability and low coercivity are required. In addition, the creation of the ultrahigh-density magnetic recording (UHD MR) systems of next generation requires magnetic materials as writing media with the minimum possible magnetic grain size, as well as miniaturization of the write/read magnetic heads.

This report presents the results of studies of the  $\text{Fe}_{1-x}\text{Co}_x$  films for write/read magnetic heads an UHD MR system, prepared by means of the RF magnetron co-sputtering method (RFNCSM) [1] on different under-layers. Also in this report are presenting the results of investigations for UHD MR applicable of multilayer  $L_{10}$  [Fe/Pt] $n$  films with controlled orientation of the easy axis and a high coercive by RFNCSM [1]. Our studies of Fe/M (M=Co or Pt) films have been focused on technological issues of high-density recording heads and media, respectively, as well as on the fundamental magnetic properties, such as the temperature dependence of the magnetic anisotropy constants, orientation of the easy axis and the exchange stiffness constant.

The film composition was determined using inductively coupled plasma spectroscopy. The magnetic properties were studied using a SQUID and vibrating-sample magnetometers. The microstructure of the films was determined by X-ray diffraction (XRD). The magnetic structure of the films was studied using Conversion Electron Mössbauer (CEM) Spectroscopy. The angle  $\Theta$  between the light axis orientation and the normal to the film plane determined using the relation of the intensity of 2-nd(5-th)/1-st(6-th) lines in the Zeeman sextet:  $A_{25}/A_{16}=3(1-\cos\Theta)/(4\sin\Theta)$ .

In result the FeCo nanostructured thin films with high magnetization ( $M_s$ ) and low coercivity  $H_c$  were obtained by utilizing suitable under-layer and optimizing the deposition conditions. It was found that the improvement of soft magnetic properties for FeCo films with an under-layer is closely related to the film texture.

In the case of FePt  $L_{10}$ -phase multilayer [Fe/Pt] $n$  thin films have been obtained. The total thickness of multilayer [Fe/Pt] $n$  was varied from 25 to 200 nm by changing the number  $n$  of deposited bilayers. We have studied the dependence of the microstructure, the magnetic structure, and the easy axis orientation in the [Fe/Pt] $n$  films on the substrate temperature as well as the pressure of Ar during sputtering, the order and thicknesses of Fe and Pt layers; and the total film thickness. These multilayers possess magnetocrystalline anisotropy ( $K_u$ ) greater compared to the existing magnetic recording media, large coercivity and saturation magnetization, high chemical stability and corrosion resistance.

The results of our studies demonstrated that prepared FeCo films and  $L_{10}$  [Fe/Pt] $xn$  multilayers meet the requirements to write/read heads and recording media, respectively, for the perpendicular recording and can be use for future UHD MR systems.

- [1] A. S. Kamzin, L. A. Grigor'ev, A. B. Sherman, and I. S. Barash, Sverkhprovodimost: Fiz. Khim. Tekh. **6**, 64 (1993).

## Skyrmion lattices in multiferroics

A. N. Kalinkin, V. M. Skorikov

*Institute of General and Inorganic Chemistry RAS, 11999 Moscow, Russia*

Collective spin excitations in the form of skyrmion lattices have recently been the subject of intense research in solid state physics and chemistry in both magnetic models and nonlinear field models for a 2D electron gas. This is due to the possibility of using such lattices to produce promising information recording/readout systems with active components (skyrmions, Fig.1) ~1 nm in size, which will enable a record high data density ~10 Tb/cm<sup>2</sup>. Skyrmion stabilization mechanism has recently been proposed for magnetics, which employs the well-known Dzyaloshinskii–Moriya (DM) interaction  $k$  with linear field derivatives [1].

We construct perturbation theory with  $k$  as a small parameter using the Belavin-Polyakov solution  $\theta_0$  as unperturbed:  $\theta(r,k) = \theta_0(r) + \kappa g(r) + \dots$ . To first order in  $\kappa$ , the lattice energy per unit area of the circular cell of skyrmion lattice has the form (for antiferromagnets):

$$E = (2/R^2) \int dr \{ (\theta_0')^2 + (1+1/r^2) \sin^2\theta_0 - (k/r) \sin\theta_0 \cos\theta_0 [1+2(1+r)g] + k \theta_0' (1+2g) \} r,$$

where  $\theta'$  and  $g'$  are derivatives with respect to  $r$ . The integration is performed from  $r=0$  to  $R$  (cell boundary) and  $\theta(r,k)_{r=0} = 0$ ,  $\theta(r,k)_{r=R} = \pi$ ,  $\theta_0 = 2\arctg(r/\lambda)$ .

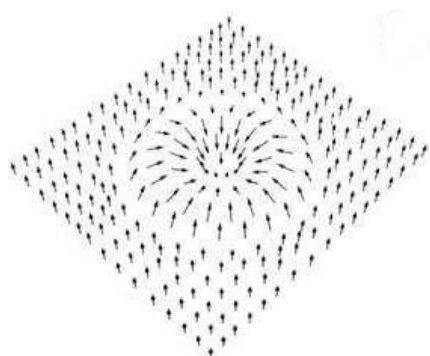


Fig.1. The Skyrmion.

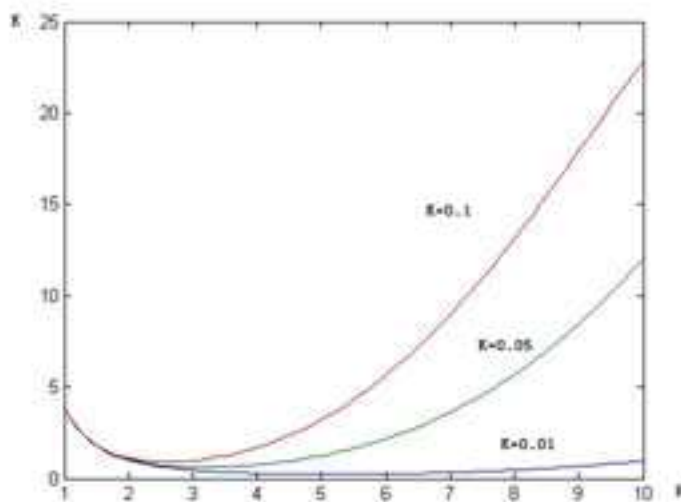


Fig.2. Energy of the cell  $E$  as a function of  $R$ .

From Euler's equation we obtain a linear differential equation in  $g(r)$ :

$$g'' + (1/r)g' - (r^4 - 6r^2 + 1)/[r^2(1+r^2)^2]g = -4r/(1+r^2)^2$$

with the analytical solution  $g(r) = -0.5r$ .

The free parameter  $\lambda = R \text{tg}(kR/4)$ . Calculating standard integrals, we find:

$$E = 2[a_0 + a_1/(\lambda^2 + R^2) + a_2 \ln(1 + R^2/\lambda^2)/R^2] \quad \text{with } a_0 = k\lambda, \quad a_1 = [(4 + \lambda^2)(1 - k\lambda) + \lambda^2], \quad a_2 = \lambda^2(2 - 3k\lambda).$$

Minimizing energy  $E$  with respect to  $R$ , we obtain the curves presented in Fig.2. As seen, at each  $\kappa$  value there is a minimum in energy  $E$  as a function of the cell radius  $R$  in the skyrmion lattice. This implies conceptual possibility of a spontaneous skyrmion lattice stabilized by DM interaction in multiferroic BiFeO<sub>3</sub> (BFO) with hexagonal sublattice of ions Fe<sup>3+</sup>. DM interaction is typical for the noncentrosymmetric antiferromagnet BFO. Multiferroic BFO is a promising material for spintronics and magnonics [2] because it has high temperatures  $T_C = 1103$  K,  $T_N = 643$  K and a giant linear magnetoelectric effect and giant polarization (in films).

[1]. A.N. Bogdanov, D.A. Yablonskii. *ZhETP*. **96**, 253 (1989).

[2]. A.N. Kalinkin, V.M. Skorikov. *J. Inorg. Chem.* **55**, 1903 (2010).

# Properties of high frequency conductivity in noncollinear ferromagnets

E. Karashtin<sup>1</sup>, O. Udalov<sup>1</sup>

<sup>1</sup>*Institute for physics of microstructures RAS, 603950, Nizhny Novgorod, Russia*

It is well-known that the symmetry of the Schrödinger equation does not allow electro-dipole transitions of electrons between two spin subbands in collinear ferromagnets. However, this restriction is removed in a media with noncollinear ferromagnetic structure. An additional contribution to the high-frequency conductivity should appear due to these transitions in such a media. We study this contribution considering two particular distributions of magnetic moments: helical distribution and noncollinear multilayer magnetic structure.

Helical magnetic structure can be found in holmium. This rare-earth metal possesses coplanar helical structure below the Neel temperature (133K) which becomes noncoplanar at the Curie point (20K). Earlier experiments [1] show that holmium demonstrates anomalous increase in the conductivity at the frequency close to the exchange splitting (0.35eV). The peak is observed below the Neel temperature and vanishes in a strong external magnetic field. We propose a theoretical explanation of this phenomenon. The exchange interaction between localized d-electrons and delocalizes s-electrons is taken into account, while the spin-orbit interaction is neglected. The results of our calculations compared to the experimental data are shown in Fig. 1. Theoretical and experimental curves fit well in the vicinity of the exchange splitting frequency. Besides, the proposed contribution to the high-frequency conductivity exists only in noncollinear magnetic structure in accordance with the experiment.

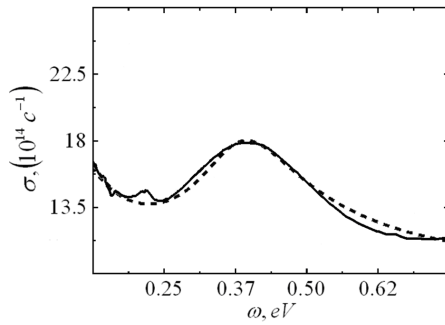


Fig. 1 High-frequency conductivity of holmium at 5K. Experiment (solid) and theoretical calculations (dashed).

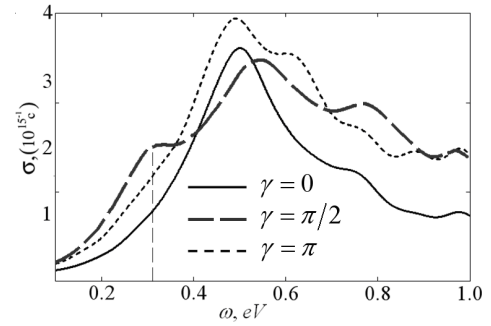


Fig. 2 Conductivity of [Ni(2nm)/insulator/Ni(2nm)/conductor] periodic structure. A peak is observed in noncollinear state at 0.31eV.

We suggest similar effect to arise in a periodic multilayer ferromagnetic structure with noncollinear orientation of magnetic moments of neighbouring layers. Such a structure demonstrates the GMR effect [2] which consists in considerable difference between conductivities in parallel and antiparallel states. Our calculations show that in addition to this effect the conductivity demonstrates an observable peak in the vicinity of the exchange splitting frequency (see Fig. 2) which exists only in noncollinear state. The peak becomes more prominent as the thickness of the layers is decreased.

This research was supported by the FTP “Scientific and scientific-pedagogical personnel of innovative Russia” (contracts No P2618, P348), RFBR (project 11-02-00294-a), and the “Dynasty” foundation.

[1] P. Weber and M. Dressel, *J. Magn. Magn. Mater.* **272-276**, E1109 (2004).

[2] M. N. Baibich, J. M. Broto, A. Fert et al. *Phys. Rev. Lett.* **61**, 2472 (1988).

# Oscillatory energy exchange between spin wave modes coupled by a dynamic magnonic crystal

A. D. Karenowska<sup>1</sup>, A. V. Chumak<sup>2</sup>, V. S. Tiberkevich<sup>3</sup>, A. A. Serga<sup>2</sup>, J. F. Gregg<sup>1</sup>,  
A. N. Slavin<sup>3</sup> and B. Hillebrands<sup>2</sup>

<sup>1</sup>Department of Physics, University of Oxford, Oxford OX1 3PU, United Kingdom, <sup>2</sup>Fachbereich Physik and Forschungszentrum OPTIMAS, Kaiserslautern University of Technology, Kaiserslautern 67663, Germany, <sup>3</sup>Department of Physics, Oakland University, Rochester, MI 48309, United States.

A magnonic crystal (MC) [1-6] is a spin-wave transmission medium which features an ‘artificial lattice’ formed by a wavelength-scale spatial modulation in its magnetic properties. Like other artificial crystals (for example optical photonic crystals [7-9]), the transmission spectra of MCs typically include band gaps; frequency intervals over which wave propagation is prohibited. In this paper, we describe the results of a series of investigations into spin-wave propagation in a *dynamic* magnonic crystal (DMC) which can be switched from a spatially uniform state with a trivial transmission spectrum (‘off’), to a spatially modulated state with a well defined band gap (‘on’) (Fig. 1). We demonstrate that if such a crystal undergoes a rapid transition from ‘off’ to ‘on’ whilst an incident spin-wave mode lying within the band gap is excited *inside* it, this wave becomes coupled to a secondary counter-propagating wave, generally of a different frequency [5, 6] (Fig. 2). We explore the features of the interaction experimentally and theoretically and show that its underlying physics reveals a fundamental result of general wave dynamics.

The interaction is characterized by *oscillatory* energy exchange i.e. the direction of energy flow between the incident and secondary waves spontaneously reverses every  $T$  seconds for as long as the coupling persists [6]. The coupled mode frequencies are related by inversion about the DMC’s band-gap centre frequency  $f_a$  (Fig. 2) so that the coupling can be used to realize *all-linear* frequency conversion and time reversal of signals; functionalities of considerable technological significance [5].

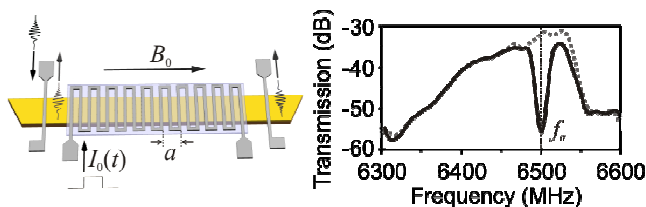


Fig. 1 Experimental DMC system and transmission characteristics in the ‘off’ state (dotted) and in the ‘on’ state in which there is a band gap centred on frequency  $f_a$  (solid).

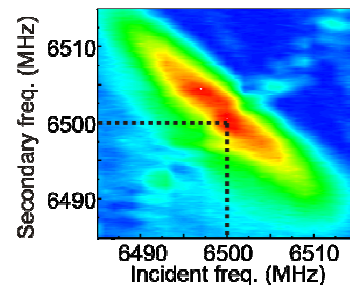


Fig. 2 Experimental data showing that coupled mode frequencies are related by inversion about  $f_a$ .

- [1] A. V. Chumak et al., J. Phys. D **42**, 205005 (2009).
- [2] K-S. Lee et al., Phys. Rev. Lett. **102**, 127202 (2009).
- [3] Z. K. Wang et al., Appl. Phys. Lett. **94**, 083112 (2009).
- [4] G. Gubbiotti et al., J. Phys. D **43**, 264003 (2010).
- [5] A. V. Chumak et al., Nat. Commun. **1**, 141 (2010).
- [6] A. D. Karenowska et al., *submitted* (2010).
- [7] J. Bravo-Abad and M. Soljačić, Nature **6**, 799 (2007).
- [7] E. J. Reed et al., Phys. Rev. Lett. **90**, 203904 (2003).
- [9] S-Y. Lin et al., Science **282**, 274 (1998).

# Some aspects of the influence of defects on the formation of thermoremanent magnetization in two-domain grains ensemble

N. Khasanov

*Bashkir State University, 450074, Ufa, Russia*

Most crystalline grains that make up rocks contain a large number of defects. Domain walls interact with these defects, which leads to the fact that the magnetic properties of rocks in weak fields are quite different from the properties calculated assuming an ideal crystal lattice. Among the magnetic properties of minerals the thermoremanent magnetization plays a special role [1]. It is useful for investigating the changes of the geomagnetic field in ancient times, the movement of continents and for obtaining of some information about the deep layers of the crust inaccessible to direct study.

There are many papers on the calculation of thermoremanent magnetization. But they are either not explicitly take into account the defects (single-domain model), or oversimplify their location. In addition, during the formation of thermoremanent magnetization or later, the rocks could undergo high pressure. Therefore, was tasked with: analytically calculate the effect of the distribution of defects, other than a purely random, the formation and destruction thermoremanent two-domain magnetization of the ensemble of grains with a light pressure.

In this case, we used the previously developed theoretical model of the thermoremanent magnetization formation in two-domain grains. According to that model for the case of moderate magnetic fields previously obtained the same expression as for thermomagnetization ( $I_{HT}$ ), measured at room temperature, and for thermoremanent magnetization ( $I_{rT}$ ):

$$\frac{I_{HT}}{I_s} = \frac{I_{rT}}{I_s} = \frac{C}{1-\zeta_0} \left( \frac{AH}{2D} \left( \frac{q}{q-1} \right) \left( \frac{W(q-1)}{AH} \right)^{\frac{1}{q}} F_1 - \frac{1}{v} F_2 \right), \quad (1)$$

$$\text{where } F_1 = F_{10} = \frac{1-\zeta_0^{3-1/q}}{(3-1/q)}, \quad F_2 = F_{20} = \frac{1-\zeta_0^2}{2}.$$

Here  $q$  is constant characterizing the temperature dependence of the coercive force,  $A$ ,  $C$ ,  $D$ ,  $W$ ,  $n$  are structure constants related to the size, shape of grains and other parameters,  $I_s$  is spontaneous magnetization,  $H$  is magnetic field.

Earlier [2] estimates obtained from the simplifying assumption that the elastic stress  $\sigma$  is small

(i.e.  $\left| \frac{\sigma \lambda_{111}}{K_1} \right| \ll 1$ ,  $\left| \frac{\sigma \lambda_{100}}{K_1} \right| \ll 1$ ) gave overestimated values. New calculations show that the

differences from the uniform distribution of defects and from a completely chaotic one lead to a decrease in average thermoremanent magnetization obtained under pressure, as well as to smaller values of TRM, obtained after partial heat-induced destruction of this magnetization. This leads to values closer to the experimental ones.

[1] Özdemir, Ö. Thermoremanent magnetization, Encyclopedia of Geomagnetism and Paleomagnetism, Editors: David Gubbins and Emilio Herrero-Bervera. Kluwer Academic Publishers, pp 609-616. (2008)

[2] N.A. Khasanov, V.I. Maksimochkin, K.A. Valeev. Izvestiya. Physics of the Solid Earth. Vol.35, No.6 (1999)

# Ground states of the triangular arrays of magnetic dots in the presence of the external magnetic field

R. Khymyn, V. E. Kireev, B. A. Ivanov

*Institute of Magnetism, National Academy of Sciences of Ukraine, Kiev, 03142, Ukraine*

The ground state of the array of small magnetic particles (magnetic dots) with the magnetic moment perpendicular to the lattice plane ordered into the 2D triangular lattice and subject to an external magnetic field was investigated. Such model is applicable for the single-domain small dots with perpendicular anisotropy and for the micron-sized dots in the vortex state, in the latter case the out-of-plane magnetic moment is specified by the vortex core [1]. The close-packed triangular lattices of the cylindrical particles considerably extended in the direction normal to the array plane are naturally obtained when the array is prepared by the self-organization method. The triangular lattice with the dipole-dipole interaction of the moments is a typical example of the frustrated system. Behavior of such arrays is defined by the long-range dipolar interaction and with account taken of the external magnetic field  $H_z$  can be described by the energy

$$W = \frac{M_0^2}{a^3} \sum_{i,j,i \neq j} |r_i - r_j|^{-3} S_i S_j - M_0 H_z \sum_i S_i. \quad (1)$$

Here the summation runs over the all pairs of the lattice sites,  $M_0$  is the magnetic moment of the site,  $a$  – distance between sites,  $S_i = \pm 1$  determines the sign of the magnetic moment projection on the axis perpendicular to the lattice plane. Dipolar interaction is not local and results in a rather simple checkerboard antiferromagnetic (AFM) orientation of the magnetic moments in a square lattice [1]. For the case of the triangular lattice in the absence of magnetic field for model (1) AFM order with two sublattices can be implemented, where from 6 nearest neighbors of each moment 2 have the same sign, and 4 the opposite sign. But the differences in the magnetization process for these two lattices, triangular or rectangular, are much more essential, either for an infinite array or finite systems. For the rectangular lattice (in particular, square lattice) the magnetization is going through the turn of some magnetic moments, leading to the multisublattice structures at finite values of the external magnetic, for finite systems such reversed moments are concentrated at the corners and edges of the array. In the triangle AFM lattice linear topological defect in the form of a magnetized domain wall appears with the increasing of the external magnetic field to the certain critical value  $H_c = 0.71 M_0 / a^3$ . The scenario with the magnetic moments reversal at the corners and edges of the array, typical for the square lattice, could appear in much higher external magnetic field and are not realized here for any geometry of the array's border. Because of the presence of the magnetic moment such defects (magnetized domain walls) repel each other. At the values  $H \geq H_c$  a finite density of such walls are present creating a new regular triangle superlattice. The increasing of the external magnetic field in the range from  $H_c$  to the saturation field  $H_s$  (when the all the moments become parallel) is characterized by the gradual parameter changing of such superlattice. Due to the discrete nature of such changing some jumps are observed on the magnetization function of the array especially noticeable in the region of relatively low external magnetic fields.

- [1] J. E. L. Bishop, A. Yu. Galkin, and B. A. Ivanov, Phys. Rev. B **65**, 174403 (2002).
- [2] B. A. Ivanov, V. E. Kireev, JETP Letters **90**, 750 (2009).

# Features of high-frequency properties of the crystal $\text{NdFe}_3(\text{BO}_3)_4$ in the incommensurate magnetic phase

M. I. Kobets, K. G. Dergachev, E. N. Khatsko, S. L. Gnatchenko  
*B. Verkin Institute for Low Temperature Physics and Engineering,  
 National Academy of Sciences of Ukraine, 61103 Kharkov, Ukraine*

In this report we present experimental results of the AFMR spectrum studying in multiferroic  $\text{NdFe}_3(\text{BO}_3)_4$  at temperature 4.2 K. The investigated crystal belongs to the noncentrosymmetrical space group  $R32$ , at high temperatures. Below 30 K  $\text{NdFe}_3(\text{BO}_3)_4$  crystal is antiferromagnetic with easy-plane type magnetic anisotropy. The magnetic phase transition in a helical incommensurate phase occurs at a temperature of 13.5 K [2]. The field-frequency dependence of quasi-ferromagnetic line in  $\text{NdFe}_3(\text{BO}_3)_4$  ( $\mathbf{H}||\mathbf{a}$ ) in the frequency range 25-33 GHz was studied and in the AFMR spectrum an intense additional absorption line ( $H_{res} \sim 6$  kOe) was detected. The resonance excitation was observed in experiment under the condition  $\mathbf{H} \perp \mathbf{h}$ . There are several significant features of additional line. First, the increasing of external magnetic field leads to appearing of additional line, and decreasing of external magnetic field leads to disappearing of this line (fig. 1).

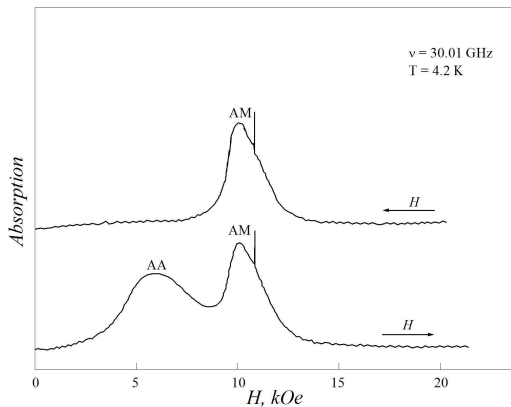


Fig. 1. Additional absorption lines and its transformation after magnetic field direction changing. AA – additional absorption, AM – acoustic mode of AFMR, narrow line – the signal DPPH.

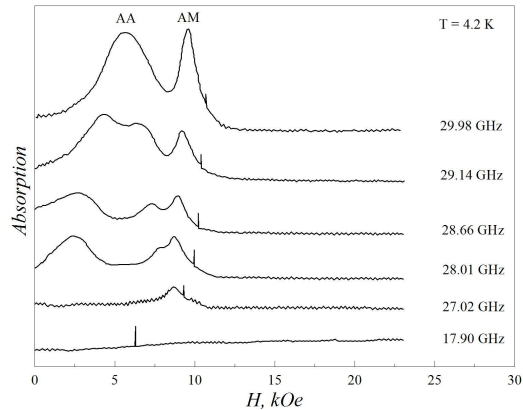


Fig. 2. Transformation of additional absorption line of  $\text{NdFe}_3(\text{BO}_3)_4$  AFMR spectrum with frequency changing. AA – additional absorption, AM – acoustic mode, narrow line - the signal DPPH.

Second, decreasing frequency leads to splitting of additional absorption line into two. First line approaches to the gap value  $\Delta\nu_{AA} = 27.58$  GHz in zero magnetic field at further decreasing of frequency. For second line, the resonance field increases (fig. 2). For orientation of the external magnetic field  $\mathbf{H}||\mathbf{c}$  the excitation was not found. In this work we assumed that additional absorption line at AFMR spectrum of  $\text{NdFe}_3(\text{BO}_3)_4$  is caused by elementary excitation spectrum of incommensurate phase

[1] W.A. Dollase and R.J. Reeder, Amer. Mineral., **71**, 163, (1986).

# Equations to describe the femtosecond magneto-optics under the electric-dipole excitation of electrons

M. I. Kurkin<sup>1</sup> and N. B. Orlova<sup>2</sup>

<sup>1</sup>*Institut of Metal Physics UrB of RAS, 620041, Ekaterinburg, Russia,* <sup>2</sup>*Department of Applied and Theoretical Physics, Novosibirsk State Technical University, 630092 Novosibirsk, Russia*

The required equations were derived using several assumptions:

1. The light wave is described by Maxwell equations in a medium taking into account the interaction of the electric dipole moment  $P$  and the wave electric field  $E(t)$  (electric-dipole approximation).
2. Dynamics of electrons under the action of  $E(t)$  is described by quantum equations with the simplified electronic Hamiltonian  $H_e$ . Simplification is connected with the femtosecond duration  $\tau_p$  of optical pulse. It consists in the fact that in the Hamiltonian  $H_e = H_0 + \Delta H$ , the terms  $\Delta H$  are neglected that do not have time to significantly change the electron wave function in the time interval  $\tau_p$ .
3. The eigenstates of the Hamiltonian  $H_0$  were assumed to describe the orbital ( $l$ ), magnetic ( $m$ ), spin ( $\sigma$ ) quantum numbers, the number of Bloch band ( $n$ ) and the wave vector in the Brillouin zone ( $k$ ). That allowed us to use the electric-dipole selection rules under the action of circularly polarized light wave:

$$\Delta l = l' - l = \pm 1, \quad \Delta m = m' - m = 1, \quad \Delta \sigma = \sigma' - \sigma = 0, \quad \Delta k = k' - k = 0 \quad (1)$$

The change in quantum number  $n$  is determined by the resonance condition

$$h\nu = \varepsilon(n', k, l') - \varepsilon(n, k, l) \quad (2)$$

In these approximations, the behavior of electrons in the electric field of the light wave  $E(t)$  is described by three dynamical variables: the non-diagonal matrix elements of electric-dipole momentum

$$P^+ = P_{n'l',nl}; \quad P^- = P_{nl,n'l'} \quad (3)$$

and the difference in population numbers of the ground and excited states  $\Delta\rho = \rho_{n'l'km'\sigma} - \rho_{nlkm\sigma}$ . The behaviour of  $P^\pm$  and  $\Delta\rho$  is described by the Bloch-type equations [1], which solutions were considered in detail in the theory of magnetic resonance [2]. In the theory of magnetic resonance the dependence of the transition frequency (2) having a continuous range of values on the wave vector  $k$  corresponds to the inhomogeneous broadening.

In the report we discuss the results of the joint solution of Maxwell and Bloch equations in the case of a large inhomogeneous broadening when the width of the spectral band  $h\Delta\nu = h(\nu(k_B) - \nu(0))$  is much larger than the interaction of the electron with the electric field amplitude of the light wave. The value of  $k_B$  is the value of  $k$  on the boundary of the Brillouin zone.

This work was partly supported by Russian Foundation for Basic Research (project 11-02-00093).

[1] L. Mandel and E. Wolf, *Optical Coherence and Quantum Optics* (Cambridge Univ. Press, 1995).

[2] A. L. Bloom, *Phys. Rev.* **98**, 1105 (1955).



# Raman image of the magnetic structure in $\text{YFeO}_3$

A. P. Kuz'menko, P. V. Abakumov

South-West State University, 305040, Kursk, Russia

The recent level of development of measurement techniques made it possible for cards to study the spectral distribution of Raman transitions in polymorphous crystallographic multiferroics type  $\text{Ni}_3\text{B}_7\text{O}_{13}\text{Br}$  (Ni - Br) [1]. According to Raman observed using probe micro spectrometer NTEGRA Spektra, were visualized with the dimensions of the DS 200 - 400 nm in  $\text{LiNbO}_3$ , which had previously formed during the laser-processing  $\text{CO}_2$  - laser [2].

Active modes of the magnetic ion  $\text{Fe}^{3+}$  in the Raman spectrum  $\text{YFeO}_3$  has only one line  $A_g$  ( $221\text{ cm}^{-1}$ ). There is a difference in the intensity of the interaction of the exciting radiation (532 nm) with a magnetic moment in the neighboring domains in mind the different orientation of the one. This leads to a difference in the intensity of the  $221\text{ cm}^{-1}$  in the Raman spectra. In all the measurements it reached 34% [3].

Area on the sample in the vicinity of the domain boundary was chosen with the help of a confocal microscope, modified for the magneto-optical studies. We used a lens with a numerical aperture of 0.28. The magnetic structure was studied by the method of mapping a lens with a numerical aperture of 0.7. Scanned sample area ( $60 \times 15\ \mu\text{m}$ ) using AFM. Raman spectra were measured at each point with a spatial resolution of 500 nm. The obtained Raman images of the domain structure are shown in Fig. 1.

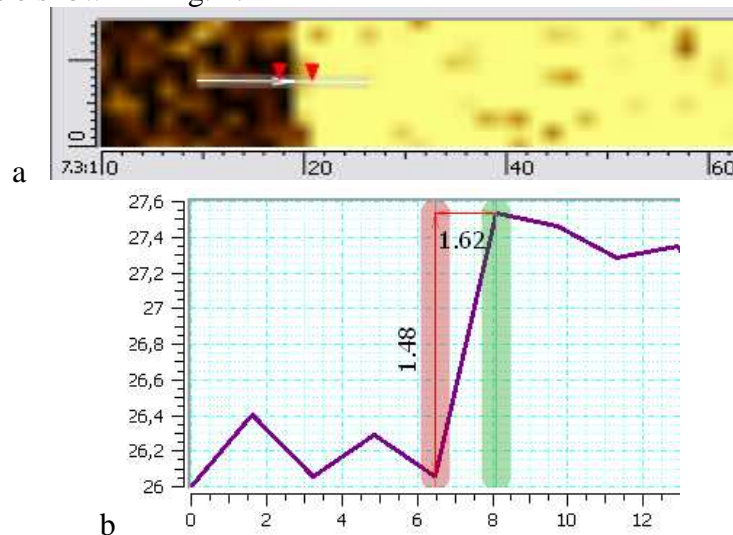


Fig. 1. The construction of hyperspectral data: a) a picture of the domain structure and b) the width of the domain wall in  $\text{YFeO}_3$

Software on the hyperspectral data obtained by mapping, presented in graphical form, are based changes in the magnetization along the perpendicular to the plane of the wall (even if it is bent). Defined in this way the width of the DW in  $\text{YFeO}_3$  was  $\sim 1.6\ \mu\text{m}$  (Fig. 1), which is consistent with measurements using magneto-optical microscope.

[1] M. N. Iliev, V. G. Handjiev, J. Iniguex, J. Pascual. Phys. Rev. B **116** (1) (2009).

[2] P. S. Zelenovsky, V. Ya. Shur, D. K. Kuznetsov et al. Fiz. Tver. Tela. **53**(1) (2011).

[3] A. P. Kuz'menko, P. V. Abakumov, A. N. Chaplygin, Proceedings of KSTU **4**(33), (2010).

# Role of the rare-earth magnetism in the magnetic-field-induced polarization reversal in multiferroic $\text{TbMn}_2\text{O}_5$

N. Leo<sup>1</sup>, D. Meier<sup>2</sup>, R. V. Pisarev<sup>3</sup>, S.-W. Cheong<sup>4</sup>, and M. Fiebig<sup>1</sup>

<sup>1</sup>*HISKP Universität Bonn, Bonn, Germany,*

<sup>2</sup>*University of California, Berkeley, USA,*

<sup>3</sup>*Ioffe Physical-Technical Institute, St. Petersburg, Russia;*

<sup>4</sup>*Department of Physics and Astronomy, Rutgers University, New Jersey, USA*

The interplay of multi-dimensional complex magnetic order parameters leads to fascinating effects like magnetically induced ferroelectricity [1]. A particular interesting example is  $\text{TbMn}_2\text{O}_5$  because of the associated magnetic-field controllable electric polarization. This material shows well defined optical second harmonic generation (SHG) features [2] related to charge-transfer transitions between oxygen and manganese ions [3]. By using SHG measurements we show that the gigantic magnetoelectric effect originates in three independent ferroelectric contributions. Two of them are related to magnetic ordering within the manganese  $\text{Mn}^{3+}$  and  $\text{Mn}^{4+}$  sublattices. The third contribution is related to the magnetism of the  $\text{Tb}^{3+}$  sublattice and has not been identified before. It mediates the remarkable magnetic-field induced polarization reversal. This model is verified by experiments on the isostructural  $\text{YMn}_2\text{O}_5$  where  $\text{Y}^{3+}$  ions are nonmagnetic. In this case only two polarization contributions due manganese sublattices are present and no magnetoelectric coupling is observed. These results underline the importance of the  $3d$ - $4f$ -interaction for the intricate magnetoelectric coupling in the class of isostructural  $\text{RMn}_2\text{O}_5$  compounds.

This work was supported by the DFG through SFB 608. The work of R.V.P. is supported by the RFBR through Projects 09-02-00070a and 10-02-90023-Bel\_a.

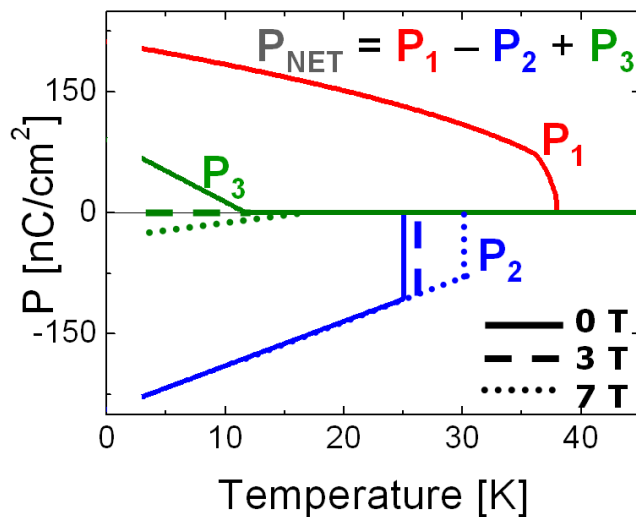


Fig. 1: SHG study allowed us to distinguish three independent contributions to the spontaneous net polarization in  $\text{TbMn}_2\text{O}_5$ . Application of a magnetic field  $H_x$  leads to a reversal of the net polarization at low temperatures, which can be related to suppression and reversal of the low-temperature rare-earth Tb-induced contribution  $P_3$ , whereas the ferroelectricity linked to the magnetic order of manganese sublattices remains robust.

[1] M. Fiebig, J. Phys. D – Appl. Phys. **38**, R123 (2005).

[2] Th. Lottermoser, D. Meier, R. V. Pisarev, and M. Fiebig, Phys. Rev. B **80**, 100101 (2009).

[3] A. S. Moskvin and R. V. Pisarev, Phys. Rev. B **77**, 060102(R) (2008).

# On the relationship between power and dispersion characteristics of a dipole spin waves

E. H. Lock, A. V. Vashkovsky

Kotel'nikov Institute of Radio Engineering and Electronics of Russian Academy of Sciences  
(Fryazino branch),

141190, Vvedensky sq.1, Fryazino, Moscow region, Russia

The ferrite-dielectric-metal (FDM) structure has one rare property: dispersion characteristic of a dipole spin wave (magnetostatic wave (MSW)) in these structure may have one or two extremum points. Thus, in some intervals of wave number the wave is forward, and in the other intervals – backward. As a distinct from other structures, where the wave is always forward or always backward, it is of interest to consider, how fundamental relationships between the propagation number, phase and group velocities, Poynting vector and power flow manifest themselves when the wave number changes near extremum points.

Basing on the Maxwell's equations the dispersion characteristics of MSW with extremum points were calculated for FDM structure (Fig.1, curves 2, 3). Then the corresponding partial and total power fluxes were calculated for the FDM structure geometries with extremum points on dispersion characteristics (Fig.2). As it is seen from comparison of Fig.1 and Fig.2, when the wave number  $k_y$  changes near extremum points, then the total power flow  $\Pi$  changes its value from positive to negative (or from negative to positive).

We have done similar calculation in magnetostatic approximation. A comparison of magnetostatic approximation results with calculations using Maxwell's equations shows that magnetostatic approximation formulas (currently used for calculation of the MSW Poynting vector and MSW power flow) are wrong. A correct formulas is proposed in [1].

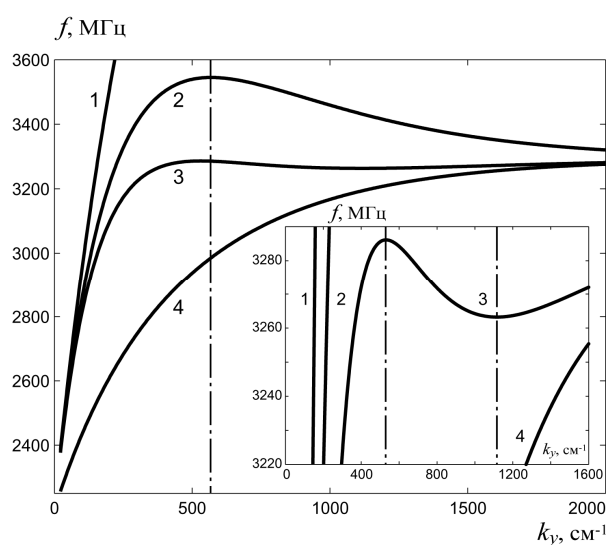


Fig. 1 Dispersion of FDM structure for various vacuum gap thickness  $w$ : 1 –  $w = 0$ , 2 –  $w = 10 \mu\text{m}$ , 3 –  $w = 15.5 \mu\text{m}$ , 4 –  $w \rightarrow \infty$ .

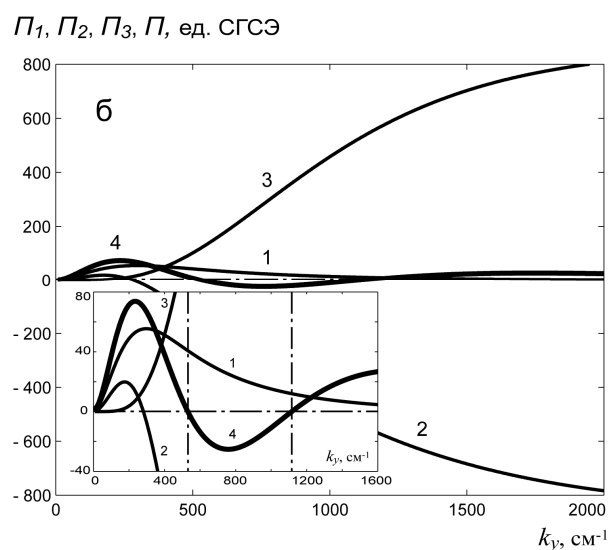


Fig. 2 Power fluxes of FDM structure for  $w = 15.5 \mu\text{m}$  for in vacuum half-space (1), in ferrite (2), in vacuum gap (3) and total flux (4 bold line).

This work is partially supported by the Program “Development of the Scientific Potential of High School” (project No. 2.1.1/1081).

[1] A. V. Vashkovsky, E. H. Lock, Physics-USpekhi, **54**(3), in press, (2011).

# spin-wave and spintronic devices on the base of magnetic nanostructures

L. V. Lutsev<sup>1</sup>, A. I. Stognij<sup>2</sup>, N. N. Novitskii<sup>2</sup>, and A. S. Shulenkov<sup>3</sup>

<sup>1</sup> Ioffe Physical-Technical Institute, the Russian Academy of Sciences, 194021, St. Petersburg, Russia

<sup>2</sup> Institute of Solid State and Semiconductor Physics, National Academy of Sciences of Belarus, 220072, Minsk, Belarus

<sup>3</sup> Minsk Research Institute of Radiomaterials, 220074 Minsk, Belarus

We consider spin-wave devices based on magnetic films of nanosize thickness and spintronic devices used the injection magnetoresistance effect in the avalanche regime in  $\text{SiO}_2(\text{Co})/\text{GaAs}$  heterostructures, where the  $\text{SiO}_2(\text{Co})$  structure is the granular  $\text{SiO}_2$  film with Co nanoparticles. In  $\text{SiO}_2(\text{Co})/\text{GaAs}$  heterostructures giant magnetoresistance effect is observed [1-3]. This effect presents the opportunity to construct magnetic sensors on the base of structures with hole traps and quantum wells that contain spin-polarized localized electrons (Fig. 1) [4]. The field-effect HEMT devices with the spin polarized electron channels are developed on the base of the n-GaAs/AlGaAs heterostructures (Fig. 2). Construction schemes of the second generation of spin wave devices (tunable filters, delay lines), which based on heterostructures containing ferrite films sputtered on semiconductors, are considered.

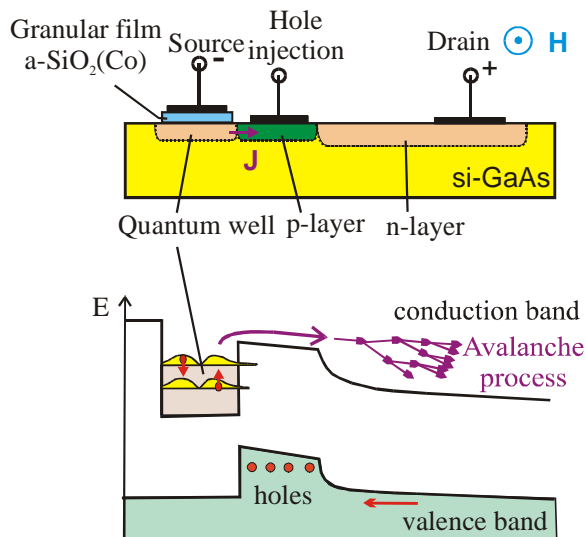


Fig. 1. Structure and schematic energy band diagram of the magnetoresistive sensor on the base of the heterostructure with a quantum well and hole trap in the avalanche regime.

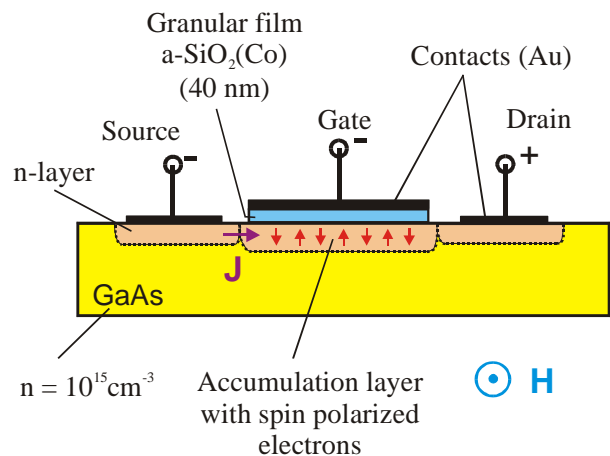


Fig. 2. Field-effect HEMT device with spin polarized electron channel under gate electrode.

This study was supported by the Russian Foundation for Basic Research (project no. 10-02-00516).

[1] L. V. Lutsev, A. I. Stognij, and N. N. Novitskii, *JETP Letters*, **81**, 514 (2005).

[2] L. V. Lutsev, A. I. Stognij, N. N. Novitskii, and A. A. Stashkevich, *JMMM*, **300**, e12 (2006).

[3] L. V. Lutsev, A. I. Stognij, and N. N. Novitskii, *Phys. Rev. B* **80**, 184423 (2009).

[4] L. V. Lutsev, A. I. Stognij, N. N. Novitskii, and A. S. Shulenkov, *Solid State Phenomena* **168-169**, 23 (2011).

## Self-action effects of magnetostatic waves in layered ferromagnetic structure

M. A. Morozova, Yu. P. Sharaevskii, S. E. Sheshukova and M. K. Zhamanova  
Saratov State University, 410012, Saratov, Russia

In recent years, the investigation of nonlinear effects in different media with Kerr nonlinearity represents a great interest. Propagation of waves in such media is described by a system of nonlinear Schrodinger equations (NSE) [1]. A similar system of equations can be obtained for the description of nonlinear effects in ferromagnetic layered structures, in which different types of magnetostatic waves (MSW) can propagate. In this case, in the long wavelength approximation the electrodynamic coupling between the waves in each ferromagnetic film play main role. This coupling is determined mainly by parameters of the MSW and thickness of a dielectric layer between films [2]. In this report, the nonlinear effects of MSW in the structure consisting of two ferromagnetic films were analyzed based on the numerical solution of the system of NSE. The coupling leads to excitation of two normal waves - fast and slow waves propagating with different group and phase velocities. When the phase relationship between the normal waves are taken into account, the presence of a coherent coupling leads to a beats (Fig. 1) and instability of fast soliton. The latter effect was observed in the presence of a strong cross-modulation and significant differences between the coefficients of dispersion and group velocities of the fast and slow waves. The nonlinear effects such as the capture and support of the soliton were observed when the system of NSE with incoherent coupling was used for investigation. The main differences between the effects described above and similar effects in nonlinear optics were studied. Generally, these differences are caused by strong dependence of the coefficients in the system of NSE on the coupling between films. The latter circumstance leads to change the character of the modulation instability for the normal modes of the MSW. The considered effects give an opportunity to manage the nonlinear pulses propagation in the coupled ferromagnetic films and can be used as the basis for a number of nonlinear magnetoelectronic devices.

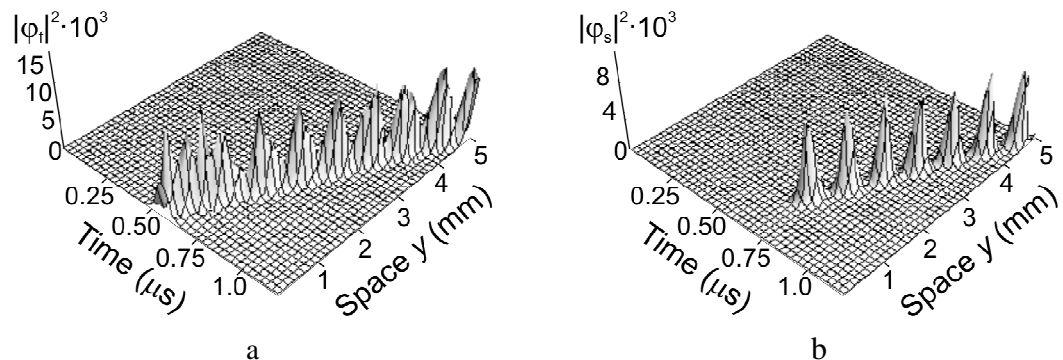


Fig. 1 The spatio-temporal evolution of the fast wave  $\phi_f$  (a) and slow wave  $\phi_s$  (b).

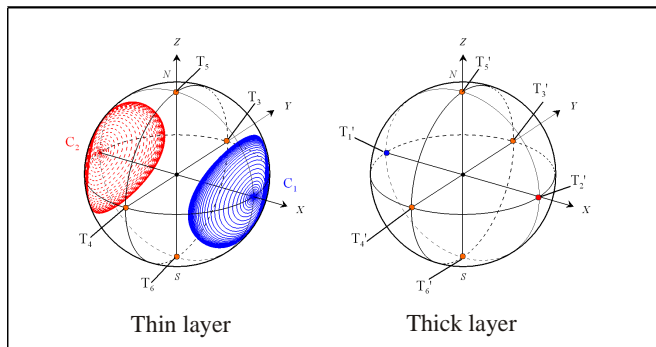
This work was supported by Federal Targeted Programme of the Ministry of Education and Science (project № 2010-1.2.2-123-019-002 and project № 2.1.1/9525)

- [1] N. N. Akhmediev and A. Ankiewicz, *Solitons. Nonlinear Pulses and Beams*. (Chapman and Hall, London, 1997).
- [2] E. N. Beginin, M. A. Morozova and Yu. P. Sharaevskii, *Physics of the Solid State* **52**, 79 (2010).

## Analysis of bifurcations in the model of a three-layered magnetic structure

N. V. Ostrovskaya, V. V. Polyakova, A. F. Popkov  
 Moscow State Institute of Electronic Technology (Technical University)  
 Moscow 124498, Zelenograd, Solnechnaya alleya, 5, Russia

The Slonczewski model of a three-layered magnetic structure driven by spin-polarized current is under consideration. In contrast to [1], [2], we studied the case of unpinned magnetic layers. The mathematical model of the structure consists of two coupled Landau–Lifshits–Gilbert equations without second-order space derivative terms. The full phase of the dynamical system is four-dimensional and represents the direct production of two spherical surfaces corresponding to the thin and thick layers of the magnetic structure. On the basis of qualitative analysis of the dynamical system, classification of stationary states of three-layered magnetic structure is performed. It was found numerically that, at some combinations of the parameters, the phase space of the system is featured with limiting cycles that indicates the precession of the magnetization vector in the structure. Before the system will reach the stable parallel-spin configuration predicted in [1], it passes through a cascade of bifurcations with different types of spin dynamics. We have outlined the intervals of current and field values for topologically equivalent phase portraits of the system.



In the figure the spherical phase spaces for thin and thick layers at  $H_0 = 10 A/M$ ,  $\alpha = 0.1$ ,  $J = 4.2 \cdot 10^8 A/M^2$  are displayed. There are six stationary points located close to the coordinate axes, namely, four four-dimensional focuses  $T_1 - T_1'$ ,  $T_2 - T_2'$ ,  $T_5 - T_5'$ ,  $T_6 - T_6'$ , and two saddles,  $T_3 - T_3'$ ,  $T_4 - T_4'$ . The spiral trajectories in the left phase portrait are the ones of the magnetization dynamical

transition from stable state to the precession around the  $x$ -axis (limit cycle), while the magnetization in the thick layer remains stable. The most interesting effects that were observed in numerical calculations are precession generation in the thick layer, sequential changing the axes of precession with the current growth, and birth of node-type singular points at high current values (saddle-node bifurcation). For each of them the threshold values of injection current were determined at various values of external magnetic field.

- [1] J. C. Slonczewski, JMMM , **159**, L1 (1996).
- [2] G. Bertotti, C. Seprico, I. D. Maryergoyz et al, Phys. Rev. Lett. **94**, 127206 (2005).
- [3] N. V. Ostrovskaya, V. V. Polyakova, A. F. Popkov, J. Phys.: Conf.Ser., **200**, 072073 (2009).
- [4] V. I. Korneev, A. F. Popkov, M. Yu. Chinenko, PSS **51**, 118 (2009).

# Magnetic, resonance and magnetoresistivity properties of trilayer NiFe/Bi/NiFe films

K. G. Patrin<sup>1,2</sup>, V. Yu. Yakovchuk<sup>1</sup>, D. A. Velikanov<sup>1</sup>, G. S. Patrin<sup>1,2</sup>, S. A. Yarikov<sup>2</sup>

<sup>1</sup>*L. V. Kirensky Institute of Physics, Siberian Branch, Russian Academy of Sciences, Krasnoyarsk, 660036, Russia*

<sup>2</sup>*Siberian Federal University, prospect Svobodny, 79, Krasnoyarsk, 660041, Russia*

Multilayer magnetic films with a nonmetal spacer, in particular, those belonging to the system *ferromagnetic metal / semiconductor* [1], or with a semimetal spacer attract close attention by virtue of a great variety of effects observed in these films. When a semiconducting spacer is used, the interest of researchers is caused by the possibility of changing the current carriers concentration in a nonmagnetic layer by means of influence of external factors, which allows controlling the interlayer interaction. For this reason, currently the creation of film structures that would keep sensitivity to external conditions and effects along with far more effective interaction between ferromagnetic layers remains the urgent problem to solve. One of the ways to accept the challenge seems to use semimetal Bi instead of semiconducting material as a nonmagnetic interlayer.

NiFe/Bi/NiFe films (Ni – 80 % at. and Fe – 20 % at.) were obtained in a single cycle by vacuum evaporation at working pressure  $P \sim 10^{-6}$  Tor. As a substrate material, cover glass was used. For all films the permalloy layer thickness and bismuth spacer thickness were  $t_{\text{NiFe}} \cong 10$  nm and  $t_{\text{Bi}} = 0, 4, 6, 12 (\pm 0.5)$  nm, respectively. The value  $t_{\text{NiFe}}$  was selected to be rather small, but at the same time, to keep a film continuous and magnetization of a magnetic layer independent of its thickness. Thickness of layers was determined by X-ray spectroscopy. Electron microscopic study showed that the layers were continuous on area and their composition corresponded to the nominal. No traces of known 3d-metal-Bi compounds were found. Magnetic measurements were made with MPMS-installation. During the measurements magnetic field was in the film plane. Magnetic resonance spectra were measured at 28 GHz microwave frequency.

It was found [2] that the bismuth spacer formation influences essentially the system magnetization. The shape of  $y(H)$  curve is changed with bismuth spacer thickness increasing. In particular, the test film with  $t_{\text{Bi}} = 0$  has the narrow hysteresis loop and magnetization curve of a ferromagnetic type. For the films with  $t_{\text{Bi}} \neq 0$  the magnetization curves are typical for films possessing either by «strong» intra-layer anisotropy or by antiferromagnetic interlayer coupling. Since anisotropy is not experimentally observed, we attribute such a behavior to the presence of interlayer antiferromagnetic exchange.

The investigations of electron magnetic resonance were made in NiFe/Bi/NiFe films. It was established that the magnetic resonance spectrum consists of solitary line for films with  $t_{\text{Bi}} = 0$  nm and  $t_{\text{Bi}} = 15$  nm, whereas for films with intermediate value of semi metal spacer the spectrum is superposition of two lines. Theoretical treatment of temperature dependences of resonance fields gives conclusion that the interlayer coupling depends on both bismuth interlayer thickness and temperature.

Also, the magnetoresistivity of order of percent units and dependence of its value on thickness of bismuth spacer were found in these films at helium temperatures.

The current investigations are being undertaken at financial support of the Russian Found of Basic Researches (Grant № 11-02-00675-a)

- [1] G. S. Patrin, V. O. Vas'kovskii, Phys. Met. Metalloved., **101**, Suppl. **1**, S63, (2006).
- [2] G. S. Patrin, V. Yu. Yakovchuk, D. A. Velikanov. Phys. Lett. A **363**, 164 (2007).

# Picosecond spectroscopy of electronic-spin excitations in magnetic semiconductor EuTe

V. V. Pavlov<sup>1</sup>, A. B. Henriques<sup>2</sup>, A. Schwan<sup>3</sup>, I. Akimov<sup>3</sup>, R. V. Pisarev<sup>1</sup>,  
D. R. Yakovlev<sup>3</sup>, and M. Bayer<sup>3</sup>

<sup>1</sup>*Ioffe Physical-Technical Institute of RAS, 194021, St. Petersburg, Russia,*

<sup>2</sup>*Instituto de Física, Universidade de São Paulo, 05315-970, São Paulo, Brazil,*

<sup>3</sup>*Experimentelle Physik 2, Technische Universität Dortmund, 44221, Dortmund, Germany*

Ultrafast electronic-spin and related optical phenomena have got a great attention of researches working in physics of magnetism. It is due to expected potentials stemming from novel high-speed magneto-electronic and magneto-optical devices, on the other hand it is related to thrilling fundamental phenomena living in femto- and picosecond time scales, see for example, [1, 2]. We present results of an optical picosecond pump-probe study of magnetic semiconductor EuTe. Magnetic semiconductors EuX ( $X = O, S, Se, Te$ ) represent compact group of materials possessing unique electronic, magnetic, optical, and magneto-optical properties. In particular, magnetic semiconductors EuX reveal a new type of nonlinear magneto-optical effects [3, 4]. In our experiment we observed strong optical response for the circular polarized pump in transmission applying magnetic field in the Voigt geometry, see Fig. 1. Temporal behaviour of optical rotation in EuTe is characterized by narrow peak around zero time delay and by broad tail with a characteristic relaxation time of 6 ps. These signals can be attributed to the strong optical nonlinearity of the third order and optical orientation at electronic transition from the localized  $4f$  states of  $\text{Eu}^{2+}$  ions on the top of valence band into  $5d$  orbitals forming the conduction band. Figure 2 shows the photo-induced rotation as a function of magnetic field for two time delays. These dependencies display appreciably distinct behaviours. The band gap of EuTe is about 2.4 eV at low temperatures, this value decreases in an applied magnetic field. At magnetic field of 5 T the band gap is about 2.2 eV.

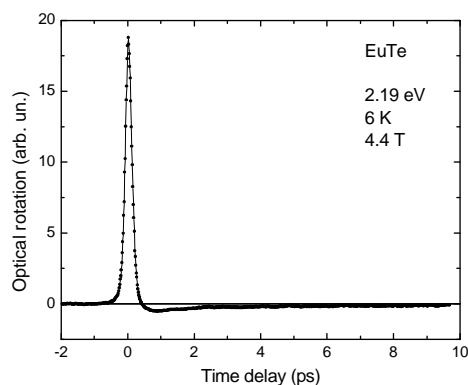


Fig. 1. Temporal behaviour of the photo-induced rotation in EuTe

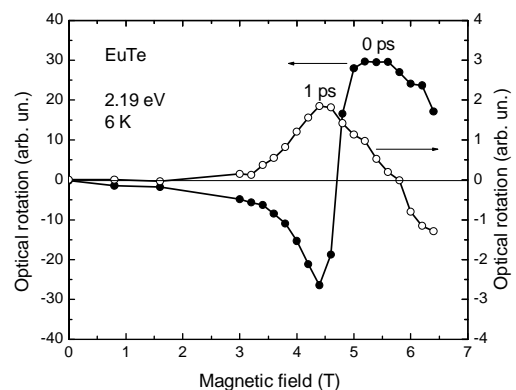


Fig. 2. Magnetic field dependence of the photo-induced rotation in EuTe for two time delays

Therefore, applying magnetic field in the range of 0-7 T one can perform a peculiar picosecond spectroscopy using the optical pump-probe techniques.

[1] V. V. Pavlov, R. V. Pisarev, V. N. Gridnev, *et al.*, Phys. Rev. Lett. **98**, 047403 (2007).

[2] A. Kirilyuk, A. V. Kimel, and T. Rasing, Rev. Mod. Phys. **82**, 2731 (2010).

[3] B. Kaminski, M. Lafrentz, R. V. Pisarev, *et al.*, Phys. Rev. Lett. **103**, 057203 (2009).

[4] M. Lafrentz, D. Brunne, B. Kaminski, *et al.*, Phys. Rev. B **82**, 235206 (2010).



# Synthesis, characterization and dynamic magnetic properties of multiferroic chromates

Anna Pimenov<sup>1</sup>, Ch. Kant<sup>1</sup>, A. Shuvaev<sup>1</sup>, V. Tsurkan<sup>2</sup>, and A. Pimenov<sup>1</sup>

<sup>1</sup> Institute of Solid State Physics, Vienna University of Technology, 1040 Vienna, Austria

<sup>2</sup> Experimentalphysik V, EKM, University of Augsburg, 86159 Augsburg, Germany

We describe the preparation routes for the series of polycrystalline  $ACrO_2$  ( $A = Cu, Ag, Li, Pd$ ) chromates using a solid-state reaction technique at different temperatures and partly using a two-stage substitution procedure. All samples have been characterized using X-ray and magnetic measurements. In addition, single crystals of  $CuCrO_2$  have been grown by flux method.  $CuCrO_2$  and  $AgCrO_2$  have been investigated using the high field ESR and quasi-optical transmittance technique in the frequency range between 100 GHz and 900 GHz. We discuss the results within the context of other known multiferroic compounds.

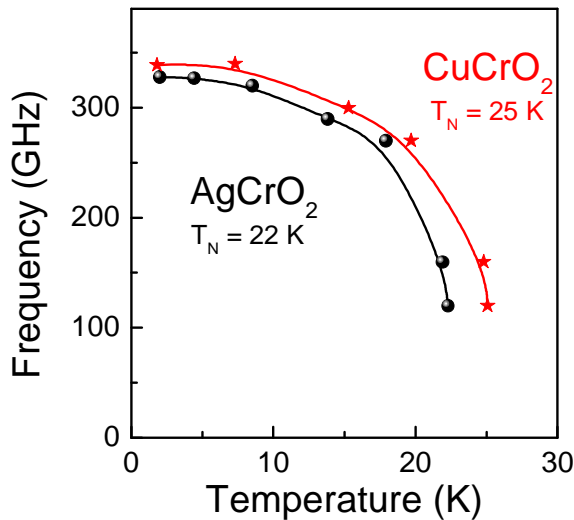


Fig. 1 Antiferromagnetic resonances in  $CuCrO_2$  and  $AgCrO_2$

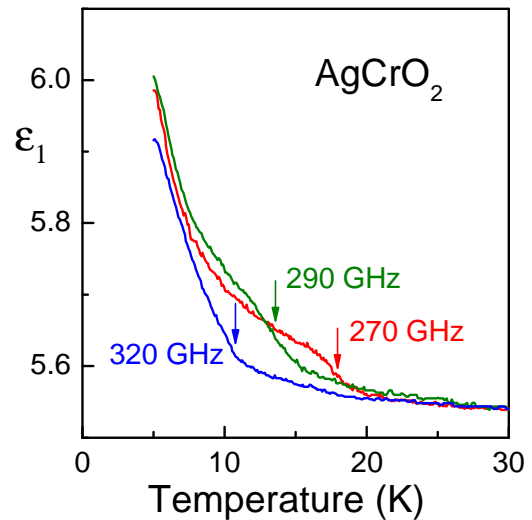


Fig. 2 Dielectric susceptibility of polycrystalline  $AgCrO_2$  at frequencies as indicated. The arrows show the positions of the antiferromagnetic resonance. The increase of the susceptibility towards low temperatures is a possible evidence of the multiferroic properties of this composition

# Magnetic structures based on periodically alternating cobalt and permalloy stripes

V. K. Sakharov<sup>1</sup>, Y. V. Khivintsev<sup>1,2</sup>, S. A. Nikitov<sup>3,2</sup> and Y. A. Filimonov<sup>1,2</sup>

<sup>1</sup>Saratov Branch of Kotel'nikov Institute of Radio-engineering and Electronics of RAS, 410019, Saratov, Russia; <sup>2</sup>Saratov State University, 410012, Saratov, Russia; <sup>3</sup>Kotel'nikov Institute of Radio-engineering and Electronics of RAS, 125009, Moscow, Russia

In this work we experimentally studied magnetic structures in the form of periodically alternating cobalt (Co) and permalloy (Py) microstripes deposited on silicon substrates (Si) – see

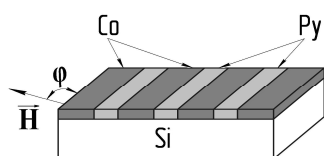


Fig.1 Geometry of the experimental structures.

Fig. 1. The structures were fabricated using magnetron sputtering, photolithography and ion etching. We fabricated and tested samples with different micron sized width ( $W$ ) of Co and Py stripes. The thickness of both Co and Py films was about 50 nm. Characterization of the samples was done using vibrating sample magnetometry (VSM) and method of ferromagnetic resonance (FMR) at 9.9 GHz.

Inset to Fig.2 illustrates a typical hysteresis loop obtained by VSM for magnetic field aligned along the striped structures. VSM measurements for various orientations of tangential magnetic field with respect to the stripes indicated the presence of the uniaxial magnetic anisotropy with easy axis aligned nearly along the stripes – see Fig.2.

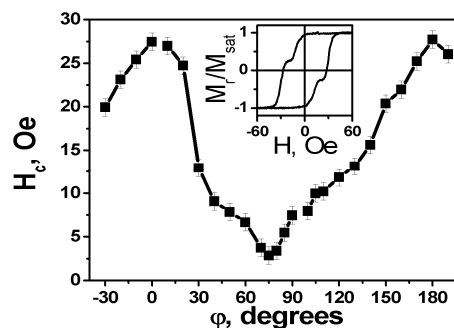


Fig. 2 Angular dependence of coercivity for sample with  $W_{Co} \approx 7 \mu\text{m}$ ,  $W_{Py} \approx 3.5 \mu\text{m}$ . Inset shows hysteresis loop for  $\phi=0$ .

Fig. 3 shows results of FMR measurements for different orientations of tangential bias magnetic field with respect to the stripes. At  $90^\circ$  one can see two responses corresponding to uniform FMR mode for Co (the low field peak) and Py (the high field peak). FMR fields for these responses decrease as magnetization angle decreases due to shape anisotropy. Besides that there are additional responses below the uniform FMR field for Py stripes. These resonances occur at angles below  $\sim 60^\circ$  and correspond to standing surface magnetostatic waves across the stripes width.

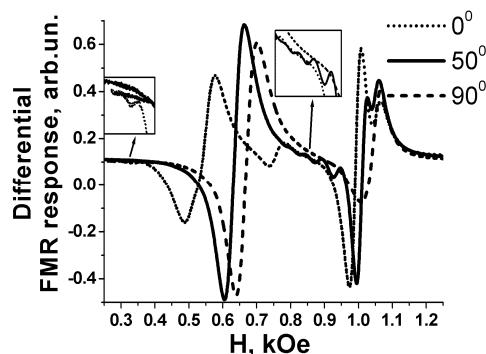


Fig. 3 FMR spectra for sample with  $W_{Co} \approx 11.6 \mu\text{m}$ ,  $W_{Py} \approx 3.5 \mu\text{m}$  for different  $\phi$ .

Thus, in this work we showed that such structures can demonstrate effect of shape anisotropy and quantization of spin wave spectrum.

This work was supported by RFBR (grants # 09-07-00186 and 11-07-00233), Federal Grant-in-Aid Program «Human Capital for Science and Education in Innovative Russia» (governmental contract # П485, 02.740.11.0014 and 14.740.11.0077), Federal Agency of Education of the Russian Federation (project # 2.1.1/2695) and the Grant from Government of Russian Federation for Support of Scientific Research in the Russian Universities Under the Guidance of Leading Scientists (project No. 11.G34.31.0030).

# Magnetoresistance and domain structure in patterned magnetic microstructures based on cobalt and permalloy films

V. K. Sakharov<sup>1</sup>, Y. V. Khivintsev<sup>1,2</sup>, S. A. Nikitov<sup>3,2</sup> and Y. A. Filimonov<sup>1,2</sup>

<sup>1</sup>Saratov Branch of Kotel'nikov Institute of Radio-engineering and Electronics of RAS, 410019, Saratov, Russia; <sup>2</sup>Saratov State University, 410012, Saratov, Russia; <sup>3</sup>Kotel'nikov Institute of Radio-engineering and Electronics of RAS, 125009, Moscow, Russia

Magnetic micro- and nanostructures are intensively studied because of their possible application in magnetic field sensors and data storage media. In this work we fabricated two types of patterned ferromagnetic structures and tested their magnetic properties. The first type of the structures is continuous permalloy films deposited on silicon substrates with 1D or 2D patterns. The second one is 1D or 2D planar structures combined of alternating areas of cobalt and permalloy films.

Fabrication procedure involved magnetron sputtering, photolithography and ion etching. The structures with micron sized lateral dimensions of the pattern were fabricated. Magnetic properties of the structures were studied using vibrating sample magnetometry (VSM), magnetic-force microscopy (MFM) and four-probe method of magnetoresistance (MR). The last was applied in wide temperature range (8 - 300 K).

VSM measurements showed the presence of the shape anisotropy in the samples due to patterning. Domain structure observed by MFM was sensitive to type of the microstructure (see Fig. 1) as well as to fabrication conditions.

MR effect occurred in a field range limited to the saturation fields. The maximum MR was observed in the case of the first type of the microstructures – see Fig. 2. We found that it can be sensitive to type of the patterning as well as fabrication conditions so that its magnitude can be larger or smaller in respect to the unpatterned film. Temperature measurements showed that MR effect increased as temperature decreased.

This work was supported by RFBR (grants # 09-07-00186 and 11-07-00233), Federal Grant-in-Aid Program «Human Capital for Science and Education in Innovative Russia» (governmental contract # П485, 02.740.11.0014 and 14.740.11.0077), Federal Agency of Education of the Russian Federation (project # 2.1.1/2695) and the Grant from Government of Russian Federation for Support of Scientific Research in the Russian Universities Under the Guidance of Leading Scientists (project No. 11.G34.31.0030).

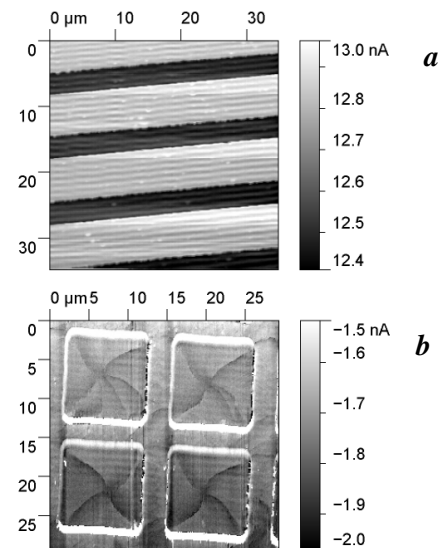


Fig. 1 MFM images for: (a) Py film on the patterned substrate; (b) Co square dots inside of Py matrix.

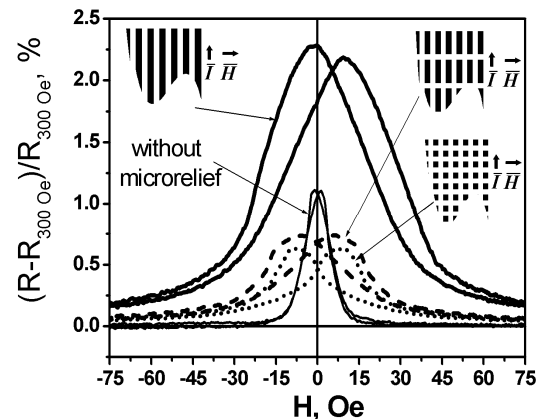


Fig. 2 MR for Py films on substrates with different patterns (see insets).

## Magnetics with large single-ion easy-plane anisotropy

A. V. Sizanov<sup>1</sup>, A. V. Syromyatnikov<sup>1,2</sup>

<sup>1</sup>*Petersburg Nuclear Physics Institute, 188300, Gatchina, St. Petersburg, Russia,*

<sup>2</sup>*Department of Physics, St. Petersburg State University, 198504, St. Petersburg, Russia*

We propose a new representation for the spin operators. It's useful for investigation of spin systems with ground state close to  $S_z=0$  at all sites of the lattice. As a realistic example of such a system we consider a lattice of spins with exchange interaction and large single-ion easy-plane anisotropy. This model describes several real compounds. Examples are  $\text{CsFeBr}_3$ ,  $\text{CsFeCl}_3$ ,  $\text{NiCl}_3\text{-4SC(NH}_2)_2$ ,  $\text{Ni(C}_2\text{H}_8\text{N}_2)_2\text{Ni(CH)}_4$ . Using our representation for this model we obtain one-particle excitation spectrum at  $T=0$  and describe transition to magnetically ordered phase in magnetic field along anisotropy axis. Spectrum is found up to the 2<sup>nd</sup> order of  $J/D$  for  $S > 1$  and up to the 3<sup>rd</sup> for  $S = 1$ . In order to check our results we compare them with numerical experiments. Namely there is a good agreement of our spectrum with Monte-Carlo calculation on 2D square lattice [1] and satisfactory agreement of critical behavior description in magnetic field along anisotropy axis [2]. To put our approach into practice we consider in details compound  $\text{NiCl}_3\text{-4SC(NH}_2)_2$  known as DTN [2, 3, 4, 5]. Magnetic subsystem of DTN consists of two interpenetrating antiferromagnetic sublattices, formed by Ni ions with  $S=1$ . Intra-sublattice interactions are known, but inter-sublattice one is an open question. There are few theoretical descriptions of experimental results. But none of them describe all experimental data at once numerically. On the base of our approach we present description of experimental data at low and high magnetic field. Exchange interaction between sublattices is proposed. We obtain for the first time numerically correct spectrum behaviour at low field and correct critical fields at once. Corrected intra-sublattice interaction parameters are acquired. And predicted inter-sublattice exchange interaction is in agreement with our previous spin-wave estimation [6].

[1] J. Oitmaa and C. J. Hamer, *Phys. Rev. B* **77**, 224435 (2008).

[2] A. Paduan-Filho, K.A. Al-Hassanieh, P. Sengupta, and M. Jaime, *Phys. Rev. Lett.*, **102**, 077204 (2009).

[3] L. Yin, J. S. Xia, V. S. Zapf, N. S. Sullivan, and A. Paduan-Filho, *Phys. Rev. Lett.*, **101**, 187205 (2008).

[4] V. S. Zapf, D. Zocco, B. R. Hansen, M. Jaime, N. Harrison, C. D. Batista, M. Kenzelmann, C. Niedermayer, A. Lacerda, and A. Paduan-Filho, *Phys. Rev. Lett.*, **96**, 077204 (2006).

[5] S. A. Zvyagin, J. Wosnitza, A. K. Kolezhuk, V. S. Zapf, M. Jaime, A. Paduan-Filho, V. N. Glazkov, S. S. Sosin, and A. I. Smirnov, *Phys. Rev. B* **77**, 092413 (2008).

[6] A. V. Sizanov and A. V. Syromyatnikov, *J. Phys.: Condens. Matter* **23**, 146002 (2011).

## Spin waves in diluted magnetic quantum wells

P. M. Shmakov, A. P. Dmitriev and V. Yu. Kachorovskii  
*Ioffe Physical-Technical Institute, 194021 St. Petersburg, Russia*

Diluted magnetic semiconductors are the subject of great interest due to their potential in combining semiconductor and magnetic properties. These materials are formed by replacing a small part of the cations in III-V or II-VI with the magnetic ions (usually, manganese ions). Many remarkable phenomena in diluted magnetic semiconductors, for example, the giant Zeeman effect and the ferromagnetic transition, are possible due to the exchange interaction between the itinerant carriers and the electrons localized on the outer shells of magnetic ions.

The exchange interaction leads to existence of spin excitations, which correspond to coherent precession of the itinerant carriers' spin and the ions' spin. Our research of these excitations was initiated by recent experimental [1, 2] and theoretical [2, 3] works that are dedicated to the study of spin dynamics in  $\text{Cd}_{1-x}\text{Mn}_x\text{Te}$  quantum wells placed into magnetic field. In the experiments [1, 2] two collective homogeneous ( $k = 0$ ) spin modes were observed (Fig.1). The most important observation is the anticrossing of the modes which occurs at a certain "resonant" field  $B = B_{\text{res}}$ .

We developed a theory of the spin waves ( $k \neq 0$ ) in diluted magnetic quantum wells placed into magnetic field. The method we use is based on studying the Wigner equation for the electron spin density together with the Bloch equation for the spin of the ions. Aside from the exchange interaction between delocalized and localized electrons, the exchange interaction of delocalized electrons among themselves was taken into account, which is crucial in the inhomogeneous case. The simultaneous existence of these two types of exchange interaction leads to a number of unusual phenomena. One of them is the "anticrossing" of two branches of dispersion (Fig. 2), which occurs at certain wave vector that can be tuned by the external magnetic field. Another interesting result is the possibility to change the group velocity sign on one of the branches by changing the magnetic field.

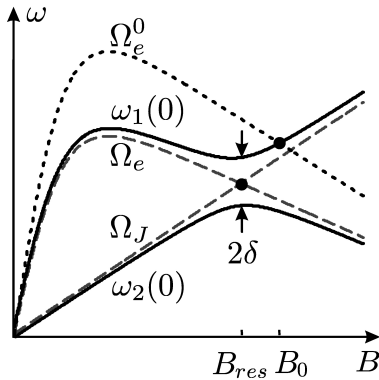


Fig. 1 The spectrum of homogeneous spin excitations

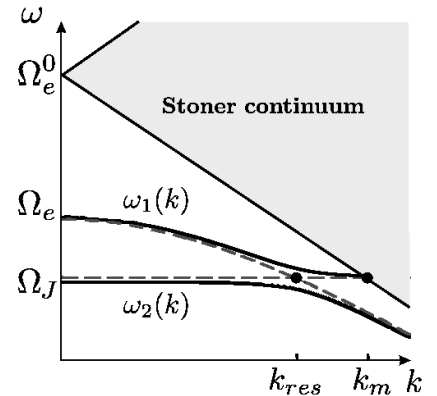


Fig. 2 The anticrossing of two branches of the spin-wave spectrum

- [1] F. J. Teran, M. Potemsky, D. K. Maude, D. Plantier, A. K. Hassan, A. Sachrajda, Z. Wilamowsky, J. Jaroszynski, T. Wojtowicz and G. Karczewski, *Phys. Rev. Lett.* **91**, 077201 (2003).
- [2] M. Vladimirova, S. Croneberger, P. Barate, D. Scalbert, F. J. Teran, A. P. Dmitriev, *Phys. Rev. B* **78**, 081305(R) (2008).
- [3] J. Konig and A.H. MacDonald, *Phys. Rev. Lett.* **91**, 077202 (2003).

## Magnetic resonance in the ordered phase of spin-1/2 antiferromagnet Cs<sub>2</sub>CuCl<sub>4</sub>

A. I. Smirnov,<sup>1,2</sup> K. Yu. Povarov,<sup>1</sup> S. V. Petrov<sup>1</sup>, A. Ya. Shapiro<sup>3</sup>

<sup>1</sup>*P. L. Kapitza Institute for Physical Problems, RAS, 119334 Moscow, Russia,*

<sup>2</sup>*Moscow Institute for Physics and Technology, 141700 Dolgoprudny, Russia,*

<sup>3</sup>*A.V. Shubnikov Institute of Crystallography, RAS, 119333 Moscow, Russia*

The spin system of Cs<sub>2</sub>CuCl<sub>4</sub> is formed by localized  $S=1/2$  spins coupled antiferromagnetically within 2D layers with distorted triangular lattice. This magnet remains in a quantum spin-liquid state at temperatures far below Curie-Weiss temperature 4 K and exhibits a transition with a spiral ordering only at  $T_N=0.6$  K. [1] We studied spin excitations in Cs<sub>2</sub>CuCl<sub>4</sub> by means of electron spin resonance at temperatures down to 0.05 K in the range 9-140 GHz. An unexpected energy gap of about 10 GHz and a splitting of spin excitation mode were found for the spin-liquid phase [2]. The observed gap and splitting are due to uniform Dzyaloshinsky-Morya (DM) interaction in the effectively decoupled spin chains of Cs<sub>2</sub>CuCl<sub>4</sub> spin structure [2]. Below  $T_N$  we have found a multibranch spectrum, coexisting with a mode at the nearly paramagnetic resonance frequency. This unusual mode is proposed to be a "spinon"-type spin resonance of excitations within the spin-liquid continuum, which is known to remain below  $T_N$ . Other modes of spin excitations of the ordered phase at low fields may be well described by a macroscopic approach for a spiral magnet. Excitations observed in high field phases still remain unclassified.

[1] O. A. Starykh, H. Katsura, L. Balents, Phys. Rev. B **82**, 014421 (2010).

[2] K. Yu. Povarov, A. I. Smirnov, O. A. Starykh, S. V. Petrov, and A. Ya. Shapiro, preprint arXiv:1101.5275v1[[str-el](#)].

# Transitions in three-dimensional magnets with extra order parameters

A. O. Sorokin, A. V. Syromyatnikov

*Petersburg Nuclear Physics Institute, 188300, Saint Petersburg, Russia*

In a phase transition, symmetry plays crucial role determining the universal properties of the systems at critical point. The order parameter space is the symmetry broken upon transition. In particular, for XY and Heisenberg ferromagnets the order parameter space is manifold  $SO(2)$  and  $SO(3)/SO(2)$  correspondingly, i.e. one- and two-dimensional sphere, describing a set of probable direction of spontaneous magnetization. In three dimensions for the systems the second order transition occurs with origin of collinear order.

For helimagnets and triangular antiferromagnets the order is planar. For XY spins in these systems  $Z_2 \otimes SO(2)$  symmetry is broken, and additional order parameter is chirality. For Heisenberg spins broken symmetry is  $SO(3)$ , and order is described by two orthogonal vectors. In three dimesions the transition is weak first order with pseudo-universal behavior.

We introduced and considered by Monte Carlo simulations two models of three-dimensional classical magnets with more complicated order parameter space. The first model is the stacked three-exchange model on a simple cubic lattice with one interlayer ferromagnetic exchange between nearest neighbor spins and three intralayer exchanges between spins of first three order of range. The second model is antiferromagnet on a stacked-triangular lattice with two competing interlayer exchanges.

Ground state of these systems is planar, but because of two helical structures are present, the broken symmetry in case of Heisenberg spins is  $Z_2 \otimes SO(3)$  similar to magnets with non-planar order. In this case we found first order transition but with probable pseudo-universal behavior. We obtained critical exponents which are in agreement with exponents of other systems of this class [1].

In case of XY spins the broken symmetry is  $Z_2 \otimes Z_2 \otimes SO(2)$  with two chiral order parameters. We found distinct first order transition.

[1] H. Kunz, G. Zumbach, J. Phys. A: Math. Gen. **26**, 3121 (1993).

# Temperature dependence of multiple spin-flip Raman scattering in magnetic quantum wells

R. R. Subkhangulov, B. R. Namozov, K. V. Kavokin, Yu. G. Kusraev, A. V. Koudinov  
Ioffe Physical-Technical Institute RAS, 194121, Saint Petersburg, Russian Federation

We performed a magneto-optical study of multilayer magnetic quantum wells CdMnSe/ZnSe with manganese concentration  $x=0.28$ . Quantum well width was 0.3 monolayer and barrier (ZnSe) width was 10 monolayer. The research was carried out in Voigt backscattering geometry, the magnetic field was parallel to the QW plane. Magnetic field, temperature and angular dependences were measured. Fig. 1 demonstrates the temperature dependence of the spectrum in magnetic field of 6 T with  $\pi$ -polarized excitation and  $\sigma$ -polarized detection. Peak series following LO phonon at energy 2.745 eV are easily seen, which we interpret as multiple spin-flip Raman scattering (MSFRS) via LO phonon.

The energy difference between peaks corresponds to  $Mn^{2+}$  Zeeman energy with g-factor 2 [1,2]. The MSFRS is usually described within a  $Mn^{2+}$  spin precession model [3], which involves deflecting  $Mn^{2+}$  magnetization in the vector sum of the external magnetic field and exchange field produced by the heavy hole. Because of the large heavy-to-light hole splitting, the exchange field is directed along the structure axis. MSFRS was excited either via LO phonon, or directly by the resonant laser excitation.

A theoretical model of the spin-flip peaks intensities distribution has been built, which accounts for thermal distribution of  $Mn^{2+}$  spins over the Zeeman-split sublevels. The model yields a good agreement with experiment (see Fig.2A).

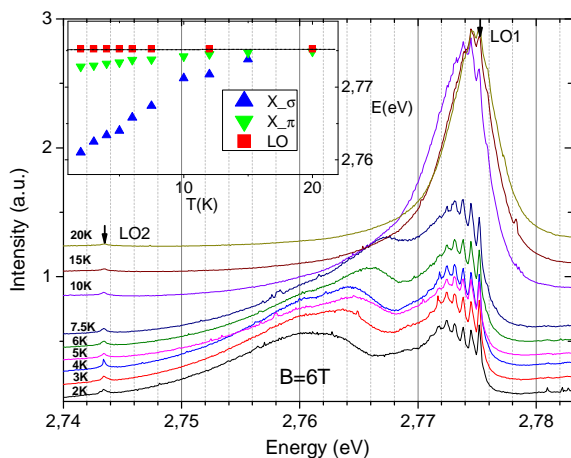


Fig. 1 Temperature dependence of MSFRS in magnetic field 6 T, Voigt geometry (excitation  $\pi$ , registration  $\sigma$ ); the inset shows temperature dependence of exciton luminescence transitions

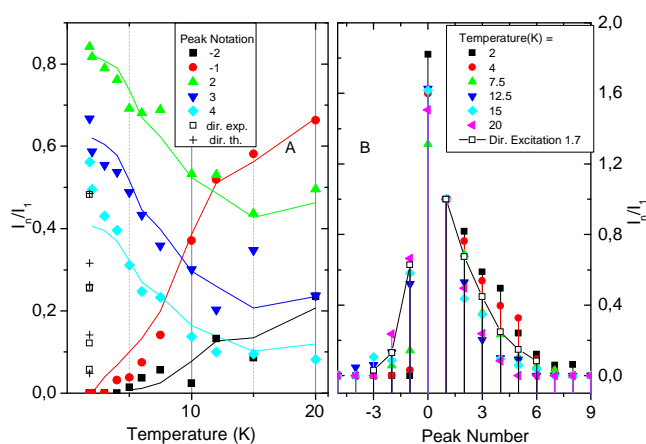


Fig. 2 Peak dependence on temperature. A contain: symbols represent experiment data given in Fig.1, lines represent theoretical simulation; unfilled symbols represent direct excitation experiment, crosses – theoretical simulation for direct excitation experiment; B is net peak intensity treated from experiment for different temperature; unfilled symbols the same meaning as in Fig.1

- [1] J. Stuchler et al, Phys. Rev. Lett. **74**, 2567, (1995).
- [2] J. Stuchler et al, Journal of Crystal Growth **159**, 1001-1004, (1996).
- [3] K. V. Kavokin, in *Optical Properties of Semiconductor Nanostructures*, L.Marcin et al (eds.), NATO Science Series 3, High Technology, **81**, p.255-268 (2000).



## XMCD studies of magnetic properties and proximity effects in Co/MnF<sub>2</sub>(111) heterostructures

S. M. Suturin<sup>1</sup>, L. Pasquali<sup>2</sup>, A. G. Bانشchikov<sup>1</sup>, D. A. Baranov<sup>1</sup>, V. V. Fedorov<sup>1</sup>, K. V. Koshmak<sup>1</sup>, Yu. A. Kibalin<sup>3</sup>, P. Torelli<sup>4</sup>, J. Fujii<sup>4</sup>, G. Panaccione<sup>4</sup> and N. S. Sokolov<sup>1</sup>

<sup>1</sup> Ioffe Physical-Technical Institute, 194021, St. Petersburg, Russia

<sup>2</sup> Università di Modena e reggio Emilia, 41125, Modena, Italy

<sup>3</sup> Petersburg Nuclear Physics Institute, Gatchina, Leningrad district, 188300, Russia

<sup>4</sup> IOM-CNR, 34012, Basovizza (TS), Italy

Cobalt nanoparticles arrays grown by molecular beam epitaxy on antiferromagnet MnF<sub>2</sub> are very attractive for basic studies of the exchange bias effect. These heterostructures can be grown epitaxially on CaF<sub>2</sub>/Si heteroepitaxial substrates. The morphology, structure and orientation of MnF<sub>2</sub>, and of Co ferromagnetic overlayer can be tailored with a suitable choice of the growth parameters (substrate orientation, growth temperature, flux and growth time). On CaF<sub>2</sub>(111) surface MnF<sub>2</sub> grows in a orthorhombic  $\alpha$ -PbO<sub>2</sub> type metastable phase presenting a (111) surface orientation, having uncompensated spin structure with magnetic moments which are out of plane by 35°.

Magnetic circular dichroism in X-ray absorption (XMCD) is a particularly powerful tool to investigate the magnetic properties of thin films and interfaces, allowing one to disentangle the contribution of different elements to the magnetic properties. In this work XMCD was measured at the Co and Mn 2p edges of Co/MnF<sub>2</sub>(111) nano-heterostructures as a function of Co thickness (3-10 nm) below and above MnF<sub>2</sub> Neel temperature (67 K). Hysteresis loops were recorded in correspondence of the absorption edges of the two elements. The experiments were carried out both at the APE beamline of ELETTRA, Italy, and at the BL7A beamline of Photon Factory, Japan. The investigated samples were grown at the Ioffe Institute and capped by a protective layer of CaF<sub>2</sub> (3 nm). All samples were pre-characterised by RHEED, AFM and MOKE, which permits us to correlate the magnetic properties with structure and morphology of the heterostructures.

It was found that the antiferromagnet showed unexpected behavior already at room temperature, with Mn presenting a weak circular dichroism and hysteresis loop aligned antiparallel with respect to the ferromagnetic Co (see Fig. 1). The magnetization of Mn ions seems to be confined at the interface between the ferromagnet and the antiferromagnet. No Mn magnetization is observed without the Co overlayer. This magnetic proximity effect was not observed previously at room temperature for Co or Fe growth on (110) compensated faces of antiferromagnetic fluorides (MnF<sub>2</sub> and FeF<sub>2</sub>) [1,2]. It could be related to Mn hybridization with the ferromagnetic metal at the interface. The authors appreciate support of European Commission via project ONDA FP7-PEOPLE-2009-IRSES-247518.

[1] S. Roy et al. Phys. Rev. Lett. **95**, 047201 (2005).

[2] H. Ohldag et al. Phys. Rev. Lett. **96** 027203 (2006).

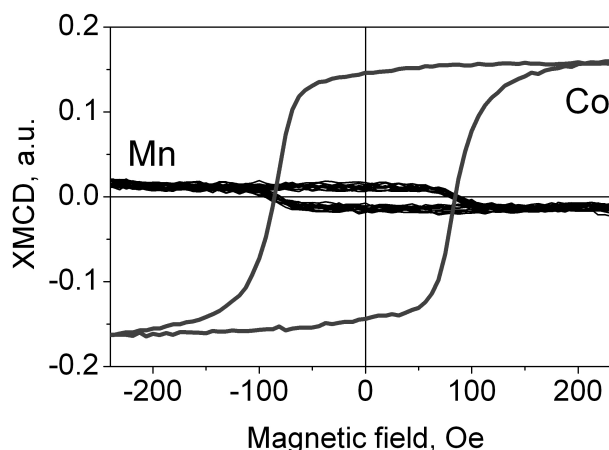


Fig. 1. Co and Mn hysteresis measured at RT by XMCD. Sample: CaF<sub>2</sub> / Co 3 nm / MnF<sub>2</sub> / CaF<sub>2</sub> / Si(111)

## ODMR of Mn-related excitations in (Cd,Mn)Te quantum wells

D. O. Tolmachev, A. S. Gurin, N. G. Romanov, P. G. Baranov, B. R. Namozov, Yu. G. Kusraev  
*Ioffe Physical-Technical Institute, Polytechnicheskaya 26, 194021, St. Petersburg, Russia*

II-VI diluted magnetic semiconductors are attractive objects to study the interaction of localized magnetic moments through indirect exchange coupling mediated by free carriers. The manganese acceptors are known to behave unusually in some semiconductors. We report here on the observation of new ODMR spectra in  $\text{Cd}_{1-x}\text{Mn}_x\text{Te}$  quantum wells (QWs) with two dimensional hole gas (2DHG).

Single 100 Å  $\text{Cd}_{1-x}\text{Mn}_x\text{Te}$  QWs ( $x=1\%$ ,  $2\%$ ,  $4\%$ ) were grown by molecular-beam epitaxy on (001)-oriented GaAs substrates with thick CdTe buffers and  $\text{Cd}_{0.8}\text{Mg}_{0.2}\text{Te}$  barriers. The QWs were covered by thin  $\text{Cd}_{0.8}\text{Mg}_{0.2}\text{Te}$  cap layers. Though these QWs are not specially doped, owing to the surface states they contain a 2DHG [1]. We studied QWs with a cap layer thickness of 170 Å, where the surface-state induced p-type doping is most effective [2] and 140 Å. 35 GHz ODMR was recorded at 1.7-4.2 K via photoluminescence (inset in Fig.1) excited with a 650 nm semiconductor laser.

Two types of ODMR signals with different angular variations were found (see Fig.1).

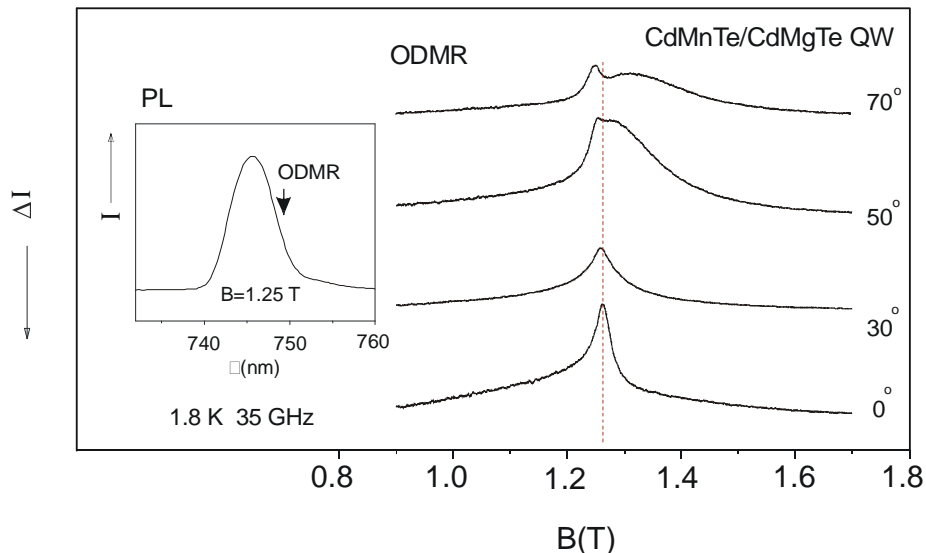


Fig. 1 Photoluminescence (inset) and ODMR at different orientations in magnetic field recorded in 100 Å  $\text{Cd}_{0.98}\text{Mn}_{0.02}\text{Te}$  QWs covered by 170 Å  $\text{CdMgTe}$  cap layer.  $0^\circ$  corresponds to  $[001]/B$ .

A strongly anisotropic wide line was found in addition to a usual ODMR signal of Mn. The effective  $g$ -factor of this wide line varies from  $g = 2.07$  at  $\theta=0$  to  $g=1.86$  at  $\theta=70^\circ$ . A more narrow ODMR line disappears with increasing temperature. No broad ODMR line was found in the sample with 140 Å cap layer. A similar behavior of the ODMR spectra was observed in the samples with the same cap layer thicknesses but different Mn content (4% and 1%). The results are discussed in terms of a possible effect of a magnetic soft mode of collective spin excitations in (CdMn)Te QWs, containing a 2D hole gas interacting with magnetic moments.

This work has been supported by the Ministry of Education and Science under Contract No. 14.740.11.0048; the programs of RAS: “Spintronics”; “Basic Researches of Nanotechnologies and Nanomaterials,” and by the RFBR under Grants No. 09-02-01409 and 09-02-00730.

[1] S. Tatarenko *et al.*, *Opto-Electron. Rev.* **11**, 133 (2003).

[2] C. Kehl, *et al.*, *Phys. Rev. B* **80**, 241203 (2009).

## Antiferromagnetic resonance and magnetic investigations of rare-earth ferrobates

V. Tugarinov<sup>1</sup>, A. Pankrats<sup>1,2</sup>, G. Petrakovskii<sup>1,2</sup>, S. Kondyan<sup>2</sup>, D. Velikanov<sup>1</sup>, V. Temerov<sup>1</sup>  
<sup>1</sup>L. V. Kirensky Institute of Physics SB RAS, 660036 Krasnoyarsk, Russia,  
<sup>2</sup>Siberian Federal University, 660041, Krasnoyarsk, Russia

The borate compounds with general formula  $RA_3(\text{BO}_3)_4$  ( $R^{3+}$  - rare-earth ion or  $\text{Y}^{3+}$  and  $A=\text{Al}$ ,  $\text{Ga}$ ,  $\text{Sc}$ ,  $\text{Cr}$ ,  $\text{Fe}$ ) have attracted considerable attention as materials for nonlinear optics and laser techniques. They crystallize in the trigonal crystal system and have the structure of the *huntite* mineral with high-temperature space group  $R\bar{3}2$ , which transforms to  $P3_121$  with temperature decreasing for the crystals with small ionic radius of the  $R^{3+}$ . Many  $R\text{Fe}_3(\text{BO}_3)_4$  crystals are multiferroics. The  $RA_3(\text{BO}_3)_4$  crystals have interesting magnetic properties due to an interaction between subsystems of  $\text{Fe}^{3+}$  and  $R^{3+}$  magnetic ions. In the present work we present data on antiferromagnetic resonance (AFMR), magnetic properties, heat capacity and magnetic phase diagrams of  $\text{GdFe}_3(\text{BO}_3)_4$ ,  $\text{GdFe}_{2.1}\text{Ga}_{0.9}(\text{BO}_3)_4$ ,  $\text{EuFe}_3(\text{BO}_3)_4$  and  $\text{Pr}_{1-x}\text{Y}_x\text{Fe}_3(\text{BO}_3)_4$  system with  $x=0\div 1$ .

The AFMR investigations of pure  $\text{GdFe}_3(\text{BO}_3)_4$  showed [1] that the competition of  $\text{Fe}^{3+}$  and  $\text{Gd}^{3+}$  contributions to total magnetic anisotropy of the crystal results in spontaneous reorientation at  $T=10$  K between states with “easy plane” (EP) and “easy axis” (EA) anisotropy. EP magnetic ordering occurs at the Neel temperature  $T_N=38$  K. Magnetic phase diagram was constructed from AFMR and magnetic measurements.

Diamagnetic substitution of  $\text{Fe}^{3+}$  leads to decreasing of the Néel temperature in  $\text{GdFe}_{2.1}\text{Ga}_{0.9}(\text{BO}_3)_4$  to  $T_N=16.3$  K. From magnetic and AFMR data the magnetic phase diagram was constructed. It follows from the data that the spontaneous reorientation does not occur in Ga-substituted ferrobate and the crystal remains easy-axis in a whole ordering area.

The investigations of magnetic and resonance properties of  $\text{Pr}_{1-x}\text{Y}_x\text{Fe}_3(\text{BO}_3)_4$  system showed the following: the crystal with  $x=1$  ( $\text{YFe}_3(\text{BO}_3)_4$ ) is an easy-plane antiferromagnet [2], the AFMR investigations of the crystal with  $x=0$  ( $\text{PrFe}_3(\text{BO}_3)_4$ ) crystal confirm that it is an easy-axis antiferromagnet in all temperature range below  $T_N=32$  K [3]. The energy gap  $\nu_c=130$  GHz allow to estimate the Pr contribution to total magnetic anisotropy as exceeding almost two times the Fe one in magnitude.

A dilution of the  $\text{Pr}^{3+}$  subsystem by diamagnetic yttrium reduces the anisotropy of the subsystem and can lead to a spontaneous transition from EA to EP state at some yttrium content. The single crystals  $\text{Pr}_{1-x}\text{Y}_x\text{Fe}_3(\text{BO}_3)_4$  with yttrium content  $x=0.25$ ,  $0.5$  and  $x=0.75$  were grown. Magnetic and resonance investigations show that the crystal with  $x=0.25$  is EA antiferromagnet with the energy gap close to 75 GHz at  $T=4.2$  K but the crystals with  $x=0.5$  and  $0.75$  are EP one.

The crystal  $\text{EuFe}_3(\text{BO}_3)_4$  is EP antiferromagnet throughout the temperature range below the Neel temperature. AFMR data show that the energy gap is about 120 GHz at  $T=4.2$  K, which is close to the value of the gap in the yttrium ferrobate. Thus, the contribution of rare-earth subsystem to the magnetic anisotropy is negligible in Eu ferrobate.

Thus, the value of the total magnetic anisotropy depends strongly on the type of the rare-earth ion, which determines the magnetic structure of the crystal.

- [1] А. И. Панкрац, Г. А. Петраковский, Л. Н. Безматерных, О. А. Баюков, ЖЭТФ, **126**, 887 (2004).
- [2] А. И. Панкрац, Г. А. Петраковский, Л. Н. Безматерных, В. Л. Темеров, ФТТ **50**, 77 (2008).
- [3] А. М. Кадомцева, Ю. Ф. Попов, Г. П. Воробьев и др., Письма в ЖЭТФ, **87**, 45 (2008).

# NMR spectrum in the non-collinear antiferromagnet $\text{Mn}_3\text{Al}_2\text{Ge}_3\text{O}_{12}$

O. G. Udalov

*Institut for physics of microstructures RAS, 603950 Nizhny Novgorod, Russia*

In the frame of the exchange approximation for spin dynamics [1] modified for description of nuclear magnetic moments dynamics [2] the calculation is carried out of NMR spectrum in non-collinear antiferromagnet  $\text{Mn}_3\text{Al}_2\text{Ge}_3\text{O}_{12}$ . The antiferromagnet consists of 12 sublattices. The spectrum of low-frequency electron magnetic moments oscillations in  $\text{Mn}_3\text{Al}_2\text{Ge}_3\text{O}_{12}$  was theoretically and experimentally investigated earlier in the work [3]. The effect of nuclear subsystem on the AFMR spectrum can be neglected in all the range of external magnetic field excluding small region near critical field, where the one of AFMR resonant frequencies becomes small and comparable with frequencies of nuclear magnetic resonance. The NMR spectrum is determined by the hyperfine interaction with electrons magnetic moments and external field. In order to get NMR spectrum it is necessary to investigate coupled oscillation of the nuclear and electrons spins. Relativistic distortions of exchange spin structure of electron subsystem play important role in the formation of NMR spectrum. If the external field is oriented along three-fold axis, the distortion of electrons exchange spin structure (due to relativistic interactions) does not appear due to high symmetry of the system. In the case NMR spectrum consists of three degenerate branches. These braches are found analytically. The NMR spectrum for the case is determined by only one additional constant (to those describing electron spin system), namely the constant of hyperfine interaction. If the external field is directed along four-fold axis 9 branches of NMR spectrum can be distinguished. In this case the distortion of the electrons exchange spin structure becomes important, namely weak antiferromagnetism, anisotropic spin reduction and the change of the angle between exchange vectors. Also the reorientation of electrons magnetic moments by the external magnetic field leads to splitting of NMR spectrum branches. It is necessary to use 5 additional constants to describe all the effects. For this field orientation the problem is solved numerically. For the general orientation of external magnetic field NMR spectrum has 12 branches.

The author thanks V.I. Marchenko for useful discussions and comprehensive assistance during this work.

The work was carried out during the stay of the author in the Kapitza institute for physical problems and under support of RFBR (10-02-90702-mob\_st).

[1] A. F. Andreev, V. I. Marchenko, *Sov. Phys. Usp.*, **23**, 21 (1980).

[2] V. I. Marchenko, A. M. Tikhonov, *JETP Letters* **69**, 1, 41 (1990).

[3] L. A. Prozorova, V. I. Marchenko, Yu. V. Krasnyak, *JETP Letters* **41**, 12, 637 (1985).

## Magneto-optical properties of Fe and Fe/Cu layered nanostructures on Si(001)

P. A. Usachev<sup>1</sup>, A. A. Astretsov<sup>1,2</sup>, V. A. Rusakov<sup>1</sup>, V. V. Pavlov<sup>1</sup>  
N. A. Tarima<sup>3,4</sup>, S. A. Kitan<sup>3,4</sup>, V. M. Iliyashenko<sup>3,4</sup>, N. I. Plusnin<sup>3,4</sup>

<sup>1</sup>Ioffe Physical-Technical Institute of RAS, 194021, St. Petersburg, Russia

<sup>2</sup>Physics and Technology Centre, 194021, St. Petersburg, Russia

<sup>3</sup>Institute of Automation and Control Processes of FEB RAS, Vladivostok, Russia

<sup>4</sup>Nanophysics and Material Science Laboratory of VSUES, Vladivostok, Russia

In last years there is growing research interest to layered nanostructures on base of transition metals, such as Cr, Fe or Co, and Cu on silicon [1]. These nanostructures may considerably differ from their bulk analogues on crystal structure, electronic and magnetic properties. But their fabrication is a complex growth problem due to a metal-metal and metal-silicon intermixing which lead to dim interfaces. Solution of the problem is formation of special interlayers on interfaces [2] or using a lowered temperature of vapor during ultrahigh vacuum thermal evaporation of metal [3]. By using the last method, Fe [4] and Cu [5] films with a thickness of 0.1-1 nm were grown on Si(001). And, in present work, layered structures of Fe and Fe/Cu/Si(001) with a layer thickness in range of 0.1-1 nm have been grown and their magneto-optical properties have been studied.

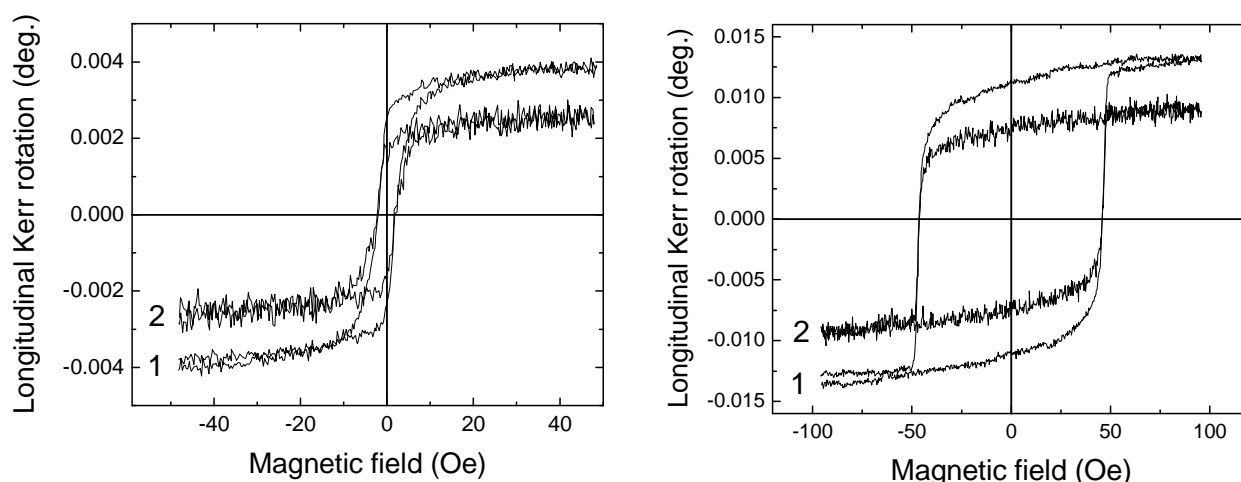


Fig. Hysteresis loops measured by the longitudinal magneto-optical Kerr effect for samples of Fe/Cu/Si(001). Left and right figures show nonannealed and annealed samples, respectively. Kerr rotation and ellipticity are shown by curves 1 and 2, respectively.

Figure shows the longitudinal magneto-optical Kerr effect for two Fe/Cu/Si(001) samples consisting of 9 and 1 monolayers of Fe and Cu, respectively. Second sample has been annealed at 250°C within 3 minutes before the iron growth. As a whole, obtained result shows that for both single-layered and belayered structures such annealing process enhances values of magneto-optical signal and also leads to an increase of coercive field. Additionally increase of effective thickness of magnetic material leads to enhance of magneto-optical signal. In summary, obtained nanosize structures of ferromagnetic metal – nonmagnetic metal – semiconductor can be used as potential materials for silicon spintronics.

[1] C. A. F. Vaz, J. A. C. Bland, and G. Lauhoff, *Rep. Prog. Phys.* **71**, 056501 (2008).

[2] G. Garreau, S. Hajjar, J. L. Bubendorff, *et al.*, *Phys. Rev. B* **71**, 094430 (2005).

[3] N. I. Plusnin *et al.*, *Tech. Phys. Lett.* **33**, 486 (2007).

[4] N. I. Plyusnin, *et al.*, *J. Surf. Invest. X-ray, Synchr. and Neutr. Techn.* **3**, No. 5, 734–746 (2009).

[5] N. I. Plyusnin, *et al.*, *J. Surf. Invest. X-ray, Synchr. and Neutr. Techn.* (2011) (to be published).

# Spin-polarized conductivity of double magnetic tunnel junction

N. Useinov and L. Tagirov

Kazan Federal University, 420008 Kazan, Russian Federation

The double magnetic tunnel junction (DMTJ) is now of magnetic nanostructure the use in spintronics. It is devise where the electron spin is the active element for information storage and transport [1]. We present a theoretical study of spin-polarized conductivity in DMTJ:  $FM^L/I_1/FM^W/I_2/FM^R$ , where the magnetization of the middle ferromagnetic layer  $FM^W$  may be changed into parallel (P) or antiparallel (AP) with respect to fixed magnetizations of the left  $FM^L$  and right  $FM^R$  ones. The two dielectric layers  $I_{1(2)}$  of the lateral size comparable with mean-free paths of the conduction electrons are considered as tunnel barriers. In Fig.1 the large parabolic curves present dispersion low for spin-up electrons ( $\uparrow$ -arrows) and correspond to the spin-up majority conductance sub-bands. The small parabolic curves belong to the spin-down minority sub-bands with spin-down electrons ( $\downarrow$ -arrows). The arrows inside the brackets of the middle layer show the electron spin direction for the AP case. The electron spin-conduction channels passing through minority or majority sub-bands are determined by the electron-tunnel trajectory with conserved spin-direction. They are shown at the bottoms of the sub-bands as dash-dot-dot lines and dashed lines for the P-case and as dash-dot and solid lines for the AP-case.

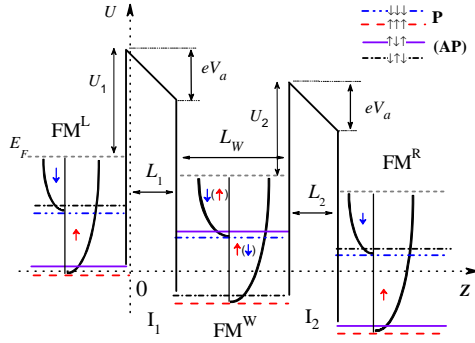


Fig. 1 Schematic potential profile of the DMTJ with applied bias  $V_a$ . The  $U_{1(2)}$  are the heights of the barriers above Fermi energy  $E_F$ ,  $L_{1(2)}$  are the thickness of the barriers, respectively and  $L_W$  is the thickness of the middle layer  $FM^W$ .

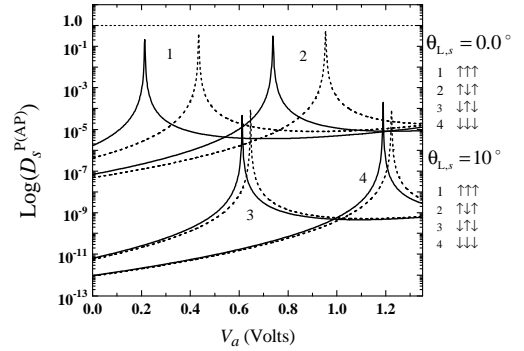


Fig. 2 Transmission coefficients vs.  $V_a$  for four configurations of the spin-conduction channels at each of the P and AP magnetic moments alignment. The arrows are related with arrows in Fig.1.

Fig. 2 shows the plot of the transmission coefficients  $D_s^{P(AP)}$  as a function of the bias  $V_a$  for two fixed trajectory angles:  $\theta_{L,s} = 0.0^\circ$  (solid lines) and  $\theta_{L,s} = 10^\circ$  (dash lines), where  $s = \uparrow, \downarrow$ . The parameters  $L_{1(2)} = 12 \text{ E}$ ,  $L_W = 13.6 \text{ \AA}$  and  $U_{1(2)} = 1.8 \text{ eV}$  are used. In the free-electron model the spin-polarized conductivity is proportional to the product of  $D_s^{P(AP)}$  and cosine of the incidence angle  $\theta_{L,s}$  of the electron trajectory in the  $FM^L$  [2]. The results show that  $D_s^{P(AP)}$  have resonant character for each conduction channels and inclination of the electron trajectory considerably influences the transmission coefficient. Thus the our calculation of  $D_s^{P(AP)}$  to show that DMTJ have spin-filtering effect and can be used as spintronics devise.

This work was supported by the RFBR (project No. 10-02-91225-CT\_a).

[1] A. Vedyayev, Phys. Usp. **45** (12), 1296 (2002).

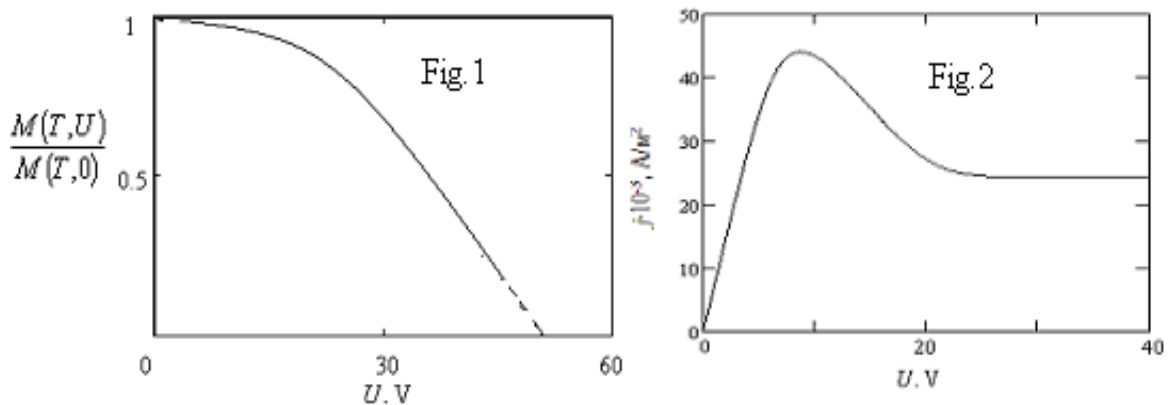
[2] A. Useinov, R. Deminov, N. Useinov, and L. Tagirov, Phys. Status Solidi B **247**, 1797 (2010).

# The nonlinear effect of external electric field on the spin excitations and the electronic structure of ferromagnetic semiconductors

A. G. Volkov, A. A. Povzner

*Ural Federal University, 620002, Ekaterinburg, Russia*

Abnormally strong electric field effects on the magnetic subsystem of ferromagnetic semiconductors are known since 1972. Observed in experiments is strong dependence of the magnetic properties (magnetization, magneto resistance and etc.) on the applied electric field for this class of substances as an indication of the strong electron-magnon interaction, realization in this class of substances. It should be noted that proposed earlier concept of "hot" magnons is based on the assumption that the heat current only the spin subsystem. At the same time unable to determine the reasons for observed in the experiment nonlinear current-voltage characteristic, which correlate with the observed nonlinear dependences of the magnetization of an external electric field.



In this paper we consider the area as weak as well as strong relaxation magnons in ferromagnetic semiconductor  $\text{EuO}_{1-\delta}$  in an external electric field. Of the subsystems of f- and d-electrons described by the Hubbard model with different values of the constants of intra-site coulomb interaction and parameters band of movement taking into account their interstitial exchange interaction. Energy exchange between electrons, phonons and magnons described by the equation of thermal balance between the joule heating up and the inside temperature of the sample. It is shown that in the framework of such a model is installed the positive feedback of the current density, the magnetization and the amplitude of thermal fluctuations of the internal exchange fields, which should be interpreted as a relaxation of spin waves. The electric field increases fluctuation internal exchange fields, suppresses the magnetization -  $M(T,U)$  (fig.1). ( $T$  - temperature of the sample surface,  $U$  - voltage). In turn, decrease  $M(T,U)$  leads to reduce the occupancy of the d-band conductivity (due to redistribution of electrons between localized f- and a band-like d-state) and appearance the energy gap between the f- and d-states. Thus, due to the joule heating increase of the magnetic excitations number, explains electronic metal-semiconductor transition and  $N$ -shaped current-voltage characteristic (fig.2). Interaction fluctuating internal exchange fields and conduction electrons should lead to an  $S$ -shaped current-voltage characteristic in the temperature region of magnetic phase transition  $\text{EuO}_{1-\delta}$ .

# Influence of metal on formation of forbidden gaps in SMSW spectrum of 1D ferrite magnonic crystal

S. L. Vysotsky<sup>1</sup>, Yu. A. Filimonov<sup>1</sup>, E. S. Pavlov<sup>2</sup>, S. A. Nikitov<sup>2</sup>

<sup>1</sup>Kotel'nikov SBIRE RAS, 410019, Saratov, Russia, <sup>2</sup>Kotel'nikov IRE RAS, 125009, Moscow, Russia

Forbidden gaps in spectra of magnetostatic waves (MSW) propagating in magnonic crystals (MC) represented ferrite films with 1D or 2D periodic surface structures are widely investigated during last years. The reason for their formation is interaction of incident  $q_{in}$  and reflected from periodic structure  $q_{ref}$  waves. The frequencies of gaps  $f_n$  can be found from MSW dispersion equation as corresponding to wave numbers satisfied Bragg condition  $q_n = \pi n / d$ , where  $d$  is structure's period,  $n=1,2,\dots$

To be used in ferrite microwave devices dispersion of MSW usually must be corrected. One of the well-known ways for correction is to use ferrite-dielectric-metal (F-D-M) structure; here the shape of dispersion curve depends, including thickness  $t$  of dielectric layer.

It is obvious that change of dispersion curve could result in shift of  $f_n$  corresponding to  $q_n$ . Though it is right only for reciprocal waves namely backward volume and forward volume MSW. On the other hand non-reciprocal surface MSW (SMSW) propagating in opposite directions are keep close to different surfaces of ferrite film. It means that in MC-D-M structure "effective" values of  $t$  for incident and reflected from periodic structure waves will differ by  $h$  (thickness of ferrite film). As a result  $q_{in}$  could be not equal to  $q_{ref}$ . The figure 1 demonstrates calculated dispersion curves of SMSW in yttrium-iron garnet ( $4\pi M_0 = 1750$  Gs) at 800 Oe for  $t=0$  (curve 1) and  $t=h=22 \mu m$  (curve 2). One can see that wave numbers  $q_1$  (at curve 1) and  $q_2$  (at curve 2) corresponding, for example, to frequency  $f^*$ , can differ significantly. So interaction of incident and reflected waves wouldn't result in forbidden gaps formation. Figure 2 presents amplitude-frequency characteristics (AFC) of SMSW delay line based on 1D MC with  $d=200 \mu m$  (a) and the MC-metal ( $t=0$ ) structure (b). Parameters of the experiment correspond to used in dispersion calculation. As it was suggested in the case (b) gaps are lost.

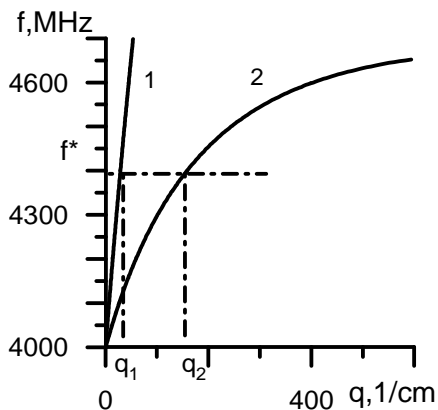


Fig.1 SMSW dispersion curves calculated for  $t=0$  (1) and  $t=h$  (2)

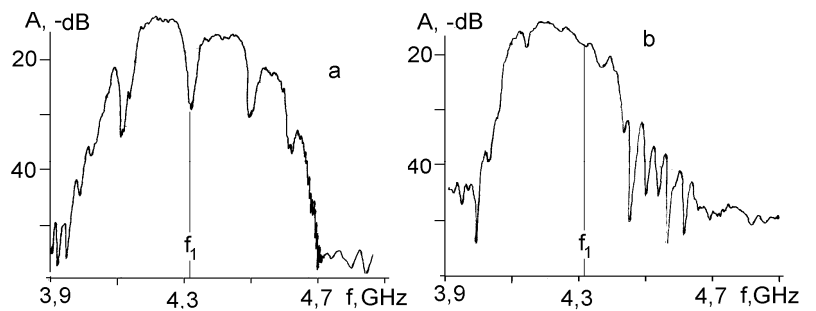


Fig.2 AFC in the cases of MC (a) and MC-metal ( $t=0$ )

This work was supported by the Russian Foundation for Basic Research (grants nos.11-07-00233 and 09-07-00186) and by the Grant from Government of Russian Federation for Support of Scientific Research in the Russian Universities Under the Guidance of Leading Scientists (project No. 11.G34.31.0030).



# Influence of three magnon parametric instability on MSSW Bragg resonances in 1D magnonic crystal

S. L. Vysotsky<sup>1,3</sup>, Yu. A. Filimonov<sup>1,3</sup>, E. S. Pavlov<sup>2</sup> and S. A. Nikitov<sup>2,3</sup>

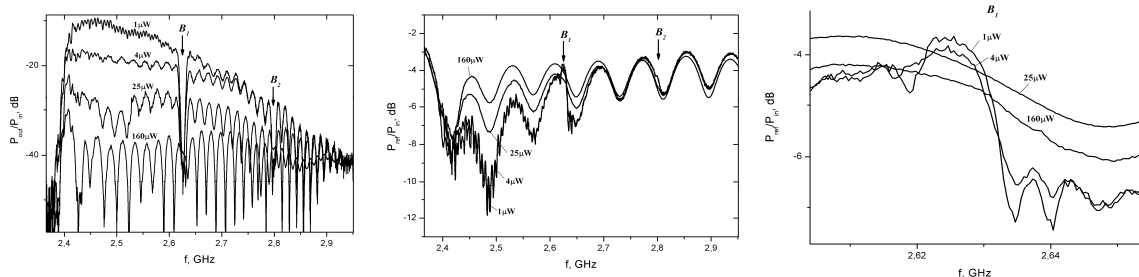
<sup>1</sup>Kotel'nikov SBIRE RAS, 410019, Saratov, Russia, <sup>2</sup>Kotel'nikov IRE RAS, 125009, Moscow, Russia

<sup>3</sup>Saratov State University, 410012 Saratov, Russia

One of the main features of magnetostatic surface wave (MSSW) propagation in 1D and 2D magnonic crystals is formation of frequency stop bands in MSSW spectra. This bands are the result of resonance interaction of incident and reflected MSSW from surface structure at the frequencies  $f_n$  corresponding to wave numbers  $k_n$  satisfied Bragg condition  $k_n = \pi n / \Lambda$ , where  $n=1,2,\dots$ ,  $\Lambda$  is period of surface structure. In this work we experimentally investigate an influence of the first-order (three-magnon) parametric instability of MSSW on Bragg resonance in 1D magnonic crystal based on YIG film.

Note that under three-magnon (3M) parametric instability both dispersion and losses of MSSW are changes. At fixed pumping frequency  $f_p$  one may characterize mentioned changes by some additions to real  $\delta k'$  and imaginary  $\delta k''$  parts of the MSSW wave number  $k = k' + i \cdot k''$  corresponding to linear wave dispersion  $k = k(f_p)$ . Due to dissipation in magnetic film this changes take place at some propagation distance  $S$  smaller then length  $L_{nl}$  of nonlinear part of the film, where MSSW power  $P$  exceeds the threshold value for 3M parametric instability  $P_{th}$ . ( $P > P_{th}$ ) and where parametric spin waves are excited by MSSW. At distances  $S > L_{nl}$  MSSW power is smaller than  $P_{th}$  and MSSW came back to linear regime of propagation. From this one may conclude that through the distance  $L_{nl}$  the nonlinear additions to dispersion and losses are not uniform and they are the functions of distance  $S$  ( $\delta k' = \delta k'(S)$ ,  $\delta k'' = \delta k''(S)$ ).

It is clear, that both nonuniformity and nonlinear losses induced by parametric instability may destroy the synchronism between incident and reflected MSSW and leads to suppression of Bragg resonances in magnonic crystal. Frequency dependencies of transmitted  $P_{out}$  (a) and reflected  $P_{ref}$  (b) MSSW power vs incident MSSW power  $P$  are shown. For  $P \approx 2\mu W < P_{th}$  at frequencies  $B_1$  and  $B_2$  corresponding to Bragg resonance both drop in  $P_{out}$  and an increase in  $P_{ref}$  are seen. For high level of overcriticality  $P > 20\mu W$  one can see that an increase in  $P_{ref}$  at frequencies  $B_1$  disappear (fig.c). It means that Bragg resonance was suppressed by parametric instability.



This work was supported by the RFBR (grants nos.11-07-00233 and 09-07-00186) and by the Grant from Government of Russian Federation for Support of Scientific Research (project No. 11.G34.31.0030).

# Author Index

## A

Abakumov	P. V.	109
Abramof	E.	27
Abramova	G.	81
Adeyeye	A. O.	28
Ahmad	E.	16
Akimov	I.	116
Alakshin	E. M.	21
Aristov	D. N.	41
Astretsov	A. A.	81, 128
Atkinson	R.	64
Au	Y.	16
Azamatov	Sh. A.	89

## B

Back	C. H.	56
Baenitz	M.	91
Balakrishnan	G.	40
Balbashov	A. M.	18
Baltz	V.	15
Banshchikov	A. G.	67, 124
Baranov	D. A.	67, 124, 125
Baró	M.D.	15
Bauer	G.	27
Bauer	H. G.	56
Bayer	M.	27, 115
Bazhanov	A. G.	82
Beginin	E. N.	60, 83, 84
Belik	A.	48
Benckiser	E.	24
Benner	H.	58
Bergman	A.	63, 65
Bergqvist	L.	63, 65
Bessonov	V. D.	85
Bezmaternykh	L.	47
Boehm	M.	80
Bogach	A. V.	39, 46
Bolsunovskaya	O.	80
Bondarenko	P.	86
Boris	A. V.	24, 31
Brunne	D.	27
Buchanan	K. S.	15
Büettgen	N.	30
Bunkov	Yu. M.	19, 21

## C

Capogna	L.	40
Caro	J.	22
Carr	L. D.	55
Charnukha	A.	31
Cheong	S.-W.	109
Cherkasskii	M. A.	57
Chumak	A. V.	103
Chupis	I. E.	53
Cristiani	G.	24
Ctistis	G.	25

## D

Davison	T.	16
Deen	P. P.	40
Deisenhofer	J.	34
Demidov	V. E.	20, 62, 85
Demishev	S. V.	39, 46
Demokritov	S. O.	20, 62, 85
Dergachev	K. G.	106
Dieny	B.	15
Dmitriev	A. P.	120
Dmitriev	D. V.	37
Dobrzyński	L.	92
Dolgov	O. V.	31
Drovosekov	A. B.	23
Drozdovski	A.	88
Dvornik	M.	16

## E

Ekomasov	A. E.	89
Ekomasov	E. G.	89
Eremin	E. V.	52, 73
Eremin	M.	74
Eremina	R. M.	34, 47
Eriksson	O.	63, 65

## F

Farzетdinova	R.M.	29
Fayzullin	M.	74
Fedin	D. N.	88
Fedorov	V. V.	67, 124
Fennell	T.	40
Fiebig	M.	54, 109
Filimonov	Y. A.	117, 118, 131, 132
Filipov	V. B.	39
Firsenkov	A. I.	88

Fridman	Yu. A.	90	<b>I</b>		
Fujii	J.	124	Ignatenko	A. N.	33, 96
Fujita	T.	30	Igoshev	P. A.	97
<b>G</b>			Iliyaschenko	V. M.	128
Gambardella	P.	15	Ilyushenkov	D.	98
Gan'shina	E. A.	66	Inosov	D. S.	44
Ganeev	V.	100	Irkhin	V. Yu.	96, 97
Gastev	S. V.	67	Ishchenko	T. V.	39
Gavrilova	T. P.	34	Iuşan	D.	63
Gazizulin	R. R.	21	Ivanov	B. A.	86, 105
Gerasimov	N.	71	Ivanov	M.	54
Gervits	N. E.	91	Ivanov	V. P.	99
Gieniusz	R.	85	Ivanov	V. Yu.	50
Giersig	M.	25	<b>J</b>		
Gippius	A. A.	91	de Jong	J. A.	18
Glazkov	V. N.	43	Jushkov	V. I.	73
Glushkov	V. V.	46	<b>K</b>		
Gnatchenko	S. L.	106	Kachorovskii	V. Yu.	120
Go	A	92	Kadlec	C.	48
Goian	V.	48	Kalashnikova	A. M.	18
Gregg	J. F.	103	Kalinikos	B. A.	55, 58, 87, 93, 94
Grigoryeva	N.	93, 94	Kalinkin	A. N.	101
Grishin	A. M.	99	Kamba	S.	48
Grishin	S. V.	60, 95	Kaminski	B.	27
Gudim	I. A.	52	Kamzin	A. S.	100
Gumerov	A. M.	89	Kang	T. D.	77
Gurevich	S.	98	Kant	Ch.	116
Gurin	A. S.	125	Kapaklis	V.	25
<b>H</b>			Karashtin	E.	102
Habermeier	H.-U.	24	Karenowska	A. D.	103
Hagiwara	M.	30	Kartashev	A. V.	52
Haug	D.	44	Katanin	A.	96, 97
Heinonen	O	15	Katsnelson	M.	63
Hellsvik	J.	63, 65	Kavich	J. J.	15
Hendren	W.	66	Kavokin	K. V.	123
Hendry	E.	16	Keimer	B.	24, 31, 44
Henriques	A. B.	27, 115	Khasanov	N.	104
Heyderman	L. J.	15	Khatsko	E. N.	106
Hillebrands	B.	78, 103	Khivintsev	S. A.	117, 118
Hinkov	V.	44	Kholin	D. I.	23
Hjörvarsson	B.	25	Khymyn	R.	105
Hoffmann	A.	15	Kibalin	Yu. A.	124
Honda	Z.	30	Kimel	A. V.	18
Huang	Y.	91	Kimura	S.	30
			Kireev	V. E.	105
			Kirilyuk	A.	18

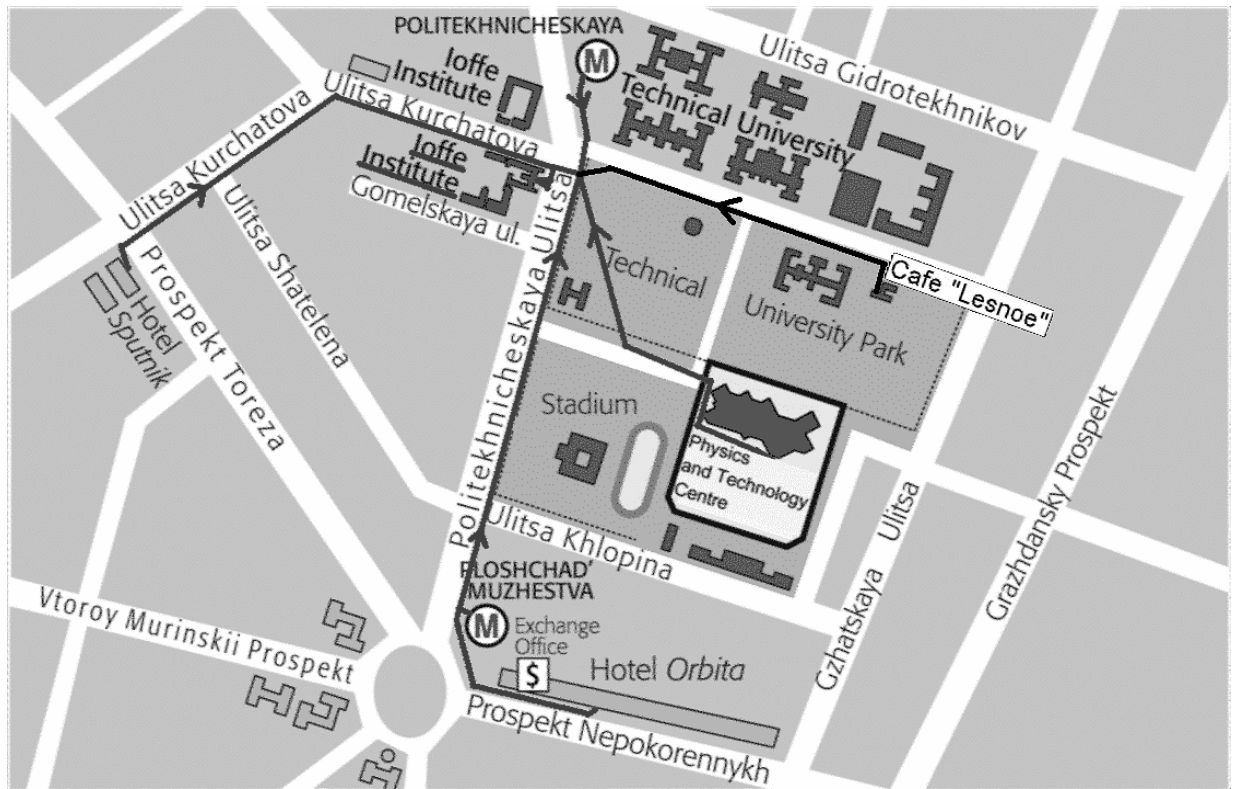
Kitan'	S. A.	128
Klevets	Ph. N.	90
Klochkov	A. V.	21
Kobets	M. I.	106
Koch	K.	91
Kohn	K.	48
Kolmychek	I. A.	66
Kondrashov	A. V.	58
Kondyan	S.	126
Koplak	O.	59
Koshmak	K. V.	67, 124
Kosmachev	O. A.	90
Kosobukin	V. A.	26
Kostylev	M. P.	28, 78
Kotelyanskii	M.	77
Koudinov	A. V.	123
Kozhevin	V.	98
Kozin	A. E.	88
Kozub	V. I.	22, 98
Kraetschmer	W.	30
Kreines	N. M.	23
Krichevtsov	B. B.	67
Krivnov	V. Ya.	37
Krivosik	P.	55
Krug von Nidda	H.-A.	30
Kruglyak	V. V.	16
Krutianskiy	V. L.	66
Kurkin	M. I.	64, 107
Kusraev	Yu. G.	123, 125
Kuz'menko	A. P.	108
Kužel	P.	48
Kuzmenko	A. M.	50
Kuzmin	V. V.	21
<b>L</b>		
Lafrentz	M.	27
Lee	J. H.	48
Lee	L. A.	73
Leo	N.	109
Li	Yuan	44
Lin	C. T.	31
Liu	W.	91
Lock	E. H.	70, 110
Loginov	N.	71
Logunov	M.	71
Loidl	A.	34
Lutsev	L. V.	72, 88, 111

<b>M</b>		
Majchrak	P.	56
Malakhovskii	A. V.	52
Maleyev	S. V.	32
Manuilov	S. A.	99
Matiks	Y.	24
Maziewski	A.	85
Meilikhov	E. Z.	29
Melander	E.	25
Mentink	J. H.	63
Mikhaylovskiy	R. V.	16
Mishina	E.	54
Mitryukovskiy	S. I.	66
Morenzoni	E.	24
Morgunov	R.	59
Morozova	M. A.	61, 112
Moshnyaga	V.	54
Mugarza	A.	15
Mukhin	A. A.	50
Murphy	A.	66
Murtazin	R. R.	89
Murzina	T. V.	66
Mushenok	F.	59
Mutka	H.	40
<b>N</b>		
Namozov	B. R.	123, 125
Nashchekin	A. V.	67
Nikitov	S. A.	68, 69, 84, 117, 118, 131, 132
Nikolychuk	G. A.	99
Nogués	J.	15
Novitski	N. N.	81, 111
Nowik-Boltyk	P.	20
<b>O</b>		
Omura	K.	30
Orlova	N. B.	64, 107
Östman	E.	25
Ostrovskaya	N. V.	113
Ouladdiaf	B.	80
<b>P</b>		
Panaccione	G.	124
Pankrats	A.	126
Papaioannou	E. Th.	25
Park	J. T.	44
Pasquali	L.	124
Patoka	P.	25
Patrin	G. S.	73, 114

Patrin	K. G.	114	Serga	A. A.	78, 103
Patton	C. E.	55	Shaginyan	V. R.	38
Pavlov	E. S.	131, 132	Shapiro	A. Ya.	36, 121
Pavlov	V. V.	27, 81, 115, 128	Sharaevskii	Yu. P.	60, 61, 84, 95, 112
Petford-Long	A. K.	15	Sheshukova	S. E.	61, 84, 112
Petrakovskii	G.	126	Shitsevalova	N. Yu.	39
Petrenko	O. A.	40, 76	Shmakov	P. M.	120
Petrov	S. V.	36, 121	Shulenkov	A. S.	111
Pimenov	A.	49, 116	Shuvaev	A.	116
Pimenov	Anna	116	Sirenko	A. A.	77
Pisarev	R. V.	18, 27, 48, 81, 109, 115	Sitnikova	A. A.	67
Platonov	S.	68, 69	Sizanov	A. V.	119
Plusnin	N. I.	128	Skorikov	V. M.	101
Pollard	R.	66	Skoromets	V.	48
Polyakova	V. V.	113	Slavin	A. N.	103
Popkov	A. F.	113	Sluchanko	N. E.	39, 46
Povarov	K. Yu	36, 121	Smirnov	A. I.	30, 36, 43, 121
Povzner	A. A.	130	Smolyakov	D.	73
Prokofiev	A.	30	Sofronova	S.	47
Prokscha	T.	24	Sokolov	N. S.	67, 124
Prozorova	L. A.	30, 45, 76	Sorokin	A. O.	122
Pyatakov	A. P.	51	Sort	J.	15
<b>R</b>			Sosin	S. S.	76
Rabe	K. M.	48	Spirin	A.	71
Rainford	B. D.	40	Springholz	G.	27
Ranzinger	A.	56	Standard	E.	77
Rappl	P. H. O.	27	Starykh	O. A.	35, 36
Rasing	Th.	18, 63, 75	Stashkevich	A.	28
Rauckii	M.	73	Stepanow	S.	15
Razdolski	I.	18	Stognij	A. I.	81, 111
Ritter	C.	40	Subkhangulov	R. P.	123
Rogers	P. D.	77	Sultanov	R.	94
Romanenko	D. V.	95	Suturin	S. M.	67, 124
Romanov	N.G.	125	Svistov	L. E.	30, 45
Rosner	H.	91	Syromyatnikov	A. V.	42, 119, 122
Rusakov	V. A.	81, 128	<b>T</b>		
<b>S</b>			Tagirov	L.	129
Safin	T. R.	21	Tagirov	M. S.	21
Sakharov	V. K.	117, 118	Tanase	M.	15
Salazar-Álvarez	G.	15	Tarima	N. A.	128
Sales	B. C.	43	Taroni	A.	65
Scherbakov	A. V.	17	Temerov	V.	126
Schmitt	M.	91	Tiberkevich	V. S.	103
Schnelle	W.	91	Tolmachev	D. O.	125
Schwan	A.	115	Tong	W.	55
Semeno	A. V.	39, 46	Torelli	P.	124

Tsurkan	V.	45, 116	Woltersdorf	G.	56
Tugarinov	V.	126	Wu	M.	55, 57
Turpanov	I. A.	73	<b>Y</b>		
<b>U</b>			Yakovchuk	V. Yu.	114
Udalov	O. G.	102, 127	Yakovlev	D. R.	27, 115
Ulrichs	H.	85	Yamaguchi	H.	30
Urazhdin	S.	62, 85	Yaresko	A. N.	31, 44
Usachev	P. A.	81, 128	Yarikov	S. A.	114
Useinov	N.	129	Yarygin	A.	69
Ustinov	A. B.	58, 87	Yassievich	I.	98
<b>V</b>			Yavsin	D.	98
Vashkovsky	A. V.	110	<b>Z</b>		
Vasil'ev	A. D.	52	Zaripova	L. D.	100
Vasiliev	A. M.	45	Zarubin	A. V.	97
Velikanov	D. A.	52, 114, 126	Zasukhin	S. V.	23
Volkov	A. G.	130	Zayats	A. V.	66
Volkov	N.	47, 73	Zhamanova	M. K.	112
Vysotsky	S. L.	131, 132	Zheludev	A.	43
<b>W</b>			Zhitomirsky	M. E.	76
Wang	Z.	57	Zvezdin	A. K.	51
Weber	A.	15	Zyuzin	A. M.	82
Wei	Fulin	100			

# Symposium location map



Spin Waves 2011  
International Symposium

The abstract book is prepared and edited by  
A. M. Kalashnikova, V. V. Pavlov, R. V. Pisarev and A. I. Smirnov





Spin Waves 2011  
International Symposium